A Dynamic Three-Dimensional Plant-Microclimate Simulation Model: "Ecospace"

Thomas David Harwood

A thesis submitted in fulfilment of the requirements for the degree of Doctor of Philosophy to the University of Edinburgh

1996

Acknowledgements

This study was funded by my parents, Jane and Pip Harwood without whom it would not have been possible. I would like to thank them, both for the opportunity and for their limitless encouragement. This thesis is dedicated to their continuing happiness.

I would also like to thank

my supervisors Robert Muetzelfeldt and Graham Russell for their patience, motivation, joviality and invaluable critisism;

Colin Legg for his heathland expertise and open door;

John Grace for his ever relevant investigations;

Alex Fiennes for his work on a visual interface for the model;

my dearest love Amanda Edwards for her endless support and optimism;

and all my colleagues at the Institute of Ecology and Resource Management for inspiration and advice.

Abstract

Growing plants modify the microclimate within which they grow by altering their physical structure. Thus individuals affect the subsequent growth of both themselves and competing neighbours. It is important that this feedback be represented in a model of dynamic vegetation change.

A flexible generalised model "Ecospace" is presented, which was designed to be applicable to all terrestrial vegetation. The model uses a three-dimensional grid of hexagonal tiles to represent space above and below ground. Each individual plant may occupy one or more tiles within the grid. Any number of individuals may occupy each tile until all space is filled. Microclimate, comprising solar radiation, wind and temperature, is calculated for each tile. Plant growth depends on the microclimate of occupied tiles. Three different plant functional groups are represented.

The current model can represent an area of up to 50 m^2 for low shrub vegetation. However, at present, computer run time and restricted memory limits the volume which can practically be simulated. There is no fundamental reason why these limits could not be overcome.

Some model runs are presented for heather plants growing under different structural and climatic regimes. Since the model represents the feedback of vegetation structure on microclimate, it is suitable for studies of the impact of changing weather patterns on ecosystems.

Table of Contents

1

Introduction

Contents

1.1 Overview

The description of the dynamic processes involved in plant interactions is central to the study of vegetation ecology. Studies in the controlled environments of forestry and agriculture and more recently in ecological science have generated much of our information on the responses of individuals to a variety of stimuli. However, the nature of interactions in both natural and semi-natural plant communities is more complex due to their inherent heterogeneity, thus making it difficult to investigate the nature of interactions between plants in controlled (i.e. uniform) conditions. As a result of this heterogeneity, each individual will be subject to a unique set of conditions for growth, which, combined with its genetic strategy, will define the survival, size and shape of that individual. Each generation of plants within a community alters the growth conditions for both present and future individuals, resulting in phenomena such as succession and cyclical regeneration. This project involves the development of a modelling framework which represents the processes described above explicitly.

The main objective of this project was to produce a prototype model outlining a general approach to vegetation dynamics modelling based on the representation of the three-dimensional spatial microclimate and plant structure at a sub-individual level. It is a common assumption in models of vegetation dynamics that the abiotic conditions are broadly constant, thus rendering them unsuitable for studies involving changes in those conditions. The modelling approach avoids the assumption of constant abiotic environment, potentially allowing simulations of the effects of a changing climate. However, this is a complex mechanistic modelling approach, and to some extent requires assumptions covering aspects of the system about which we know very little at present. It is expected that such an approach

would require a considerable body of work involving model development with concurrent field studies to yield reliable results. This project aimed to test the practicality of the approach.

The upland heath moorland of the British Isles was chosen as a basis for the project because it is a comparatively well studied semi-natural system. Nevertheless, the model framework has been designed such that it may be applied to any terrestrial vegetation. This requires that all modelling decisions are based on a firm ecological footing thus avoiding the use of empirical modelling abstractions (e.g. coefficients of competition) for the sake of simplicity. The structure of most models is such that it will only allow change in a certain number of variables immediately relevant to the model purpose. This can severely limit the applications of the model, and, particularly where abiotic conditions must be assumed constant, (e.g. Botkin, Janak & Wallis, 1972; van Tongeren & Prentice, 1986) its ecological generality. The "Ecospace" model is designed to minimise the constraining effects of the structure of the model on model behaviour, thus representing ecological knowledge in as direct a way as possible. The model should be viewed as a prototype, moving some way towards a closer relationship between simulation modelling and descriptive ecology, but being imperfect because of the scale of the task of mathematically representing all relevant ecological knowledge and the limitations of computing power.

In order to achieve ecological and application generality, the "Ecospace" model uses a three-dimensional spatial grid within which plants grow as individuals occupying a number of grid units. Conditions at each point in the grid are generated from the vegetation structure and are used to calculate plant growth which is then applied spatially.

The "Ecospace" model is described and discussed in this thesis. The remainder of this chapter puts the model in an ecological context. Chapter 2 justifies the modelling approach used in the framework. Chapter 3 is a description of the spatial grid and the rules of occupancy associated with it. Some field studies describing elements of spatial structure used in the model are presented in Chapter 4. Chapter 5 is a description of the weather and microclimate generation sub-models. Chapter 6 is a description of the growth generation and spatial allocation of individual plants. Chapter 7 presents some results and preliminary validation. Chapter 8 is a discussion of the completed model. The Appendix contains a full listing of the "Ecospace" program in ANSI C.

The heathland ecosystem

Heath vegetation has a relatively simple community structure. It is a successional community maintained by human management (burning, cutting and grazing) at a level where ericaceous dwarf shrubs are dominant. Succession eventually leads to birch or pine woodland (Miles, 1974; Hobbs, 1981), whilst nutrient enrichment shifts the competitive advantage towards grasses (Heil & Diemont, 1983; Berendse & Aerts, 1984). Heather (*Calluna vulgaris* (L.) Hull) and the other ericaceous shrubs (e.g. *Erica tetralix* L., *Erica cinerea* L.) form a dense canopy at a height of around 20-50 cm above the ground surface, depending on stand age, which may be interrupted by competing species such as bracken (*Pteridium aquilinum* (L) Kuhn) in dry areas or grasses (e.g. *Deschampsia flexuosa* (L.) Trin.). Below this canopy, at around 0-8 cm, there is a layer of smaller plants, usually mosses such as *Hypnum jutlandicum* Holmen & Warnke and *Dicranum scoparium* Hedw.. In peat bog communities, the dominant moss is usually a *Sphagnum* species and the shrub vegetation roots in the moss column. The horizontal structure shows a shifting pattern over time due to the cyclical development of *Calluna* in uneven aged stands (Watt, 1947), herbivory (Diemont & Heil, 1984) and probably vegetative propagation through adventitious rooting (Miles, 1981). The range and nature of dynamic processes in heathlands have been well reviewed in Gimingham (1972), Webb (1986), Hobbs and Gimingham (1987) and Thompson, Hester and Usher (1995). However, although it is known that the structure of the *Calluna* canopy has a significant influence on most heath processes, it is not known what the factors controlling *Calluna* structure are. In the present work, field studies were undertaken in order to describe the dynamic growth form of *Calluna*.

1.2 The mechanisms of plant competition

The dynamics of vegetation are influenced by the spatial relations of individuals within the system (Greig-Smith, 1964), through heterogeneity of resources (e.g. light, nutrients) and limiting factors (e.g. temperature, wind), and through modification of the microclimate surrounding individuals by the individuals themselves (Blad & Lemeur, 1979), and by neighbouring individuals (Monsi & Saeki, 1953; van Eimern *et al.*, 1964; Grace, 1977).

Ford and Sorrensen (1992) defined a five axiom theory of plant competition in even-aged plant communities as summarised below.

1. Plants modify their environment as they grow and reduce the resources available for growth by other plants. This defines the existence of inter-individual competition.
2. The primary mechanism of competition is spatial interaction.
3. Plant death due to competition is a delayed reaction to reduced growth following resource depletion.
4. Plants respond in plastic ways to environmental change, and this affects not only the result of competition, but its future outcome.
5. There are species differences in competition processes.

This approach may be extended to communities with uneven distributions of age, size, species and spatial structure where the above rules apply once selection for establishment has occurred. The second axiom emphasises the dominance of spatial interactions on competition. Individual plants exist in a spatial environment defined by their own structure and the structure of the vegetation and ground surrounding them. All above-ground competition apart from mutualistic or parasitic contact must necessarily act through the medium of the air which lies between individual plants. It follows that by defining the structure of an individual and the structure of the surrounding community we can calculate the individual's response directly.

Species interactions, microclimate and soil

Plants present at a site necessarily modify their environment, altering the microclimate and soil conditions both directly and indirectly. These in turn affect the growth and survival of the plants which in turn modify their environment and so on. The end result of a period of change is therefore dependent upon the species composition and structure during the period of change. At each point that a new species invades, or a species already present becomes more influential on the conditions in the community, the direction and rate of community change is altered. The timing of alterations in species dominance and the extent of their modification of the environment is critical to the nature of the resultant communities.

Plant competition may be defined as in Figure 1.1 where two individuals are physically separate from one another and no direct symbiotic relationship exists. In order to influence one another, the influence must pass through the medium of either the air or the soil, such that even allelopathy may be treated as an indirect effect. It is not possible to justify the

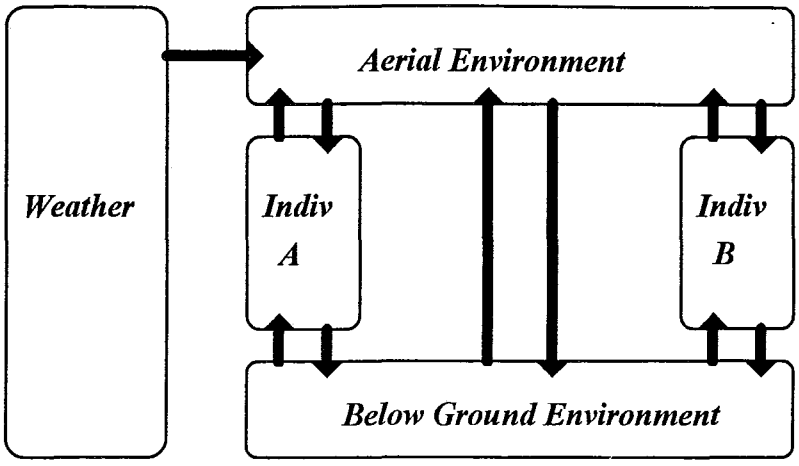

Figure 1.1. A model of plant competition: two individuals. Arrows represent influences.

use of a direct link between the two individuals except as a simplification. Thus we may say that in the absence of parasitism or epiphytic processes there are no direct influences between plants. Individuals may affect the growth of one another only through modification of the soil or microclimate. Survival of an individual is thus determined solely by the conditions in the soil and microclimate. The precise state of these two media in the vicinity of the individual is thus crucial to the success of that individual. Therefore:

-an individual is responsive only to the conditions in its immediate vicinity.

-an individual affects the conditions around it, with the amplitude of the effect decreasing with distance from the individual.

Plants of different species survive within the same area by occupying space which is suitable for the growth of each plant type. The heterogeneity of a vegetative stand is thus an inevitable component of the system. The fundamental niche occupied by a species may be defined as a multi-dimensional hypervolume (Hutchinson, 1958) where the dimensions represent gradients of influencing variables (temperature, prey size, humidity etc.) which may vary over time. For an animal the definition of its fundamental niche may be complex since it must include not only physical and chemical dimensions over time, but also four dimensional (three spatial dimensions and time) behavioural patterns. For example, Lawton and Strong (1981) stress the need for inclusion of avenues of predator escape as a niche dimension. However, the fundamental niche occupied by a plant may be defined precisely in physical and chemical terms over time. Each individual has an inherited inflexible strategy for resource capture. This may be defined qualitatively according to the three extremes of competitor, stress-tolerator and ruderal described by Grime (1979; Grime, Hodgson & Hunt 1988), or quantitatively according to potentially measurable properties such as phenology, allocation

and branching patterns, response to external factors and reproductive mechanism. The success of this strategy is dependent on the location and time of germination on which all other aspects of competition (e.g. abiotic conditions, neighbour structure) are dependent.

Cyclical, seral or long term change can therefore be viewed as a continuous period of modification of the soil and microclimate. The state at any given point in space and time will determine the success of an individual at that point, whilst the sum of the success of the individuals modifies the soil and microclimate.

1.3 Community ecology and abiotic change

An ecosystem may be viewed either as a collection of individual organisms or as a discrete community. In the context of abiotic change, the concept of discrete communities has little theoretical relevance since one can expect continuous change in community structure. However, the community approach to the study of plant systems has been a long standing principle in ecology. It is based on the assumption that certain associations of organisms occur in response to abiotic conditions and that these associations may have properties that are more than the sum of individual effects plus their interactions. A number of distinct community types may be defined for each ecosystem. For example *Calluna vulgaris-Deschampsia flexuosa* heath, *Molinia caerulea* sub-community (H9e) and *Scirpus cespitosus-Erica tetralix* wet heath (M15) (Rodwell, 1991b) are both NVC communities which might be found in heathland. However, these community types do not have clear cut boundaries, and may instead be viewed as part of a continuous gradient.

A relatively stable climax community may be regarded as an optimum solution to a given set of abiotic conditions. In practice however, abiotic conditions tend to change gradually over time, both independently of, and resulting from biological change, so that alterations in the community structure will occur to compensate for the change. A constant community composition and structure where recruitment and mortality are balanced for all species is only possible in entirely stable abiotic conditions. Stevenson and Birks (1995) present evidence that the species composition of heathlands during past interglacial periods (with similar abiotic conditions) was different from the currently *Calluna* dominated structure indicating the importance of the role of the path by which a community structure is reached. Invading species, be they plant or animal, also hold the capacity to disrupt a community.

It may be expected that one community type may shift to another in response to abiotic changes. This process is driven by the selection of individuals. Changes in the species composition may have a feedback effect on the system, forcing it to a new equilibrium.

Although there is much debate as to the validity of the community approach, the concept remains useful where dealing with conditions within the range of our past experience. Thus we can suggest possible community types which might develop at a site given the conditions at that site by drawing parallels with sites with similar conditions.

Climatic change

Climatic change occurs over a number of temporal and spatial scales, driving changes in the biosphere. Where previously unknown conditions are indicated it follows that an unknown community type might develop in response. The predicted changes in climate following a CO_2 doubling (IPCC, 1990) present us with a range of conditions, many of which have no geographical analogue (Department of Environment, 1991). The combination of solar inclination, geology and climatic regime are unique in most cases.

The fossil record might be used to find possible parallels although inaccuracies in the assessment of past climate presents difficulties. In addition, the rates of change associated with this anthropogenic warming are probably considerably faster than any previously observed changes (Davis 1989). Dispersal rates may fail to meet up with requirements and extinctions may occur across a wide range of vegetation types. Therefore we may expect existing species associations to be disrupted. Since each species has a different dispersal strategy, timing of release of propagules and life history, it would be unrealistic to expect the even migration of whole associations, but rather a fragmented response from species altering their ranges at different speeds (Peters, 1992). An added complication is the need for dispersal to take place through suitable sites. Much vegetation world wide has been fragmented through human development, and dispersal to a suitable area may be blocked by settlements, mountains or coastlines. Because of the potential difficulty that many plant species will have in attaining the rates of dispersal necessary for survival, we can expect that highly competitive, rapidly dispersing species, (including those often treated as pests) will be conferred an advantage whilst the change is occurring. The magnitude of this effect will be related to the length of time over which continuous change occurs. Slowly dispersing species may find themselves growing in unsuitable conditions but may yet be able to keep pace with

change if there are respites in the rate of change. However, the rates of change predicted could well leave many species hundreds of kilometres outside their optimal range.

Where one expects a change in existing community associations, the application of a community-based approach is questionable. The future development of ecological theory may be viewed in the context of a continuously changing climatic regime. Whether the predicted CO_2 driven changes occur or not, the issues brought up by this problem need to be considered. Long-term climatic change is a well established fact, and it is difficult to continue to extend the number of possible communities researched to cover each combination of climate and site since, if carried to its logical conclusion this leads to the continuum of ecosystem structure implied by an individual-based approach. An individual-based theory appears at the present to be a suitable approach to the problems of vegetation dynamics as influenced by climate forcing.

2

Approaches to Vegetation Dynamics Modelling

Contents

2.1 Introduction

Vegetation dynamics models provide a simulated environment within which to study the mechanisms of vegetation change. They also present the opportunity for experimentation which would be destructive, expensive or time consuming if performed on the system in the wild. The structure of a predictive simulation model should not cause significant differences between the model behaviour and the behaviour of the natural system. In addition, the model should be valid for all situations within the prescribed boundary conditions.

In the following paragraphs, I argue that, within the described modelling context, it is appropriate to model plant vegetation dynamics spatially and mechanistically at the individual level. Such an approach has been limited in the past both by computing resources and by the extent of our ecological knowledge. With the evolution of computers we are no longer limited to those mathematical models which may be calculated by simple programs, and are thus freed from the need for the more biologically unreasonable simplifying assumptions required by many such models.

Models of vegetation dynamics may take several basic forms. The system may be modelled as a collection of distinct communities where the state of the whole system is dependent on the relative amounts of different community associations. Individuals may be grouped into competing species and interactions at the species level used to determine

community structure . The system may also be modelled as a mosaic of interacting patches or gaps containing a certain number of individual plants. An alternative is to model the ecosystem as a collection of individuals. These individuals may either be represented explicitly with some properties unique to each individual (*i*-state configuration) or as a whole population distribution where individuals are not treated separately (*i*-state distribution) as defined by Metz and Diekmann (1986). It is argued that in order to represent spatial elements crucial to vegetation dynamics in a natural system, an *i*-state configuration model is required.

Modelling context

The "Ecospace" model has been developed in the context of long-term climatic change. The abiotic inputs to the system are viewed as non-constant. When the time-lag between change in abiotic conditions and biotic response is also taken into account, the concept of an equilibrium becomes inappropriate. The process of change is therefore viewed as a continuous process which is in itself a component of the system, altering the nature of other components and their relationships. In this chapter, approaches to vegetation dynamics modelling are reviewed within the limits imposed by such a view. Many of these approaches may be suitable for the examination of systems or for the representation of aspects of ecosystem behaviour within a defined model purpose, but may fail to represent the feedbacks required for simulation in constantly changing conditions.

When modelling the impact of a changing climate on an ecosystem, it is not sufficient for the model to represent only a fixed community structure. If the abiotic forcing functions are expected to undergo large changes, one would expect corresponding changes in ecosystem structure and species composition. Any model of an ecosystem which is being tested for its responses in such conditions should allow for these changes (Nielsen, 1992; Jorgensen, 1992) in order to be applicable to the problem.

2.2 Abiotic change

The limitations of different modelling approaches need to be recognised. This is of particular importance when dealing with processes of abiotic change. When a model is used to explore conditions outside the range of conditions within which that model has been developed it is necessary that the model be suitable for this. Most correlative models are only of value within the range studied. Many other models will state in their assumptions that certain abiotic factors have been assumed to be constant (e.g. Botkin *et al.*, 1972; Noble & Slatyer, 1980).

Modelling of the effects of climate change on vegetation presents a unique problem (see section 1.3). Here it is necessary that the model include mechanisms for response to a wide range of climatic effects and, importantly, the main feedbacks in the system. If one expects a change in the physical structure of the sward it is essential that the effect of that change on the behaviour of the system be modelled (Nielsen, 1992; Jorgensen, 1992). However, most models of vegetation have been developed in a different context or for a different purpose and do not represent this feedback adequately. Failure to include this feedback would be expected to invalidate the model if a significant change in structure occurs.

Forest gap dynamics models, following the FORET model of Shugart and West (1977), are a class of individual-based succession model which has been widely applied to mixed species forest ecosystems (see the review by Shugart, 1984). The approach has also been extended to other systems such as semi-arid grassland (Coffin & Lauenroth, 1990). These are individual-based models, where individual plant location is not defined within a plot assumed to be representative of conditions in a given neighbourhood. Shugart and West (1977) found that plot size was critical to the behaviour of the model and that when the plot size was reduced to the size of a dominant individual, the "gap dynamics" phenomenon was reproduced. Models of this class have been applied to the problem of climate change (Solomon, 1986; Pastor & Post, 1988). However, the applicability of these models to steady-state ecosystem dynamics does not necessarily imply their suitability for the problem of modelling the effects of climate change. The plot size which reproduces "gap dynamics" is linked to climate. Conditions in the gap must be representative of the establishment conditions for competing trees within the plot. If the changing climate were to alter the plot dimensions required to adequately simulate "gap dynamics" either through modification of gap microclimate or through a change in the size of a dominant individual this will have a critical effect on the model behaviour. Thus, although the structure itself is not necessarily changing, the microclimate, which is derived from climate but defined by vegetation structure, is changing, such that the effective structure of the community is also changing. It is necessary to determine whether or not this effect will be significant as far as model dynamics are concerned before drawing conclusions from the simulations of Solomon (1986) and Pastor and Post (1988).

The extent to which the physical composition of the system is represented is critical to the validity of the model if the effect of abiotic change is being simulated. Even in systems where aspects of physical structure are unimportant at present (e.g. Coffin & Lauenroth, 1990, where semi-arid grassland is modelled by representing only below-ground processes), a

change in structure may well alter the driving variables within the system (development of continuous ground cover altering the soil water relations).

2.3 Modelling heterogeneity

The survival and growth of an individual plant is dependent upon that plant's access to resources and its exposure to limiting conditions. The distribution of resources throughout natural systems tends to be patchy. Heterogeneity of the environment operates at all ecological scales and is essential for the maintenance of diversity in ecosystems. When dealing with individual plants it will be found that in most natural systems each individual is in a unique environment. A large proportion of vegetation models to date have been developed for even aged monocultures, especially agricultural crops (e.g. Wisiol & Hesketh, 1987) and forests (e.g. Munro, 1974; Shugart & West, 1980). Unfortunately, conditions in these managed systems are very different from the conditions in natural communities, since steps will be taken by the manager to reduce heterogeneity. In an idealised crop system with regular spacing between rows and within rows, each individual will be subject to identical conditions. Consequently, if the responses of all individuals to conditions are equal, all individuals will theoretically grow at the same rate, thus maintaining constant conditions for all individuals. However, in real crop systems, only in exceptional circumstances will variation in yield between individuals be negligible. Nevertheless, for the purposes of modelling in such a system, it is reasonable to simplify or ignore spatial relationships since similarity may be attained between the real and model systems with regards total plot yield, thus giving application validity.

If one is treating a multispecies ecosystem, then the effects of patchiness in resource availability are of great importance (Caldwell & Pearcy, 1994). Each individual will be in a unique set of circumstances, and this has important implications for the preservation of diversity (De Angelis & Rose, 1992).The establishment of an individual may well be dependent upon a certain set of conditions being met, but only at the point of establishment, rather than over the whole system. Each species occupies a niche in the community which may be defined multidimensionally by a number of environmental variables. Within an ecosystem the conditions required for survival of a species occupying a certain niche may only be found in a small part of that community. Where the species involved is of particular ecological importance, (for example the establishment of birch, *Betula sp.*, in the heathland ecosystem leading to succession towards woodland) it becomes important to model this aspect accurately. If the model plot is regarded as homogenous, it is unlikely that conditions will arise over the whole plot which favour the establishment of an invading species without some

preconditioning by small numbers of that species. Indeed, in homogenous conditions, one would expect the principle of competitive exclusion to act, resulting in species impoverishment. Ebenhöh (1994) demonstrates how the introduction of temporal heterogeneity allows coexistence of species in a class of food web model which would demonstrate competitive exclusion in a steady state form. Given that coexistence is critical to the process of vegetation change it is important that modelling assumptions do not act to prevent it.

Spatially homogenous vegetation dynamics models (e.g. Kauppi, Hari and Kellomaki, 1978, Noble & Slatyer, 1980, Cannell, Grace & Booth, 1989) may well simplify the real system to the extent of inadequate simulation. Depending on the aims of the model, a homogenous approach may be justified. However, where the model is to be used to test the effects of changing heterogenously distributed variables upon species composition, a homogenous approach becomes very difficult to justify, since it cannot implicitly represent establishment. In this case heterogeneity would ideally be represented at a scale sufficient to mechanistically capture its effect on vegetation dynamics.

2.4 Model complexity

Model complexity or simplicity are not desirable properties in themselves. The relative complexity of a model should be the result of a reasoned process as to the best way to represent the system for the model purpose. It is important not to under-represent our knowledge of the system for the sake of simplicity, or conversely model in unnecessary detail. Explicit representation of biological processes is likely to simplify the interpretation of the results of a simulation, since the ecological interpretation of a model using abstractions requires interpretation of those abstractions (Kimmins & Scoular, 1984). Complexity can, however, make interpretation difficult due to the amount of information which must be assimilated.

In the context of a changing climate (section 2.2), and where heterogeneity of the system is an important component of the system (section 2.3), the extent to which the real system is simplified is critical to the applicability of the model. Where simplification is such that these aspects are under-represented the model is no longer suitable for predictive simulation.

An approach to ecological modelling based on a search for generalities has predominated for a number of years. In addition, simulation modelling has developed in a climate of limited computer resources, thus reducing the possibilities for complex models. As a result, a modelling philosophy based on considerable simplification of the real system has arisen. Although some simplification is necessary in order to reduce any system to computer algorithms, beyond a certain level of simplification the model ceases to be representative of the real system, thus severely limiting its applicability. Although the model may demonstrate behavioural validity at the chosen level of simplification (e.g. one community shifting directly to another in response to increased nutrients, with measurements for validation based on a simplified community definition), it does not follow that this behaviour is representative of the non-simplified system (the rate and sequence of species replacement will have an effect on the composition of the resultant community).

For an example we may consider the model by Slatkin and Anderson (1984) of competition in communities of static organisms such as plants or barnacles. Hereafter these organisms will be referred to as plants. The individual plants are represented as two-dimensional discs randomly distributed across a homogenous surface. Growth monotonically increases with time, and is applied as a radial increase. When two discs touch, competition occurs and one of the two plants is selected randomly for survival whilst the other instantly dies and disappears. The model is shown to conform to the -3/2 thinning law (Yoda *et al*, 1963), if mass is taken as the cube of the radius. What relevance has this model to plant competition? What are the real system parallels of the processes described? The degree of abstraction and simplification is such that the processes occurring have no direct parallels in a plant community, where growth is proportional to resource capture and plants may grow at different vertical levels. The fact that it shows a single property of real communities does not necessarily mean that the model correctly simulates the key features of the real system.

A chess tournament

We may also consider an extreme case of a model of a chess tournament starting with dozens of players in pairs, competing, with the losers being removed until only the champion remains. The modeller has chosen to view proceedings from a vantage point on the ceiling of the venue (Figure 2.1.a.). A chess board is composed of a number of black and white tiles and a number of black and white pieces. If viewed from a great enough distance (the ceiling), the board will appear to be a uniform grey and may be represented as such. The players interact through the

medium of the board. If measurements for validation are also taken from this distance we can confirm that the board remains a constant uniform grey throughout the game.

Since it is not possible to represent the actual game at this level of simplification, and the board appears constant, one could model the game as direct competition between the two players based on an abstract competition coefficient based on some property or combination of properties of each player. The players will compete until only the champion remains and the model behaviour may be said to be reasonable provided that the model is not used to draw conclusions on the relative competitive ability of the different players.

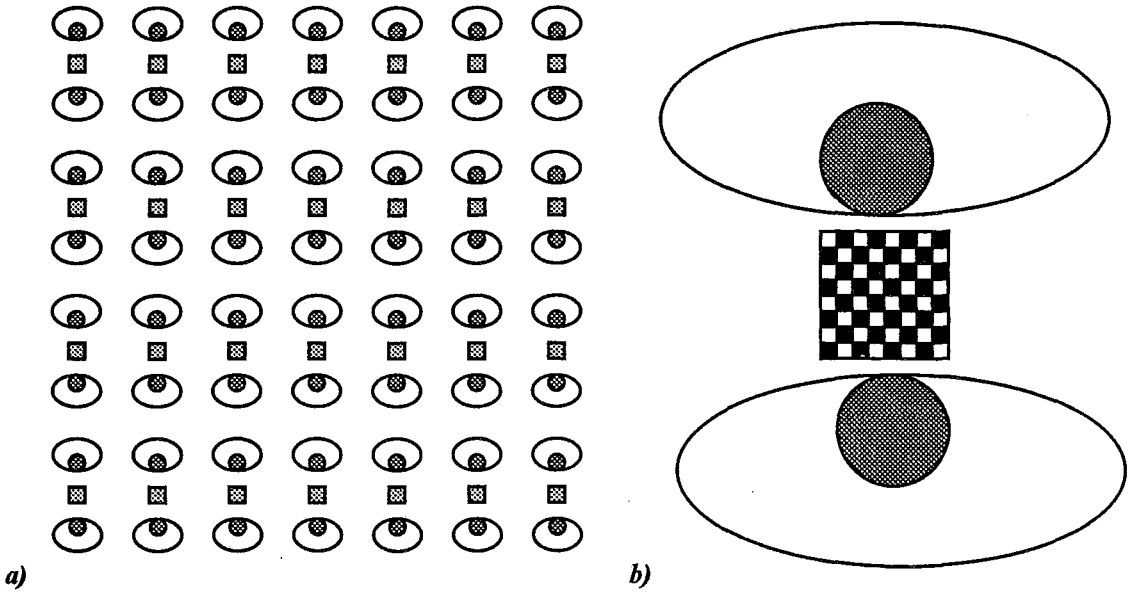

Figure 2.1. Modelling a chess tournament. a). The tournament viewed from the ceiling where all the boards appear to be a uniform grey. b). An individual game with black and white board.

We may examine this approach as a model to determine the relative competitive ability of the different players and to predict the outcome of the tournament. If one is not aware of the existence of the heterogeneity of the board it would be reasonable to adopt the above approach. If, however, one is aware of the true nature of the game and yet choose to deliberately ignore it we are moving into difficult territory. The model has a certain structural validity and yet does not represent the full extent of our knowledge. Consequently, the competition coefficient will fail to represent the results of different combinations of strategy, with the "best" player (with the highest competition coefficient) always winning. The model cannot therefore reasonably be applied to predict the outcome of the chess tournament. However, it should be noted that a complex approach, although perhaps theoretically more satisfying, would not guarantee an improved result even if shown to be possible.

Competition coefficients

Consider also the use of the concept of competition. Ekschmitt and Breckling (1994) point out the ambiguity of definition of this concept, with indefinite mechanism and effect. It is common practise when modelling vegetation dynamics spatially to view plants as competing against their immediate neighbours for resources with competition derived from "nearest-neighbour" distance and relative size (e.g. Mead, 1968; Diggle, 1976; Gates, 1978; Ford & Diggle, 1981; Cannell *et al.,* 1989). The model of Diggle (1976) first defined competition as a one-sided process by which large plants influence small plants, but small plants have no influence on large ones. One-directional and sometimes two-directional (Kenkle, 1988; Thomas & Weiner, 1989) competition between neighbouring individuals interacting in pairs has become the basis of this class of model.

In the context of the model of competition outlined in section 1.2 and in the context of abiotic change, such an abstraction has no place. Competition coefficients are an anthropomorphism (Ekschmitt & Breckling, 1994), attributing to plants a characteristic which they do not have. It is possible that this concept may have arisen from the modelling of animal populations using Lotka-Volterra type competition equations, where the competition coefficient is used to represent complex animal strategies, and where the approach may be the most valid representation. It is potentially a more straightforward task to describe the interaction of plant allocation strategies with the volume surrounding the plant, due to the sessile nature of plants and their lack of conscious thought (see section 1.2, p 5,). Knowledge of the community structure around an individual, combined with external influences (e.g. weather, hydrology) may be used to predict the response of a plant with a particular inflexible strategy. It is not therefore necessary to apply the abstraction of a competition coefficient, although such an approach may be justified within a narrow range of modelling objectives. However, it is possible to include in the coefficient a representation of some aspects of the environment local to an individual, particularly light, but this must necessarily assume homogeneity of conditions throughout the individual.

As an alternative approach, I propose that instead of individual plants being assumed to compete against other selected individual plants, these plants are assumed to compete against the community as a whole, where the effect of the community can be defined in terms of the abiotic conditions in the particular space occupied by that individual.

A complex model structure is used in the "Ecospace" model in order to represent competition between plants according to the theory outlined in section 1.2. This inevitably

leads to complex model behaviour, which slows analysis of model behaviour. Where the behaviour is the result of a fault in the model, the complex nature of the model makes detection of the fault difficult. In addition, the complexity of a model may introduce significant difficulties of formulation and parameterisation throughout model development. However, the difficulties in producing a complex model do not represent an ecologically based reason for avoiding this approach.

2.5 Morphological abstraction

Where plants are being represented explicitly by spatial forms in ecological models, abstractions may be used in order to simplify the real structure of the plants (Fig.2.2). Often these will bear little resemblance to actual plants. For example, the model of Korzukhin (1995) represents trees as flat screens, oriented in either the horizontal or vertical planes, and the model of Luan (1994) uses cylindrical crowns. Depending on the calculations performed using these abstractions, such assumptions may well be reasonable. However, Kurth (1994) points out that the integration of process-based models using different abstractions presents a problem, and argues for the use of morphological models.

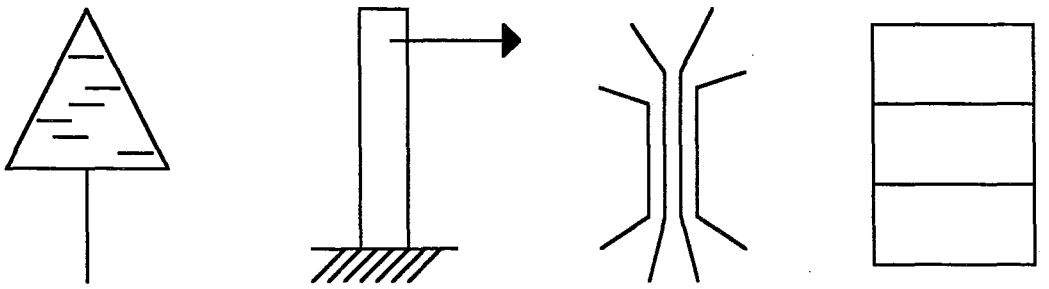

a) *b)* *c)* *d)*

Figure 2.2. Specialised simplifications of trees used in modelling (after Kurth 1994). a). light model, b). mechanical model, c).hydraulic architecture (pipe model), d). allocation model with leaves, stem and roots as compartments.

Morphological models of plants have largely been developed as computer graphics models (e.g. Prusinkiewicz & Lindenmayer, 1990; Aono & Kunii, 1984). Branching L-systems models (Lindenmayer, 1975) have developed to the stage where complex structures identifiable as distinct species can be generated from a limited number of rules. However, little work has been carried out to link such models to biological processes with the exception of the model of Ford, Avery and Ford (1990). The potential application of such models to ecological systems, as advocated by Bassow, Ford and Kliester (1990) and Kurth (1994), requires an effort by ecologists to work towards the combination of the two approaches. The "Ecospace"

model presented in this thesis is designed such that any defined plant structure may potentially be converted to the cell-based representation used in the modelling framework, since the cells are defined on a three-dimensional Cartesian grid.

2.6 Individual-based models

As argued in section 1.3, a community-based approach to modelling (e.g. Hobbs, 1983) is inappropriate where the system being modelled moves outside the studied range of abiotic conditions. The argument may be extended to cover any grouping of individual plants. The categorisation of plants requires the use of generalisations. Spatial generalisations are necessarily scale-specific and abiotic change alters the effective ecological scale of interaction. An individual-based modelling approach avoids this problem because the definition of an individual remains constant.

Metz and Diekmann (1986) developed a useful classification of individual-based models which will be used to distinguish individual model types. Each individual is considered to have an "*i*-state" which is defined as all the information needed to calculate the response of that individual to its environment, such as age, sex, size and condition. The state of the population (the *p*-state) may be derived from the properties of the individuals comprising that population and their dynamics i.e. the *i*-state dynamics. The two classes of model are the *i*-state distribution model (where individuals are grouped according to common characteristics) and the *i*-state configuration model (where the conditions for each individual are modelled explicitly). The latter models represent individuals as discrete entities. The more detailed *i*-state configuration models may be used to derive *i*-state distribution models, but not the reverse.

Huston, DeAngelis and Post (1988) and Caswell and John (1992) argue that, for plant populations, the sedentary nature of individuals and the spatial heterogeneity of the environment render an *i*-state distribution approach inappropriate. It is a fundamental assumption of the *i*-state distribution model that all individuals within a class are subject to the same conditions. In most plant stands there is a degree of heterogeneity of the environment of the individual, ranging from small variations in an even-aged even-spaced monoculture up to complex patchy multi-species systems. This heterogeneity has important effects on vegetation dynamics and an *i*-state configuration approach becomes more appropriate as one moves to more heterogeneous systems.

2.7 Models of heathland vegetation

The heath ecosystem has been modelled using a number of approaches summarised below. It was considered that none of the approaches adequately represented the ecology of the system for a study of abiotic change, but that the development of a fresh approach allowing the synthesis of aspects of the different models would be of value.

The production of *Calluna vulgaris* has been modelled empirically in relation to temperature and light by Grace (1970, Grace & Woolhouse 1974). This model does not represent individuals explicitly and does not involve any dynamic competition, concentrating instead on net production, and assimilate partitioning between different plant organs. This model was used as the basis of the three-dimensional model presented here.

Hobbs (1983) and Hobbs and Legg (1983) have modelled community and patch shift respectively between heathland types using Markov processes. These models are very simple association-based models allowing the development of no associations outside those represented and generating change by stochastic mechanism. The authors conclude that this approach is inappropriate for all but simple systems, and should only be used comparatively. In the context of abiotic change, this approach has little relevance.

Van Tongeren and Prentice (1986) presented a general spatial model of vegetation dynamics and applied it to the heathland dwarf shrub community. The model uses a horizontal grid over which individual plants occupying one or more grid squares compete. Only a single occupant is allowed in a given grid square. Plants grow about a central stem, with their height estimated as a function of horizontal extent. Establishment and mortality are calculated stochastically. Growth is calculated according to competition-modified relative growth rates, with horizontal spread to new cells calculated using a stochastic mechanism. This simple spatial model is shown to reproduce shifting mosaic behaviour over time for competing species. No abiotic elements are represented, although it is suggested that these could be added to the equation for areal spread.

The dynamics of the dry inland heathlands of the Netherlands (*Genisto-Callunetum*) are dominated by nutrients and this has received considerable research attention (Aerts & Heil, 1993). Nutrient enrichment has led to succession towards grassland (Heil & Diemont, 1983), and this process is modelled by a compartment-flow model "Calluna" by Heil and Bobbink (1993). The model is non-spatial, describing only relative cover of *Calluna vulgaris* and two grasses, *Molinia caerulea* (L.) Moench and *Deschampsia flexuosa* (L.) Trin..

Competition is calculated from available nitrogen-modified relative growth rates and mean replacement rates, and as such is unresponsive to abiotic or structural change. It was considered that the equations for the modification of relative growth rate with available nitrogen could be of potential use in a dynamic model of nutrient response, although the transferability of response data to upland heath (*Callunetum*) is questionable due to the difference in the below-ground component of the two systems.

The phosphorus dynamics of dry heathlands have been modelled in two compartment models, NUCHE (De Jong & Klinkhamer, 1983) and PCAL (Chapman, Rose & Clarke, 1989).

Noble and Slatyer (1980) present a general model of post-disturbance succession based on "vital attributes". This is an extension of the principle that most phenomena of succession are the consequences of differential properties of species (Drury & Nisbet, 1973), such that the course of succession at a disturbed site is an inevitable consequence of the relative availability of a range of species and their life history characteristics. The model is based solely on the properties of species over time. No abiotic conditions are represented. It does not seem reasonable to ignore the effects of environmental variability on the course of succession, yet the principle on which the model is based is valuable. An analysis of Scottish heathland vegetation using the approach of Noble and Slatyer has been carried out by Hobbs, Mallik and Gimingham (1984), where key species are classified and a diagram representing post-fire recovery times formulated.

A land use model of the effects of climatic warming on the extent and quality of heather moorland in Great Britain has been produced using the ITE land classification system (Bunce, Howard, Clarke & Dean, 1991) by Bardgett and Marsden (1992; Bardgett *et al*, 1995). The model is based on the shifts in cover of land classes at a resolution of 1 km^2 in response to climate change predicted by Hossell (1992) and a survey of the current quality of moorland. The model predicts a relatively constant areal cover of open moorland and heather on moorland within a 3°C temperature rise. However, the model also predicts the loss of approximately a quarter of the blanket bog cover, requiring significant relocation of heather to meet the first model prediction. There is little similarity between land cover approaches and mechanistic ecological approaches to the effects of climate warming.

2.8 Summary of the "Ecospace" model

The "Ecospace" model has been developed in order to provide a framework for modelling vegetation dynamics in the context of the whole ecosystem. It attempts to provide a flexible framework which is applicable to all terrestrial vegetation systems. It has been designed such that each sub-model of the system may be replaced by an alternative version without altering the model structure. A three-dimensional spatial grid of hexagonal tiles is used as a common link for the different components of the model. Each grid unit has certain physical, chemical and biological properties which represent their spatial distribution in the system.

In order to avoid confusion between the terms "framework" and "grid" as applied to the "Ecospace" model, these will be defined below.

Framework:- refers to the entire "Ecospace" model structure, where the framework supports the different sub-models.

Grid:- refers to the spatial grid of hexagonal tiles used to represent space.

"Ecospace" is based on the model of competition outlined in Chapter 1, where plants directly modify the abiotic conditions which directly affect the plants. In order to capture this process at a scale suitable for individual plants at all stages of their life cycle it was decided to explicitly model space using a sub-individual resolution. Each unit of volume has certain properties (e.g. irradiance, temperature, wind speed, volume occupied by plants) which at different levels may be either beneficial or detrimental. Plants may therefore compete by occupying units of volume which will alter their growth rates.

Plants are grown as individuals, each occupying a number of units of volume, both above ground and below ground. The representation of below-ground processes is simple and essentially non-spatial. Individual growth is calculated directly from the conditions in the units of volume which that individual occupies on an hourly basis. The structure of the vegetation is used in conjunction with generated weather conditions to calculate the three-dimensional microclimate.

The model is designed to capture the effects of spatial and temporal heterogeneity at a resolution suitable for the level of germination and establishment but below the level of the fully grown individual. The scale of the units of volume is flexible such that the grid can be altered to fit a number of vegetative systems. By representing competition mechanistically it is possible to apply the same model of vegetation dynamics to all terrestrial ecosystems.

"Ecospace" is a complex model, based on a principle of representing our knowledge of the different ecosystem components and their relation to each other explicitly. Although simplification of the system may be reasonable in some cases, it is recommended that all the components are modelled initially and the sensitivity of the system under the experimental regime be determined before decisions are made, since the combined behaviour of two or more components may be different from the sum of their separate behaviour. In its present state, the model should be viewed as a prototype, demonstrating the potential of the system, since it has not been possible due to time limitations to represent all the different ecosystem components to the best of our knowledge, and also because aspects of the system (particularly spatial plant allocation and the horizontal variation of microclimate) are modelled at a level of detail close to the limits of our current understanding. It was considered that these components of the system are likely to be researched in the near future and that the framework should have the capacity to represent this new knowledge.

The complexity of the model framework makes computer run time a severe limitation at the present. However, again it was felt that advances in computing power, particularly with the use of parallel computing (Haefner, 1994) could reduce run time. The model has been written in the ANSI C programming language in order to allow the potential development towards an object-oriented C++ approach. The "Ecospace" model has been developed and run on a mainframe computer, WAVERLEY, at the University of Edinburgh.

The main influences in the model are summarised in Figure 2.3., where it can be seen that the new individual growth is applied to the vegetation structure, and it is the combination of this structure with the incoming weather which defines microclimate which in turn drives the next round of growth. Thus there is no direct influence of one plant on another.

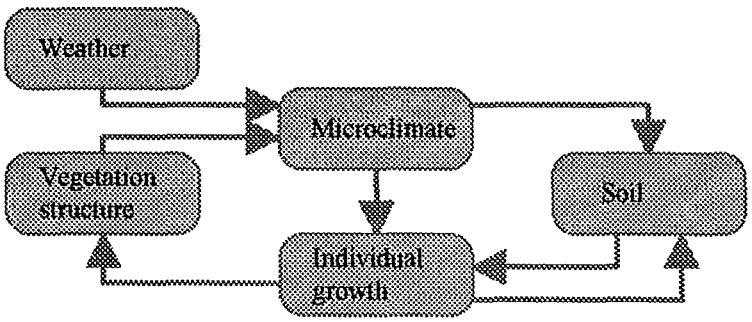

Figure 2.3 Essential influences and feedbacks in the model. Arrows represent influences. Soil feedbacks are at present very simply represented by the model.

Time and the model

A number of different time steps are used in the model framework in order to integrate the different sub-models used. These are summarised in Figure 2.4.

Individual growth is calculated on an hourly basis from spatial light and temperature which are generated hourly. This growth is accumulated and added weekly to the plant for partitioning and spatial allocation so that sufficient growth is accumulated to enable division between a number of tiles. The new spatially-added growth thus alters the vegetation structure weekly.

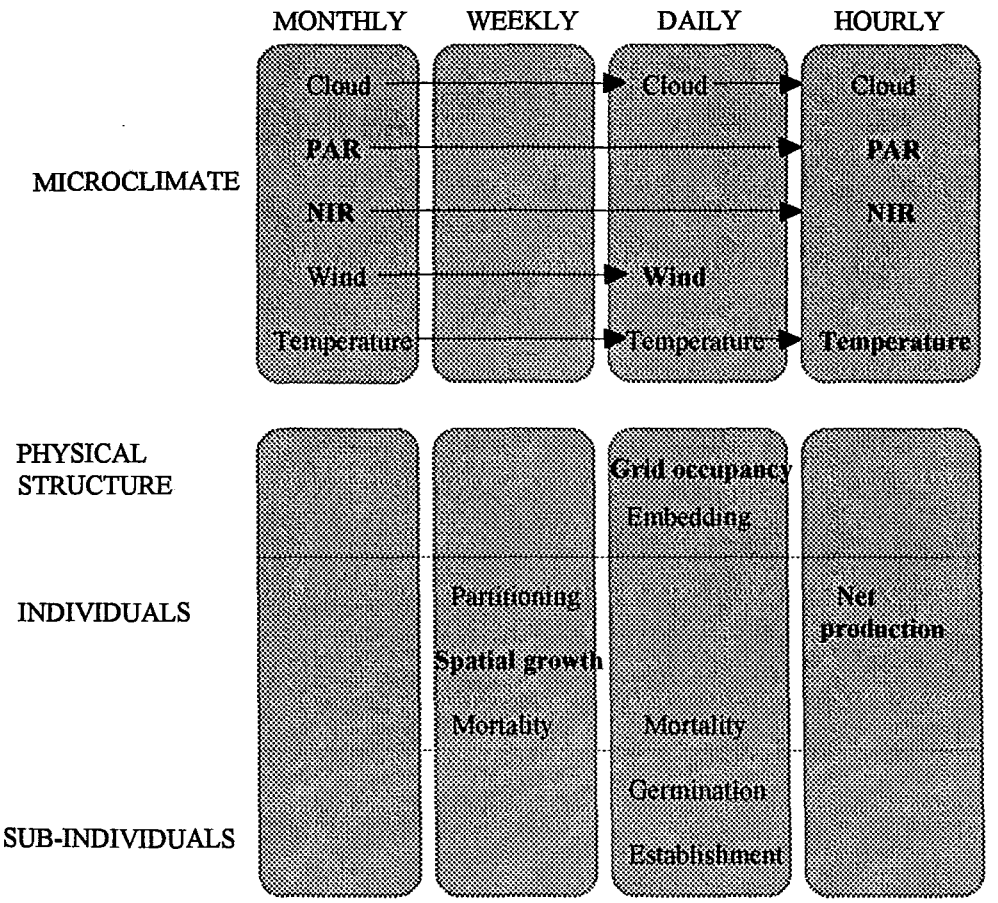

Figure 2.4. Time steps used in the "Ecospace" model framework. Bold type indicates three-dimensional spatial calculations.

The temperature and wind sub-models are responsive to this weekly change in vegetation structure, but the main spatial light sub-model is calculated monthly due to its lengthy computation time. It was considered that the minor changes in vegetation structure in most months would have little effect on the light environment relative to day to day variation.

Weather is generated daily and this is used to generate diurnal variation in temperature and light.

Germination and the growth of establishing individuals (calculated according to a simplified model) are calculated and added to the grid daily, based on average daily conditions, until each plant becomes established and is treated as an individual. Stress related and stochastic mortality are also calculated daily.

3

The General Spatial Modelling Framework.

Contents

3.1 Introduction

A general spatial framework was developed to allow 3-dimensional modelling at a sub-individual level. The framework comprises both a spatial grid and a set of rules for occupancy and growth. Plants are represented as individuals with specific spatial forms. In this chapter the static properties of the modelling framework is described in terms of the geometry of the grid and the plant growth forms and the non-dynamic interactions between the two. The dynamics of the growing plants are described in Chapter 5, whilst Chapter 4 describes the use of the spatial grid to generate a microclimate for the plant growth..

3.2 The 3-dimensional spatial grid

In order to represent realistically the three-dimensional space within which real plants interact, it was decided that all space within the community must be represented. In many models (see Chapter 2), the abstractions of form that are used cause parts of the plant (especially stems) and environment to be ignored or poorly represented spatially in model calculations. This is likely to cause errors in model output directly attributable to the representation of spatial structure in the model (e.g. ignoring stems in light transmission models).

The present model is built around a structure of tessellating solids that fill all space in the community, and which correspond to volumes in real space. Such a representation allows

a flexibility and adaptability lacking in approaches which do not fully define the geometric structure of the community. For example, a variety of different community structures can be defined, allowing the adequate representation of any terrestrial vegetation, or model behaviour may be examined in response to irregular ground surface.

The shape of these units of volume is critical since it may limit the nature of calculations performed using the grid. Ideally these units of volume should all have the same positional relationship to each other in order that each may be treated identically, thus ensuring that no structural bias is incorporated. We shall first consider a single plane and then apply these principles to a three-dimensional grid.

Horizontal grid considerations

A grid of tessellating hexagons was decided upon as the best way of dividing up space in a single plane. An equal relationship with all neighbours can only be achieved within a single plane using hexagons. Each hexagon has six equal neighbours, each abutting a side of equal length. This minimises the limitations imposed upon the geometry of the modelled system by the spatial framework. Hexagonal grids have been used two-dimensionally as the basis of cellular automaton models (e.g. Gardner, 1971; Comins, 1982) and in the seed dispersal model of Weiner and Conte (1981) for this reason.

Other systems were considered. Most regular polygons do not tessellate. Only triangles, squares and hexagons tessellate. For the triangular and the square grids a proportion of the neighbouring polygons make contact through a vertex rather than a side (Fig.3.1.). The area of contact at a vertex is infinitely small, and yet the space within the neighbour is approximately as close to the original polygon as that of the other neighbours. This relationship is unequal. If one considers transport through the surfaces of a polygon where the transport can be made proportional to the length of surface contact between neighbours, those neighbours at vertices will receive an infinitely small proportion. This throws up complex questions when dealing with spatial relations between neighbours in a model based on such a grid and is best avoided.

The simplicity of a square grid is desirable for geometric calculations, and yet is inadequate for the above problems of neighbour relationships. An offset brick-like grid was considered to give all neighbours a surface of contact. However, despite the added complexity of this system, it still makes it difficult for even spread in all directions to be characterised.

The hexagonal grid is the most theoretically satisfying choice for a 2-dimensional grid, but this approach cannot unfortunately be extended to three-dimensions.

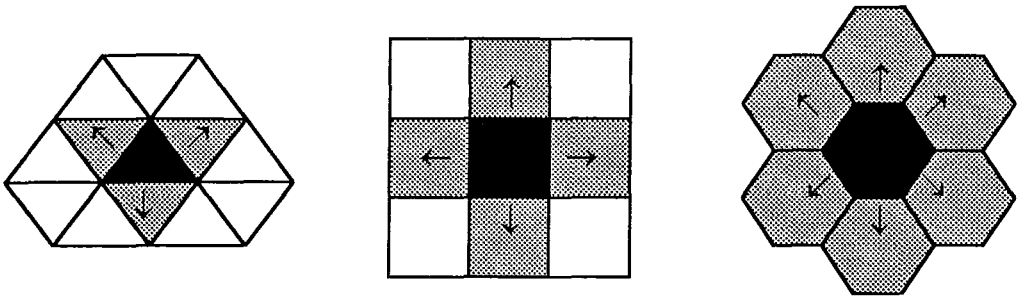

A **B** **C**

Figure 3.1. Transport between tessellating polygons. In the triangular grid (**A**), only the grey triangles have surface contact with the black central triangle. The clusters of white triangles at the vertices have an infinitely small point of contact only, and as such transport from the black triangle must be assumed to be minimal. The square grid (**B**) has four neighbours with surface contact and four with point contact, but in the hexagonal grid (**C**) all neighbours have an equal area of surface contact to one another. This minimises the effects of the grid on transport through the system.

The third dimension

The vertical component would ideally be represented in a non-limiting manner similar to a 2-D hexagonal grid. Only one three dimensional shape allows for each solid to relate equally to all its neighbours, and that is a dodecahedron (with twelve pentagonal sides). The complexity of this structure presents problems for direct geometric representation in the model. A compromise is therefore necessary. It was decided therefore that the use of hexagonal "tiles" (Fig 3.2.a) stacked directly on top of one another would reduce neighbour effects sufficiently if care was taken to allow for transport problems between layers. Assuming that transport may only occur through the faces of the tiles, no diagonal transport is allowed (Fig 3.2.b).

The model grid

Hexagonal tiles are defined in the model as having a depth equal to the length of one side. Each tile is referenced by a set of x,y and z co-ordinates. The extent of each of the three dimensions of the grid is limited by fixing the number of tiles in each direction, nx, ny and nz. The geometric nature of tessellating hexagons means that in the horizontal plane, each column is offset by 0.866 hex sides with respect to the next. The x dimension is defined as that perpendicular to the columns, such that the y referenced hexagons do not lie on a straight line.

In order to perform geometrical calculations using the hexagonal tiles, the tile grid is superimposed over a Cartesian co-ordinate grid *X, Y, Z*, with the unit of measurement defined as one hexagon side (Fig. 3.3). All *X, Y* measurements are taken from a point (0,0) situated at

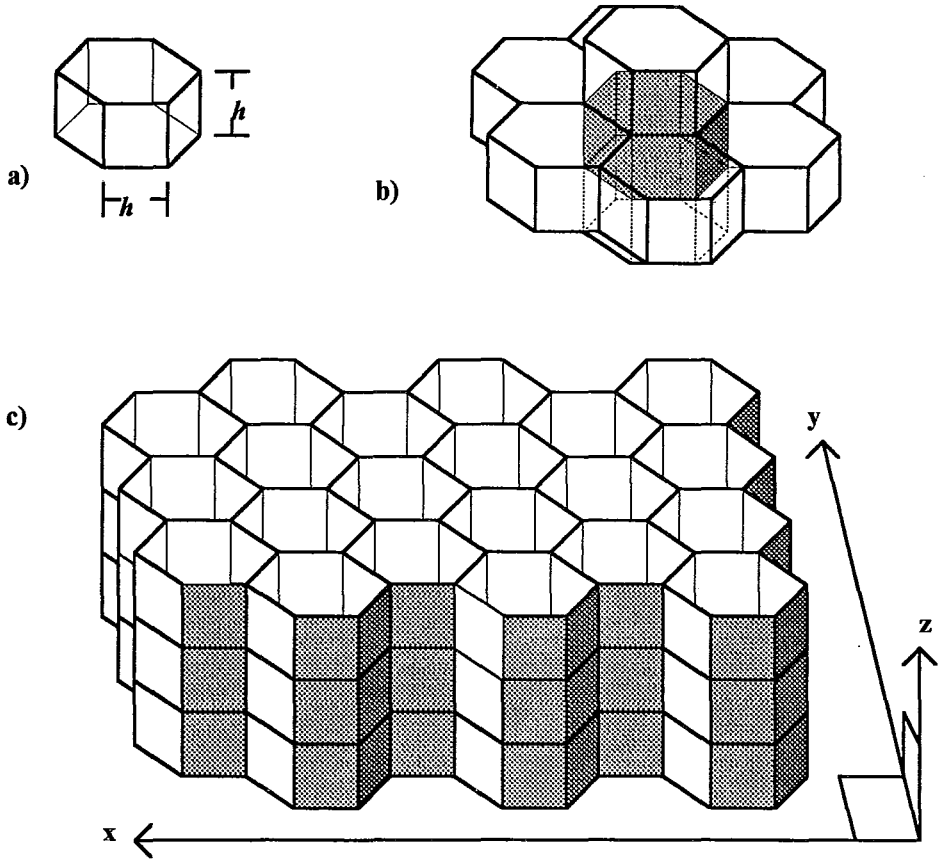

Figure 3.2. The hexagonal tile grid. a) single tile with all sides of length *h* cm.; b) a single tile (filled grey) with its eight immediate neighbours shown, six in a horizontal ring, one above and one (dotted) below; c) a block of the tessellating grid with the horizontal *x, y* and vertical *z* dimensions marked. The rows of tiles in the *y* dimension can be seen to lie along straight lines whilst the rows in the *x* dimension zigzag.

the intersection of the outermost edges of the even numbered hexagons, where the bottom of a tile in layer *z* lies at a Cartesian *Z* co-ordinate of value *z*, and the top of the tile at $Z=(z+1)$. A single tile is thus defined by an *x, y, z* co-ordinate, but the co-ordinates of its centre and vertices are more precisely defined on the *X, Y, Z* grid (see description of *hexcord()* at end of chapter for definitions).

System variables in the model may either be local to a tile or independent of the spatial grid. For example the amount of solar radiation, which will vary in space, varies between tiles, whilst species properties and individual age are independent of spatial location. For those variables local to a tile there is no further spatial definition: the value is an attribute

of the whole tile. In order to model the system with no spatial definition below the level of a tile, all properties of each tile are assumed to be uniformly distributed throughout the tile. As will later be seen, tiles can hold a number of individuals and sources of material, but this is all assumed homogenously distributed within the tile.

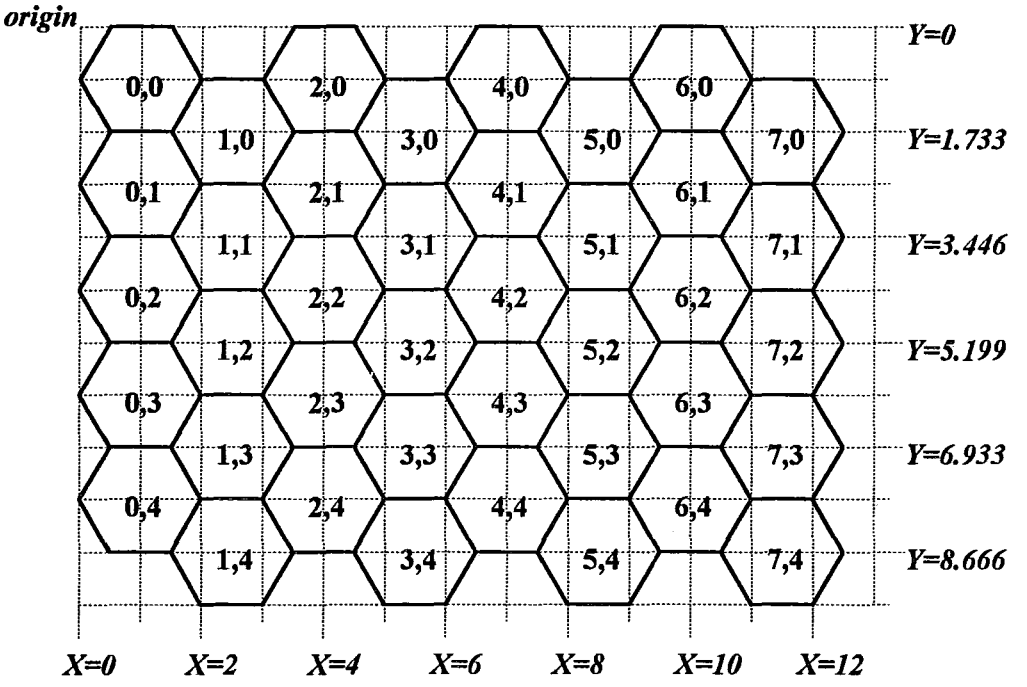

Figure 3.3 The *X/Y* sub grid in relation to the hexagonal grid. Tile co-ordinates (*x,y*) are shown within each tile. As can be seen, tiles with identical *y* co-ordinates fall into two offset classes, those with an even value of *x* and those with an odd value. Both their actual position and the relative numbering of their immediate neighbours vary accordingly. The *X/Y* sub grid is shown as dotted lines, with scale of *h*, i.e. one hexagon side. This allows precise location of each vertex of a tile. In the vertical dimension, *z* and *Z* overlap since each layer of hexes is *h* thick.

This abstraction allows mathematical treatments which would not otherwise be possible. The use of tiles to store information on the three-dimensional state of the system enables calculations to be performed using the physical and biological state at a given moment. For example, the calculation of the transmission of light beams needs to assume homogeneity within the tile in order to allow derivation from shaft length within the tile as described later. Provided that the tile size is sufficiently small relative to the vegetation processes being modelled, it is reasonable to assume that this simplification will not introduce significant errors. However, if the tile size becomes too large relative to plant size, the model becomes cumbersome and increasingly less accurate.

Another important limitation is that the greater the level of detail in the model, the more difficult it becomes to ignore areas where our knowledge is limited, and the more limited our knowledge of spatial relationships at the scale of the model becomes.

The "Ecospace" model is designed to be flexible and applicable to any terrestrial vegetation system. It is therefore important that the scale of the hexagonal tiles and the dimensions of the grid can be varied such that ecosystems from forest down to lichen growth on rocks may be represented. Since there is no spatial resolution within tiles, the tiles should ideally be small enough to prevent important spatial processes acting at a scale below that of the tile. At some point a compromise must be made between detail and area covered because of limitations of computer memory and run time.

The resolution of the model as developed is designed such that a dominant individual will be represented by a number of vertical layers and tiles rather than lie within a single tile. Sub-dominants and smaller plants may lie within a single tile, but it is hoped that the effects of the structure of plants at this scale on the abiotic environment will be limited.

The model framework was developed whilst working on the heath ecosystem. A hexagon side length of 50mm. was decided upon as a reasonable scale for this system, giving around ten above ground layers for a large heather plant, and allowing the microclimate underneath the canopy to be described. This scale also seems appropriate for the description of tile sized gaps for germination and establishment. The volume of a tile works out as 325ml. Grid sizes of up to $100 \times 100 \times 20$ were used for model runs.

Because the model is based on a grid of tiles with known abiotic properties, the growth of an individual plant can be calculated from the sum of the production of each of its component tiles. It is hoped that this will lead to a more accurate representation of individual growth than would be achieved in a model assuming uniform conditions across the whole plant. This is not an entirely new approach. Trees are often modelled as a number of layers or concentric solids with properties allocated to each level, but these properties are rarely modelled explicitly or fully spatially. An exception is the MAESTRO model of Wang & Jarvis (1990), where production for an array of identical trees is calculated for radially distributed points at each level, for each of which radiation balance is calculated by direct ray tracing. However, in the "Ecospace" model, the points of calculation are distributed evenly throughout the plant volume, thus avoiding modelling bias due to the selection of model sample points.

3.3 Plants within the framework

The framework is used to define the spatial relationships between the various elements of the ecosystem. The three dimensional structure of the ground and litter surface is described, and individual plants grown relative to this, with roots below and shoots above. At the end of each time step the altered state of the various solid components of the system are converted from whichever data structures are being used for calculations within the separate sub-models into the volumetric occupancy of hexagons. The absolute physical state of the system is thus represented by the grid. This can then be used to determine the spatial distribution of the abiotic components of the system, which can in turn be used to generate the potential spatial biotic responses, which can then be used to generate a new grid.

Plants are spatially modelled as individuals growing according to defined three-dimensional growth forms. The maximum number of individuals allowed in the grid at the same time is limited by computer memory according to the grid dimensions. The size of the grid and number of individuals were tested against each other to obtain the optimum use of memory space in terms of area covered and maximum size and number of individuals. It is important that the number of individuals allowed in the grid should be sufficient to cover virtually every possible situation. Should the maximum number of individuals be reached in a run it is essential that some adjustments be made to prevent computer memory limitations affecting model behaviour.

3.4 Individual plant representation

In this section the rules for representation of individual plants within the grid are outlined. Having decided to model plants spatially as individuals there arises the need to develop a three-dimensional model which can adequately represent the behaviour of real plants. There exists a wide range of plant growth forms, from the prostrate mosses, through bushes, to single stemmed trees (see Raunkiaer, 1937). It is important that the 3-dimensional form of a plant be adequately represented.

Plants are modelled as individuals, defined as a plant coming from a single point of origin at the top of the ground surface (*Xcent[indiv][z], Ycent[indiv][z]*), lying within a tile *xcord[indiv][z], ycord[indiv][z]*. When an individual is initialised, the X and Y co-ordinates are generated randomly within the tile of origin, x,y using the function *xyconvertB()*.

It was decided that to limit the occupancy of single tiles to a single individual was not suitable. This has no real world parallel unless the size of the tiles is very small relative to the size of the plants, and would impose unnatural limitations on the three-dimensional behaviour of the plants.

Each tile can therefore contain any number of individuals.

If one were to use a presence/absence method to record the plants present in a tile, such as in cellular automata, one would lose valuable information for calculations of growth and physical conditions in the grid as a whole. A measure of the amount of each individual within each tile must be recorded to maintain the accuracy of such calculations. In the "Ecospace" model the distribution of matter is represented by units of volume (hereafter referred to as units *dens[][]*) defined such that a single tile (325ml.) contains 10000 units. This was extended from a percentage density approach (where tile divided into 100 units) in order to capture the small weekly increases in volume. The number of units *dens[][]* in a tile is held as a constant *DCON*. The use of a volumetric measurement is similar to an areal measurement in a two-dimensional model, and enables the spatial structure of the system to be represented directly, making it easier to avoid overfilling a tile. A mass-based approach would require run-time conversion to volume in order to calculate spatial relationships.

Each individual may occupy space within a tile up to the point where the tile is full of vegetation (*dens[indiv][tile]*=10000=*DCON*) whatever individual its origin.

This means that although two individuals may occupy the same tile they can be assumed not to occupy the same space. However, different species will have different architecture and different tolerances to physical conditions, such that they will not continue to grow in an area beyond a certain plant density. Ideally directional growth responses would be precise enough to prevent an individual growing in an area that is unfavourable. In the absence of modelled responses of such precision a simple limiting factor has been applied. Therefore, individuals may continue to grow within a tile up to a species specific vegetation density (total for all individuals) *densmax[sp]*.

This approach was then taken further with the introduction of an optimum density (*densopt[sp]*) which represents the density to which the plant will grow in the absence of competition. Plants continue to fill tiles up until *densopt[sp]* is reached and then only apply further growth in such a tile (up to *densmax[sp]*) if it cannot reasonably be applied elsewhere. Plant occupation per tile is thus constrained by three factors, the total volume of the tile, the

optimum density to which a species will aspire, and the maximum density that a species can attain. The model here deviates from the general modelling philosophy, with the variables *densopt[]* and *densmax[]* imposing behaviour on the system which would ideally be emergent properties. Real plants reach a point where they will not allocate further material to a particular volume. This may be for two reasons:

a). unsuitable abiotic conditions (e.g. insufficient light, excessive exposure),

b). limitations of the plant branching structure.

Although the model may reasonably be expected to be able limit spatial growth according to the first reason, in the absence of a direct representation of the branching structure, the variables *densopt[]* and *densmax[]* are used as an abstraction of this structure. In addition they provide a safeguard against unrealistic behaviour which might be necessary to cope with extreme behaviour once a reasonable representation of the branching structure is installed.

An individual plant is thus composed of a number of tiles, each of which contains a certain amount of plant material (separated into short {*sshoot_dens[indiv][tile]*} and long shoot {*dens[indiv][tile]-sshoot_dens[indiv][tile]-woodens[indiv][tile]*} leaf material and wood {*woodens[indiv][tile]*}). The proportion of each tile occupied as a percentage of the total volume of the tile is stored in the array *dens[indiv][tile]*. The size of the array for a given individual is determined by the number of tiles occupied by that individual, *nntile[indiv]*.

A plant species may take one of three basic forms (Fig. 3.4):

i) Central stem limited plants (gform[sp]=0)

These plants are defined as growing about a central stem with a *trunk_length[indiv]*, bearing *rtrunk_angle[indiv]* and angle of elevation *vtrunk_angle[indiv]*. Radial spread about this trunk is allowed within each *z* layer, defined as *rsq[indiv][z]* (radius squared). The plants can thus develop as stacked discs within the grid. This enables representation of plants with central trunks and approximately radial branching structures and potentially of moving trunk structures. More importantly, this form is closely related to the abstractions of form common in light interception and simple competition models (e.g. ellipses, cones and cylinders on central trunks) facilitating an interface between different modelling approaches.

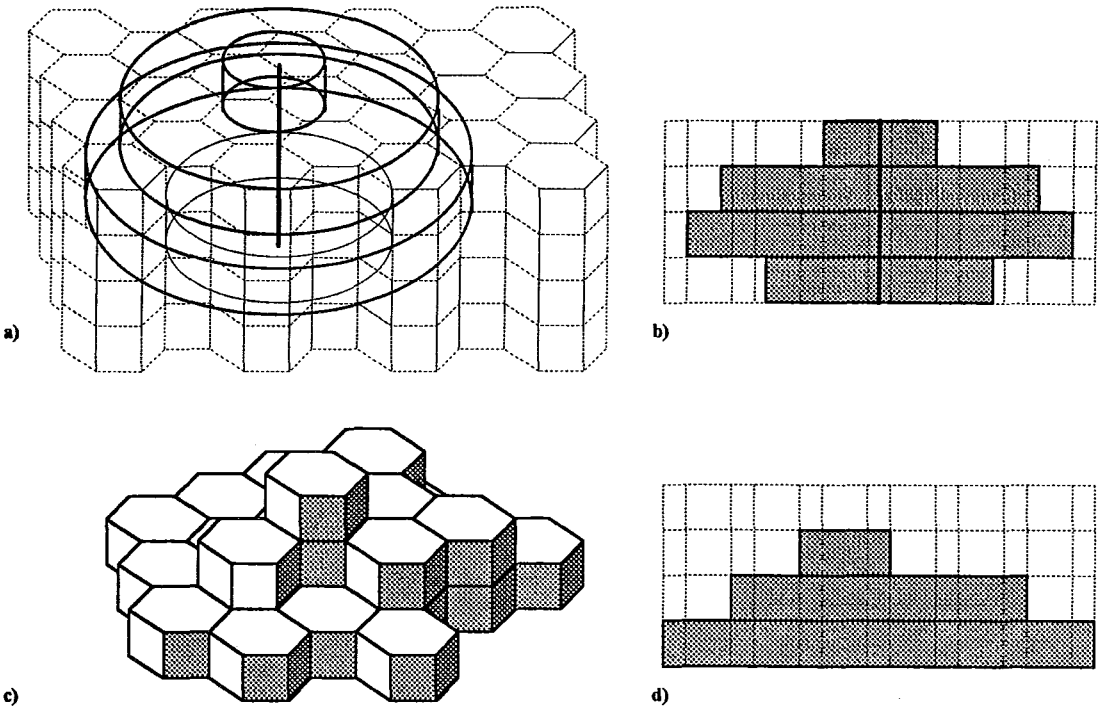

Figure 3.4 Plant growth forms in the hexagonal grid. **a/b).** Central stem limited growth (*gform* 0), with a disc of material lying within each layer. **c/d).** Tile limited growth (gforms 1&2); all material assumed distributed evenly throughout whole tile. N.B. This does not imply that only a single individual can occupy a single tile.

ii) Prostrate/ rambling plants (gform[sp]=1) and Phototrophic plants (gform[sp]=2)

These plants have no structure other than that of the hexagonal tiles, although a vertical limitation may be imposed through *zmax[ageclass][sp]* in order to prevent species from growing too high. This growth form is suitable for the representation of mats of moss or grasses, where the whole mat grows independently of a central stem, or perhaps for the modelling of simplified shrub structures, where the mass of branches might be expected to allow spread in any direction.

The difference between these two growth forms lies in the allocation of resources to new growth, where the phototrophic form allocates new growth where light is most abundant in order to simulate the process of positive phototrophic growth responses. This allows plants to optimise their interception of light and would be expected to result in improved photosynthetic rate compared with the other growth forms.

Rooting

Roots are represented at present using a single growth form for all species. The "Ecospace" model has been initially developed without accurate dynamic three-dimensional representation of below-ground resources, thus limiting the possibilities for a root model. The spatial distribution of roots is a dynamic and trophic process (e.g. Hutchings & De Kroon, 1994), which is as yet still poorly understood due to the difficulties of studying below-ground processes dynamically. Root responses to nutrient and water distributions are plastic (Duncan & Ohlrogge, 1958; Fitter, 1994). Since roots tend to lack a predictable segmented metameric form (Steeves & Sussex, 1989), an approach based on a predisposition towards a certain form is less desirable than a spatially responsive approach. The lack of any spatially-distributed abiotic reference due to current limitations of the model presents difficulties for a responsive form.

However, a certain amount of plant growth is allocated to the plant roots and it was felt that a simple spatial representation would allow the development of links between the above-ground and below-ground components of the system and individual. A hemispherical form was developed because it is easily linked to the dome functions (section 5.9) and, since it is based on discs within each layer, can very easily be converted to an inverted cone or an exponential decrease with depth. The hemispherical root structure is in the form of an inverted dome spreading out from the point at which the individual enters the ground. The radius of the dome is a function of the root volume.

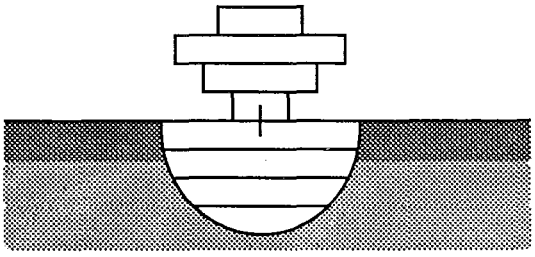

Figure 3.5 Hemispherical root form.
This simple form extends from the point of insertion of the individual in the ground. For growth form 0 as illustrated, this is the base of the trunk; for the tile based growth forms this is the original tile.

As for the above ground forms, this is not intended as a comprehensive representation of all possible forms, but rather a working module to further development of the grid system. A more flexible approach similar to the stacked discs of *gform[0]*, or perhaps a trophic, tile-based approach similar to *gform[2]* would be a more suitable course of development.

3.5 Calculation of the overlap of discs over the hexagonal grid

The central stem-limited growth form represents plants as discs within a single layer. In order to link the growth form to the hexagonal tile grid, it is necessary to calculate the extent to which a given disc fills each tile. This requires the two-dimensional calculation of the intersections of a circle with each tile, from which the area subtended can be calculated. The disc thickness (*discthick[indiv][z]*), can then be used to convert the area into a volume. For every growth increment a new disc overlap must be calculated.

The calculation process is controlled by the function *overhex()* which is called from *potentialindivgrow()* from within an *indiv* loop and a *z* loop. *Overhex()* fills the global array *potvol_overlap[x][y][z]*, which is implicitly specific to *indiv*. The function loops over the grid in layer z and for each tile (*x,y,z*) and calculates the area of overlap of the disc. In order to do this it calls a number of other functions:

1. Hexcord()

This function calculates the co-ordinates of each of the vertices of the given hexagon (*x,y*) on the *X, Y* sub-grid, and stores them in the arrays *Xcord[vertex]* and *Ycord[vertex]*. Vertices are numbered from 1 to 6 (Fig.3.6.a) clockwise from the vertex closest to 0,0 and defined as;

Position.	Xcord[vertex]	Ycord[vertex]
Centre 0	1.5*x + 1	1.7321*y + 0.866
Vertex 1	1.5*x + 0.5	1.7321*y
2	1.5*(x +1)	1.7321*y
3	1.5*x+ 2	1.7321*y + 0.866
4	1.5*(x+1)	1.7321*(y+1)
5	1.5*x + 0.5	1.7321*(y+1)
6	1.5*x	1.7321*y + 0.866

2.*Cpoint_test()*

This function uses Pythagorean relationships on the *X/Y* grid to determine which of the vertices lie within a circle of radius $\sqrt{rsq[indiv][z]}$ with centre *Xcent[indiv][z]*, *Ycent[indiv][z]* (Fig 3.6.b). The array *point[vertex]* is used to record these results in binary

form, where a value of 0 indicates that the vertex lies outside the disc and a value of 1 indicates that it lies within the disc.

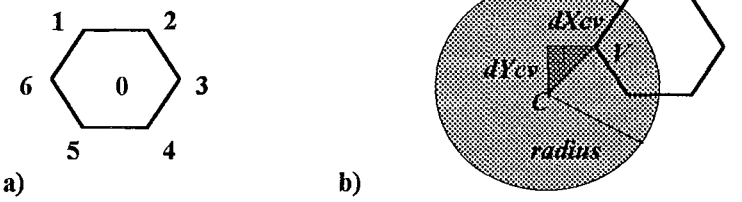

Figure 3.6 a) Numbering of vertices for calculation. b) In order to determine which vertices lie within a circle, simple Pythagorean calculations are used such that a vertex *V* is considered to lie within a circle with centre *C* if $dXcv^2 + dYcv^2 < \text{radius}^2$. The diagram shows the calculation for vertex 6, which lies within the circle.

3. *Cside_test()*

This function uses the array *nextvert[vertex]* which holds the nearest vertex in a clockwise direction from a given *vertex,* and the array *point[vertex]* to calculate which whole sides are within the disc. These are recorded in the array *sidestart[scount]* where *scount* is the number of sides totally enclosed, again counting clockwise around the hexagon. The counter *intcount* (6= no intersect, 7 or 8 for the intersects) is used in place of *scount* where the intersect of the circle with the hex occurs along the length of the side and only one vertex lies within the circle.

At this point, in *overhex()*, the arrays are checked. If *intcount* is still 6, no sides are crossed by the circle and the area of overlap is either 0 or 100. The function *circhexarea()* is called immediately to calculate the area, since the shape involved is simple and no chord calculations are necessary. If *intcount* has been increased, then the circle crosses through the hex tile and the co-ordinates of the intersects with the hex sides must be calculated in the function *cintersect()*.

4.*Cintersect()*

This function sorts through the sides of the hex and for each side crossed, works out which end vertex lies within the circle, (*v*) and which lies without (*w*) from the *sidestart[]* array. Using co-ordinate geometry, (see Fig.3.7) the points of intersection are calculated and held in the arrays *Xcord[]*, and *Ycord[]*, referenced by the integer *chord* (e.g. *Xcord[chord]*).

These arrays now hold all the co-ordinate information required for the calculation of the area of overlap.

It should be noted that this function has been adapted (using the control variable *dcheck*) for use in the calculation of dome overlaps as well as discs, where the same calculation is required.

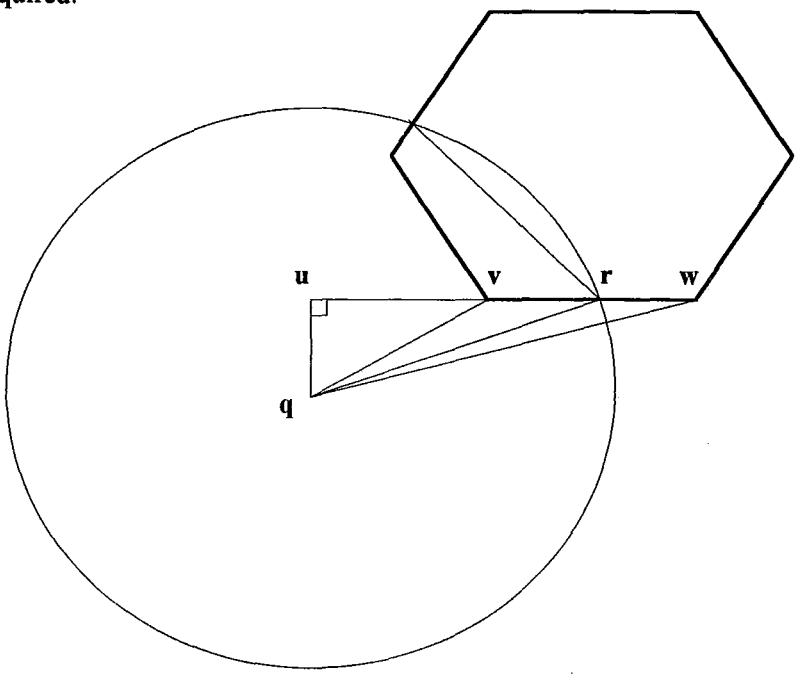

Figure 3.7 Example calculation. Here vertices 5 and 6 lie within disc. Thus *point[1-4]*=0 and *point[5-6]*=1. One side is totally enclosed so *scount*=0 and *sidestart[0]*=5, *sidestart[7]*=6 and *sidestart[8]*=4. Calculation of intersect as performed in *cintersect()* is illustrated for one side only, between vertices 4 and 5. Vertex 5, lying within the disc is labelled *v*, whilst vertex 4 is labelled *w*. (The point labels q, u, and r are not used in the model but are here used for clarity.) Using Pythagorean theory the sides $\underline{qv}$ and $\underline{qw}$ can be calculated. The radius, $\underline{qr}$ is known. From the cosine rule, the angle rwq can be calculated for the triangle q*vw*. The angle rq*w* and thus the side $\underline{rw}$ can be calculated in the triangle rq*w*. Since $\underline{vw}$=1, $\underline{vr}$ can be calculated as 1-$\underline{rw}$. The co-ordinates of the point of intersect can then be calculated from the co-ordinates of the vertices *v* and *w*.

5.*Circhexarea()*

This function uses the co-ordinate arrays to calculate the area of overlap, with which it fills the array *potvol_overlap[x][y][z]*, thus fulfilling the purpose of *overhex()*. Where the value of *scount* is 0 or 7 the areas 0 and 100 are returned respectively. Since *scount* cannot by definition be 2 (since any circle which includes a vertex must define an area with a minimum of 3 sides), *scount* must lie between 3 and 6.

The area of the polygon defined by the hex sides and the chord between the intersects is calculated by dividing the area into a number of triangles (Fig. 3.8) whose area is calculated in the function *tcalc()*. The area of the segment subtended by the chord (*chordarea*) is calculated in *csegment()*, using the formula

$$\text{Area of segment} = \tfrac{1}{2} * R^2 * (\emptyset - \sin\emptyset). \qquad \text{(Feldman 1935)}$$

implemented as

chordarea = rsq[indiv][z](angle-sinang)/2*

where R ($\sqrt{}$*rsq[indiv][z]*) is the radius of the circle, and Ø (*angle*) is the angle at the centre of the segment (*SQU* in Fig3.9) which is calculated from the known lengths SQ, QU and the calculated chord length SU (see Fig.3.9). The total area of triangles and segment is then summed and recorded in *potvol_overlap[x][y][z]* in units of *h*/100 such that 100% cover gives a result of 260.

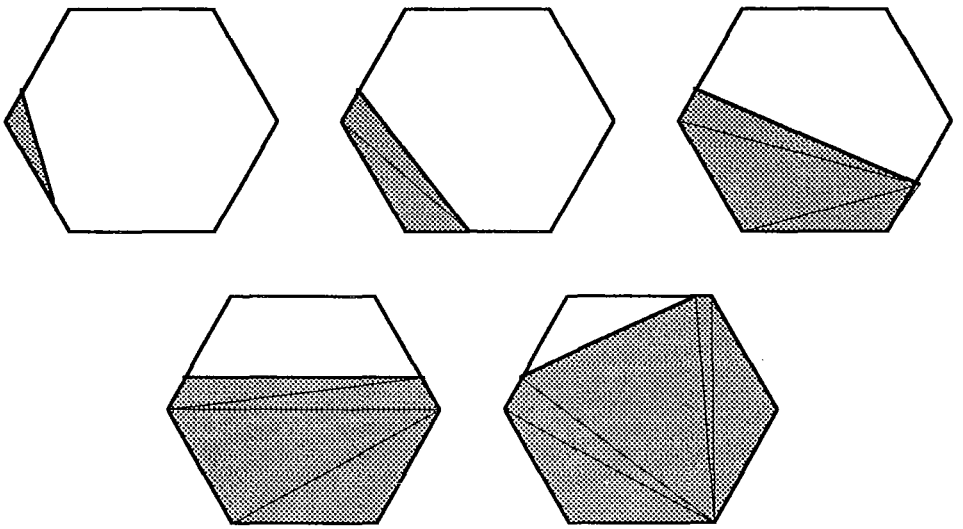

Figure 3.8. Division of area subtended by chord into triangles for area calculation.

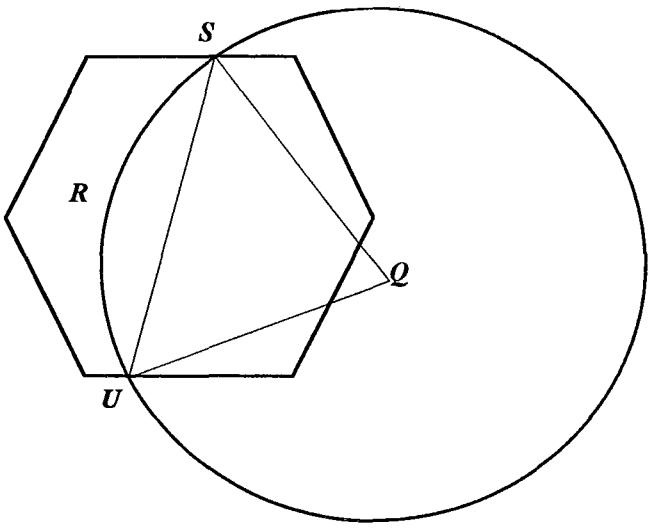

Figure 3.9. Diagram showing segment *RSU* subtended by the chord $\underline{SU}$.

3.6 The surface of the ground

The aim of the model is to describe the three-dimensional structure of the whole community. This must necessarily include the ground surface. Raised areas and small pits in the soil surface provide distinct microsites, altering the competitive relations of plants. The surface of the ground has been modelled in three dimensions using the spatial grid.

It is a complex problem to model steeply sloping terrain since difficulties arise at the edges where assumptions have to be made about the structure outside the model area to enable microclimate calculations to be carried out. This imposes limits on the extent of the variation in ground surface height that is possible without resulting in inadequate model representation. Because of these limits, the ground surface represented within the grid is at present assumed to be embedded in a larger area which is essentially level but which has surface variation similar to that represented within the grid (section 3.7). The effects of continuous slopes outside the grid area cannot therefore be represented.

The position of the soil surface within the grid is defined using the array *ztop_soil[x][y]*, (Fig.3.10) which holds the first unoccupied *z* level above the soil surface at point *x,y*. Since litter builds up on the soil surface, a similar array *ztop_lit[x][y]* is used to describe the litter surface. In the model at present, the soil surface is set constant at the start of a run, but litter is allowed to build up and decompose such that *ztop_lit[x][y]* is not static. A degree of heterogeneity in the soil surface is permitted such that the restraint that it should be approximately level is not violated, although there can be no clear point at which a surface ceases to be level.

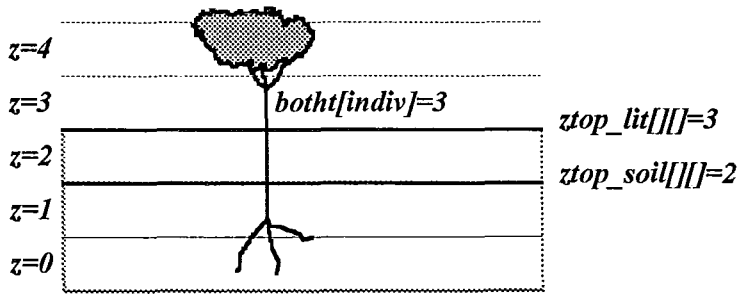

Figure 3.10 Definition of ground surface. An example showing a section of the grid with strictly level surface for clarity. Note that the base height of an individual at point of contact *x,y* is equal to *ztop_lit[x][y]* where litter present.

3.7 The volume surrounding the spatial grid

In order to reduce the effects of the edges of the spatial grid on its behaviour, the grid is assumed to be embedded in a horizontally homogenous volume with the average properties of the grid. This volume is defined within the function *embdens_update()* as a one dimensional stack *embeddens[ez]* holding the mean of *absdens[][][]* for each layer *ez* where *ez* is the vertical distance from the ground surface *ztop_lit[x][y]* rather than the base of the grid. By defining *embeddens[]* in terms of height above ground, the effects of uneven ground surface are reduced.

This approach was used rather than a torus (e.g. van Tongeren & Prentice 1986) because a torus (where the edges are rolled around to meet each other) has no parallel in the real system and may result in sharp changes at the border if the simulation becomes too heterogeneous. By taking an average value for each layer, sharp changes at the edge will be minimised although there will be a relatively constant edge effect for non-level ground. The embedded approach is recommended in the review of solutions for edge effects by Haefner, Poole, Dunn and Deeler (1991).

The homogenous embedding volume is used to calculate the attenuation of light rays passing through the sides of the grid and to generate a wind profile by assuming it to be representative of the wind field.

4

Field Observations on the Growth Form of *Calluna vulgaris*

Contents

4.1 Introduction

The "Ecospace" model was developed in the context of the heathland ecosystem. Despite years of study, our knowledge of both the mechanisms of vegetation dynamics in general and the specific processes within heathlands are incomplete. In particular, our understanding of the mechanisms controlling spatial resource allocation in plants is limited. As the dominant, *Calluna* defines the microclimate of heathlands. In order for the model to in be in any way representative of the microclimate it must therefore adequately represent *Calluna*. A programme of study was developed in parallel with the model to attempt to describe the growth of the plants in terms easily incorporated into the model and to assist in the development of appropriate modelling decisions. Due to time constraints on the project, it has not been possible to pursue these studies beyond initial observations, and the results tend towards qualitative generalisations.

The heathland ecosystem has been extensively studied and yet the growth form of *Calluna vulgaris* is far from fully understood. Standard horticultural texts describe the classic hemispherical form of individual heather plants, although it should be noted that this often achieved by pruning and is the case only for isolated plants. Gimingham (1972 Chapter 6) provides a detailed description of the development of the growing plant with some qualitative mention of the range of variables influencing plant form; neighbours, topography, light levels and exposure. The effects of these variables on whole plant structure may be described in terms of their effects on individual branches, but this is difficult to quantify. In a natural system heather plants may be expected to have a form deviating from the hemispherical

individual. A number of simple descriptive studies were carried out at field sites across the Pentland Hills south of Edinburgh.

4.2 Direct destructive measurement

Methods

In order to measure a stand of heather in terms of the hexagonal grid used in the model the heather was measured directly in tile form. A simple template was developed to be inserted into a stand without disturbing the structure so that each hexagonal tile's worth of vegetation could be cut away. This took the form of a series of thin metal rods, each of which passed through the vertex of a hexagonal tile. These rods were graduated in units of one hex side (50mm.) and inserted into the stand and on into the soil until all rods were stable and all graduations were aligned. Spacing was achieved by inserting each rod through a hole in a light plastic board fixed above the canopy by a stout metal frame. The board was designed to allow the insertion of enough rods to define a rectangular array of five by two contiguous hexagons in the horizontal plane.

Destructive sampling was begun on an area to be extended as appropriate in order to include several complete heather plants per sample. Once the template was in place the portion of each separately rooting plant in each tile was removed using secateurs and clipping along the line between rods and placed into a marked sample bag to be returned to the laboratory for separation into components (individual, short shoots, long shoots, dead leaves and woody stems) for measurement of volume (by Archimedes Principle) and dry weight.

Problems in the measurement arose once the sampling had proceeded below the topmost layers of tiles. It was found that due to the multi-directional growth of heather, it was often impossible to sample from a single tile without removing supportive tissue for a series of other tiles. A significant amount of material thus fell to the ground with each cut. The effect of this could be minimised if plants were clipped from the outside in, but this was prevented in most cases by the presence of other separately rooting plants in the tile being sampled. Almost inevitably the structure of those other individuals was disrupted by sampling from within their structure. Added to this was the effect of leaving sample areas overnight. The action of wind and rain tended to distort the shape of the damaged plants, even when the rods were left in place to give added support.

It was decided that the results obtained were not representative of the structure of the heather since the measurement itself disrupted the structure, and that the method of measurement was impractical. After the aborted measurement of two sample sites each comprising at least five separate main stems, this approach was abandoned. However, in the course of measurements, a number of important observations were made.

Observations

1. Each hexagonal tile was found to contain vegetative matter from between zero and four separately rooting plants in the small number of tiles sampled. These individuals grew through each other to form a continuous mass not easily distinguished from a single individual. Although a proportion of the separately rooting plants might come from a common germination, some were of essentially separate origin when rooting was examined. This indicates that at the scale of tile used in the model competition is not spatially exclusive.

2. Single plants were often found to grow in a convoluted form, approaching a given tile through a number of tile faces, sometimes on opposite sides of the tile. This means that it is inappropriate to limit model growth such that a plant cannot fill all space within itself, even if the route to a vacant space is complex.

3. Within the canopy, there was a considerable amount of dead brown leaf material, no longer photosynthetically active, but still attached to the plant. Although fragile to the touch, much of this brown material appeared to have been inactive for more than a season, although further study would be needed to confirm this. These observations are consistent with the distribution of dead plant material in the one dimensional destructive measurements of McKerron (Gimingham 1972). The implication for modelling is that care should be taken when dealing with old shoots and litter.

4. The volume and dry weights of leaf and woody material were determined for 150 tiles for which no clear sampling error occurred. The maximum volumetric occupation of the tiles studied was found to be 23% (converting to *densmax[Calluna]*=2300) near the top of the canopy. The mean estimated conversion factors for mass to volume (*masshoot* and *masswood*) were as follows;

1g leaf occupies 21.4 ml air-free volume (*masshoot*=0.0065895)
1g wood occupies 11.59 ml air-free volume (*masswood*=0.00356879)

Due to the difficulties in measuring litter volume and the variable composition of litter it was decided simply to use the conversion factor for leaf material as an estimate. This will underestimate the volume for leaf litter which is likely to be less dense, but will overestimate wood litter.

5. The "Ecospace" model requires a scale for each tile side, allowing the general framework to be applied to a number of ecosystems. Ideally this tile size should be selected to operate at a sub-individual level for full grown plants, but also to capture the varaition in germination microsites at a suitable scale for juvenile plants. Observations of the dimensions of plants in the field led to the selection of a 0.05 m hexagon side for the initial modelling study. This was selected as an apparently appropriate value, but it is likely that the size of the tile will have a significant effect on the behaviour of the model, particularly regarding establishment, where the extent of representation of heterogeniety is critical. The selected tile size should not therefore be taken as a definitive value. This problem of appropriate scale is critical to all spatial models. It is hoped that the model will provide a framework for the investigation of the effects of varying tile size.

4.3 The hemispherical dome form

A dome-based form was identified through field observation as being a possible super-clonal-individual structure since it can dominate more than one clone. Some measurements were made to attempt to detect properties of domes rather than clones.

An attempt to relate the relative performance of six segments of each separately rooting stem to the conditions incident upon that segment (e.g. open sky, nearest neighbours) was made. It was hoped that this would allow the development of simple empirical rules to apportion growth radially about each stem. However, whilst taking measurements it became clear that the direction of growth and the shape of the leafy head were very closely linked to the structure of the whole community and that the resultant stem angle and orientation of the leafy head overrode radial growth features.

The tussocky nature of most heather communities is immediately evident (Fig. 4.1), although this form may be hard to detect in some communities. At the edges of blocks of Calluna, the heather will tend to meet the ground in a smooth curve, and when viewed from above, a curved perimeter composed of a number of bulges is evident. These observations

could be attributed to the presence of a number of hemispherical clones. Observations of branching structures within the canopy would appear to support this theory, with each peak corresponding to the centre of a radial network of branches similar to that of an isolated individual plant. Closer examination of these hemispherical structures, however, reveals them to be composed in many cases of more than a single clone. Up to nine separate clonal root systems were observed within a single dome.
The internal branching structures tend towards radial extension towards the dome surface rather than from the centre of each clone.

The surface of the dome tends to be fairly smooth, with all plants growing to form a single continuous surface. This behaviour is consistent with the observations of Metcalfe (1950) where plants growing in troughs in the ground grew taller than usual and plants growing on raised areas were shorter.

The outer surface of the *Calluna* community may be considered as a single photosynthetic surface similar to a tree canopy. Phototropic responses will lead to stems growing towards and filling any gaps in the canopy, acting to maintain a continuous surface. However, emergent stems will be subject to exposed conditions, an effect which is magnified by the laminar flow around the aerodynamically smooth domes.

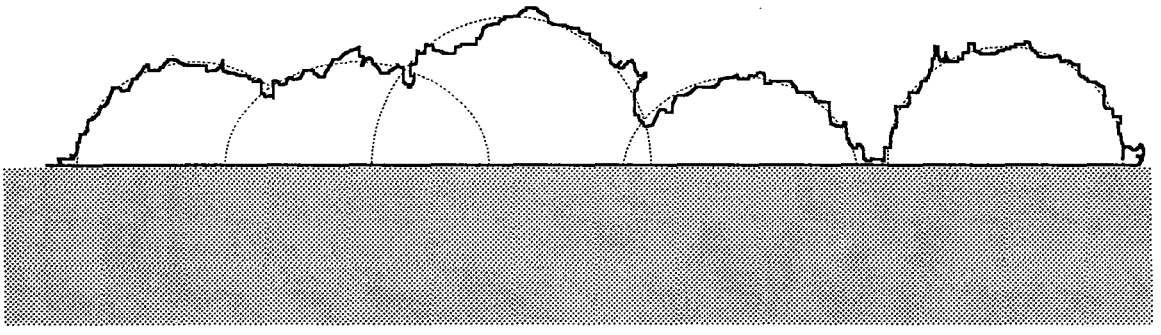

Figure 4.1: Apparent dome structures in the canopy of *Calluna vulgaris*.

The development of distinct individual hemispheres is complicated by the presence of other individuals which are growing in the same volume. However, as shown in Figure 4.2, if the development of stems is controlled by directional growth responses alone, the clonal origin of the component stems in a dome is of little significance. Consider stems ***A*** and ***B***. Conditions affecting the directional development of these stems will be the same in both situations. It follows that directional growth within a dome may be independent of the number of clonal individuals in the dome.

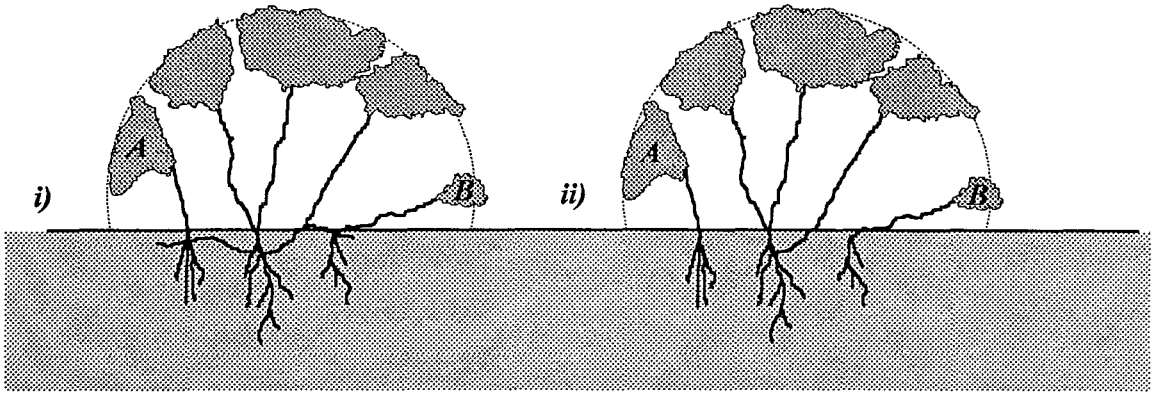

Figure 4.2. Two similar domes. i). Single clone, with connected root sytem, and ii). Dome composed of three separate clones.

The decision was made to model this process using a hierarchical system, modelling both at the level of the separate stem, and of the hemispherical dome, such that the origin of the stem has no effect on morphology. In order to facilitate the modelling process, an attempt was made to correlate stem angles from the ground surface to the first node with position within the dome, but the measurement of the geometry of fifty domes failed to produce any statistically significant results. This was partly due to the problem of definition of a dome in the natural canopy, and partly due to the complexity of stem form. In addition, individual stems may have a variety of origins, (seed, adventitious rooting, and vegetative propagation) occurring over a number of years at different stages in the development of a dome, such that orientation to the dome will occur at different stages of plant development. Superimposed over the dome structure is the phenomenon of stems tending to grow over one another in a downhill direction, which was present even though the field site was relatively level.

The potential for the generation of useful results from further study appeared to be poor, since extremely detailed measurement of stems and origins in relation to the somewhat abstract concepts of domes and layering direction would be required to separate out the causes of variation. This had implications for the modelling approach, since the functions for initialising stem angles and moving whole stems through the grid were dependent on a quantitative theory for stem orientation and position over time. The whole-plant morphology of shrubs is a suitable area for future research (see review Wilson, 1995), since an understanding of the mechanisms used by plants to capture three-dimensional space is critical to the process of vegetation dynamics. The results of the above studies, both in terms of calibrated variables and more general observations, were useful in the development of the modelled individual plant growth form presented in Chapter 6.

5

Microclimate Sub-model

Contents

5.1 Introduction

Microclimate is generated by the interaction of plants, soil and weather, and is spatially variable within a patch of vegetation. In the "Ecospace" model, weather is generated according to a simple random weather generator either daily or hourly according to the weather variable, and these inputs are combined with the current state of the system in terms of microclimate and structure to give the new microclimate. Radiation and wind are used to generate local temperature assuming that all of the plants in the model are able to transpire freely. The generated abiotic values are spatially distributed throughout the grid and can be used for the generation of plant growth.

The movement of water in the system is not fully represented since this was considered beyond the present scope of this prototype model. Since plant structure, radiation, temperature and wind have now been modelled, a water sub-model could be added relatively easily. This is an area for future development of the model.

Plant material is represented in the model in such a way as to allow direct estimations of the microclimate within the system. Once the total volume of solid material, including all plant material or soil, in each hex tile (*absdens[x][y][z]*) has been calculated (in function *absdens_update()*), the microclimate can be derived from the weather above the canopy. As stated in Chapter 3, the spatial resolution of the model is one hex tile and it is assumed that all material is distributed evenly throughout the tile occupied. Plants of all species and sizes are

thus represented similarly within the grid, and competition can be calculated according to the capture of volumes with explicit abiotic properties.

Solar radiation and temperature are calculated for each tile on an hourly basis (see Fig.2.4), whilst wind and precipitation (including snow cover) are calculated daily. Values from the weather generator and the physical structure are used to calculate radiation and wind, which in turn are used to calculate temperature.

5.2 Weather generation

The weather generator provides values for input into the spatial grid which represent weather variables immediately outside the grid. The "Ecospace" model is designed so that it requires the minimum of input data. This is of particular importance when dealing with weather generation, since if full site specific weather records are required, it is not easy to change the potential weather conditions for climate impact analysis. It was decided that a model which could generate daily weather conditions for input into the model from monthly means and variances would be of great use. A simple stochastic sub-model was developed, with some correlation between consecutive days. The sub-model uses statistical distributions to generate weather, allowing simple alterations in weather by the alteration of the monthly means. Alternatively, the probability of extreme events may be increased by increasing the variance.

A similar sub-model (WEATHER_CLASS) was developed simultaneously by Strandman, Väisänen, and Kellomäki (1993) at the University of Joensuu in response to the need for a sub-model for predictive forest modelling in the context of climate change. Both sub-models derive their stochastically generated values from published weather data, with simple correlation between variables, although the "Ecospace" model is based on normal distributions rather than Markov processes. Autocorrelation between consecutive days' weather is dealt with continuously in the WEATHER_CLASS sub-model allowing monthly autocorrelation coefficients to be determined. The periodical approach in the "Ecospace" model is less flexible but potentially more realistic. Combination of the best features of both sub-models would be a suitable course of action although both function adequately in their present state. WEATHER_CLASS also contains functions for the representation of long-term changes in weather variables.

The weather generator gives daily values for air temperature, precipitation, wind speed and mean wind direction. It was initially assumed that weather variables were not

correlated. However, since the surface radiation balance is strongly influenced by cloud cover, correlation between temperature and cloud cover has been introduced. The lack of correlation between the different weather variables makes the sub-model mechanistically unsatisfying, but the range and variable extent of links between the different elements of the weather, their past history and geographical position was considered beyond the scope of the model. However, it was felt that the use of monthly means should capture a proportion of the correlation between variables (particularly solar radiation and temperature) caused by seasonal cycles. The approaches of Linacre (1992) for weather estimation are based on site latitude, elevation and empirical relationships whilst ignoring other weather variables. If correctly parameterised, the weather generator returns reasonable weather data over a monthly period.

The stochastic basis of the weather generator is the function *normal_distribution()* which is given input values for mean and standard deviation and returns a randomly generated value from within a normal distribution. Monthly means and standard deviations for each weather variable are read in as a data file for each site.

The weather generator is in the function *weather_master()*, and returns daily wind speed, and direction, precipitation (including snow cover) and maximum and minimum temperatures. The temperature values are used to generate diurnal curves in the function *tempvar()* and radiation is varied diurnally according to an hourly cloud distribution. Although both precipitation and wind can be expected to vary diurnally these are assumed constant throughout the day. Precipitation is modelled very simply because at present it has no effect on the rest of the model and is in place largely to provide an input into a potential water sub-model. Microscale wind calculations are time consuming even when modelled daily, and so variation of the input wind (*windspeed*) may not reasonably be calculated hourly, as for light calculations. An hourly variation about the generated daily mean local wind value (*wind[x][y][z]*) as applied in *lvar()*, *nvar()* and *tvar()* was considered inappropriate because of the likely variation in wind direction which would require recalculation of the spatial wind environment. Wind is thus assumed constant throughout the day.

Weather patterns tend to occur in periods dependent on the airflow direction or isobaric pattern (e.g. Lamb, 1950). Simulation would ideally take into account the general weather characteristics associated with particular airmass types, but this would present problems when attempting to generate weather within statistical distributions. It was decided instead to use an index of periodicity (*period*) to describe the mean length of periods of similar weather. A random integer (*val*) where $0 \leq val \leq period$ is generated daily to determine whether the weather will continue as it is ($val>0$), or move to a period of fresh conditions

(*val*=0). When a new period of weather begins, weather values are generated directly from normal distributions by input of corresponding monthly means and standard deviations. If in a period of continuing similar weather, the new generated values for each weather variable are averaged with the corresponding values for the previous day's weather (stored in *ystrday*). This is a simplification of the actual nature of weather, but should result in values lying within the correct distributions. The effects of this simple mechanism can be seen in Figure 5.2, where periods of similar temperature of varying lengths are visible. In the model of Strandman *et al.* (1993) specific monthly autocorrelation coefficients derived from the meteorological data are used in the daily generation of each weather component. This approach allows more flexibility than the straight average used in *weather_master()* and could be incorporated. However, the estimation of autocorrelation coefficients directly from meteorological data will underestimate the correlation between consecutive days in periods of similar weather, and overestimate the correlation between different periods. Care should thus be taken in the combining of the two methods.

Temperature

It was decided to base the temperature sub-models on maximum and minimum temperatures, because standard meteorological records (e.g. Meteorological Office, 1972) present temperature data in this form. This also facilitates the calculation of diurnal temperature curves. The meteorological records are presented as monthly values for "average daily" maxima and minima, defined as the average of all daily maximum and minimum temperatures for the month respectively; "average monthly" maxima and minima, defined as the average of monthly maximum and minimum temperatures respectively; and "absolute" maxima and minima, defined as the maximum and minimum temperatures recorded for the entire period of measurement. Statistical analysis of tabulated values for several sites over a thirty year period indicated that if the deviation of the average monthly maximum from the average daily maximum temperature were taken to represent two standard deviations from the mean, the absolute values were almost certain to fall within four standard deviations, which is reasonable for the large sample size (eleven thousand days). It was decided therefore to calculate the standard deviations for maximum and minimum temperatures on this basis, taking the average daily maxima and minima as the mean.

For realistic simulation of temperature data, however, it is not sufficient to generate maximum and minimum temperatures independently of each other and of previous temperatures, since the resulting chaotic diurnal curves bear little resemblance to reality. It

was decided to base daily temperature calculations on a randomly generated normally distributed maximum. Correlation between the day's maxima and minima is achieved by generating two minimum values, one dependent on, and one independent of the maximum, and averaging them. The first value is generated by subtracting the difference between the monthly means for maximum and minimum temperatures from the generated maximum, which would give a constant daily temperature range. The second value is generated directly from the monthly mean and standard deviations. Due to the semi-random nature of this method it is possible that the generated minimum temperature could exceed the maximum, in which case they are simply substituted for one another.

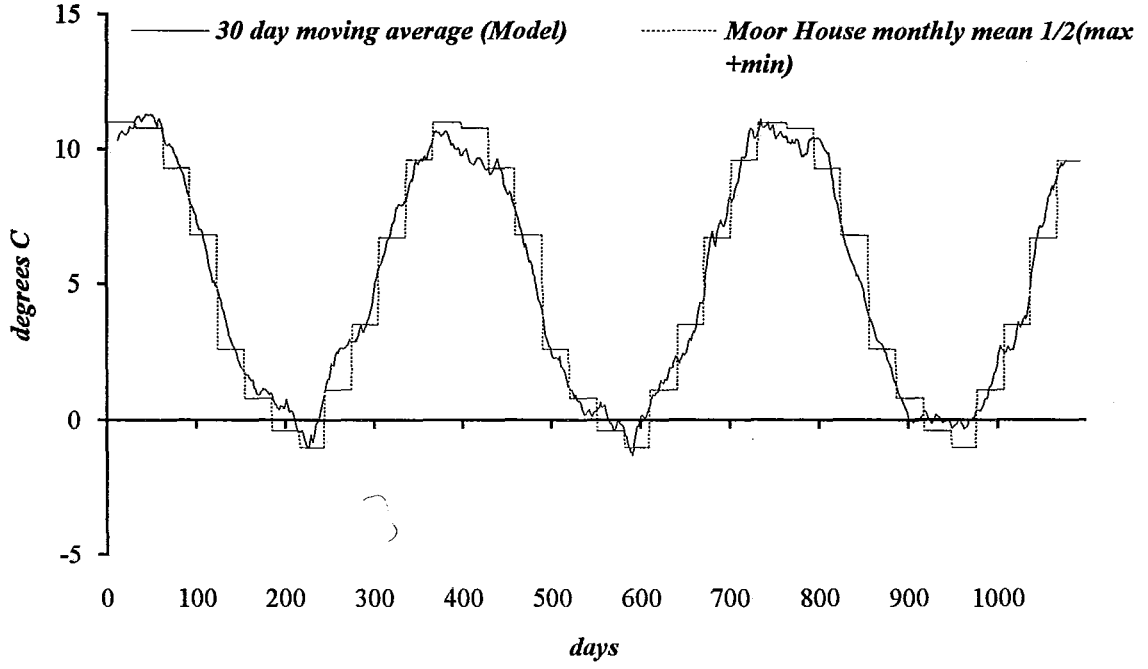

Figure 5.1. Annual cycles of temperature as generated by the model.

The daily temperature cycle above the canopy is calculated using a standard sinusoidal progression during the day and exponential decrease during the night (Parton & Logan, 1981; Goudriaan & van Laar, 1994) in the function *tempvar()*. This differs slightly from the sinusoidal increase followed by linear decrease to the minimum used the simulations of Grace (1970) but more closely conforms to average diurnal curves. The function is called hourly from *temp_regime()* which then uses the above canopy temperature in the microscale temperature calculations. The day's maximum temperature is reached two hours after solar noon to allow for the lag between solar radiation and temperature.

Figure 5.2 shows the temperature regime for a number of days. Periodic correlation between consecutive days leads to periods of fairly constant weather (days 12-18)and gradual changes (days 2-7). Breaks between periods of similar weather may lead to sharp changes (days 10-11). Where the temperature at the end of the day is less than the coming night temperature a rapid increase followed by a constant night temperature results (days 2,7,10). This was considered to be reasonable behaviour (e.g. passage of warm front) and unlikely to have much effect on model behaviour.

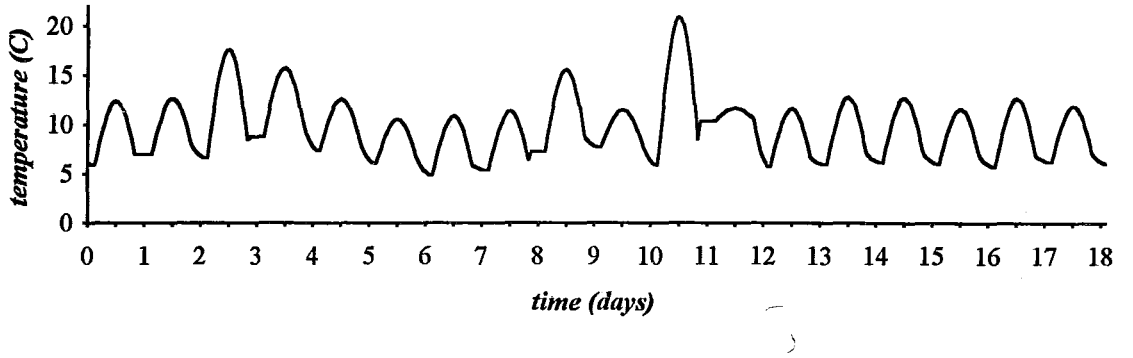

Figure 5.2 Diurnal variation in July screen temperature as generated by the function tempvar().

Precipitation

For both precipitation and wind velocity a problem arises because naturally occurring frequency distributions are truncated, taking an approximately normal shape, the lower end being cut off sharply at zero. Because a normal distribution is used to generate values, a method to deal with negative values needed to be developed. In the case of rainfall, weather data may contain the number of rain free days per month as well as the average rainfall. The calculation thus takes place in two stages. Firstly the daily percentage probability for the month (*ppt_prob[month]*) is used to determine whether the day is likely to be rainy or not. If the *period* of weather does not change, it is assumed that the rain conditions will remain constant. Secondly, the actual daily amount of rain is generated randomly, if the day is likely to be rainy. This distribution is set up with a variance to return a low number of rainfall values below zero. When a value falls below zero it is set to zero. This will result in the mean of the generated distribution being skewed away from zero, and a correction of the mean is necessary in order that the real and simulated distributions remain similar. This is not an ideal solution since it does not allow the direct use of actual weather statistics, and an alternative should be sought.

Snow cover can significantly alter the growth of plants, both through reduction of growth due to low light and temperature and through selective exposure to desiccation (browning of heather, Watson, Miller & Green, 1966), particularly in upland environments where snow cover may be present for more than half the days on average in some winter months. It was considered to be important to represent this aspect of precipitation. However, a complex mechanistic approach was rejected due to time constraints and the difficulties of achieving the correct number of days snow cover with such a sensitive subject. A purely stochastic approach was used, generating a presence/absence value for each day according to the monthly mean number of days snow cover (function *snow_master()*). Importantly, in its present state, there is no correlation between precipitation and snow cover. For every day of snow, a random variation in depth is applied such that the depth of snow in z levels above the ground surface (*snowht*) is given by

$$snowht = 4.0 + val$$

where *val* is a random number between one and ten. This depth of snow is assumed to be constant across the vegetation surface, and no drifting is modelled, although this could have a significant effect. Snow prevents the penetration of radiation and allows exposed plant parts to be desiccated by the wind (assuming frozen ground-water) in the function *browning()*.

Wind

Wind velocity distributions are skewed significantly towards zero and as a result the proportion of generated points falling below zero will move the generated mean away from zero. This bias must be compensated for in order to ensure that the generated distribution matches the desired distribution. Because the proportion of the distribution truncated at zero is dependent on both the distance of the mean from zero and the standard deviation and the desired distribution is rarely symmetrical in shape, a simple numerical solution is not available. Currently the distributions are aligned by ignoring all values falling below zero and compensating by adjusting the input mean in proportion to the amount truncated, such that the two annual means are identical. A reduction of 0.35* *windmean[month]* is used for the Moor House data set. No compensation for this effect is modelled by Strandmann *et al.* (1993). The resultant distribution is compared with the distributions for 3 sites across Europe taken from Troen and Petersen (1989) in Figure 5.3.

The function *wind_direction()* is called, to return a bearing for the wind. This is achieved by a simple method whereby the wind direction is assumed to be normally distributed about the prevailing wind. By altering the standard deviation, the relative probabilities of non-prevailing winds can be altered. Since all values generated will be radial angles with the form prevailing wind ± *ú*, where *ú* is the generated variation, it is possible that the value of *ú* will be greater than 180° such that the tails of the distribution overlap opposite the mean. This method

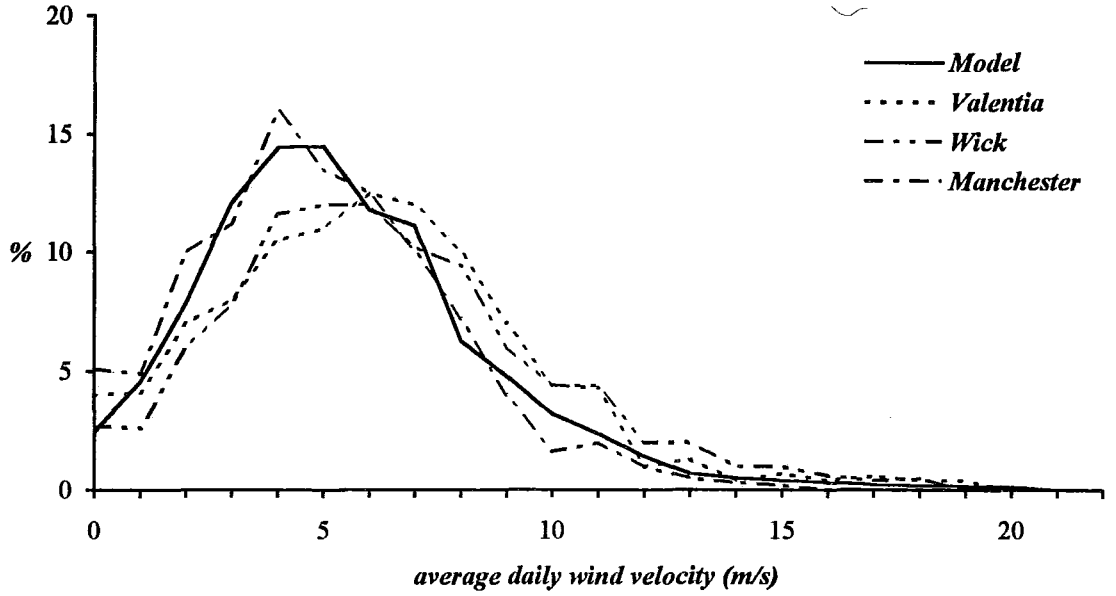

Figure 5.3. Output from the wind generator compared with a number of annual distributions in Europe (Troen & Petersen, 1989). The data is presented as a line graph of a frequency distribution rather than a bar graph to enable comparison.

allows some flexibility, but if compared to the complexity of a wind rose for most sites, (e.g. Shellard, 1976) the method fails to capture the complexity of wind direction. However, it was considered adequate for the initial version of the model, especially if exposure is calculated using the simple method (*turbulence_cat()*) rather than by directional ray tracing, so that wind direction is not used in the model. It would be possible to generate values from a wind-rose distribution, but these are not universally available.

Cloud

Within-grid solar radiation conditions for each hour of the day are calculated once a month rather than daily because of the complexity of the calculations used. The monthly values, which are the monthly mean of the mean daily radiation during hours of daylight are used as

inputs to drive diurnal variation in the function *lvar()*. Daily cloud conditions are generated in the function *lcloud()* called from within *weather_master()*. The monthly distribution of the number of hours of bright sunshine (defined by *sunmean[month]* and *sundev[month]*) is used to generate a stochastic normally distributed value, *sunhours*. An occasional dependency on temperature is imposed since in summer months a clear sky may be correlated with a warm day but the reverse may be true in winter (Strandmann *et al.*, 1993). A random number *dice* between zero and five is generated and used as a switch for dependency (i.e. *if(dice>3){...}*). The value against which dice is tested can be increased to reduce dependency. Where dependency is selected, between *month* 3 and *month* 8, a daily maximum value of temperature greater than *tmaxmean[month]* ensures a daily value of *sunhours* greater than *sunmean[month]*, and a daily maximum temperature less than *tmaxmean[month]* ensures a daily value of *sunhours* less than *sunmean[month]*. For the remaining months the correlation is reversed. The dependency is calculated by moving any generated values of sunhours lying on the wrong side of the mean to the other side of the mean, using in all cases, the correction equation

$$sunhours \mathrel{+}= 2 \times (sunmean[month] - sunhours)$$

The value of *sunhours* after these tests is then autocorrelated as before according to *period*. This value of daily hours of bright sunshine is used to generate hourly cloud cover using a random process, filling the hours of the day with cloud twenty minutes at a time until all cloud (*cloudhours=dayhours-sunhours*) has been allocated to the array *c_cover[hr]* used in *lvar()*. Further calculations of radiation are described below.

4.3 Solar radiation sub-model

Introduction

The passage of incoming solar radiation through the canopy can be more clearly defined than other microclimatic variables because light travels in straight lines. The solar radiation climate at a given point in the canopy with the sun at a given position is calculated directly from the vegetation structure using ray tracing techniques. Reflected radiation within the canopy is not calculated by ray tracing since this has little effect on photosynthesis, acting instead through temperature increase and may not reasonably be represented by straight lines due to diffraction. This saves on complex light dispersal calculations. All reflected radiation is instead assumed to travel vertically into the tile directly above the reflecting tile for temperature calculations (section 5.6). The nature of the grid allows direct geometric

calculations to be used in order to calculate transmission to a given point in space. The solar radiation outside the canopy is calculated first. Ray tracing through the grid and calculation of transmissivity allow the estimation of the light environment in terms of photosynthetically active radiation (PAR) and near infra-red radiation (NIR) which are calculated separately. The details of this process are given below. This process is time consuming (at least ten minutes for ten occupied cells in a 10×10×10 grid) and as a result is performed only monthly to determine the mean radiation (PAR and NIR) for each hour of daylight per tile. Diurnal variation about this is calculated daily from hourly cloud cover and the relative hourly proportions at the top of the canopy in the function *lvar()* to give hourly values for each tile.

Incoming solar radiation outside the canopy

A model of solar radiation outside the canopy was developed as a Microsoft Excel spreadsheet program since the calculations are performed only once to parameterise the site. Values for hourly incoming solar radiation may then either be calculated using the spreadsheet model as described below for a particular site or may be taken directly from solar radiation tables. They are then read into the model as a data file. The spreadsheet model returns hourly values for a given day for solar altitude (*altitude[hr]*), solar azimuth (*azimuth[hr]*), direct PAR (*par_dir[hr]*), diffuse PAR (*par_dif[hr]*), direct NIR (*nir_dir[hr]*), diffuse NIR (*nir_dif[hr]*) with angles in radians and irradiance in W m^{-2}. Inputs of site latitude, altitude and day number are required. The transmission of the atmosphere is assumed to be constant over time for simplicity.

Calculations of solar position with time are performed according to standard procedures (e.g. Brock, 1981; Linacre, 1992). Thus

$$D = 23.45 \times \sin[\, 360 \times (\, 284 + N\,) / 365\,] \qquad \text{(Cooper, 1969)}$$

where D is an approximation of the angle of declination and N, the day number. For the monthly light model the representative day number and declination were read in directly from the table in Duffie and Beckman (1980). Since these representative angles of declination differed from the approximation from the representative day due to the non-linear relationship between the two, the representative values were used for the monthly light calculations rather than those generated. The hour angle at sunset can then be calculated as

$$W_s = \arccos\{\, -\,[\, \tan(L) \times \tan(D)\,]\,\} \qquad \text{(Milankovitch 1930)}$$

where W_s is the sunset hour angle in radians and L the latitude (negative in southern hemisphere). From this, daylength can be calculated as

$$\text{Daylength} = 24 \times W_s / \pi$$

The hour angle (W) for the sun for any hour of the day (T, measured in hours after solar midnight) can be calculated as

$$W = 15 \times (T - 12)$$

from which the angle of the sun at each hour can be calculated.

$$\cos(sz) = \sin(D) \times \sin(L) + \cos(D) \times \cos(L) \times \cos(W)$$

$$sa = \pi \times sz / 2$$

$$\cos(az) = \sin(D) - [\sin(L) \times \sin(sa)] / [\cos(L) \times \cos(sa)] \text{ (Hay \& Davies, 1980)}$$

where sz is the solar zenith angle, sa the solar altitude and az the solar azimuth. Allowing for the eccentric orbit of the earth using the radius vector (R)

$$R = 1 / \{ 1 + [0.033 \times \cos(360 \times N / 365)] \}^{1/2} \qquad \text{(Nicholls \& Child, 1979)}$$

the amount of radiation incident at the top (I_{top}) of the atmosphere can be calculated from the solar constant ($I\Theta = 1353$ W m^{-2}) as

$$I_{top} = I\Theta / (R^2 \times \cos(sz))$$

When moving further towards the earth, it is possible to take into account sinks for solar energy in the atmosphere to varying degrees of detail. The model of Wiess and Norman (1985) was selected since it uses simple extinction coefficients to calculate atmospheric transmission for diffuse and direct radiation in both the photosynthetically active and the near infra-red wavebands. This allows treatment of photosynthesis separately from temperature conditions. Although Wiess and Norman (1985) propose a method for combining calculated radiation with measured monthly site totals to give site specific values, this approach was not used since cloud cover is taken into account separately, and hourly values are required. Site

atmospheric pressure (P) is assumed to be constant over the year and approximated from altitude (H km) and mean pressure at sea level (P_0 = 101.325 k Pa) as

$$P = P_0 \times \exp(-0.12 \times H) \qquad \text{Linacre (1992)}$$

Radiation may then be calculated after dividing I_{top} into PAR and NIR according to Moon (1940) where 45% of radiation is in the visible waveband.

Direct PAR $I_{DV} = I_{topV} \times \exp[- 0.185 \times (P/P_0) m] \times \cos(sz)$

Diffuse PAR $I_{dV} = 0.4 \times (I_{topV} - I_{DV}) \times \cos(sz)$

Direct NIR $I_{DN} = \{ I_{topN} \times \exp[- 0.06 (P / P_0) \times m] - w \} \times \cos(sz)$

Diffuse NIR $I_{dN} = 0.6 \times (I_{topN} - I_{DN} - w) \times \cos(sz)$

where $m = 1 / \cos(sz)$

and $w = I \times \Theta \times \text{antilog}_{10}[- 1.1950 + 0.4459 \log_{10} m - 0.0345 (\log_{10} m)^2]$

This gives hourly vectors and intensity for solar radiation in the four radiation classes which enables the light to be calculated within the grid. The effect of cloud is taken into account later in the light model. The data provided by the spreadsheet model are read in monthly as the data file *solardata* by the function *sun_month()*.

Radiation within the grid

Incoming shortwave radiation per tile is calculated using ray tracing techniques (see below). Longwave radiation reflectance within the canopy is presently treated simply as part of the temperature model, since it has no direct effect on photosynthesis. Because the hexagonal tiles may contain not only leaves, but wood and dead material from many individuals, it was decided to use the total volumetric occupation of the tile, *absdens[][][]* to calculate transmissivity. This was considered a more flexible approach than Leaf Area Indices, since these are an essentially two-dimensional measurement, linked to radiation interception on a horizontal surface. In addition there is no direct conversion between the two units, particularly

when dealing with shading by structures other than leaves such as above-ground dead material and stem.

In order to calculate transmissivity from *absdens[][][]*, and in keeping with the principle that there is no spatial definition below that of the tile, it is initially assumed that all material is distributed evenly throughout each tile. To visualise this, one may think of each tile being composed of a uniform soup. As such, a tile has no orientation to a given beam of radiation, only a path length through the tile (*shaft_length[][][]*). This assumption allows the use of Beer's Law extinction equations which assume homogeneity of the medium through which the beams passes. By reducing each beam into a number of shaft lengths, each in a homogenous tile, the passage of a beam of radiation through the canopy may be described. If one considers a tile cross section presented to the beam of light, filled with an opaque material the transmissivity will vary from zero at *absdens[][][]*=10000 (when all available space is occupied) to transparency at *absdens[][][]*=0. A direct conversion is therefore possible such that the extinction coefficient k_b (for one-sided black material) can be given as

$$k_{xyz,b} = absdens[x][y][z] \,/\, 10000$$

It is normal to double the value of k calculated for an assumed leaf angle distribution to represent the two sided nature of individual leaves (Monteith & Unsworth, 1990). All solids will effectively have two sides from which to absorb radiation and so the above equation is multiplied by two to account for this. Allowing for this and the absorption coefficient (α) of the material for a particular wavelength, k can be modified by the equation

$$k = 2 \times ab \times absdens[x][y][z] \,/\, DCON$$

where k is the transmission coefficient, *ab* is the root of α, and *absdens[x][y][z]* is the total volumetric occupation of tile *x*, *y*, *z* up to a maximum *DCON*. The above equation is equivalent to

$$k_{xyz} = 2 \times \alpha^{0.5} \times k_{xyz,b}$$ (Monteith & Unsworth, 1990)

A constant absorption coefficient of 0.8 is assumed for all material at all wavelengths, which avoids analysis of the material composition of each tile. The above equation yields values of k of 0.358 and 0.447 for volumetric vegetation densities near the maximum of 20% and 25% respectively. The values of k measured by Grace (1970) for reconstructed *Calluna* canopies, were found to range between 0.25 and 0.40. Since it is

unlikely that *Calluna* will develop to a density of 25% (see Appendix I), the above equation seems to generate reasonable results. Interestingly, the values of k from the study of reconstructed canopies were found to be largely independent of the incident angle of light and to conform to Beer's Law, (Grace 1970). These results are consistent with a conical leaf angle distribution where the conical angle is less than the angle of solar elevation. It is assumed for the heather model that there is such a leaf angle distribution. However, for other plant species a different leaf angle distribution may be required.

Transmission per tile can now be calculated according to the standard Monsi and Saeki equation (1953)

$$transmission = I \times e^{-(k.d)}$$

where d is the length of passage of the ray through the medium (i.e. *shaft_length[x][y][z]*) in metres.

If the leaf angle distribution deviates significantly from the above pattern it may become necessary to include the distribution of leaf orientation to each beam of light for reasonable calculations. Attention must here be paid to the description of the contribution of each ray to the total irradiance. It is common practice to firstly divide the sky into regions described by inclination angle. Goudriaan (1977) and later Van Kraalingen (1989) and Bartelink (1993) have used nine inclination categories each of which is ten degrees wide. The contribution from each slice of sky may then be calculated. However, the descriptions of Goudriaan are based on the projection on to a horizontal surface, which is poorly suited to any but a horizontal leaf area distribution. Bartelink corrects for this by dividing by a factor sin(inclination) which transforms the distribution back to "the illuminance of a plane normal to the ray direction" which for a uniform sky equals simply the relative areas of the sky in each class. This approach results from the methods of light measurement commonly used and enables simple comparisons between model and measurement but introduces a bias which must be used carefully especially when the results are described by terms such as uniform overcast sky (UOC) as in Goudriaan (1977) where the actual meaning is "UOC projected on to a horizontal surface". A model is presented below (function *soc()*) which avoids the inclusion of the surface intercepting the radiation when calculating the input from each ray, thus allowing calculations based on the leaf angle distribution relative to the ray angle at the stage of light attenuation (i.e. in functions *light_attenuation()* and *kcalc()* rather than in *soc()*).

Overcast skies may be simulated using two approaches, the uniform overcast sky (UOC) which assumes that the brightness of the sky is uniform, and the standard overcast sky (SOC) which assumes that the brightness of the sky increases towards the zenith. The empirical SOC was proposed by Moon and Spenser (1942) and verified by Grace (1970, 1971). However, the SOC is generally considered to be appropriate only for a range of temperate climates for which it was developed where brightness does increase towards the zenith. The SOC was considered to give a better representation of actual conditions than the UOC for the purposes of this model in the context of the temperate heather moorland. The equation for the SOC is given as

$$L_\theta = L_z \times (1 - \sin\theta) / 3$$

where L_θ is the brightness of the sky at inclination θ relative to the brightness at the zenith L_z. The approach of Goudriaan (1977 eq.2.14) to this distribution converts it to the incidence on a horizontal plane which is inappropriate for the "Ecospace" model for reasons described above. A simple alternative approach is used, multiplying the relative areas of each slice of sky given by Kimball (1921) with the relative brightness from the SOC to give the relative contribution to illuminance for each slice. When compared with the curves for incidence on a horizontal plane, this method gives greater weight to the lower sky fractions.

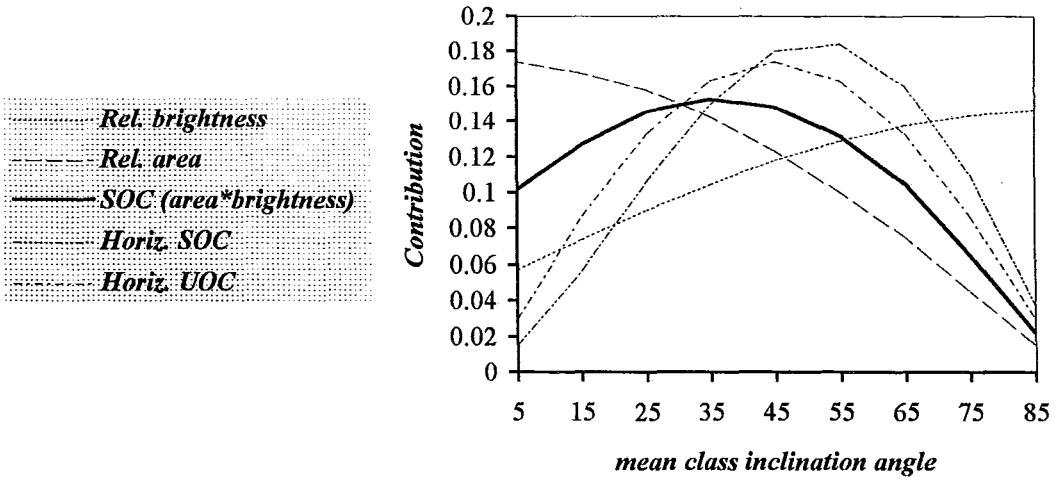

Figure 5.4. Contributions from ten degree inclination classes of an overcast sky. The graph shows the SOC for illuminance of a plane normal to the ray direction used in the model as a solid line, with the component relative brightnesses (Moon & Spenser 1942) and areas (Kimball 1921) overlaid. The curves for illuminance of a horizontal plane for both brightness distributions (Goudriann 1977) are given for comparison.

This method is based on an overcast sky and does not fully take into account the hourly variation in the distribution due to rings of increased brightness around the solar disc which are evident even in blue skies as described by Pokrowski (1929). Since all light which is not direct is treated as diffuse it would be appropriate to work towards the inclusion of this variation, although it would require modification of the data structure and calculation approach in the model.

The contributions for each inclination class are stored in the array *sky[*inclination class*]* and the fraction *sky[]/BSTEP* used to determine the contribution of each ray within an inclination class, where *BSTEP* is the number of classes of azimuth angle or bearing used in calculation.

Computation of monthly light environment

Once the solar radiation environment above the canopy has been calculated it is possible to proceed with calculations within the grid. The radiation environment for each tile is calculated by ray tracing for each hour of the representative day of each month and then converted to a single value (*lt[x][y][z]* and *nir[x][y][z]*) representing the mean of radiation for each hour of daylight. This can then be used to calculate diurnal curves for each point in the grid without the use of ray tracing.

These calculations are controlled by the function *light_regime()*, called monthly to generate the average radiation for an hour of daylight for each tile. Assuming the mean monthly cloud is distributed evenly over the day, diffuse radiation for each hour is calculated as

$$startlight = (par\_dif[hr] \times sunhours / dayhours) + (par\_dif[hr] \times 0.36 \times cloudhours / dayhours) + (par\_dir[hr] \times 0.36 \times cloudhours / dayhours)$$

$$nirlight = (nir\_dif[hr] \times sunhours / dayhours) + (nir\_dif[hr] \times 0.3 \times cloudhours / dayhours) + (nir\_dir[hr] \times 0.3 \times cloudhours / dayhours)$$

where startlight and nirlight are the totals of diffuse radiation for PAR and NIR respectively unaffected by cloud and the cloud dispersed elements of both direct and diffuse radiation, and where 0.36 and 0.3 are the transmissivities of cloud for PAR and NIR respectively (Wiess &

Norman, 1985). The ratio *sunhours/cloudhours* is generated in *lcloud()* as described above. These hourly values are used to generate mean hourly diffuse radiation, *startlight* and *nirlight* used as inputs for diffuse light calculations. The effects of cloud on direct radiation are calculated in the function *light_direct()* for each hour as

$$startlt_{PAR} = par\_dir[hour] \times sunhours/dayhours$$
$$startlt_{NIR} = par\_dir[hour] \times sunhours/dayhours$$

where *startlt* is the direct radiation equivalent of startlight and nirlight.

Light_regime() then scans the grid and calls the functions *light_direct()* and *light_diffuse()* to calculate direct and diffuse components of average hourly input to each tile. These functions are essentially similar, differing only in that direct calculations are performed for a single ray representative of the sun's position and intensity at that hour, whereas diffuse light calculations assume an even distribution of rays across the sky as described below. The co-ordinates of the tile and irradiance (for diffuse radiation) at the top of the canopy are fed in, and the amount of light not intercepted returned. The calculations take the following basic form:-

For each hour: Generate and algebraically characterise hourly ray or selection of rays across the whole sky.

For each ray: Calculate shaft length projected across horizontal surface for each stacked column.
Divide amongst tiles stacked in column.
Attenuate light according to density in tile.
Calculate contribution of the ray to total light and accumulate total.

i). Generation of rays across sky.

Light_diffuse(): Rays are generated at a regular angular spacing for both bearing in radians (0 to $2 \times \pi$) and inclination (0 to $0.5 \times \pi$). A step of $\pi/20$ is used for both inclination and bearing to give an array of 40 points across the sky. This value was selected to maximise detail whilst minimising run time.

Light_direct(): The hourly bearing *azimuth[hour]* and angle of elevation *altitude[hour]* are used to define ray direction. The function *light_path()* is called to convert each combination

of angles into a pair of rays defined by $y = m \times x + c$ style equations, one for the horizontal and one for the vertical plane.

ii). Calculation of shaft length per tile.

The function *light_shaft()* was used to perform the two-step calculation of shaft length. The calculation is first performed for a single horizontal layer and then extended to the third dimension. The grid is considered as a horizontal layer with the radiation ray defined by its bearing to the centre of the subject tile. The routines *stathexcord()* (generating co-ords of each hex), *slinegenerate()* (generating the equations for the sides of the hex), and *lintersects()* (a variation on *cintersect()*), were used to calculate the points of intersect of the ray of light with the hex sides where the equations for the two lines meet. The length of the horizontal trace of the shaft from the point of origin to each point of intersect on the tile can then be generated from the co-ordinates as shown in Figure 5.5 below, where the distance AB is named *hdisp* and the distance AC is named *hlength*. Provided *hlength-hdisp* is less than or equal to two hexagon sides (the maximum length of a horizontal trace of any line through a hexagon) the ray is assumed to pass through the stack.

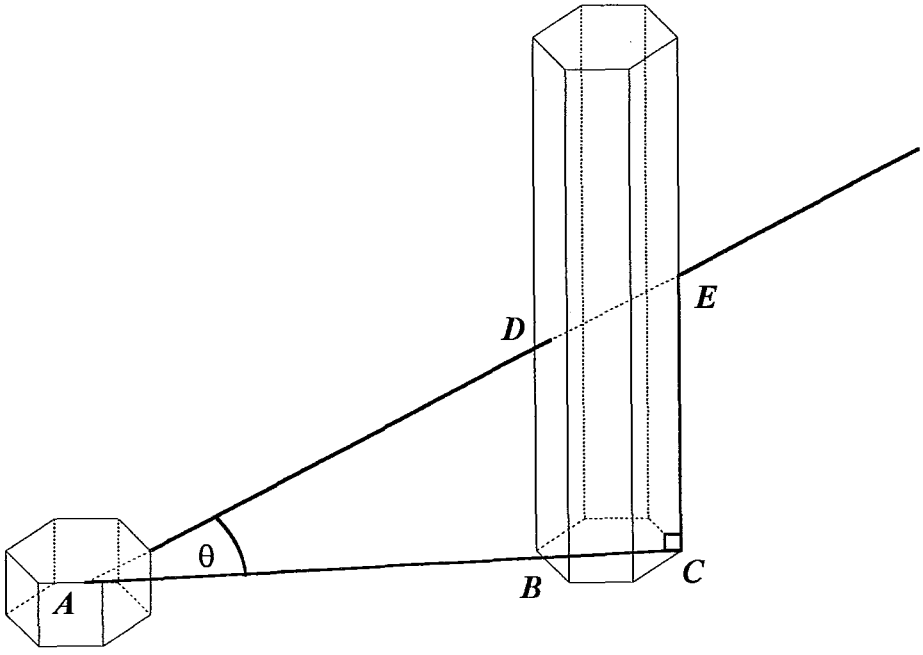

Figure 5.5. Calculation of light trace through a stack of tiles ***BCDE*** to centre of selected tile at ***A***.

Each stack is then analysed in the function *lvert_distribute()* to divide the horizontal trace of the ray between *z* layers according to their position using simple trigonometry based on the value *horiz* defined as the horizontal distance from *A* to the top face of that layer of tiles. Thus for the example ray below (Fig. 5.6) *horiz=*$\underline{AG}$ for the lower tile and *horiz=*$\underline{AC}$ for the upper tile. Using the ray inclination, the horizontal trace in each tile is converted to a diagonal trace (e.g. $\underline{BG}$ to $\underline{DF}$, $\underline{GC}$ to $\underline{FE}$). An exception was made for the case of the vertical light beam which fails to cross tile sides. The length of the shaft in each tile (*shaft_length[x][y][z]*) is thus calculated.

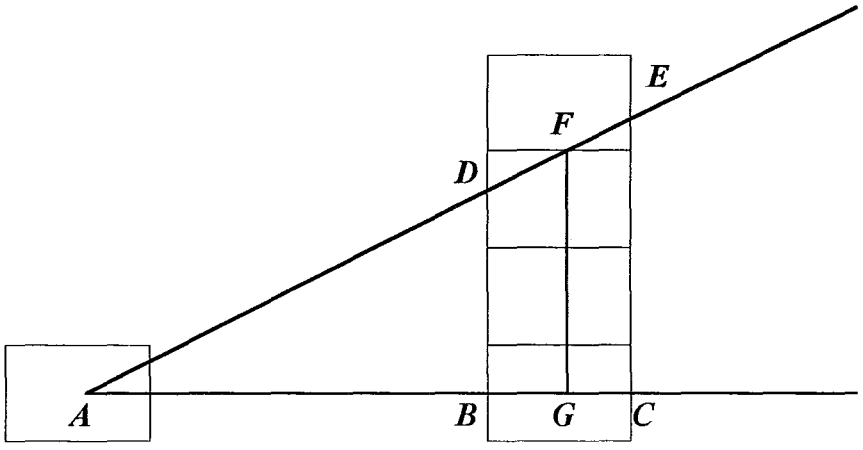

Figure 5.6 Calculation of shaft length per *z* layer.

iii). Attenuation and Contribution.

The amount of light attenuated by each tile is calculated from a combination of *shaft_length[x][y][z]* and *absdens[x][y][z]* (see "*Radiation within the grid*" above). Transmission is calculated using the Beer's Law extinction equation, by the functions *light_attenuation()* and *kcalc()*. An incoming irradiance for each ray is thus generated. The relative contribution of each angular slice of light was calculated assuming a standard overcast sky (Moon & Spenser 1942) such that the sum contribution of all the slices is one. The function *soc()* is called to return this contribution for each ray. For each slice the total transmitted light is accumulated using

$$irrad = irrad + (irr \times contr)$$

where *irrad* is the cumulative radiation, *irr* is the radiation transmitted though the slice and *contr* is the contribution of the slice. Once all slices have been treated, the radiation incident at that point has been calculated.

iv). Light rays outside the grid

The nature of the grid means that, for any tile, a proportion of the rays contributing to its illumination will pass out of the sides of the grid below the top height of the vegetation. In order to reduce edge effects due to this, the spatial grid is assumed to be embedded within a large area of horizontally uniform vegetation, such that ray tracing, and radiation attenuation may continue outside the grid (see end of Chapter 3). The function *lembed()* is called from *light_attenuation()* to quantify attenuation outside the spatial grid for each ray.

Figure 5.7 demonstrates the approach to calculation for a single ray (dotted line) and a single tile (light shading) at *x, y, z.* The heavy shading shows a transect of ground surface in the plane of the tile. As can be seen, the embedding volume is positioned relative to the tile such that the layer *ez*=0 lies on the surface at *ztop_lit[x][y]*. Attenuation outside the grid can be

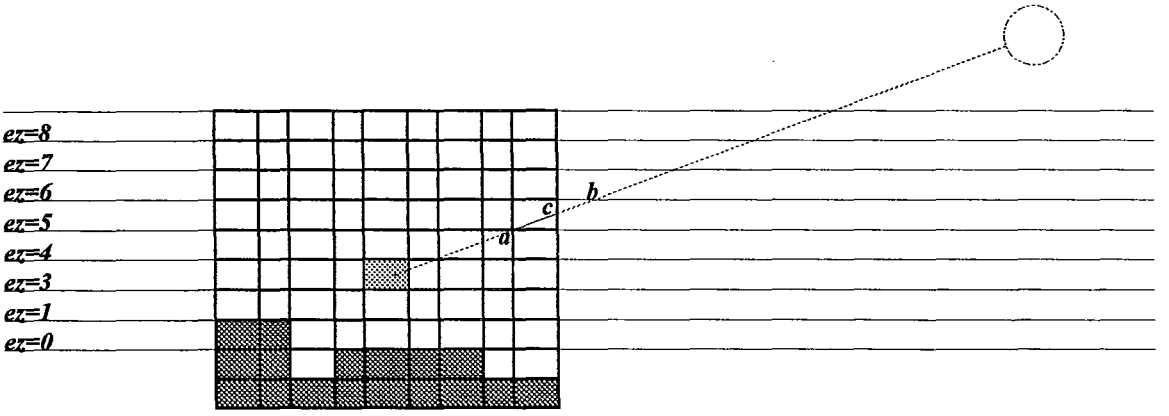

Figure 5.7 Calculation of light attenuation outside the grid.

calculated directly from the shaft length in an *ez* layer and the density *embeddens[ez]* as for all other attenuation. Shaft length per *ez* layer (*outshaft*) is calculated as 1 / sin(*elevation*) and converted to metres using *SIDESCALE*. The only problem arises at the very edge of the grid where a proportion (*ac*) of the shaft (*ab*) lies within the grid. The total length *ac* (*edgeshaft*) of the shaft in *ez* lying within the grid is recorded from *shaft_length[][][][]* in the function

ledgend() whilst defining the shaft in *light_shaft()*. The length ***ab*** can thus be calculated as 1 / sin(*elevation*) - *edgeshaft*.

Computation of daily light environment

Since it is too time consuming to calculate light at each point on an hourly basis, the results from the monthly radiation sub-model are used to generate a diurnal variation (Fig. 5.6). The variables *lt[x][y][z]* and *nir[x][y][z]* are defined as the mean of hourly irradiances (during daylight hours) for a day of average conditions. As such this is a useful relative measure of radiation conditions at a given point during that month.

Diurnal variation will occur about this mean according to the relative intensities of light at that time and the relative cloud cover (*c_cover[hr]*). Since the fraction of transmitted light is constant with intensity it is possible to apply this variation to all points in the grid. The function *lvar()* for PAR (*nvar()* for NIR) is called to return hourly values for a given tile. Modification of the monthly value to an hourly value, *lhour*, is performed as:

$$lhour = \{ lt[x][y][z] \times dayhours \times (par\_dir[hr] + par\_dif[hr] / totpar) \} \times \{ 1 - (0.64 \times c\_cover[hr] / 100) \} / \{ 1 - (0.64 \times (dayhours - sunmean[month]) / dayhours) \}$$

where the first half of the equation generates variation due to variation in irradiance at the upper atmosphere, and the second half corrects for cloud cover. The coefficient 0.64 for PAR

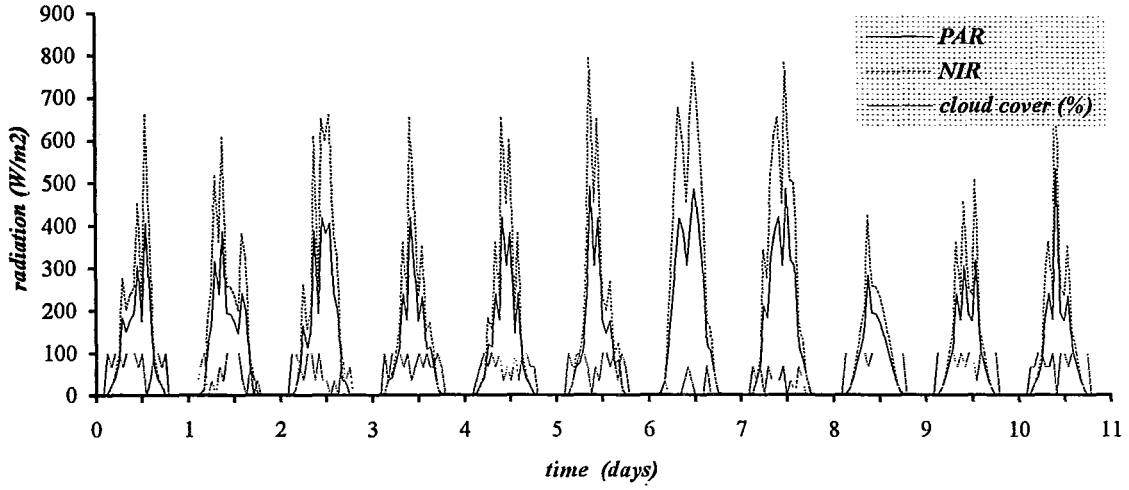

Figure 5.8. Diurnal variation of radiation at the top of the canopy as calculated from mean monthly values *lt[x][y][z]* and *nir[x][y][z]* in combination with relative light intensity.

represents energy absorbed or reflected by the cloud (1 - transmission coefficient). The corresponding coefficient 0.7 is used for NIR in *nvar()*. The above equation yields a smooth curve in constant cloud conditions. Figure 5.8 shows several days consecutive running of the light sub-model above the grid as the incoming light environment. This behaviour is comparable with that of the real system. Performance of the model in a simulated canopy is outlined in section 5.6 at the end of the chapter.

5.4 Wind sub-model

Overview

Wind is modelled daily in three-dimensions within the grid. The daily mean wind speed and direction from the weather generator are used to generate a one-dimensional wind profile in conjunction with the vegetation structure represented within the grid, and this mean value with height is converted into a distribution of values within each z layer according to the relative exposure of each tile.

Wind may affect plants by altering rates of mass and energy transfer and by mechanical disruption and abrasion. As such it is an essential component of the aerial environment of plants (e.g. Grace, 1977), and its effect must be represented in some way in any system subject to significant wind. In addition, this representation must be at a scale appropriate to the scale of the model vegetation. The modelling of canopy transfer processes is a field in which current modelling is largely inadequate. The complexities of turbulent air flow, the interdependence of all microclimatic variables, the difficulties of defining the boundaries of "units" of air, and the poor quality of three-dimensional vegetation description both in models and the field, make for a complex modelling task.

In recent years the well-used K-theory models (Philip, 1964; Waggoner & Reifsnyder, 1968) have come to be considered inadequate for many applications because of the relatively large scales of eddies within canopies (Raupach & Thom, 1981). These simple models work on the principle of diffusion between layers of air (flow is assumed to be essentially laminar) controlled by transfer coefficients (K values) and relative concentration gradients. Where eddy scale is large enough, the assumption of laminar flow is violated. Sauer and Norman (1995) demonstrate that this approach may still be used in short canopies (less than 1-2 m) where K-theory models can produce similar results to recent higher-order closure models. This is based on the assumption that the canopy is horizontally uniform. However, in sparse heterogeneous

canopies, the scale of eddies may be expected to increase and the use K-theory models even for low canopies becomes doubtful.

In order to model turbulent transfer processes within the canopy effectively, it is necessary to solve the momentum equations for each layer of air simultaneously. This presents a complex mathematical problem (since not only do the equations of motion and the non-hydrostatic, incompressible atmospheric continuity equation need to be balanced, but also, importantly, the equations of turbulence resulting from these). Various solutions to this problem have been presented (Wilson & Shaw, 1977; Raupach & Shaw, 1982; Finnigan, 1985) allowing a number of higher-order closure models to be developed (e.g. Meyers & Paw, 1986; Li *et al.*, 1989). An alternative approach is the use of Lagrangian theory (e.g. Raupach, 1989; McNaughton & van den Hurk, 1995) where profiles are expressed as the sum of a 'far-field' component (which obeys K-theory) and a 'near-field' component (which does not). Both these approaches have been used effectively for one-dimensional model canopies.

All the above models require the input of detailed turbulence structure. This presents a problem when attempting to generate transfer conditions directly from the vegetation structure model. In the absence of a mechanism to generate turbulence structure from vegetation structure the model will not respond to changes in vegetation and is thus inappropriate for analysis of change. In addition, all the above models are at present one-dimensional, since most have been developed for agricultural crops and forests where the canopy is managed for uniformity. Recent measurements of horizontal gradients of wind speed within a maize crop using a hot-sphere anemometer by Jacobs *et al.* (1995) reveal variation in wind speed of 20-30% at a single height within the canopy, across the space between rows. Failure to represent this type of variation in a model will result in significant errors at or below individual level, and it becomes questionable whether a one-dimensional model is appropriate for studies at this level.

The introduction of the second and third dimension complicate the computational problems extensively, with the introduction of effects from upwind and downwind vegetation structure and non-vertical eddies. The conversion of any of the above approaches to a three-dimensional model is a task of much mathematical complexity, and indeed may not presently be practical. The "Ecospace" model is designed to allow simple three-dimensional spatial calculations based on the absolute physical state of the system. It was decided that the use of semi-empirical modelling of transfer processes could produce realistic three-dimensional results without the input of measured turbulence properties. It was hoped that any inaccuracies generated by the simplified three-dimensional approach would be less significant

at the scale of a tile than the inaccuracies of any one-dimensional model which ignores horizontal variation.

Model structure

Air speed in the model is calculated daily according to a simple model. First, the wind profile for the plot is generated from the vegetation profile. This gives a mean wind speed for each *z* layer in the model. An estimate of air speed for each tile within a layer can then be obtained by variation about the mean wind speed according to the relative exposure of each tile within the layer. Wind in the model is assumed to travel in a certain direction for part of the calculation of exposure, but in order to be a useful value it is necessary that the generated values of wind speed per tile represent wind in all directions. The output array, *wind[x][y][z]*, is defined as the mean daily air speed in all directions within a given tile. It would be appropriate to simulate wind at an hourly time scale in response to changes in wind speed and direction throughout the day, but this is computationally very intensive. Mean daily air speed is used as an initial simplification, allowing the development of a temperature sub-model and the modelling of some plant response to wind, but using the minimum of computer run time. The calculations required involve most of the sub-routines required for a more frequent model.

Wind profile

It is assumed that the modelled site is a part of a uniform wind field with the mean structural properties of the model grid, such that the wind profile is constant across an area far larger than the modelled site. As such it is possible to generate the wind profile from the site conditions. Mean site conditions are represented in the *embeddens[ez]* array and all calculations are performed using *ez*, the height above ground surface rather than the absolute height. First the wind profile above the canopy is calculated and this is then used in combination with the vegetation structure to derive approximate wind speeds within the canopy. Provided that the scale of spatial inhomogeneities in the canopy is less than a few times the canopy height, a wind profile may reasonably be defined from roughness length and zero plane displacement derived from vegetation structure (Lewellen, 1985). Further inhomogeneity may well result in the disruption of a constant flux layer immediately above the canopy. It is assumed that the vegetation structure will not reach a state where the constant flux layer is disrupted.

Vegetation height (*ht*) in metres is defined simply as the topmost *z* layer containing *embeddens[ez]* greater than an arbitrary 50. The additional height from the vegetation within the topmost layer is estimated from *embeddens[ez]*/2500 (where 2500 is the maximum expected density, see Chapter 4). The estimation for roughness length (z_0) of Lettau (1969) is used for calculations in the function *wind_rough()*.

$$z_0 = 0.5 \times ht \times (A^*/A')$$

where A^*/A' is the ratio of the area of upwind face of roughness element (A^*) occupying a ground area of A'. For a hexagonal tile with average surface area in a horizontal plane of 0.9339 tile-sides (h) squared and ground area (A') 2.6 h^2 the upwind area of each tile is given by

$$A^*_{tile} = 0.9339 \times absdens[x][y][z] \,/\, 10000$$

thus where A^* is the sum of A^*_{tile} for *hcount* tiles roughness length is given as

$$z_0 = 0.5 \times ht \times (A^* / (2.6 \times hcount))$$

Zero plane displacement (d) is estimated as 2/3 the vegetation height as is standard for shrub vegetation (Monteith & Unsworth, 1990). Friction velocity u^*, an expression of the velocity of turbulence elements, is estimated within a range 0.2 to 0.45 m s^{-1} for incoming wind speeds of 0 to 10 m s^{-1} from the simple equation

$$u^* = 0.2 + 0.125 \times windspeed$$

This produces values suitable for short vegetation, but greatly simplifies the relationship by ignoring the effect of vegetation structure, assuming that variation in structure over the vertical scale in the model will have little effect. It should here be noted that this compromises the generality of the model, and a more suitable form of the above equation should be substituted for taller vegetation (e.g. Jaeger, 1985).

Wind speed above the canopy can thus be calculated from the standard wind profile equation

$$u_z = \left(\frac{u^*}{k}\right) \ln\left(\frac{(ez-d)}{z_0}\right)$$

where k is the von Karman constant (≈0.41). Assuming a constant friction velocity, the first term in the equation remains constant for all heights and the wind speed at any height can be calculated as a fraction *wfract[ez]* of the reference windspeed at 10 m (*windspeed*).

Within the canopy a semi-empirical approach is used to generate a profile based on the exponential reduction of Inoue (1963) and Cionco (1965) where

$$u_z = u_h \times \exp\left[\alpha \times \left(\frac{ez}{h} - 1\right)\right]$$

where u_h is the windspeed at the canopy air interface and α is the canopy flow index which is an index of airflow response to vegetation roughness. This equation ignores the effect of vertical inhomogeneity in the canopy and always results in a smooth curve. It was decided that vertical variation could reasonably be introduced by modifying α to take account of the differences between layers. Thus each layer is effectively calculated at the correct height within a canopy of uniform flow index assumed to be equal to the canopy flow index at that height. Variations about the exponential curve are then produced. This approach can thus represent the effects of a through-draft resulting from low vegetation density near the ground if the variation in density with height is sufficient.

The canopy flow index is calculated empirically from the relationships recorded in Cionco (1978) where self-sheltering of roughness elements results in a relatively constant canopy flow index of around unity when a crop is between 68% and 100% of its natural maximum density, with a peak of $\alpha \approx 1.5$ at a density of 36%. From the assumptions that a crop density of 100% is reached at *embeddens[ez]*≈2500, and both increase and decrease of α with density are linear, the canopy flow index can be estimated by three equations

$$\alpha_{ez} = 1.5 - 0.0555\ (9 - ed_{ez}) \qquad \text{for } 0 < ed_{ez} < 9$$
$$\alpha_{ez} = 1 + 0.0625\ (17 - ed_{ez}) \qquad \text{for } 9 < ed_{ez} < 17$$
$$\alpha_{ez} = 1 \qquad \text{for } 17 < ed_{ez} < 100$$

where ed_{ez} is the mean percentage of tile filled at height *ez* above the ground surface, given by *embeddens[ez]* / 100.

In a simple canopy, an exponential curve is a reasonable approximation of air speed down to 0.1.h but the quality of simulation is reduced in complex canopies (Cionco, 1978). In

order to take account of this the *ez* layer closest to the ground (*ez*=0) is modelled using a different approach from the canopy above. For a typical heather canopy 0.50 m high this layer represents 0.1 × *ht* with an increasing proportion of the canopy height being represented for lower canopies. When *Calluna* is at this height, it is usually in the building or mature phase with a fairly uniform structure. Where the canopy is shorter, and probably more complex (pioneer and senescent stages), the bottom layer takes up an increasing proportion of the profile to compensate for inaccuracies. Working on the principle that the wind speed is zero at the ground surface, and that there is a linear decrease in wind from the second *ez* layer to the ground, the wind speed in the bottom layer is approximated as

$$u_0 = \frac{u_1}{3}$$

where u_1 is the wind speed in level *ez*=1 and u_0 the wind speed in the bottom *ez* layer.

Given that a mechanistic modelling approach which can adequately describe vertical profiles in response to vegetation structure in the absence of flux measurements has not yet been developed to the awareness of the author, all models must necessarily be approximations of wind conditions. The simple model outlined above allows a direct effect of vegetation porosity on the wind profile through the action of skin friction and form drag. The estimations of canopy flow index do not take into account the effects of a varying wind speed since it is assumed that the drag coefficient of the vegetation will remain constant in the range of wind speeds experienced within the canopy. Although this simplification (Cionco 1978) may result in poor estimates at low wind speeds where skin friction becomes dominant it was considered an adequate assumption for this model.

Relative exposure

The wind profile model yields a vertical distribution of mean wind mean velocity as a proportion of the wind speed above the canopy. Together with the direction of the wind at a given time this is a useful description of wind conditions within the canopy. However, when viewed in the context of the three-dimensional vegetation structure, where some tiles within a layer may lie within a group of dense tiles and others may lie in the open, wind profiles seem inadequate to describe conditions for a given tile. It is desirable that the profile be extended to the second and third dimensions i.e. to the horizontal plane, to enable temperature and potentially vapour transfer to be calculated in each tile. An estimate of the degree of exposure

experienced by each tile is calculated for a given wind direction using ray tracing techniques as used in the light model. The representation of wind as straight rays is a necessary simplification. Although criticism may be made for failing to allow for funnelling and eddies, alternative approaches would require complex mathematics (increasing computer simulation time unacceptably), and at the present state of the art would be unlikely to yield results of any improved degree of accuracy within a heterogeneous canopy.

For each layer above the ground, the wind profile sub-model returns a value of average daily wind speed as a proportion of the wind speed at 10 m. This is averaged over time and horizontal space. In a normal canopy, air movement may be expected in any number of directions and intensities, and a minimum time of 30 minutes is recommended (Monteith, 1973) for averaging to capture variation. On a horizontal scale there may be significant variation in local wind speed and turbulence due to inhomogeneities in the canopy. The use of *exposure()* is intended to represent this variation by assuming that the wind speed at a given point is proportional to the amount of vegetation upwind and the amount immediately surrounding it. From this assumption, the mean wind speed can be converted into the theoretical spatial frequency distribution which defined it, directly from the distribution of vegetation elements within that horizontal layer.

Calculations for three-dimensional wind model

The three-dimensional wind sub-model is calculated in *wind_master()* which first calls the function *wind_profile()* to generate a vertical profile as described above. Each *ez* layer (i.e. layer above ground surface at *x, y*) is then scanned and for each tile the function *exposure()* is called to return a value between zero and one (fully covered to fully exposed). The total exposure for each *ez* layer is recorded in the array *exposum[ez]*.

In *exposure()* two methods are used to calculate the exposure of a given tile to wind. The first method is based on the ray tracing routines of the light sub-model. Nine evenly spaced rays are defined, in a radial arc five degrees to either side of the wind bearing (*windbearing*) and a vertical arc from horizontal to ten degrees above the centre of the tile. This is a limited scan only in the direct direction of the wind. The functions *light_path()* and *light_shaft()* are called to determine which tiles are passed through. For each ray exposure is measured as the sum of *absdens[][][]* for each tile passed through. The mean *absdens[][][]* for all rays is then calculated and converted to a 0-1 scale (*sumshaft*). This method automatically weights the mean towards those tiles closest to the subject tile because the rays

are closest at this point. Since this method assumes that the wind travels in straight lines, the second method (*turbulence_cat()*), was developed to include the effects of all the subject tile's neighbours which affect wind speed in the tile but are not necessarily represented by the first approach. This second method simply converts the total density for the tile and all eight neighbours to a linear 0-1 scale (*surroundens*). Exposure is calculated simply as the average of these two values. Although this relationship could be modified, insufficient data at this scale makes any decision somewhat arbitrary. Due to the length of time required for the first ray tracing method when calculated daily, a shortcut option (*EXPOCUT*) is provided which uses only the shorter second method.

Once exposure has been calculated for each tile in a *ez* layer and recorded temporarily in *wind[x][y][z]* the variation about the mean wind speed for that layer may be calculated. As stated earlier, mean wind speed may vary up by ±30% (Jacobs, Vanboxel & Elkinlani, 1995) within a horizontal canopy layer. The distribution about the mean wind speed for each layer is based on a linear relationship between variation in exposure from the mean exposure and variation in wind speed from the mean wind speed such that

$$wind[x][y][z] = wfract[ez] \times windspeed \times hvar$$

where *wind[x][y][z]* is the wind in m s^{-1} per tile, *wfract[ez]* is the fraction of the reference wind speed, *windspeed* at height *ez*, and

$$hvar = 1.0 + 0.4 \times (\text{"exposure[tile]"} - (exposum[ez] / en[ez]))$$

where *hvar* is a coefficient of relative exposure, "exposure[tile]" is the exposure of the tile (at this point stored in *wind[x][y][z]*) and *exposum[ez]/en[ez]* is the mean exposure at height *ez*. This gives variation about the mean of up to a maximum of ±40%, although in practice it is unlikely that the exposure of a tile should differ more than 0.75 (±25%) from the mean.

5.5 Temperature sub-model

Temperature is calculated hourly for each tile in the grid. As mentioned previously in this chapter, the use of K-theory models for transfer presents certain difficulties when dealing with a variable canopy structure. A simple temperature model was developed, based on isothermal net radiation and leaf temperature, with limited representation of three-dimensional air transport processes. Temperature is calculated hourly in proportion to leaf temperature for each tile in the grid. It was hoped that this sub-model could produce heterogeneity in air/leaf temperature at a suitable scale for photosynthesis and respiration calculations. However, the flow of energy is not modelled explicitly and the system is not closed. A more mechanistically satisfying sub-model was considered to be beyond the scope of the current model.

The leaf temperature calculations are based on the approach of Jones (1983), as adapted by Friend (1995) drawing from Monteith (1973). This approach calculates the difference between leaf and background air temperature from the sum of two terms, one depending on isothermal net radiation (from the solar radiation sub-model) and the other on vapour pressure deficit. It is employed for all occupied tiles and used to generate air temperature. All unoccupied tiles are assumed to be at the air temperature above the canopy (*tt*).

Background temperature profile

The function *etemp_update()* calculates a simple vertical heat profile during daylight hours as a background for the three-dimensional calculations. It was considered that, in the absence of a carefully considered diffusion model, an approximation would be superior to an assumption of spatially constant temperature. Tile air/leaf temperature for the previous hour is held in the three-dimensional array *temp[x][y][z]*. The mean temperature for each *ez* layer is calculated from this. The extent of vertical mixing is made proportional to the mean wind speed in that *ez* layer (*embed_wind[ez]*), assuming that the horizontal and vertical components are equal. A mixing coefficient, *mix*, is calculated as

$$mix = 2.5 \times embed\_wind[ez]$$

which is used to weight the temperature towards *tt*, air temperature above the canopy (*mix* = 0, low mixing; *mix* ≈ 6, high mixing). A minimum value of one is imposed on *mix* such that maximum mixing is achieved at a local wind of 2.5 m s^{-1}. Temperature is calculated as

$embed\_temp[ez]_t =$

$$\frac{\left(embed\_temp[ez]_{t-1} + mix \times tt + embed\_temp[ez-1]_{t-1} + embed\_temp[ez+1]_{t-1}\right)}{mix+3}$$

for the middle layers of the grid. For the top of the grid and near ground level, (at the edges of the *ez* profile) modification of the above equation is necessary such that for the top

$$embed\_temp[ez]_t = \frac{\left(embed\_temp[ez]_{t-1} + mix \times tt + embed\_temp[ez-1]_{t-1}\right)}{mix+2}$$

and for the ground surface,

$embed\_temp[ez]_t =$

$$\frac{\left(embed\_temp[ez]_{t-1} + mix \times tt + 2 \times esoil + embed\_temp[ez+1]_{t-1}\right)}{mix+4}$$

where *esoil* is the topsoil temperature. *Esoil* is calculated simply as

$$esoil = (embed\_temp[0] + soil\_temp)$$

where *soil_temp* is the subsoil temperature at an arbitrary depth calculated daily in *soiltemp()* as a fifty point running average of half daily maximum plus minimum temperature (*temperature[2]*) by calling *hcalc()*.

This is clearly an extreme simplification of the true nature of within-canopy mixing, but it is felt that any further detail is beyond the scope of this model. As with the wind sub-model there arises a need to generate transfer coefficients from the canopy structure in order to model the process dynamically.

Calculations for the three-dimensional temperature sub-model

The background air temperature for each layer above the ground is combined with the grid-based output from the radiation sub-model to generate hourly three-dimensional temperature. The leaf temperature equations of Friend (1995) are used to determine the instantaneous difference between leaf and background air temperature, which is then used to calculate tile

air temperature according to a simple model. Unless otherwise stated the equations and default values below have been taken directly from the PGEN v2.0 model of Friend (1995). These equations are presented immediately below, as initially implemented. The conversion from leaf to air temperature is presented in subsection *ii)*.

Leaf temperature (T_l) is given by the equation

$$T_l = T_a + \left(\frac{r_w \times \gamma \times \Phi_{ni}}{\rho_a \times c_p} - \partial W \right) \Big/ \left(\frac{r_w \times \gamma}{r_{HR}} + s \right)$$

where:

T_a is the temperature (K) of the air outside the leaf boundary layer as calculated in the function *embtemp_update()* described below;

r_w is the total resistance to water flux across leaf surface and boundary layer, (s m^{-1}) given by

$$r_w = 0.607 \times r_{c,a} + 0.704 \times r_{c,s}$$

where: the coefficients assume still air across the leaf surface and laminar flow in the leaf boundary layer,

$r_{c,a}$ is the resistance to CO_2 flux across the leaf boundary layer (s m^{-1}) given as

$$r_{c,a} = 132.51 \times \left(\frac{u}{d} \right)^{-0.5} \times \left(\frac{\overline{T}}{T_0} \right)^{-1.75} \times \left(\frac{P_0}{P} \right)^{-1}$$

where: u is the wind speed (m s^{-1}) taken as *wind[x][y][z]*,

d is the leaf characteristic dimension (m) taken as the default value 0.005 m,

$\overline{T}$ is the initial leaf temperature (K) given as *temp[x][y][z]* + 273.15 K,

T_0 is the air temperature outside the leaf boundary layer (K), given as *embed_temp[ez]* + 273.15 K,

The ratio P_0 (standard atmospheric pressure) to P (site atmospheric pressure) is at present assumed to be one (default value).

and $r_{c,s}$ is the resistance to CO_2 flux across the leaf surface (319.5 s m^{-1}), default value.

γ is the psychrometer "constant", given by

$$\gamma = \frac{P \times c_p}{0.622 \times \lambda} \times \frac{1}{R \times T_a}$$

where: P, site atmospheric pressure is assumed constant at present at 101325 Pa,

c_p is the specific heat of air (1012 J kg^{-1} K^{-1}),

λ is the latent heat of vaporisation of water (J kg^{-1}) given as

$$\lambda = 3.152 \times 10^6 - 2.38 \times 10^3 \times T_a$$

R is the gas constant (8.3144 J K^{-1} mol^{-1}),

and T_a is the temperature (K) of the air outside the leaf boundary layer (as above).

Φ_{ni} is the isothermal net radiation calculated in the function *radcalc()* described below.

ρ_a is the density of dry air given as

$$\rho_a = 2.42 - 4.12 \times 10^{-3} \times T_a$$

c_p is the specific heat of air (1012 J kg^{-1} K^{-1}),

δW is the water vapour concentration deficit of the air outside the leaf boundary layer,

$$\delta W = W_{s(T_a)} \times (1 - f_w)$$

where: $W_{s(T_a)}$ is the saturation concentration of water at air temperature (mol m^{-3})

$$W_{s(T_a)} = 610.78 \times \left(\frac{P_0}{P}\right) \times \left(\frac{1}{R \times T_a}\right) \times \exp\left(\frac{17.269 \times (T_a - 273.15)}{T_a - 35.85}\right)$$

and f_w is the relative humidity of air, assumed constant in space and time (0.893, {89.3%}). In the absence of a water sub-model to represent the humidity dynamically this was considered a reasonable temporary assumption, allowing the calculation of local temperature which would be required as an input for a spatial water sub-model.

r_{HR} is the total thermal resistance to heat loss from the leaf by convection and radiation (s m^{-1}) from

$$r_{HR} = \frac{1}{r_{aH}} + \frac{1}{r_R}$$

where: r_{aH} is the leaf boundary layer resistance to convective heat loss (s m^{-1}) given by

$$r_{aH} = \frac{2}{12.09 \times \left(\frac{u^{0.6}}{d^{0.4}} \right)}$$

where: u is taken as *wind[x][y][z]*,

d is the leaf characteristic dimension (0.005 m).

This is equation 3.32 of Jones (1983) for cylindrical objects with a correction of 2/3 to allow for the effects of turbulence.

r_R is the radiative "resistance" to heat loss (s m^{-1}), given by

$$r_R = \frac{\rho_a \times c_p}{4 \times \sigma \times T_a^3}$$

where: σ is the Stefan-Boltzmann constant (5.6703×10^{-6}), and all other terms are defined above.

i). Isothermal net radiation

The isothermal net radiation, Φ_{ni} (i.e. the net radiation received assuming the object to be at air temperature) in each tile is calculated in the function *radcalc()*. The hourly irradiance of both PAR and NIR are calculated for both the subject tile and the tile directly below. In order to model reflectance within the canopy simply, it is assumed that all incoming reflected radiation to a tile comes from the tile directly below, and that all reflected radiation from the tile below is reflected directly upwards. Since the reflected radiation is almost entirely non-PAR it is of no direct import to the photosynthesis sub-model. The proportions of reflected light for each wavelength are representative values for a range of vegetation, taken from Jones (1983) such that

lt[x][y][z] += *lt[x][y][z-1]* × 0.12 × *absdens[x][y][z-1]/DCON*
nir[x][y][z] += *nir[x][y][z-1]* × 0.5 × *absdens[x][y][z-1]/DCON*

Total absorbed incoming shortwave radiation (*is*) can thus be calculated as

is = *lt[x][y][z]* × 0.88 + *nir[x][y][z]* × 0.5

This allows calculation of isothermal net radiation Φ_{ni} assuming leaf temperature to be equal to air temperature such that

$$\Phi_{ni} = is + I_{Ld} + \sigma \times \left(T_b\right)^4 - 2 \times T_a^4$$

where: I_{Ld} is the net downward flux of longwave radiation approximated as

$$I_{Ld} = \sigma \times \left(T_a - 0.825 \times \exp\left(0.00354 \times is\right)\right)^4$$

T_b is the background temperature estimated as *embed_temp[ez]*, and T_a is the air/leaf temperature *temp[x][y][z]*.

ii). From leaf temperature to tile air temperature

Sensitivity analysis of the equations of Friend (1995) as presented above revealed that even in strong sunlight the leaf temperature was not raised more than 0.0002°C over background air temperature (i.e. the air within the tile). This conforms with the common assumption that leaf temperature is the same as air temperature (Rabbinge, 1976) in most conditions. However, the measurements of MacKerron (in Gimingham, 1972) show the temperature of air within a *Calluna* canopy warming to up to 4°C above the air temperature immediately outside the canopy on a sunny day in June. We would expect a corresponding increase in leaf temperature. In addition, measurements of the dwarf shrubs *Artcostaphylos uva-ursi* (L.) Spreng and *Loiseleuria procumbens* (L.) Desv. (Wilson *et al*, 1987) recorded meristem temperatures as much as 15°C above the air temperature at 1 m at altitudes above 400 m. The leaf temperature sub-model is, in this state, inadequately simulating the process of leaf warming, even allowing for the difference between air temperatures across the canopy surface. Importantly the process of warming is driven by radiation interception by the canopy, (balanced by wind driven cooling). If we examine the main equation

$$Ti = T_a + \left(\frac{r_w \times \gamma \times \Phi_{ni}}{\rho_a \times c_p} - \partial W\right) \Big/ \left(\frac{r_w \times \gamma}{r_{HR}} + s\right)$$

it is clear that the influence of isothermal net radiation, Φ_{ni} , on the second half of the equation cannot be very great due to the structure of the equation. Presumably this is because the equation is instantaneous, and the leaf is well coupled to the air immediately surrounding

it. The leaf will thus not heat up far above the surrounding air, but will instead continually lose energy to the surrounding air. If this air were not to mix with the surrounding air it would be expected to heat up significantly, although this effect will be reduced with increasing mixing. Assuming that the degree of warming or cooling of the air is proportional to the difference between leaf and air temperature (second half of equation), the amount of leaf material present (*absdens[x][y][z]*) and the amount of air movement (proportional to r_w), an additional term (m) was added to the above equation to give the change in surrounding air temperature per hour, such that

$$T_{tile} = T_a + m \times \left(\frac{r_w \times \gamma \times \Phi_{ni}}{\rho_a \times c_p} - \partial W \right) \Big/ \left(\frac{r_w \times \gamma}{r_{HR}} + s \right)$$

where m is given by

$$m = 4 \times (r_w - 200) + absdens[x][y][z] / 2$$

when r_w is greater than 200; otherwise

$$m = (200 \times absdens[x][y][z] / 2.5) / 10$$

This modification allows air temperature in the tile surrounding leaf material to warm up as much as 4°C above previous air temperature (bright sunlight, still air and maximum vegetation density) within an hour. It should be noted that this is a pre-mixing value, and most of the energy thus accumulated is lost to mixing with incoming air before the calculation of the next hour's temperature regime, although in conditions of continuous bright sunshine and low wind speed an accumulation of energy in the canopy occurs. The modified equation produces temperatures in the broad range expected, although at present not allowing increases as large as 15°C allowing further calcuations requiring the input of local temperature. However, the extent of the modification renders the sub-model open to critisism. It is suggested that although this sub-model functions adequately as a temporary sub-model, it should be replaced with a superior model with mechanistic response to radiation, wind and evapotranspiration after the addition of a water sub-model.

All unoccupied tiles are set at the incoming air temperature *tt*. After sunset the sub-model is set to return *tt* for all tiles since the temperature otherwise falls too slowly compared to observed data and fails to simulate the expected nocturnal temperature inversion. At present this has little effect on the performance of the growth sub-model.

5.6 Validation of the microclimate sub-model

In order to test the microclimate sub-model for behavioural validity, the model was tested for behaviour relative to the measurements of MacKerron (in Gimingham, 1972) taken on an even-aged stand of building *Calluna*. This is a far from comprehensive validation, but demonstrates that the sub-model behaves realistically.

During the initial testing of the model no counter-intuitive behaviour was observed and the model can produce realistic looking three-dimensional distributions relative to vegetation structure (see Chapter 7).

Measurements of above-ground biomass, air temperature, wind speed and radiation were taken by D.K.L. MacKerron and presented in Gimingham (1972, pp. 48-51) for an even-aged stand of building *Calluna* during "a fine day in June". Since the "Ecospace" model has a stochastic weather generator, it is not possible to force the weather to produce certain weather patterns, so the model was run for a month, and a fine day was selected and compared with the validation data. Consequently the precise patterns of weather throughout the day are not directly comparable, but broadly similar.

The vegetation structure was set up as a horizontally homogenous canopy with the vertical profiles converted from the biomass profiles of MacKerron using the conversion factors *masshoot* and *masswood*. The distribution of vegetation can be seen in Figure 5.9. Firstly, the light environment was tested on a grid $30x \times 30y \times 15z$. The resultant light environment is shown in Figure 5.10. Ideally the sub-model would produce an even surface for each level. A slight striping is evident, with some significant edge effects in the outer ring of tiles, but otherwise the light sub-model performs adequately. It is felt that the striping is not significant as far as plant growth is concerned, remaining less than 10 W m^2 at its most extreme. Since the cause of these anomalies is unknown there is some cause for concern, particularly where the edge effects (see level 9) are significant.

Profiles for modelled microclimatic variables in relation to vegetation structure and the MacKerron light attenuation data are shown in Figure 5.10. The light sub-model appears to overestimate the attenuation of light, at both the density of a building stand and at half density, but it is thought that this could well be the result of gaps in the natural canopy, or an uneven top surface allowing full sunlight deep into the canopy in the natural system. Since the model was run for a homogenous canopy it will not capture such effects, and it is felt that this underestimation of light is not necessarily a fault in the sub-model. However, it is also

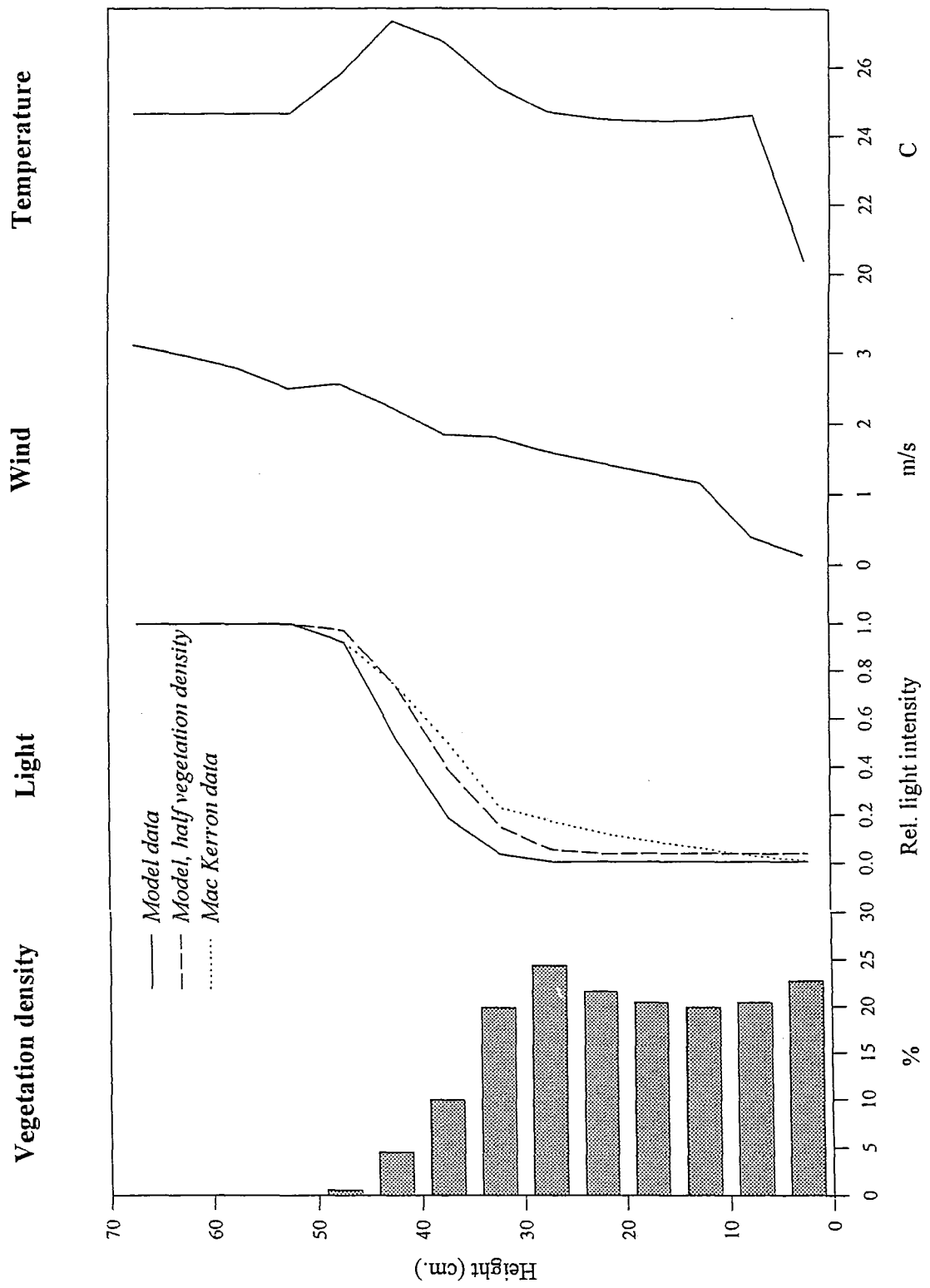

Figure 5.9. Profiles of plant material, light, wind and temeprature through a stand of building *Calluna* for a fine day in June. The light model is compared with the data of MacKerron (see text).

possible that the absorption coefficient which is assumed to be a constant 0.8 for all material may overestimate absorption in the upper canopy, where a greater proportion of leaf to wood is to be expected. Further validation with spatially explicit data is required. The wind model is not shown with the corresponding field measurements since these show a through-draft near the ground attributed to the measurements being taken near the edge of a vegetation mass. Although the model is capable of such effects, at least to a limited extent, the high densities of dead plant material near the ground used in the validating vegetation structure would be expected to generate a wind profile close to the one shown. Again, further testing of the sub-model with spatially explicit data is required.

The resultant modelled temperature profiles over the day are compared with the recorded profiles in Figure 5.11, and show a reasonable correlation. There is a difference in the diurnal progression of air temperature above the canopy between the modelled and the real data due to the difficulties in generating results comparable to a specific measured day. Allowing for this, the two sets of profiles show broadly similar behaviour over the course of the day, although the model appears to cool too slowly after sunset. This was a property common to many other days' simulation, and although in the present version of the model this is likely to have very little effect on plant growth, a more satisfying simulation of cooling and night temperature would be desirable.

Overall, the microclimate sub-model appears to produce reasonable output, with three-dimensional variation within the expected range (see Chapter 7). Consequently the sub-model has achieved the objective of spatially representing the effects of vegetation structure on microclimate, allowing the individual plant growth sub-model to be run in a dynamically responsive microclimate. However, there are some elements of concern, notably the edge effects of the light sub-model, the modified temperature sub-model and the limited treatment of wind. These will be discussed further in Chapter 8.

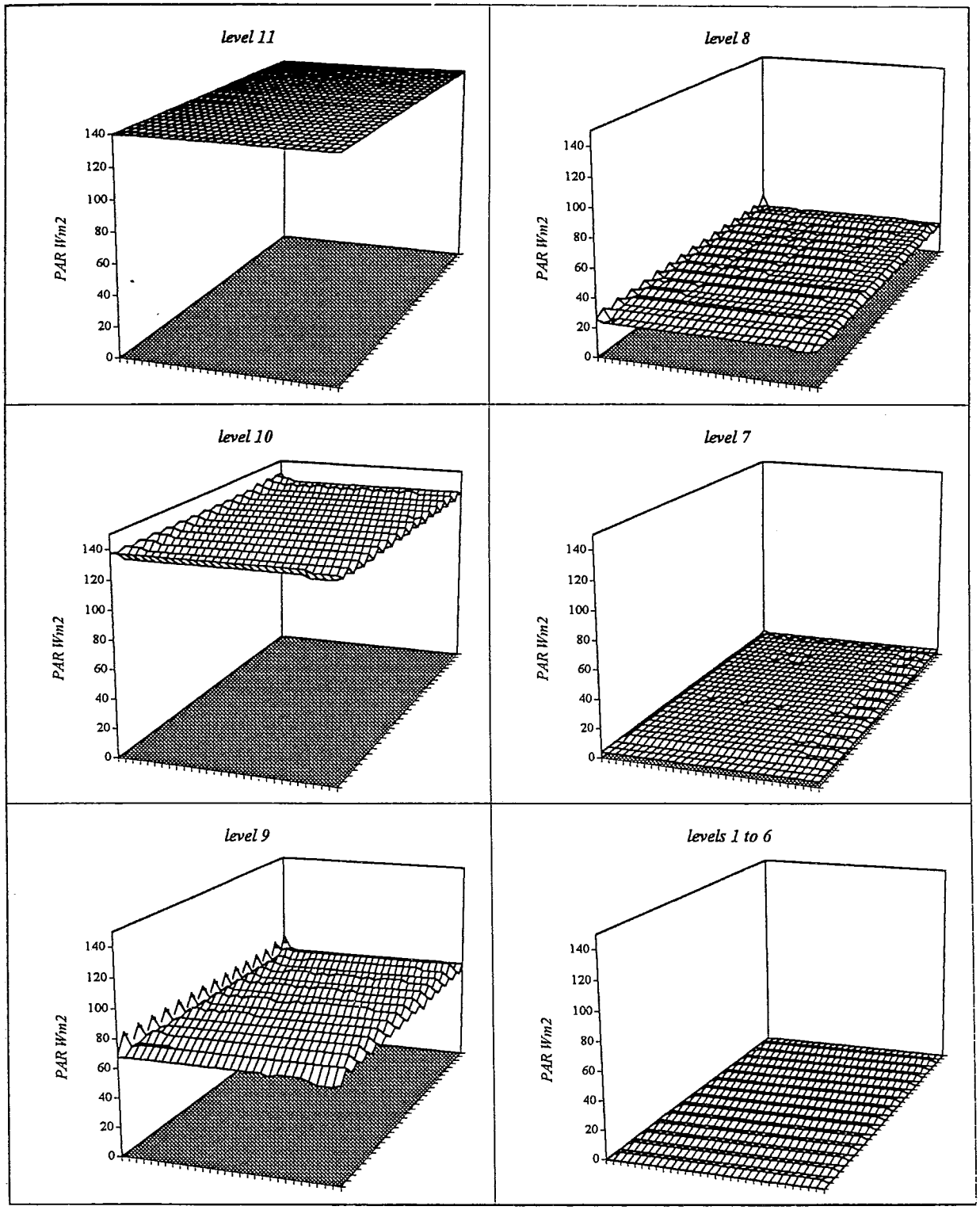

Figure 5.10. The three-dimensional light environment generated for a fine day in June on a $30x \times 30y \times 15z$ grid. Each graph shows the environment for a different *ez* level, where level 1 is at the ground surface.

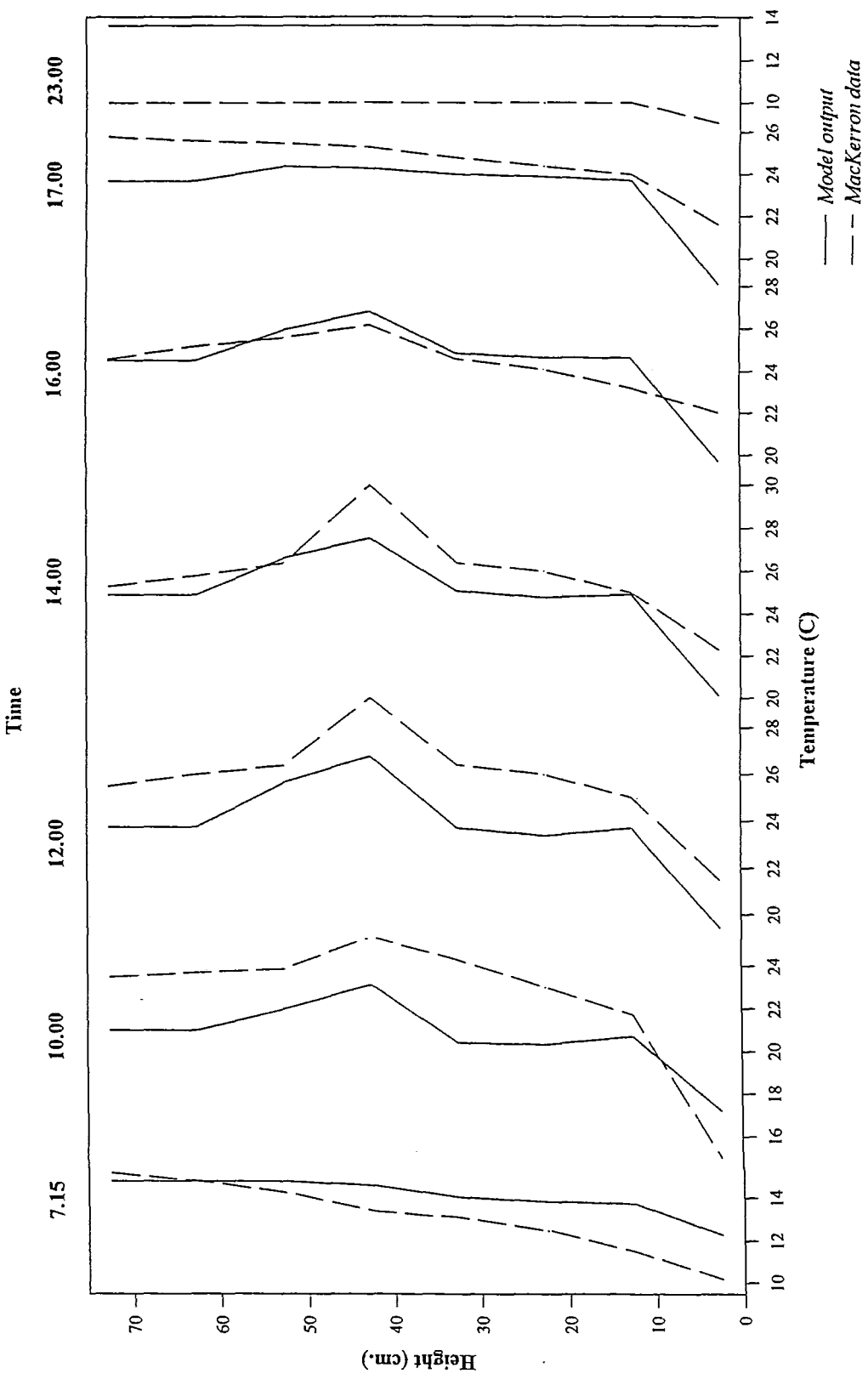

Figure 5.11. Temperature profiles through a real and modelled stand of even-aged *Calluna* on a fine day in June.

6

Individual Plant Growth Sub-model

Contents

6.1 Introduction

The hexagonal grid allows for conditions to be specified separately in each tile at the soil surface. This allows for the description of "gap" conditions for germination and establishment. Germination is calculated stochastically from a seed bank when germination microsite conditions are met.

Plants are grown as individuals within the spatial grid. Two types of individual are defined in the model, juveniles and adults. Juvenile plants are limited to a single tile at ground level, but adult plants may occupy any tile within the grid. Juveniles are initialised as adult individuals when they achieve a species-specific size. Individual production is calculated on an hourly basis using an empirical light and temperature response, as a value for each tile in the whole plant. This growth is divided between the plant organs and distributed spatially over the whole plant as potential growth at the end of each week. The potential growth for all plants is added simultaneously to the grid, and, where space is limiting, any surplus is applied elsewhere using a recursive loop. Mortality occurs both continuously and in response to stress from low production and senescence.

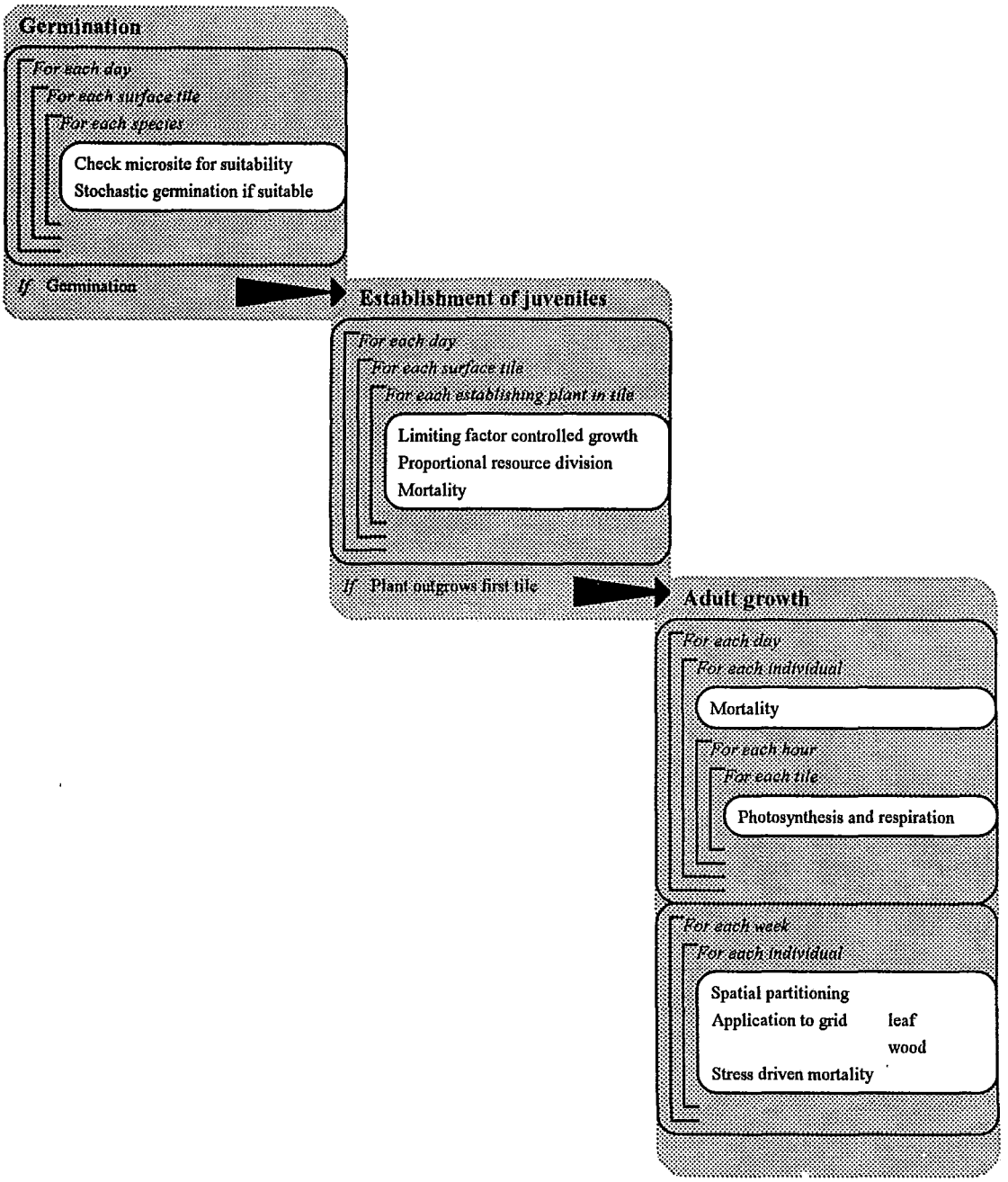

Figure 6.1. The individual plant growth sub-model, showing the three stages of an individual's life and the important processes calculated for plants in each stage at different spatial and temporal scales.

Competition

Since the abiotic and biotic environments are clearly defined on a tile basis, the growth of plants within the grid can be calculated solely from the conditions within the tiles which that individual occupies, with each growth increment resulting in changed conditions in the rest of

the grid. Competition can consequently be worked out in relation to the whole community rather than selected local individuals. This potentially allows non-living structures such as rocks to affect the growth of individuals. Where two or more individuals occupy the same tile and resources are limiting, the resources may be divided up according to the amount of each individual in that tile, and the relative resource capturing abilities of those individuals. In the model's present state, competition is based on the spatial distribution of radiation, temperature and wind, which are not all strictly resources: each may be a limiting factor. Competition for light is the most significant aspect of competition in many plant communities, including heathlands. Nutrients and water may also have a marked effect on competition in many communities but are at present assumed to be non-limiting. They are not modelled dynamically, although a simple limiting factor approach is used for establishing juveniles which could potentially be extended to the adult individuals (function *soil_limits()*).

6.2 Germination

Individual plants are created from seed in the model, germinating in response to abiotic stimuli. In the natural system germination occurs at or near the soil or litter surface in most species. This is the crucial first stage in the survival of an individual, and cannot be passed without a suitable germination site. It is essential that conditions at the point of germination are represented. Germination is not a horizontally homogenous process even with an even distribution of seeds. Seeds germinate only at suitable sites, lying dormant until either these conditions arise or the seed becomes non-viable, and it is by this temporal process that individual plants select their germination sites.

In order to model this process, each ground level tile is examined separately, every day, to determine which species could germinate, and then stochastic, seed-bank-related germination is applied.

For each x, y column, the z height of the soil and litter surfaces are recorded. This allows the conditions for germination to be described at each point across the soil surface. Shugart and West (1977) found that by varying the size of horizontal plots for plant germination, establishment and development in a grid; their forest "gap" model's behaviour could be altered. By reducing the plot size to the size of a full grown individual, the exact spatial locations of individuals could be ignored and forest dynamics adequately simulated. However satisfactorily this approach simulates forest behaviour, it ignores the heterogeneity

of the environment at the scale of the juvenile plant (Figure 6.2 below). It is this heterogeneous environment which determines the selection process for individual survival in the natural system. Consider the case illustrated in Figure 6.2. Plot size is shown below, and a gap has just been freed. In a gap model, plants *A* to *D* would all be considered to be at the same spatial location. However, in the natural system each individual will be in a unique environment. Gradients of light across the gap would favour B and C, whilst shelter is greatest at the edges of the gap.

In addition to the microclimate modification by the dominant canopy plants, it is also necessary to consider the understory vegetation. Where continuous ground cover exists, seedlings may have difficulty in surviving. It is an oversimplification to consider dominants in isolation and to ignore this crucial stage of competition, where seedlings of the dominants compete directly with understory plants and not just with each other. The only case in which competition with understory plants may reasonably be ignored is where the understory is horizontally homogenous, which is extremely unlikely in a gap-regenerating system. Plant *C*, although situated favourably for light at the scale of the dominants, is disadvantaged by the ground vegetation which will shade the seedling, and indeed which may take at least temporary advantage of the newly formed gap.

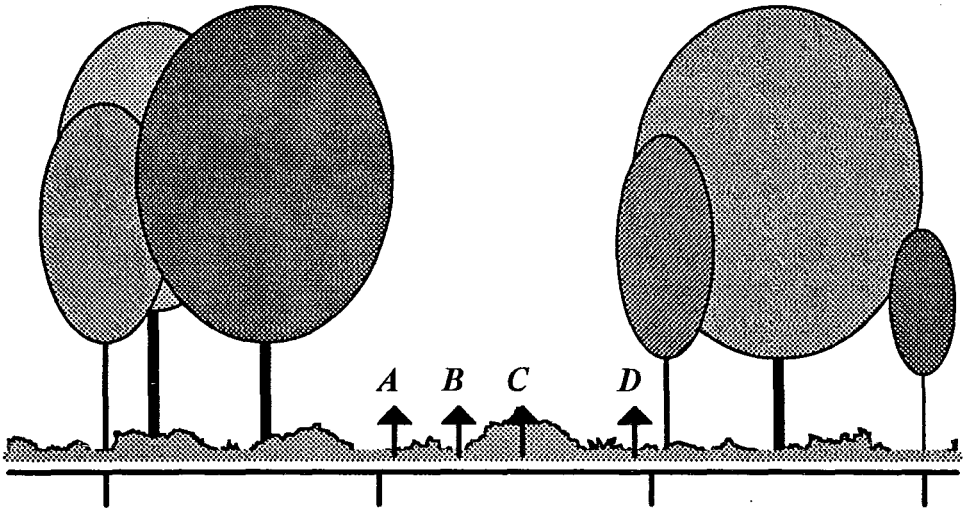

Figure 6.2. A forest "gap" with four competing seedlings.

"Ecospace" allows germination and establishment sites to be more precisely defined at a scale below that of the adult plant. It is assumed that the variation in microclimate and soil conditions is insignificant within a single tile. This requires that tile size be carefully selected for each system, although the variation in spatial relationships between systems is such that a general scaling rule would be inappropriate.

In the model the soil surface is scanned, (in function *germination()*) and for each tile the species which could potentially germinate in those conditions are recorded, and then germination is calculated stochastically in relation to the seed resources available below that tile. At present, due to the time considerations, no distinction is made between vegetative reproduction and seeds and each plant is treated as a separately rooting individual with the same pattern of development. It would be possible to model vegetative reproduction within the grid and this would be a desirable addition to the model, particularly as applied to heathlands.

Calculation of germination

Each tile is tested daily for each species to see if conditions are met for germination. Species specific minimum levels of soil moisture, temperature prehistory (using the adjustable prehistory function *hcalc()*, which allows a prehistory of between 1 and fifty days) at ground level, and irradiance and maximum and minimum daylight hours are tested against the state of corresponding variables in that tile (function *germ_gap()*). Where germination for a species is possible in a tile, the function *seedbank()* is called. Here the daily probability of germination for each species in the tile is calculated using the following expression:

daily probability of germination = *GERM*seedens[spe][x][y]*

where *GERM* is the proportion of the seedbank germinating per day (set constant for all species during initial model development),

and *seedens[spe][x][y]* is the seed density for a single species per tile.

At present, the model has no dynamic seed production and the number of seeds per tile is set as a constant. In addition to the species-specific seed densities, the variable *GERM* represents the proportion of the available seeds germinating in a suitable day. In the natural system, this proportion might be expected to change dynamically in response to germination site conditions.

It is then possible to generate new plants, which are initialised first as "juvenile" establishing individuals, local to a single tile, in the function *est_initialise()*.

6.3 Establishment of juveniles

Plants which have germinated pass through a stage of being establishing juvenile plants before becoming adult plants. Juveniles are defined more simply than adults and are limited to a single tile at ground level until they pass the threshold required to leave. Juvenile individuals are defined separately from adults for two reasons. Firstly, adults require the allocation of large amounts of memory space. Since the high rates of germination and mortality expected in establishing plants could result in the temporary presence of large numbers of juvenile plants, the resultant memory allocation could severely limit the computable grid size. The separate treatment of juveniles using a simplified version of the model for adult growth reduces this problem. Secondly, the early growth of seedlings is affected by the size of its seed reserves and developmental strategy of the species and might be expected to exhibit different properties from later growth. It was considered that a different allocation pattern or photosynthetic response might be appropriate at this stage, but at present production is calculated as for individuals, although all production is channelled into green leaves. The term "juvenile" as used in the model is defined simply as a non-adult plant and has no direct developmental implications.

Initialisation

Juvenile individuals are held in the array *estdens[i][x][y]*, where *i* is the establishing individual number in tile *x,y* at the ground surface *ztop_lit[x][y]*. Plants are defined as juveniles as long as they stay within a single tile. As soon as they pass *occtreshold[sp]* and become capable of growth into an adjacent tile they immediately become adults, and are initialised as adults in the function *indiv_initialise()*. The function *est_kill()* is then called to remove that juvenile individual from the arrays of juveniles.

When the function *est_initialise()* is called from the germination sub-model, an initial density, *seed_reserve[sp]*, representing the energy stored in the seed is immediately allocated to the *estdens[i][x][y]* array. A ten percent random variation about this value is used to represent variation in seed size and weight. *Estpress[i][x][y]*, the stress level of the establishing individual, is set to zero. The species number, carried in from the germination sub-model, is stored in the array *estsp[i][x][y]*.

Growth

The net production of juveniles is calculated using the same equations used for adults (see section 6.6), and then modifying this growth rate according to limiting abiotic factors. Species are assumed to have an optimum response to abiotic factors, and the limitations imposed by sub-optimal conditions are calculated for each factor and combined into a single multiplier (*p*). Net production is calculated as photosynthesis (function *est_photo()*) minus respiration (function *est_resp()*) as for the adult production model and the resultant value is multiplied by an index *p* representing abiotic limitations on growth.

Each species has a response curve to a number of abiotic factors: pH, soil moisture and potentially nitrogen and phosphorus. In the present state of the model, all species are set up to have no response to nutrient limitation or pH because these are not dynamically represented. Each curve is defined by three values, an optimum, a maximum and a minimum (e.g. *ph_opt[sp], ph_min[sp], ph_max[sp]*). These do not need to be regularly distributed, allowing asymmetrical response curves. Figure 6.3 shows the response curve increasing sinusoidally from the minimum to the optimum and decreasing sinusoidally to the maximum. At the optimum no limitation is imposed upon growth and this is represented as an index of one. The function *sindistribution()* returns an index in the range zero (no production) to one (maximum production) in response to a given input value. This index is then used as a multiplier to convert potential to actual growth.

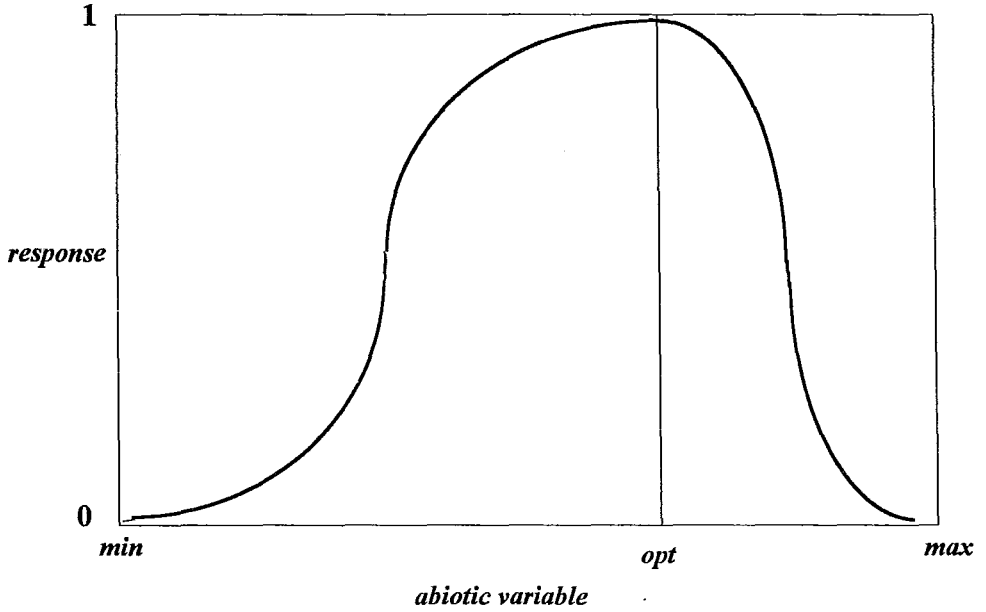

Figure 6.3. Species response curve as used in function *sindistribution()* to calculate limitations on growth due to abiotic limitation. The curve is defined by three points, a maximum, an optimum and a minimum. A response can be read off the y axis for a given value of the abiotic variable.

The function *sindistribution()* is called from a set of functions (*response_ph(), response_sm(), response_nit()* and *response_phos()*) used in *est_limits()*. These functions each return an index (*phmod, moistmod, nmod, pmod*) for a given value of their associated abiotic variable. For pH the input value is taken simply as the value of pH in the sub-surface tile. The other variables are resources and as such must be divided between competitors. The proportion of a resource available to an individual is calculated simply in proportion to the total occupation of that cell using the general formula:

$$\text{available resource} = \text{resource}[x][y][z] \times estdens[i][x][y]/competition$$

where *competition* is the total density of establishing individuals in that tile and z, the tile level is taken as *ztop_lit[x][y]*-1 for below-ground resources and "resource" may be any of the abiotic resources. At present a juvenile's responses are assumed to be directly proportion to the available resource per tile and the individual's requirements are not modelled.

The effect of limiting factors on species relative growth rate is calculated by a weighted average of two values. One value (*prodlim*) is defined as the single most limiting factor, i.e. the abiotic response index with the lowest value. The other (*prodmin*) is the product of all the limiting factors (i.e. *phmod*×*moistmod*×*nmod*×*pmod*). It was felt that neither approach could adequately describe the process in isolation. The weighting *LIMIT*, ranging from a value of zero (*prodmin* only) to one (*prodlim* only), was used to enable the flexible use of this approach. Thus

$$p = prodmin \times (1 - LIMIT) + prodlim \times LIMIT$$

where p is the index used as a multiplier for growth in the function *establishment()*. A value of *LIMIT*=1 was used for the simulations presented here.

All growth is converted directly to green leaf material and can continue up to a total tile density of *densmax[sp]*. When the density of an establishing individual passes *occthreshold[sp]*, the plant will move out of the single ground level tile and continue growth as a full individual. The function *indiv_initialise()* is called where the plant density transferred from the juvenile *estdens[i][x][y]* array to the adult *dens[indiv][tile]* arrays, all other individual arrays are initialised and the sub-grid co-ordinates of the individual generated randomly within the tile by the function *xyconvertB()*.

Stress-related mortality

The mortality of establishing individuals is calculated as a function of the total amount of stress experienced by the individual. Stress in the model results exclusively from a negative plant energy balance at present. It is a somewhat abstract concept, having no physical parallel in the real world, but is useful as a simplification of plant resistance to unfavourable conditions. Each species has a certain index of tolerance to stress (*press_tol[sp]*), being the number of days consecutive stress that species can survive. If the establishing individual's stress level, *estpress[i][x][y],* exceeds *press_tol[sp]* the plant dies and the function *est_kill()* is called.
Each plant starts life with *estpress[i][x][y]* set to zero. The value increases by one for every day when production is less than a species specific *min_prod[sp]* (currently set to zero for all species) or when soil moisture falls below the level required for germination (i.e. *if(moisture[x][y][z]<smoistgerm[sp])*). However, for every day that these conditions are not met, *estpress[i][x][y]* is decreased by one, allowing the plant to recover from periods of stress.

The productivity of plants as small as the establishing individuals can vary considerably from day to day, and model plants rarely remain energetically feasible for long enough to be initialised as adults. Consequently it is necessary to increase the value of *press_tol[sp]* so that the individuals are extremely tolerant to negative net growth. This approach seems to be mechanistically unsatisfying. An approach using a sugar pool similar to that used in the adult individual model might be appropriate, but this would involve the definition of another array, and would be finely balanced due to the small size involved, such that utilisation would need very careful modelling.

6.4 Overview of adult growth

Juvenile plants which have grown large enough to extend out of a single tile are initialised as adult individuals, which can occupy any number of tiles in the spatial grid. These individuals grow mechanistically and partition assimilate spatially.

It is necessary to define the term "individual" as used in the model (see also sections 3.3.& 3.4). An individual is a plant which grows essentially independently of other plants. This definition can include a separate individual originating through vegetative propagation where adventitious rooting occurs, although adequate representation of this process would

require a modification of the germination and establishment routines. It has been shown that vegetatively reproducing *Calluna* can establish in a broken canopy where germination of *Calluna* seeds will be unsuccessful (Miles, 1981).

Individual plants in the model are grown according to the conditions local to the tiles which they occupy. Net production (section 6.5) is calculated hourly for each occupied tile according to the empirically-derived model of Grace and Woolhouse (1974, also Grace, 1970) for the production of *Calluna* in an upland bog community. The net sugar production is added to a non-spatial sugar pool, (*storage[indiv]*), from which a certain proportion is partitioned (section 6.7) into leaf, stem and root material. Each component is converted into units of *dens[][][]* and applied to the grid using the spatial growth model (section 6.8) according to the individual's growth form.

6.5 Photosynthesis and respiration

Production is calculated for each tile according to the empirical production model of Grace (1970; Grace & Woolhouse, 1974) which was derived from laboratory measurements of the responses of separately rooted heads of *Calluna* collected from the field site. The model is driven by temperature, temperature pre-history, light and leaf age. As such it is responsive to the variables generated in the microclimatic sub-model. However, it was developed entirely through work on *Calluna* in a bog community and so may not reasonably be extended to other species or systems and this compromises the generality of the model. Although C 3 photosynthesis is common to most heathland plants, other physiological differences e.g. partitioning, phenology, may be expected to give species specific response surfaces.

The more mechanistically-based biochemical approaches to photosynthesis (Farquhar *et al.*, 1980; Farquhar & von Cammerer, 1982; Friend, 1995) were considered. However, these models rely on adequate model description of limiting leaf physiological characteristics, which in the absence of a water sub-model are not present in "Ecospace". An approach based on these more general equations would be a desirable future addition to the model once other aspects of the model have been brought up to a similar level of detail, although a number of empirical species specific parameters would still need estimating for both CO_2 assimilation and respiration. Our present understanding of these processes is such that it is not possible to account mechanistically for differences in production between all but a few well-studied species.

Given that *Calluna* is the dominant species in the heathlands for which the model was initially developed, the *Calluna*-based production seemed a useful starting point. The model structure has been developed in order to allow the input of alternative production models, by substituting a new production function. It was initially planned to also use the studies of Grace (1970) on *Sphagnum rubellum* Wils. (*S.capillifolium*) production, but this model is considered by the author to suffer from significant experimental error.

In order to account for some of the differences in photosynthetic response between species, as a temporary measure, it was decided to alter the input values to the production model. Thus, for example, the effective optimum temperature (*temp_opt[sp]*) for a species other than *Calluna* can be raised by reducing the input temperature (*tt*) to the production using the difference between *temp_opt[sp]* and *temp_opt[calluna]*.

$$tt = tt + (temp\_opt[0] - temp\_opt[sp])$$

Light saturation may be altered in a similar way (using *lt_opt[sp]*). This approach has limitations in that it may only be applied within a narrow range of species with responses similar to *Calluna*, and can only describe species in an approximate way. However, it may be expected that most species in a given community will have similar metabolic responses in order to survive in the same area, although it may be the differences in their responses which account for differences in their spatial distribution. Maximum deviations of 1 °C in *temp_opt[sp]* and 50 W m^{-2} in *lt_opt[sp]* from the optima for *Calluna* are permitted in order to limit error. This severely limits the application of this function. A stricter representation of production using species-specific response surfaces would be required for any species with a greater variation from the *Calluna* response surface.

The resultant net production is corrected for different species-specific amounts of photosynthetic tissue present per unit volume of leaf by multiplying by a factor *p_fract[sp]*.

Photosynthesis and respiration are controlled from the function *growth_gen()*, (called from *indiv_master()*) which calls the functions *photosyntheather()* and *respiration()*. These functions use the revised equations (Grace & Woolhouse 1974) such that net production in terms of CO_2 assimilated (μg g^{-1} min^{-1}) can be calculated hourly as the difference between gross photosynthesis and respiration (P_g-R). The CO_2 assimilated is multiplied by a conversion factor (0.75) to convert to plant dry weight. This conversion factor is likely to vary over time according to season, nutrient conditions and plant structure in the real system (Grace, 1970).

The regression equations used are as follows.

Gross photosynthesis:

$$P_g = \exp(q_1 \times tt + q_2 \times tt^2 + q_3 \times hh + q_4 \times hh^2 + q_5 \times A + q_6 \times A^2 + q_7 \times F + q_8)$$

where

$$q_1 = 0.4758 \times ll - 0.3608 \times ll^2 + 0.01879,$$
$$q_2 = -0.01212 \times ll + 0.0112 \times ll^2 - 0.000208,$$
$$q_3 = 1.943 \times ll - 3.5439 \times ll^2 - 0.1628,$$
$$q_4 = -0.278 \times ll + 0.5257 \times ll^2 + 0.03511,$$
$$q_5 = -0.09259 \times ll + 0.1663 \times ll^2 + 0.006079,$$
$$q_6 = 0.000171 \times ll - 0.00031 \times ll^2 - 0.0000141,$$
$$q_7 = 5.348 \times ll - 9.130 \times ll^2 - 0.6831,$$
$$q_8 = 22.588 \times ll - 45.885 \times ll^2 - 0.5463.$$

Respiration:

$$R = \exp(0.09196 \times tt - 0.009633 \times A + 0.00001625 \times A^2 + 0.2116 \times F + 1.1927).$$

In the above equations;

tt is the temperature in °C (*tt = temp[x][y][z]*),

hh is the mean previous temperature (temperature prehistory) in °C (*hh = hcalc()*), see below,

A is the shoot age measured in days from budbreak (*sshoot_age[indiv]* and *lshoot_age[indiv][tile]* for short and long shoots respectively),

F is the flowering index, 1 = flowering, 0 = not flowering (*flower[indiv]*),

ll is the PAR per tile in W m^{-2} (*ll = lvar()*, i.e. hourly value of *lt[x][y][z]*).

The temperature prehistory term used here differs from that used by Grace. In the original study temperature prehistory was calculated as a thirty day moving average from climatic records apparently both before and after the day of calculation. In the present study future results are not available, and moreover it is not reasonable to assume that a plant's growth may be affected by future weather. A thirty day moving average is calculated by the function *hcalc()*, for the thirty days immediately prior to the day of calculation from the values of *temperature[2]* (i.e. half daily max. + min.) stored in the array *htemp[ago]* by the function *temp_record()*.

Input values for the above equations are checked against each other for combinations outside the range of the experimental conditions used to generate the regression equations (see Grace 1970, sub_routine PHOTOSYNTHESIS). Where necessary, the input values are

rounded up to the nearest tested input value (function *phot_inputs()*). Since the regression model was developed over a wide range of conditions it is unlikely that any significant error would result from this approach, especially since production is close to zero at the limits of the study. A trap is used in common with the original model, setting net production to zero for cold nights.

Net production is calculated hourly, using the average conditions for that hour of the day, as generated by the function *temp_regime()* (called from *indiv_master()*) and *lvar()* (called from *photosyntheather()*). Values generated are in units of $\mu g\ g^{-1}\ min^{-1}$ CO_2 assimilate and are multiplied by a factor of 60 to convert to hourly values. This value is then scaled according to mass of leaf material per tile and the production of each tile summed to give a whole plant value ($\mu g\ CO_2$).

An option, not currently exercised, is provided to limit production in the same way as for establishing individuals, (see section 6.3) in the function *soil_limits()* (called from *growth_gen()*). Effects of sub optimum pH, soil water, nitrogen and phosphorus are modelled as sine responses, and an approach using a weighting *LIMIT* for the relative contributions of the single most limiting factor and the combined limits is used. At present, pH, water, nitrogen and phosphorus are not modelled dynamically, and although the static distribution of these soil properties could be used to investigate competition in different conditions it was considered that the model must be validated for a range of simple conditions and scenarios before introducing additional factors.

The CO_2 assimilate ($\mu g\ CO_2$) thus generated is converted to grammes by division by 10^6 and then to grammes dry weight plant material by multiplying by a conversion factor, as described above, currently set constant at 0.75 (after Grace, 1970). The resultant growth is accumulated on a weekly basis in *growth[indiv]*, which is forwarded weekly to the function *grow()* for partitioning and spatial growth.

6.6 Assimilate partitioning

The net production for each individual per week must be allocated to different parts of the plant. The carbohydrate is first taken to the non-spatial storage pool, where a proportion is stored and a proportion utilised. A proportion of the utilised carbohydrate is used for wood production and a proportion for leaf material. These are then sub-divided into roots and stems, wood and leaf, and short and long shoots non-spatially before being applied to the tiles (Fig.

6.3). For simplicity, a single model for partitioning was developed, on the basis that the same principles apply, even though the partitioning coefficients and indeed the precise definition of the plant material types may differ between species.

The partitioning of weekly growth as described above is controlled by the function *grow()*. Storage is dealt with as in the model of Grace (1970). Firstly, the function *store()* is called to return the weekly growth in units of *dens[][][]*. Here, *growth[indiv]* is added to *storage[indiv]* (total sugar pool in grammes). Since net growth may be negative, this may result in a reduction in the sugar pool. Should the stored sugar fall below an arbitrary low value then the individual becomes stressed (see section 6.7). Provided there are sufficient

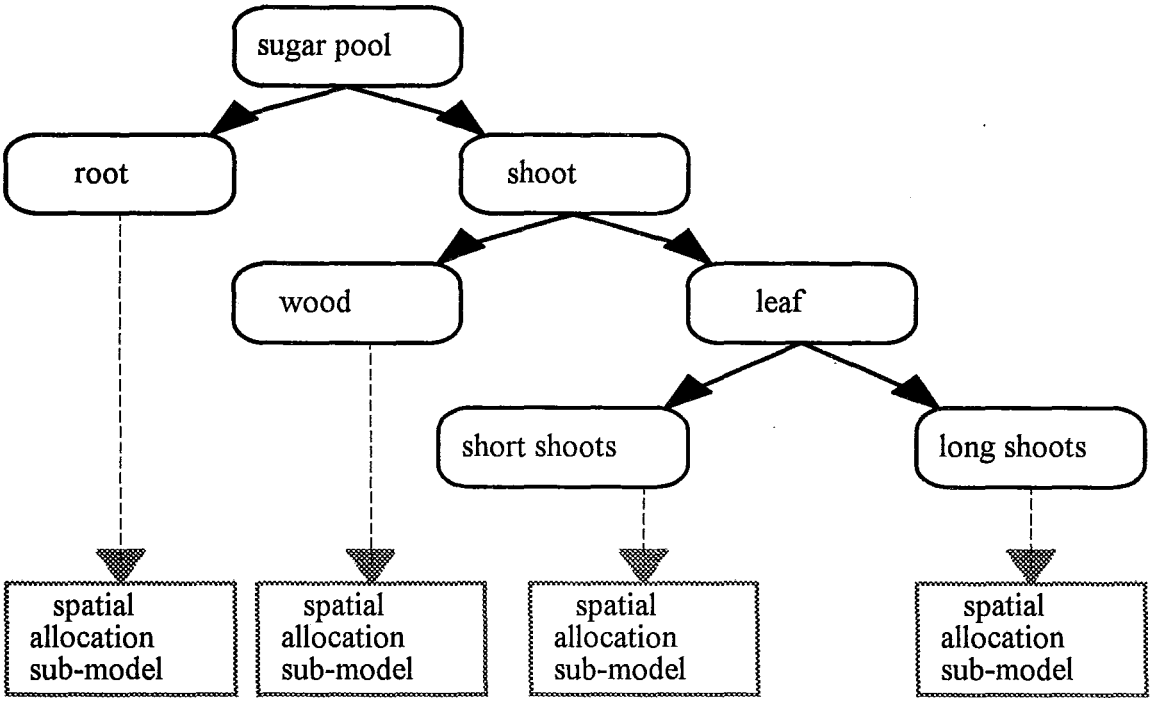

Figure 6.3. The fate of assimilate stored in the sugar pool, showing the order of partitioning. The growth for each of the four end categories is applied separately to the spatial grid.

resources a constant species-specific proportion, *utilise[sp]*, of *storage[indiv]* is taken from the store and converted to growth (*util*). Thus

$$storage[indiv] = storage[indiv] + growth[indiv]$$

$$util = storage[indiv] \times utilise[sp]$$

In the model, the returned value (*util*) is stored in the array *growth[indiv]*, at this point holding the new growth to be applied in grammes carbohydrate. This array is used to hold the growth increment for each individual for a number of different time scales and units. For clarity this array will henceforth be subscripted.

$$growth[indiv]_{whole\_plant} = util$$

This is carried into the function *partition()* which divides the growth between the different vegetative components according to the partitioning of photosynthate estimated by Grace and Woolhouse (1973).

A constant ratio, *rs_ratio[sp]* (currently set at 50%) is used to allocate the growth increment between roots (*rootgrowth*) and shoots.

$$rootgrowth = rs\_ratio[sp] \times growth[indiv]_{whole\_plant} / masswood$$

$$growth[indiv]_{shoots} = growth[indiv]_{whole\_plant} - rootgrowth$$

At this stage, the function *rootgrow()* is called to apply *rootgrowth* as an increase in the root volume, converting the growth in grammes to units of *dens[][]*, by dividing by a conversion factor *masswood* (0.00356879).

As shown in figure 6.3, the remainder of the sugar to be utilised is allocated to either leaf or woody material. The ratio of assimilate allocation between woody material and leaf material is expected to change with time after budburst. Grace and Woolhouse (1973) describe the variation in utilisation for wood and leaf in *Calluna* after budburst as moving from 100% leaf at budburst down to 33% at around 7 weeks after budburst and rising again. Such a significant variation renders a constant ratio based partitioning approach inappropriate. The relative proportions allocated to root and shoot for the first fourteen weeks following budburst are held in the array *wl_ratio[sp][week]* after which the ratio is assumed constant (for species other than *Calluna*, care should be taken, since most will not have a woody component above ground, but will need to partition towards woody material for the roots). The weekly growth of leaf material in units of *dens[][][]* is given by

$$leafgrowth = wl\_ratio[sp][week] \times growth[indiv]_{shoots} / masshoot$$

where *masshoot* is a conversion factor (0.0065895) for grammes dry weight to *dens[][][]* as determined in the field studies (Appendix I). *Growth[indiv]* here represents the growth in grammes after root allocation. The surplus growth is allocated to *woodgrowth[indiv]*, using a conversion factor *masswood* (0.0035687).

The above ground growth increments are dealt with separately, with leaf material processed by the function *greengrow()* and wood in *woodgrow()*. Both functions use the spatial growth sub-model described below (section 6.8), differing only in the method used for the calculation of potential spatial allocation.

6.7 Mortality

Death occurs when a plant becomes physically or chemically damaged (disease, herbivory, trampling, poisoning etc.), when the plant becomes too old, or when a plant has insufficient access to the resources required for maintenance. In the "Ecospace" model, all three types of mortality are represented. The first two types of mortality are represented by simple stochastic processes in the function *mortality()*, whilst the third type is linked to the production model such that when an individual loses most of its sugar pool it becomes increasingly stressed. In all cases, a living individual has a value of *life[indiv]*=1, which is converted to zero if mortality is successful.

Stochastic mortality

The stochastic mortalities take two forms. The first form representing all random age-independent factors is set at a constant daily probability of 1/60000 for all species. This is a low rate which would result in an unrealistic average life span of 164 years in the absence of any other mortality.

Age-dependent mortality is calculated according to the individual's ageclass (*ageclass[indiv]*). Plants enter a period of senescence (gradual cellular decline) at a certain characteristic age (Leopold, 1961, 1980). This has certain effects on the plant, with reduced efficiency leading to increased mortality and changing balances of plant growth substances altering plant behaviour. The function *classify_age()* keeps track of each individual's ageclass which is advanced according to species-specific ages held in *class[sp][aclass]*. These age classes could potentially be used to control the growth characteristics of each individual

according to an approach similar to that of Noble and Slatyer (1980; Hobbs *et al*, 1984). At present, however they are used solely to determine the onset of senescence.

The function *senesc_test()* is called, which returns a value, *stest,* having a value of 1 if the plant has passed the ageclass *senesc_age[sp]*. A senescing individual is considered to have an additional probability of mortality defined as 1/*dietime[sp]*, which is applied only at this stage of its life. Because this is a constant rate, *dietime[sp]* is twice the average number of days survival after becoming senescent excluding other forms of mortality. Since this is a probability it is possible for some individuals of the same species to last considerably longer than others.

Stress-dependent mortality

Stress-dependent mortality is calculated in the function *store()*, when the weekly net growth is added to the sugar pool. Each species has a stress tolerance of *stressdays[sp]*, defined as the number of consecutive days an individual can survive with no surplus carbohydrate. This is measured against the number of consecutive days each individual has been without surplus, *storeshort[indiv]*. For each week that the individual has a sugar pool *storage[indiv]* less than an arbitrarily selected 0.01 g, *storeshort[indiv]* is increased by seven days. When *storeshort[indiv]* becomes greater than *stressdays[sp]*, the individual is subject to a fifty percent chance of mortality. Importantly, should the individual produce enough carbohydrate to ease the stress (i.e. *storage[indiv]*>0.01) the value of *storeshort[indiv]* is reduced by seven days, such that it is possible for a plant to recover from a period of stress. This approach is designed to imitate stress-tolerant strategies such as short periods of dormancy and recovery of material by the sacrifice of leaves.

Once an individual has died and has a value of *life[indiv]*=0, it is not permitted to grow further, although the dead plant still persists as a structure. In the case of an old *Calluna* plant this structure will continue to have a significant effect on the surrounding microclimate. One need only visit a patch of heather burnt several years ago to see the persistence of those woody stems which have survived the fire. Dead plants provide shelter, soil stability and a structure upon which smaller plants (e.g. *Cladonia sp.*) may grow. This is an important spatial property of dead plants very often overlooked in ecological models, in which plants very often are assumed to decompose instantly. This has probably arisen out of the agricultural and forestry basis of most vegetation models, where, in the first case there will be little persistence, and in the second case the dead tree will be removed by the forest manager.

A notable exception is the patch dynamics model of Boersma, van Schaik and Hogeweg (1991) in which dying trees are modelled as falling to the ground, possibly killing neighbouring trees.

In the "Ecospace" model, dead plants are converted directly into above-ground litter, and are henceforth dealt with by the litter sub-model (section 6.10). In order to capture the effects described above, living plant material converted into litter (either as a result of whole plant death or local leaf loss) is initially allocated to its tile of origin. Consequently, above-ground "litter" structures can be created. These structures then decompose over time, falling to the ground where they are added to the ground-litter layer

When the dead individual is reduced to its last tile, the option arises to remove the individual and update the array of individuals using the function *indiv_remove()*. However, provided the model is not run for long enough for the maximum number of individuals (*SETINDIV*) to be reached, it is desirable that the individual arrays remain as they are, so that individuals retain the same number throughout the simulation and no new individuals adopt the number of a deceased individual. The defined option *ATOPT* is used to switch between *indiv_remove()* (*ATOPT*=1) or simply setting *nptile[indiv]* (number of potential tiles) to zero.

6.8 Spatial growth

Overview

The spatial growth sub-model allocates the weekly growth increment for each individual to the three-dimensional spatial grid. Individual plants grow a certain amount per week, all of which must be allocated to the individual during that timestep. In order to ensure that this is the case, the development of individuals must be flexible to allow for limitations on spread in certain areas of the grid.

The addition of growth is carried out in three stages, with all individuals being processed in parallel.

i).Potential growth (function potentialindivgrow())

Firstly the ideal spread of an individual to each tile (*potdens_overlap[indiv][tile]*) is calculated on the basis of calculated growth assuming the absence of spatial limitations,

according to the controlling factors for each species. All growth is notionally allocated to selected tiles within the grid.

ii). Application of potential growth (function appliedindivgrow())

This potential growth is then applied to the existing plant structures. Where there is space, as much of the potential growth per tile is allocated as actually possible. Where there are limitations on growth, spatial competition occurs. Growth which is not actually allocated is recorded as the total surplus growth per plant, *rdensum[indiv]*.

iii). Recursive application of surplus (function surplusindivgrow())

An attempt is made to apply this surplus growth to a new set of locations randomly distributed over the plant volume. The surplus is recalculated and the process repeated until all the growth has been applied.

A more detailed explanation of each stage is presented below. This process is used separately for the treatment of leaf material (controlled by function *greengrow()*) and wood material (controlled by function *woodgrow()*). This minimises the requirement for large temporary arrays. The two approaches differ only in the rules for the calculation of potential growth, with wood being allocated in direct proportion to the relative occupation of each tile, such that it may only be potentially allocated to tiles which have already been selected by the leaf allocation procedures. This seems to be a reasonable approach, since wood tends to develop from leafy stems and not advance in the absence of leaves.

The definition of the grid structure is such that the grid fills all space in the system. Consequently it is not possible for a plant to spread into a tile which has no neighbouring tiles occupied by that individual. This would have no real-space parallel, since all individual plants can only grow as a contiguous mass. A level, *occthreshold[species]*, is used to describe the minimum amount of vegetation required by a species in a single tile to support occupation of a neighbouring tile. *Occthreshold[]* may be lower for a species spreading by thin straight tendrils and higher for a plant growing as a dense mass.

Potential Growth

The potential growth of wood and leaf material are treated separately as described above. The wood increment is simply divided between all tiles occupied above an arbitrarily selected density of 200.0, using the equation

$$ddens\_overlap[indiv][tile] = woodgrowth \times dens[indiv][tile] \,/\, dsum$$

where *ddens_overlap[indiv][tile]* is the growth increment in units *dens[][]* per tile,
woodgrowth is the total woody growth for that individual per timestep,
and *dsum* is the sum of *dens[indiv][tile]* for all tiles above the threshold 200.

Leaf material, which must be present before wood material can be deposited in a tile, is distributed strictly according to growth form as follows:-

i) Central stem limited growth (gform[0])

This growth form develops as a series of stacked discs, each with a certain radius and thickness. Each individual has its trunk in a specific position, and the point of intersection of the trunk with the lower surface of a given *z* layer is represented by *Xcent[indiv][z]* and *Ycent[indiv][z]*. (At present, all trunks are assumed to be vertical). A new radius and thickness must be calculated for each *z* layer. The function *shoot_share()* is used to divide *growth[indiv]* between layers already occupied, recording results in *zgrowth[indiv][z]*. For leaf material this division is allocated in proportion to the amount of short shoots in each *z* layer, such that

$$zgrowth[indiv][z] = leafgrowth \times ss[z] \,/ sstot$$

where *leafgrowth* is the total growth of leaf material for that individual,
ss[z] is the total short shoots in that z layer,
and *sstot* is the total number of short shoots in the whole plant.

For each *z* layer occupied, *zgrowth[indiv][z]* is converted into a radial increase (added to *rsq[indiv][z]*, the radius squared for that level) and a vertical increase (added to *discthick[indiv][z]*, the disc thickness for that level). This process is carried out in the

function *shoot_disca()* called from *shoot_share()*. Growth is first divided between horizontal and vertical growth according to the species-specific ratio *hv_ratio[sp]*, such that

$$vgrowth = hv\_ratio[sp] \times zgrowth[indiv][z]$$

and $$hgrowth = zgrowth[indiv][z] - vgrowth$$

where *vgrowth* and *hgrowth* are the amount of growth allocated to vertical and horizontal growth respectively. These are then applied as growth increments:

$$rsq[indiv][z] = rsq[indiv][z] + \{hgrowth \times DCON / (CONVERT \times \pi \times densopt[sp] \times discthick[indiv][z])\}$$

where *DCON* =10000 is the maximum number of units dens[][] allowed per tile,
CONVERT = 3846.153 is a constant for the conversion of *dens[][]* to sub-grid area,
and *densopt[sp]* is the optimum vegetation density for the species.

$$discthick[indiv][z] = discthick[indiv][z] + vgrowth / (CONVERT \times \pi \times rsq[indiv][z])$$

When the thickness of a disc has increased above the fraction *occthreshold[sp]/DCON* (i.e. the disc equivalent of passing *occthreshold[sp]*, allowing spread to the next layer) the proportion *newgrow[sp]* is used to divide growth between that *z* layer and the layer above such that

$$zgrowth[[indiv][z+1] = zgrowth[indiv][z+1] + vgrowth \times newgrow[sp]$$

and the remainder is applied as above.

The function *overhex()* is now called to generate the overlap of the disc with updated radius over each hexagonal tile in that layer, *potvol_overlap[x][y][z]*. This is then scaled to a percentage overlap per tile occupied by the individual (*potdens_overlap*) and the temporary array *nptile[indiv]* (the potential number of occupied tiles per individual) used in the place of *nntile[indiv]*, (the actual number of occupied tiles per individual) , to hold the number of potential new tiles. Since it is assumed that there is some form of radial branching structure constraining the individual to circular growth it is also assumed that this structure will potentially allow the individual access to all tiles covered by the disc. The rule limiting occupancy of neighbouring tiles to those with occupied neighbours is not being broken here,

since potential growth only is being defined. The occupancy rule is only used when potential growth is converted into actual growth.

Figure 6.4. overleaf shows the development of an individual of this central stem limited growth form under accelerated growth using a simplified version of the model (see standard runs, Chapter 7). The figure covers two pages, with Fig.6.4a covering the lower 3 layers and Fig.6.4b the upper 3. To the left is shown the individual after 500 days simulation (starting from a disc radius 1.05 *h* in level 1), whilst to the right is shown the same individual after a further 500 days growth. The Figure is at a scale of 1: 11.3 as printed, with a real tile side length of 0.05 m. A grey scale (top right) is used to represent the total plant volume (*dens[][][]*) per tile.

The circles laid over the graphs show the radii of the disc in each layer. Although the process of allocation may cause this disc to cover unoccupied tiles, the reverse would not be expected in the absence of competition. As can be seen, all the densities lie within the range expected from the area of disc overlap. It is interesting also to note how the allocation of growth between layers according to short shoot position has allowed the growing plant to move from a pyramidical form towards a more complex form with a narrowing in level 2. The plant dimensions at 1000 days are diameter: 0.19 m, height: 0.30 m, which seems a little tall, although possible. The overall form of the plant is flexible and may be adjusted by the variables mentioned previously.

ii) Tile-based growth (gform[1])

In this growth form, the plant is allowed to spread independently of any structure other than the hexagonal tiles, by direct occupation of tiles adjacent to those already occupied. The grid is scanned to find those tiles which,

a) are already occupied by that individual;
or b) have an occupied neighbour of that individual;

and these are filled according to species specific rules of spread.

The function *nextscanA()* is used to check the immediate neighbours in both the horizontal and vertical dimensions (held in the array *nexthex[][][]*) of a given unoccupied tile for occupancy according to the rule limiting individuals to contiguous tiles. All available tiles abutting the individual are recorded in the arrays *x/y/zavail[indiv][count]*, where *count* is the total number of new tiles available to that individual.

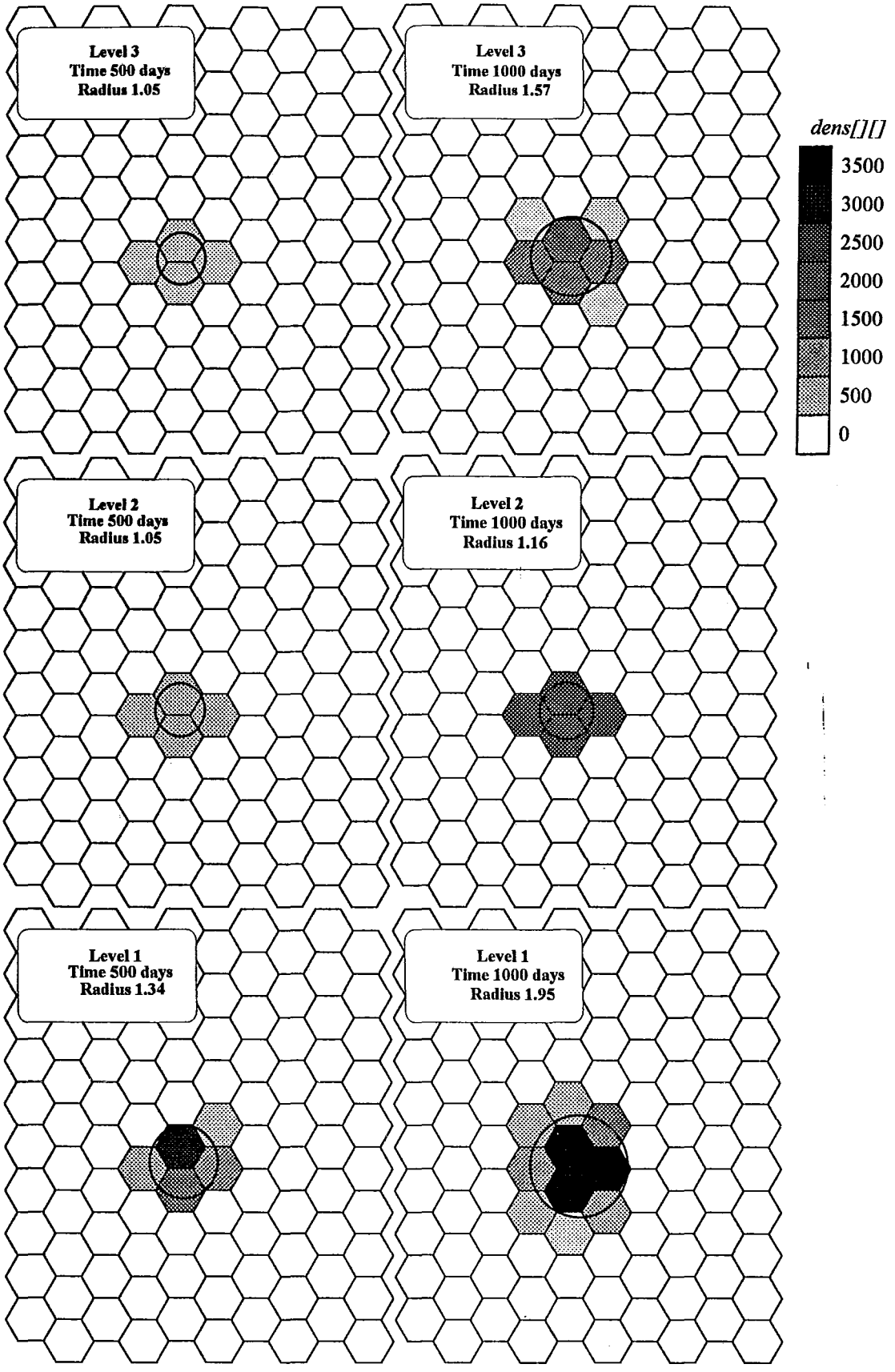

Figure *6.4a*. The development of an individual of *gform[sp]=0* over time. Scale 1:11.3.

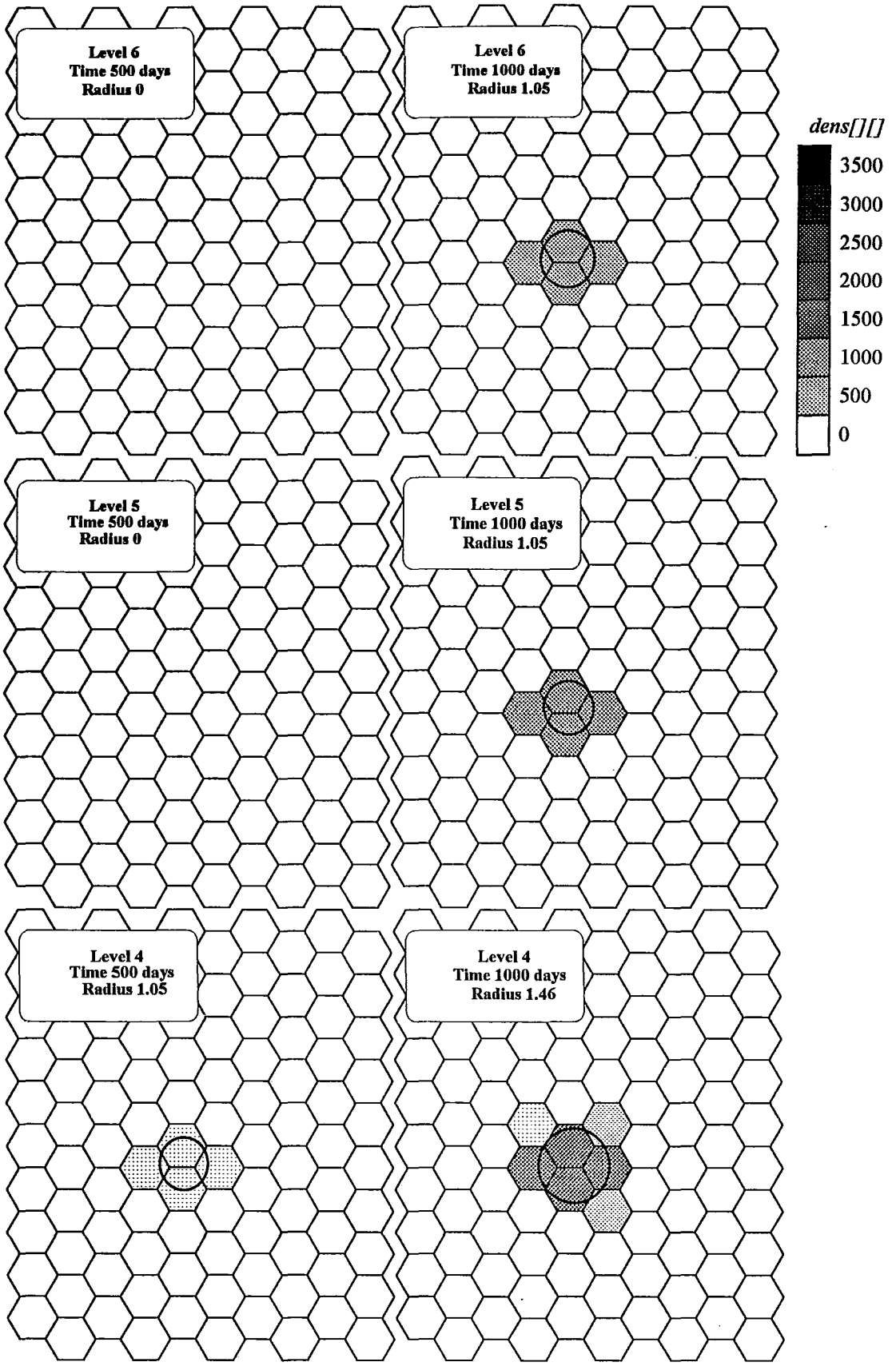

Figure *6.4b*. The development of an individual of *gform[sp]=0* over time. Scale 1:11.3.

A species-specific proportion (*newgrowth[species]*) of *growth[indiv]* is then divided between those tiles already occupied and a species-specific proportion (*spreadfactor[species]*) of the available tiles. These two variables may be varied in order to represent different plant strategies. A low value for *newgrowth[]* could represent a conservative, spatially dense strategy whereas a high value would allow rapid, sparse growth. *Spreadfactor[]* allows for a continuum of strategies for the occupation of new space, varying from a concerted effort in a single direction in a given time step to an even spread of growth around the circumference of the plant similar to radial growth. The proportion *spreadfactor[]* of the available space is selected randomly from the *x/y/zavail[][][]* arrays.

A further variable, *lingrow[sp]* is superimposed on this system. The available hex tiles are sorted into those abutting only a single tile occupied by the same individual and those abutting more than one (*x/y/zduplicate[][][]*). The proportion *lingrow[]* is the relative proportion of these two classes of tiles selected. This may be viewed as a simple way of describing growth strategies, where a high value of *lingrow[]* will result in a strategy of growing towards open space, and a low value a strategy of space conservation. The relationship between *lingrow[]*, *spreadfactor[]* and *newgrow[]* is important, and care must be taken when selecting these proportions in order to represent an actual species. For example, it is likely that a plant predisposed towards growing into new space will invest a larger proportion of its growth into this new growth than a plant with a conservative strategy. In the present version of the model, these variables were varied until *Calluna*-like forms developed in the initial growth stages. However, it would be possible with more rigorous spatial field measurements to calibrate these variables better.

The results of these selections are recorded in the array *potdens_overlap[indiv][tile]* as for growth form 0.

iii). Phototropic tile-based growth (gform[2])

As for *gform[1]* above, this growth form spreads directly through the grid of hexagonal tiles. However, in this growth from an attempt has been made to make the plant shape more self-determining by applying growth where the light is the brightest. Unfortunately development of this growth form has been hindered by the slow running time of the light model, which is required to calculate light for tiles adjacent to the occupied tiles for this growth form in addition to those occupied.

Each tile is assumed to be only able to spread into a limited number (*spreadfactor[sp]*) of its eight neighbours, thus giving increased significance to the selection of appropriate tiles. At each point a selection is made for a new tile, the lightest tile is chosen. At all other points in the individual's growth, fresh growth is applied to all tiles in proportion to both the light and density of short shoots. The growth form is controlled by the function *potformtwo()*.

When no new tiles are being selected, the total short shoots (*ssum*) and the total light (*lind*) for the whole plant are recorded. Two variables *dgr*, and *lgr*, representing the division of growth between all tiles on the sole basis of one method or the other are calculated as

$$dgr = growth[indiv] \times sshoot\_dens[indiv][tile] / ssum$$

$$lgr = growth[indiv] \times lt[x][y][z] / lind$$

A weighting *ltweight[sp]* is applied such that a weighting of one applies all growth according to *lgr*. This result is averaged with even spread in order to limit the impact of this growth form. Thus

$$potdens\_overlap[indiv][tile] = dens[indiv][tile] + ((lgr \times ltweight[sp] + dgr \times (1 - ltweight[sp])) + (growth[indiv] / ntile)) / 2$$

Selection of fresh tiles is carried out in the function *occtrigger()* called from within *dens_update()* just before the addition of new growth (*ddens[indiv][tile]*). A new tile is triggered when the occupation of the tile of origin passes a certain threshold, *thresh*. *Thresh* is incremented in steps of *(densopt[sp]-occthreshold[sp]) × spreadfactor[sp]* from the minimum *occthreshold[sp]*. If *dens[indiv][tile]* is less than *thresh* and *dens[indiv][tile] + ddens[indiv][tile]* is greater than *thresh*, a new tile will be selected. The function *nexthextwo()* is called, and the lightest tile unoccupied (by that individual) is returned and initialised.

In this way, the growth form allocates its growth towards the light. However, because the growth form requires the calculation of the light environment in all tiles rather than those occupied, since otherwise all unoccupied tiles are assumed to have a uniform illumination, development of the form has been hindered by time constraints. Although spread can initially be seen to occur in the direction of light, as more tiles become occupied the form becomes indistinguishable from growth form one, the tile-based form. Careful balancing of the rate of spread, microclimate and the relative directional allocation of resources is required in order to generate more phototropic behaviour.

Conversion of potential growth into actual growth

Now that the potential growth has been calculated for each growth form, and is represented for all forms as potential densities per tile, all the growth forms can be calculated using the same method. The potential growth for all the individuals can be compared with the available grid space and applied where possible, leaving a surplus where space is limiting. The *potdens_overlap[indiv][tile]* arrays are converted into incremental arrays *ddens_overlap[indiv][tile]* by subtracting the amount of material already present (*dens[indiv][tile]*) for all individuals, by calling the function *ddensgenerate()*. These arrays can be used to calculate the relative amount of pressure, (assumed to be proportional to the amount of vegetative matter each individual is attempting to grow into a given tile) being applied by each individual to each tile. Although there is no competition index as such in the model these relative pressures have a very similar function at the level of the single tile. Competition must occur for space where space itself is limiting in a tile and the model has already calculated potential growth. Living plants do not compete for space directly, but by local allocation of resources in response to directional stimuli. In order for a model to be theoretically consistent with these responses it is necessary to include a modelled version of these responses. The grid-based structure of the "Ecospace" model allows conditions at each point in space to be represented, and is thus well suited to the modelling of directional growth responses. The phototropic tile-based growth form (*gform[2]*) is an attempt to capture this.

For individuals of growth form 0, dome limitations are applied at this stage through the function *pressuredome()*. The dome form, which affects more than one individual of growth form 0 at once, will be described in section 6.9.

The arrays *ddens_overlap[indiv][tile]* are carried into the function *appliedindivgrow()*. In this function the grid is scanned, and potential growth applied to each tile separately. Firstly, the amounts of available space (*available_d*) and the amount of pressure from all individuals (*ddensum*) in each tile are calculated. The pressure from each individual is checked for validity using *nextscanA()* as before.

Where potential growth is less than the available space, all growth is allocated without question. However, when potential growth is limited by availability, the relative proportions of each competing individual to be allocated to that tile have to be calculated. This is done on the basis, as stated above, that pressure is proportional to the size of *ddens_overlap[indiv][tile]*, and the available space is divided proportionally amongst all competing individuals such that

ddens[indiv][tile]= ddens_overlap[indiv][tile](available_d / ddensum)*

where *ddens[indiv][tile]* is the incremental density for each tile.

The amount of potential growth which has not been allocated by each individual is summed and recorded in *rdensum[indiv]*. The sum of *rdensum[indiv]* for all individuals is returned as *surplusum* (the total amount of growth which is not allocated to tiles within the function). Where *surplusum* is zero, growth allocation for all individuals has been successful.

Addition of surplus growth

The function *surplusindivgrow()* is called where *surplusum* is greater than zero, to apply all surplus. Surplus growth (*rdensum[indiv]*) is that growth which has not been allocated within the prescribed growth form for each individual. According to the rules of the model, this growth has to be allocated at some point in the grid, since the plant has produced that much growth. A decision here needs to be made as to the route towards this application. There is no direct parallel of this situation in living plants to be used as a guideline. A new set of potential densities in a new set of tiles must be calculated, and competition for space worked out as before.

In an early version of the model, radial growth was again incremented for growth form 0, but it was found that where barriers to growth occurred in *appliedindivgrow()*, the same barriers frequently prevented growth in *surplusindivgrow()*. Given the amount of work involved in each calculation of radial growth it was decided that, if the ideal radial form had been thwarted, the plant could be assumed to apply its growth elsewhere. All growth forms are thus treated identically at this stage, and the variable *spreadfactor[sp]* is used to select a proportion of suitable hex tiles.

It was decided that growth in these circumstances should be allowed at all points around the surface of the plant and within the plant which still contain vacant space. Using *nextscanA()*, the arrays *x/y/zavail[][]* are filled and *rdensum[indiv]* divided amongst a proportion *spreadfactor[]* as in *potindivgrow()*. The same competitive rules are used as in *appliedindivgrow()* and *surplusum* is recalculated. The process is repeated until there is no surplus growth. After three loops, it is assumed that there is some problem limiting growth so *spreadfactor[]* is ignored and all available tiles are used.

Since the growth may be applied at any point, all growth will eventually be applied for each individual, provided that there is space in the area surrounding the existing plant. Where an individual has been boxed in, and no further growth is possible, *rdensum[indiv]* is reset to zero to avoid infinite recursion, and an ALERT message is printed. Resource starvation is expected to prevent growth occurring in this situation. However, at the edges of the grid, where artificial limits on spatial growth are imposed, the situation may occasionally be such that this occurs, and the escape clause is then necessary.

All growth has now been converted into *ddens[indiv][tile]* for a number of tiles *nptile[indiv]*. This growth is added to the array *dens[indiv][tile]* in the function *dens_update()*, where *nntile[indiv]* is updated to *nptile[indiv]*. It is important that the growth be worked out for all individuals before updating the *dens[indiv][tile]* arrays in order to avoid biasing results according to the order of calculation.

6.9 Domes in the model

Introduction

Heather growth is dominated by a hemispherical growth form. Although this form is generally associated with discrete individual plants, it may also include a number of individuals growing together. This was discovered through field investigations as described in Chapter 4. It was considered that the dome form should not be restricted to discrete individuals but rather should be separately defined. A natural dome can contain several separately rooting plants, so a model dome might be expected to contain several sets of individuals. In the model, a single heather plant may comprise a number of model "individuals" and a single dome, a number of heather plants.

The natural dome is probably a product of the branching structure of *Calluna*, combined with some pruning by wind and herbivory. The result is aerodynamically smooth and suited to maximising light interception. Domes are present in most heaths when growth of *Calluna* moves out of the pioneer phase.

Plants rarely rise through the surface of the dome, which may be considered similar to the surface canopy of a forest. Those individuals which exist as emergents generally appear to be isolated parts of older plants. It is therefore assumed that it is advantageous for individuals to remain within a dome form, and disadvantageous for them to grow outside a dome.

The model dome is a restriction on the growth of individuals. It is an attempt to limit the behaviour of the model plants such that they do not behave inappropriately. Representation of the branching and budding structures of plants is currently not included in the model. This is partly due to currently limited knowledge of the mechanisms controlling whole plant directional morphology, and partly due to the simplification of branching structure developed in the model. Consequently the growth forms are not in themselves sufficient to restrict plants to an overall dome structure.

The growth of individual stems is essentially a product of the conditions impinging on those stems. Three-dimensional growth is then determined by the structure of that stem and its position within a dome structure. In biological terms this implies that the hemispherical growth form of *Calluna* is for some reason an inherent property of the growing plant and will be present wherever conditions allow. It is difficult to test whether this assumption is correct, but it may be said that the dome structure appears to reflect the behaviour of the real system. When modelling in a field such as this, where there are significant knowledge gaps, modelling decisions and simplifications need to be made to cover these gaps such that the system may be adequately represented, but without prejudicing the validity of the simulation. The dome structure is of this type; the precise nature and causes of this behaviour are unclear and yet are essential to the system as whole. However, it may be hoped that with the development of the model to include increasing detail, the dome may become an emergent property.

Rules of the dome form

A dome is defined in terms of a base radius (*rad[dome]*) about a central point, (*Xdomecentre[dome], Ydomecentre[dome]*) lying within a tile at (*xdome[dome], ydome[dome], baseht[dome]*). The radius of the dome (*rad[dome]*) may then be converted into radii at each level (*domersq[dome][z]*) such that the dome is represented as a series of stacked discs.

The dome may act in two ways. Firstly it may limit the growth of individuals within that dome such that they conform to an approximately hemispherical shape. Secondly, the dome may have an effect on the orientation of stems, with branching tending towards a radial structure. The effect of these properties may be varied in intensity in order that the species be represented.

The limitation is applied using the function *pressuredome()* (called from *potentialindivgrow()*) to limit the potential growth. The limitations are applied at this point so that any surplus incurred may still be applied (in *surplusindivgrow()*), thus ensuring that the total growth still matches the generated growth. At the point of application of surplus growth, the dome structure is ignored, and surplus is applied over the whole plant with no locational preference. This means that the dome is not a strict structure and may be likened to a hemispherical sieve being pressed down on the plants, where the plant will conform to the sieve up to a certain point and then begin to leak through the holes. The apparent domes observed in natural systems are not perfectly smooth and so this seems to be a reasonable modelling approach. The lack of strict rules is particularly important in situations where most of a plant lies within a dome and yet the top of the plant lies outside the dome. In a natural system one would not expect the plant to stop growing in the part of the plant which lies outside the dome, but rather might expect that it would experience reduced growth in that part. The function *pressuredome()* acts by simply reducing the potential growth (*dens[indiv][tile] + ddens[indiv][tile]*) in each tile to the overlap of the dome in that tile (*domedens[dome][dile]*) where the potential growth is higher than the dome structure would imply.

Dome initiation and allocation

In an isolated heather plant, the dome structure does not begin to develop until the building stage has been reached in about 6-10 seasons (Gimingham, 1972). The plant grows pyramidically up until this point and then moves towards a hemispherical form as the budding system fills out the plant. In the model the point at which the growing plant begins to modify its shape is represented as a height threshold (*domethreshold[sp]*) at which the dome form will be triggered. This allows for the fastest developing plant in an area to define the first dome in that area, thus affecting the growth of its neighbours some of which might be expected to form part of the dome.

In the real system this point of dome initiation is triggered by the developmental plant morphology rather than a simple height threshold. Therefore, in certain circumstances of extreme clipping, grazing or wind pruning, a miniature heather dome or dwarf heather may develop. Such a dwarf plant may never attain the model dome threshold and yet still exhibit dome properties. It was decided, however, that the morphology of the model at a level below that of the dome will adequately simulate these effects, and that the simulation of dome behaviour involving a number of individuals was the prime problem. The use of an age

dependent trigger for dome initiation was therefore rejected on the principle that it is the individuals surroundings which determine its dome behaviour.

The function *domegenerate()* is used to create new domes. Here, each individual is tested, and the distance from the top of the litter surface at the point of the stem entry to the top of the individual determined. Should this exceed the dome threshold (*domethreshold[sp]*), the dome is initialised as a dome with a dome number (*domenumber[indiv]*) and the individual allocated to that dome. The centre is defined as the centre of the individual in the topmost level and radius calculated as *domethreshold[sp]* + 0.6 so that the outer curve of the dome includes the bottom half of the top tile. The function *domerefresh()* is called to initialise the height-specific radii, defined at the point at which the curve cuts the middle of the level of tiles, and then calculate from these the area of overlap in each tile (*domedens[dome][dile]*) in that layer by using the *overhex()* function.

As stated previously, individuals falling under the influence of a dome are then allocated that dome number and will continue to develop within that dome. The allocation of dome numbers takes place in the function *domeallocate()*, which checks the relative positions of plants and domes at regular intervals. A plant is defined as being under the influence of a dome when the curve of the dome cuts through the individual above a point a certain proportion (*htconstant[sp]*) up the plant, directly below the centre of the top layer of that individual.

Where the plant falls under the influence of more than one dome at this stage (before it has been allocated to a dome), it is allocated to the dome which has the greatest cover in the tile defined by *htconstant[sp]* and the co-ordinates of the centre of the top layer.

Growth of the dome

As the plants increase in size, so must the dome, in order that it may have a consistent effect. Originally the volume of the dome was increased in line with the total growth of all plants lying within that dome, but this was found to force the plants into a dome structure in an unrealistic manner, especially where a large part of the plant lay outside the dome, resulting in phenomena such as downward growth. This simple approach was therefore rejected as unsuitable, and a more responsive approach was selected. This is now modelled in the function *dome_align()*.

The ratio between the amount of vegetation belonging to the dome lying outside the dome relative to the amount lying inside the dome is calculated (*ioratio* = out / in). If there is more than a certain proportion (*ratmax[sp]*) outside the dome, the volume of the dome is increased by an amount proportional to the amount of vegetation lying outside the dome (i.e. dome volume × *ioratio*). The value of *ratmax[sp]* may thus be varied in order to vary the extent to which the dome affects the growth of individuals, increasing the flexibility of the model. At a low value, the dome may be quite large relative to the plants, and will only affect the growth of the extremities of the plant, whereas at higher values, the dome will restrict increasing proportions of the plant. This approach is preferable to the original method since it only applies dome growth when necessary.

The dome and heather senescence

It is a property of growing heather that it reaches a certain age at which the plant opens out, with the older branches falling towards the ground. In order to capture this effect a set of routines were developed in order to simulate the process of moving vegetation. These are controlled by the function *hexmove()* and calculate the overlap of tiles attached to trunks (which move according to revised trunk angles) over the spatial grid. This approach was developed with a single property of each individual (*dens[][]*) in each tile part way through model development. Consequently these functions do not work with the data structures used in the model in its present state. This requires some work to bring the sub-models into a compatible state. In addition, issues of allocation occur when the branch moves into occupied tiles. The sub-model is currently inactive and is not listed in the Appendix, although listings may be obtained from the author on request.

However, it has been demonstrated by the working functions at an earlier stage of model development that the grid allows the movement of plant parts, and as such could potentially explicitly represent the process of senescence in heather. The dome form is possibly an important component of this process, affecting the radial orientation of branches.

6.10 Litter sub-model

All non-living plant material is treated as litter in the model. In order to capture the effects of above-ground dead material, the development of litter structures throughout the grid is permitted. Above-ground material is assumed to fall to the ground gradually, contributing to the ground-litter layer. At present no nutrient release is modelled, and decomposition is set at a constant rate to prevent excess litter build-up, although it would be possible to draw on the data collection and modelling of decomposition carried out for the Moor House system as part of the IBP study (Jones & Gore, 1978; Clymo, 1978) in order to do this. This aspect was considered beyond the scope of the initial spatial modelling project.

The array *litter_dens[x][y][z]* is used to hold the volume of litter in units *dens[][]* both above and below ground. *Ztop_lit[x][y]* holds the height in units *z* of the litter surface at each horizontal co-ordinate, and is increased by one if the value of *litter_dens[x][y][z]* at that height exceeds *DCON* (10000).

Plant material is converted to litter by two methods, whole-plant mortality (section 6.7) and local shoot loss. Local shoot loss occurs continually over the year as a steady rate in function *litter_create()* and due to winter browning in function *browning()*. Once most of the leaf material has left a tile, the woody component of the tile begins to die.

The function *litter_create()* is called daily, and leaf loss is calculated for each tile in relation to microclimate. The variable *fpress* (proportion *dens[][]* lost) is set as

$$fpress = 2.0 \times wind[x][y][z] \times fallrate[sp][month]$$

where *fallrate[sp][month]* is the monthly species specific rate of loss, adjusted to a suitable value for wind conditions. The value of *fpress* is increased by 50% where the tile is in a light environment less than *shade_tol[sp]*, the species lower light limit, hastening leaf loss from the underside of the canopy. Leaf loss is calculated as

$$litter\_dens[x][y][z] = litter\_dens[x][y][z] + fpress \times sshoot\_dens[indiv][tile]$$

This process is repeated for long shoots, and (where *woodens[indiv][tile]/ dens[indiv][tile]* is greater than 0.95) for wood. The *litter_dens[][][]* array is thus filled directly in the tile being dealt with.

The conversion of living to above-ground dead due to browning is carried out in the function *browning()*, in a very similar way to that in *litter_create()*. Browning only occurs when the three day moving average of temperature has fallen below -1°C (assuming that this will be sufficient to limit available water), the wind speed in the tile is greater than 1.5 m s^{-1} and the tile is above any snow surface. A variable *brown* is applied in the same way as *fpress*, although for short shoots only, with no effect of light, and assuming the fall rate (*brrate* = 0.01) to be at a constant low rate. It is expected that this method will underestimate the amount of loss due to browning, but this was considered reasonable in the absence of a direct treatment of plant water.

Above-ground litter thus created falls slowly to the ground, again in proportion to wind. This is carried out daily for each tile in the function *litter_fall()*. No litter falls if the tile is under snow (Forrest, 1971). Otherwise the loss to the ground surface tile (*zz* = *ztop_lit[x][y]*) is calculated as

$$litter\_dens[x][y][zz] = litter\_dens[x][y][z] \times blow$$

where *blow* is set to a minimum of 0.01, but calculated as

$$blow = 0.05 \times wind[x][y][z]^2$$

Litter on the ground surface builds up and its depth is recalculated daily in the function *litter_level()*. When this depth becomes greater than the depth of a tile, the value of *ztop_lit[x][y]* is increased accordingly. Surface litter decomposes in the function *decomposition()* at a constant daily rate of 0.0002739, scaled to the proportional losses recorded by Heal, Latter and Howson (1978). This is a great simplification of the process, but in the absence of any use for decomposed material this approach was considered reasonable.

7

Results

7.1 Overview

The "Ecospace" model was run for a number of trial scenarios to test sensitivity and aid in validation. The scenarios and corresponding results are described below. This section is not intended to be a comprehensive validation of the model: many of the spatial measurements required have not yet been made. Rather, the aim is to demonstrate that the model behaves reasonably over a range of conditions and produces no counter-intuitive results. Due to run-time limitations and the requirement for simplicity, the model is mainly run for a single growing individual in a static spatial environment, although a simulation with a number of individuals is also presented. The results show that the model performs broadly as expected, although some anomalous results are presented which give some cause for concern

7.2 Constraints in undertaking simulations

It has been possible to test the plant growth sub-model within the framework of the microclimatic generator. The cell-based growth form (*gform[]*=1) was adjusted to produce a three-dimensional form close to that of *Calluna* and behaved consistently. Due to time constraints it has not been possible to validate the other two growth forms within the three-dimensional microclimate. Both demonstrated behavioural validity in simple conditions.

Grid size and run-time

The complexity of the model makes for a long run time. In particular, the calculations involved in the light sub-model and the ray tracing wind sub-model are very time consuming, and become increasingly so with increased grid dimensions. For example the light sub-model takes approximately 7 hours to calculate the light environment for all cells in a $12x \times 12y \times 15z$ grid, (as used in the majority of runs presented here) and 24 hours for a $30x \times 30y \times 20z$ grid. In order to limit the need for ray tracing calculations, simple forms of the radiation and temperature sub-models were used for unoccupied tiles, assuming conditions to be the same as those above the canopy. Thus the calculations need only be performed where their results are used and the light sub-model takes only approximately 10 minutes for a 6 tile plant in a standard $12x \times 12y \times 15z$ grid. The ray-tracing wind model was not used, using simply the relative density of tiles, thus removing any effect of wind direction. This was considered a reasonable simplification for these simple studies.

The model was developed on a $10x \times 10y \times 10z$ grid, which is smaller than a full sized individual might grow. Unfortunately, the model becomes very slow to run as the grid dimensions are increased. A model of grid size of $100x \times 100y \times 20z$, representing an area of 7.5m by 8.6m by 1m (at a tile side length, *SIDESCALE*=0.05 m) appeared to exhibit behavioural validity in its early run stages. This grid size was only possible by limiting the number of individuals to 200 because of memory limitations. However, the calculations are slow for such a large grid, since each task must be repeated for 200,000 cells, taking over 6 hours to calculate the light environment for a single tile, making the model impractical. The grid size could at present not be extended much beyond about $40x \times 40y \times 20z$ if a reasonable number of individuals were permitted although run time becomes limiting with a heavily occupied grid. This represents a space 3 m × 3.46 m × 1 m.

Mortality and establishment

The runs presented here have been carried out without the inclusion of the germination and establishment sub-models. The simple sub-model representation of stress and mortality requires the use of controlling variables (e.g. number of days a plant can survive with no surplus; cumulative number of days with negative energy balance which a plant can survive) which must be selected at least partially arbitrarily due to the limited extent of our knowledge. If these variables are set too favourably, all the individuals will survive, and if set too harshly, all the plants will die. Importantly there is a very fine line between these two states for small

plants, with the survival rate showing marked sensitivity to these variables near the expected survival rates of juveniles to adulthood.

It was considered that the mechanistic aspects of the model had less influence on the survival of individuals than these arbitrarily-selected variables. As such it was considered to be an inappropriate sub-model for the mechanistic representation of plant competition. For the adult model the sugar-pool related mortality was included, since the larger sugar-pools involved reduced the sensitivity of mortality to the model variables, allowing survival through and recovery from periods of stress. However, even in the adult model it was felt that the mortality model was unsatisfactory. As one of the key aspects of the selective process, it is essential that this be represented adequately in a model of vegetation dynamics.

7.3 Single plant simulations

Single plant simulations were carried out to both examine the typical pattern of behaviour of the model during simulations and assess the effect of stochastic elements on the model behaviour. The examination of the typical behaviour of the model is not intended as a rigorous validation, but is rather presented in order to demonstrate the working processes.

A $12x \times 12y \times 15z$ grid (0.9m × 1.04m × 0.75m), was used as standard for the single plant runs described here, to limit run time sufficiently to allow multiple runs. The ground level was set at a constant height of *ztop_lit[x][y]*=1 and *ztop_soil[x][y]*=1. Runs were carried out within the standard grid to investigate the sensitivity of the modelled growth of a growing *Calluna* individual in a number of different simple scenarios. A run length of 5 years was used for all simulations. Light was modelled by only calculating ray tracing for occupied tiles to reduce run time. Under these conditions it took 4-8 hours of run time for a 5 year run depending on the speed of the computer.

The individual plant was initialised as a full adult of two seasons with an initial above-ground biomass of 46 g dry weight (thus total including roots is 92 g dry weight). The tile-based growth form, *gform[sp]*=1, was used for all runs and the plant set up as a low dome within the ground level z layer (z= 1, ez= 0) with densities apportioned between five tiles as shown in Table 7.1. As such, all the tiles are above *oecthreshold[sp]* and are able to grow into new tiles. All species-specific parameters were set as appropriate for *Calluna vulgaris*. These are listed in Table 7.2.

The weather conditions were set up to simulate the conditions at the Moor House study site using the long-term climatic averages of Heal, Jones and Whittaker (1975) with standard deviations estimated from meteorological tables where data were incomplete for model parameterisation. The cloud cover was generated from the above source, but incoming radiation was estimated directly from the radiation spreadsheet for an altitude of 500 m (approximate average height for Moor House site). For the majority of runs, radiation was calculated for the Moor House latitude 54° 65' N although this was varied for some runs where mentioned.

Table 7.1. Initial co-ordinates for standard individual scenarios.

tile number	0	1	2	3	4
dens[][tile]	2100	2000	2000	1800	1900
co-ordinates	4,5,1	3,5,1	3,6,1	4,4,1	4,6,1

Table 7.2. Species-specific parameters used for species= 1, *Calluna* *asterisk denotes variables currently not in use or inactive.

budlight[sp]	6.0 hours	*occthreshold[sp]*	500
budtemp[sp]	7.2 °C	*p_fract[sp]*	1
densmax[sp]	3000	*part_start[sp]*	0.7
densopt[sp]	2000	**ph_max[sp]*	6
dietime[sp]	3650	**ph_min[sp]*	2
dormtemp[sp]	5.6 °C	**ph_opt[sp]*	4.5
expolimit[sp]	1	**phos_max[sp]*	0 g m^{-2}
flowera_off[sp]	160	**phos_min[sp]*	0.7 g m^{-2}
flowera_on[sp]	100	**phos_opt[sp]*	0.3 g m^{-2}
flowerb_off[sp]	240	*press_tol[sp]*	10
flowerb_on[sp]	200	*rs_ratio[sp]*	0.5
germlimit[sp]	60000	**seed_reserve[sp]*	100
gform[sp]	1	**seedrgr[sp]*	0.5
htconstant[sp]	0.6	*senesc_age[sp]*	8
hv_ratio[sp]	0.1	*shade_tol[sp]*	0.5
**lhoursgerm[sp]*	10 hours	*sl_ratio[sp]*	0.9
**light_germ[sp]*	0 Wm^{-2}	**sm_max[sp]*	77%
lingrow[sp]	0.5	**sm_min[sp]*	10%
**ltweight[sp]*	0.99	**sm_opt[sp]*	30%
**min_prod[sp]*	0	**smoistgerm[sp]*	20%
newgrow[sp]	0.5	*spreadfactor[sp]*	3
**nit_max[sp]*	0 g m^{-2}	*stressdays[sp]*	10
**nit_min[sp]*	0.7 g m^{-2}	**tempgerm[sp]*	6.0 °C
**nit_opt[sp]*	0.3 g m^{-2}	*utilise[sp]*	4

class[sp][aclass] {-1: 1: 2: 3: 6: 10: 15: 30: 50}
fallrate[sp][month] {0.01: 0.01: 0.01: 0.01: 0.01: 0.01: 0.01: 0.05: 0.05: 0.05: 0.01: 0.01}
wl_ratio[sp][week]
{1: 0.99: 0.97: 0.92: 0.72: 0.52: 0.35: 0.32: 0.41: 0.56: 0.68: 0.76: 0.81: 0.85: 0.88: 0.9}

With the present mortality model, it was found that the fluctuations of the weather model throughout the winter tended to lead to plant death due to depletion of the sugar pool. This occurred on a scale greater than that expected, although for those individuals surviving the winter there was very little net change in the size of the sugar pool. It was therefore assumed that the sugar pool would remain constant throughout the period of winter dormancy in the absence of a better model treatment of stress-related mortality.

Growth and partitioning

Before examining the variation between runs under different conditions, the normal pattern of behaviour of the model is first demonstrated. Five years of growth were simulated, with a typical pattern of development shown in Figure 7.1. There is a degree of variation in the rate of growth due mainly to weather, but also to the three-dimensional development of plants. The pattern of allocation of material over the plant volume through time is affected by a random number generator which selects each fresh tile (see section 6.8ii). This in turn affects the growth rate. Unfortunately, due to the nature of the tile-based growth form it is not possible to remove this source of variation without distortion of the growth form. It would therefore be desirable to use independent random number generators for the weather and the growth forms, thus allowing direct comparison of runs with an identical sequence of weather. However, this was not a practical adjustment at this stage in the project. The run presented below is slightly higher than the average but is otherwise typical of the results. The most obvious feature of the growth pattern is the short growing season, resulting in increased sensitivity to summer weather patterns.

The proportion of wood in the plant can be seen to remain fairly constant over time at a leaf:stem ratio of 2.4: 1 which lies within the range expected for individuals of *Calluna* at an age of 2 to 7 seasons. However, there should be a steady increase in the woody component to approximately 1:6 by the age of 15 (Robertson & Davies, 1965) and although one might expect the relative permanence of woody material to lead to this type of behaviour, there is no evidence of the process occurring in the period modelled. This process is sensitive to the rates of leaf fall and the composition of litter, with high rates of litter fall increasing the proportion of wood, and it is hoped that either an improved calibration of the litter sub-model or a greater run time would generate an increase. Sensitivity to the rate of litter fall is examined later in this section. The allocation functions currently in use in the model remain constant relative to the dimensions and proportions of plant materials. This simplification may be responsible for the lack of an increase in the woody component.

The individual at the end of the fifth season has an above-ground biomass of 320 g and covers a ground area of 0.2665 m^2. The total accumulation of root material is 630 g, but it must be remembered that no decomposition or loss of roots is modelled at present, so this would be expected to be considerably too high. Production data are usually presented per m^2. In order to allow comparison, the single individual data were scaled up in proportion to ground area. This will result in an overestimation of the growth rates due to the difference in light conditions. However, it was considered that this overestimation would be low due to the fairly flat dimensions of the plants. This method is far from ideal, but it was felt that it would still allow a check that the production values are of a suitable order of magnitude. At this stage in the development of the model, with uncertainty regarding the rates of leaf fall and partitioning, a more rigorous test of the whole model would be of little value.

The multiplication gives an above-ground standing crop of approximately 1200 g m^{-2} assuming continuous cover. It should be noted that this is a direct multiplication of results for a single individual and as such would tend to overestimate production. However, The above-ground biomass may be compared with the biomass estimates recorded by Forrest (1971) at Sike Hill, Moor House in 1968, (although this is a value for *Calluna* in a mixed community, 73% *Calluna*). The above-ground summer biomass at Moor House was 970 g m^{-2} for *Calluna* and 1300 g m^{-2} for all species. The model appears to be producing results in the broadly correct range. However, one must bear in mind that these are only 7 year old plants, and as such one would not expect biomass to be as great as that for a fully developed stand. This is borne out by the results of Bellamy and Holland (1966, Upper Teesdale blanket bog), where 6 year old plants had a biomass of 600 g m^{-2}, with this value rising to 2000 g m^{-2} at 14 years. Larger above ground biomasses (1800-2900 g m^{-2}) than that recorded at Moor House have also been recorded at other sites at lower altitude (Chapman, 1967; Summers, 1978), and on different soil conditions (Robertson & Davies, 1965; Kayll, 1966). However, lower values of 450-600 g m^{-2} (Allen, 1964) and 790 g m^{-2} (Gore & Olson, 1967) have been recorded elsewhere on the Moor House site. A great deal of variation between these estimates, combined with the variation in proportions of shoot and wood and above- and below- ground make comparison between results difficult. In addition it is important to consider the effects of year to year variation in production which may account for much of the variation apparently occurring between sites. The majority of these studies have been carried out for a single season or pair of seasons. An examination of Table 2. in Summers (1978) showing production for a number of sites in the Cairngorms for 3 successive years illustrates the dangers of estimating production from a single year's data. The seven sites measured across the 3 year period all show significant ($P<0.01$) difference between years. The degree of variation is not consistent across all the sites, with the lowest production for the 3 years varying from

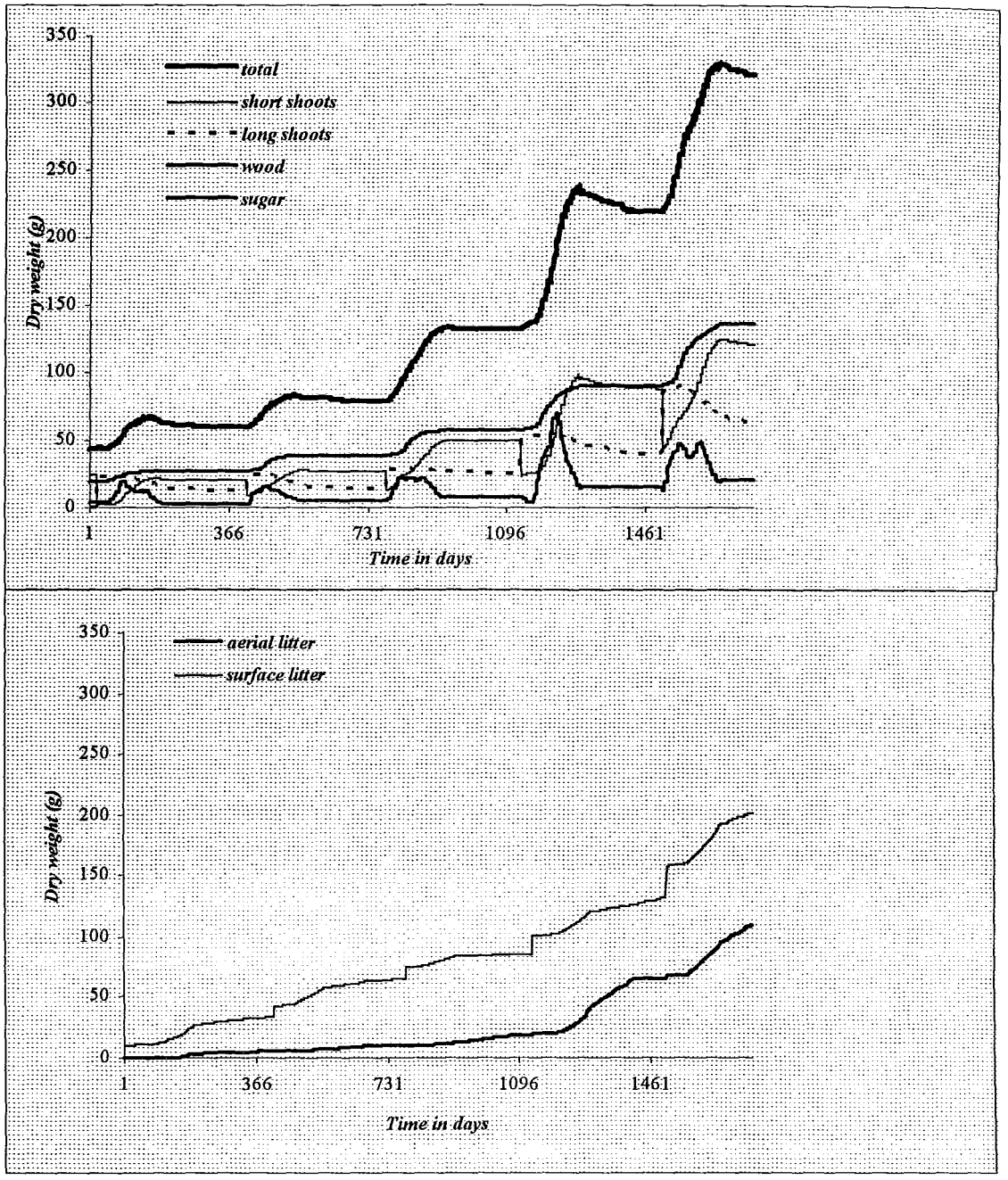

Figure 7.1. Partitioning of growth in simulated *Calluna* in standard conditions at Moor House.

0.34 to 0.68 of the highest value. It is not therefore appropriate to consider any of the measurements presented above as truly representative of their site. This variation has important implications with regards the variation generated by the model as discussed later.

The mean production rates for the fourth and fifth seasons are 92 g and 100 g respectively. If simply multiplied by horizontal area these seasons yield production rates of 426 gm^{-2} and 374 gm^{-2}. These rates are considerably higher than the field measurements of

200 gm^{-2} (Forrest, 1971) and 298 gm^{-2} (Forrest and Smith, 1975), but this may be explained by the assumption of continuous cover required to scale directly up and by increased production rates of isolated individuals. The use of relative growth rates avoids the inclusion of area in the calculation, although it does not allow for the difference in radiation environment. If given as a relative growth rate, the mean for the last two seasons is 0.54 which compares favourably with the value of 0.55 from Forrest (1971). The model appears to be generating rates of production in the expected range, although possibly overestimating production. However, this is a comparison between production rates for a community and an isolated individual, and the model needs to be further validated and its sensitivity to input variables investigated before proceeding further.

Litter can be seen to accumulate over the run time, both above-ground and on the surface. The development of above-ground structures of dead plant material is a significant improvement on previous models of heathlands (e.g. van Tongeren & Prentice, 1986), which ignore this crucial element of the system. As can be seen from Figure 10 in Gimingham (1972), there may be considerably more standing dead in the lower levels of the canopy than leaf material, and this contributes to the dense shading characteristic of Calluna. Although this process may be more common in dwarf shrubs than other plants, it is a useful treatment of dead plant material. Forrest (1971) recorded a ground litter fall of 108 gm^{-2} and an above-ground litter production of 60 gm^{-2} for 1968, representing relative litter production rates of 0.3 and 0.17 respectively compared with the model values of 0.375 and 0.25 for the last two seasons. This would indicate an over-production of litter, although production is broadly in the expected range. This is an important element of the model, having a critical interactive effect on production. A simple test of sensitivity is presented later in this section.

Modification of microclimate

It is important that the model simulates appropriate changes in microclimate in response to changes in vegetation structure. In the following analysis, the microclimate surrounding an individual grown under standard conditions is described, at the start time and after two years. Due to the random variation in the weather sub-model it is not possible to generate identical days. In order to facilitate comparison, the values of the PAR sub-model have been scaled to the same irradiance above the canopy and the wind speed has been scaled similarly. The temperature regime has not been scaled due to the extent of the difference between mean temperature, which, unlike light (or wind as represented in the model), can have significant effects on the temperature regime.

All the microclimate graphs (Figures 7.2-5) are presented as sets of four, showing two levels of tiles, the ground level, (lower pair) and the second level (upper pair), with the left-hand pair showing initial conditions and the right-hand pair showing conditions after two years' growth. North in all cases is to the top of the page. The graphs are all shown at a scale of 1:11.3. The graphs allow, the demonstration of the development of heterogeneity of microclimate in parallel with plant growth. The outline of the individual is marked with a bold line on all the graphs in order to assist with comparison of plant form and microclimate.

Figure 7.2. shows the spatial growth of the individual plant (*gform[]*=1). As can be seen, the plant extends its spread, but loses a degree of density due to litter loss. A small amount (approximately 10% of total mass) of dead plant material is also suspended above ground from this structure and will affect microclimate. This dead material is not shown on the diagram.

Figure 7.3. shows the light regime plotted for *lt[x][y][z]*, the mean monthly light per tile as an average for each hour of daylight. The modelled shadow would be expected to be smaller than the maximum (i.e. low sun angles) since the plot is an average for the whole day. Edge effects are dominant at this grid size. The embedding profile acts as a low porous wall on each side, resulting in the reduction of light towards each corner at ground level. The results surrounding the plant are more complex. shading effects continue beyond the plant boundary. One would generally expect most shadow towards the north (top) of the diagram, but this is not evident. Instead we see the area of deepest shade lying to the west and south-west of the plant. This may be explained by the fact that the plant is closer to the western and southern edges, and thus receives more shading from the embedding profile on these sides, creating an area of relative shade. This could be reasonable behaviour from the embedding profile, but must be borne in mind whilst working on such a small grid. The low value of 64 W m^{-2} directly south of the plant at time 0, seems unlikely. as previously stated, the model requires a more rigorous validation. As stated in Chapter 5, there are occasional anomalous results from the model, particularly near the edges (Fig 5.10). The precise cause of this variation is not known, but since this is largely limited to the edges, a larger plot size reduces the effect. It is important to note that the modification of the light environment extends considerably beyond the edges of the plant structure, particularly as the plant increases its height. It is by this modification of microclimate that individuals may affect one another, and it is therefore essential that the modelling be accurate. The light sub-model has been tested rigorously in isolation but needs further testing in the context of the whole model.

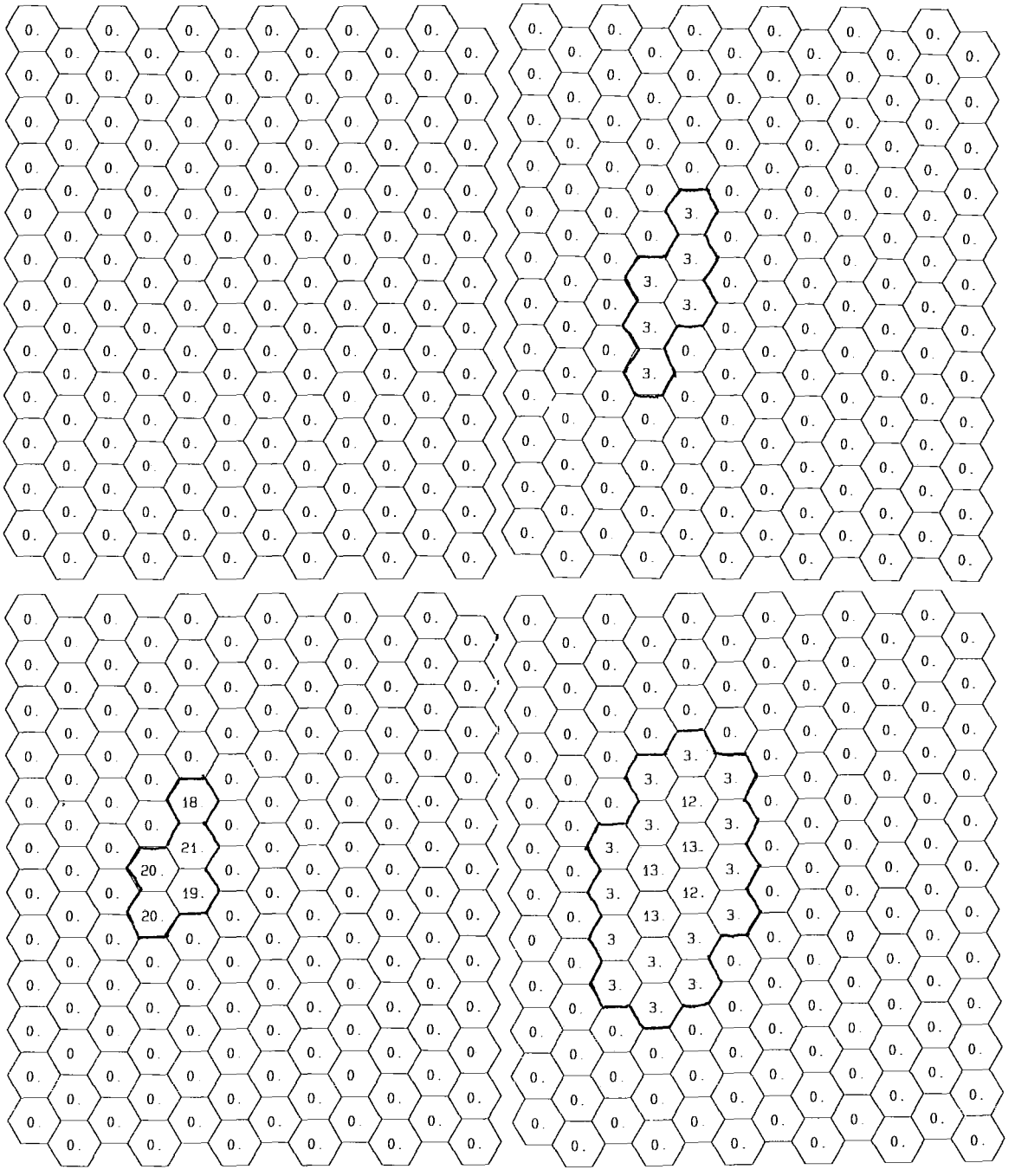

Figure 7.2. Change in individual structure over two years' growth. Plots show the x and y horizontal dimensions. The upper pair of plots represent z=2 and the bottom pair z=1, ground level. All figures are in % volumetric occupancy. Scale 1:11.3. North to the top.

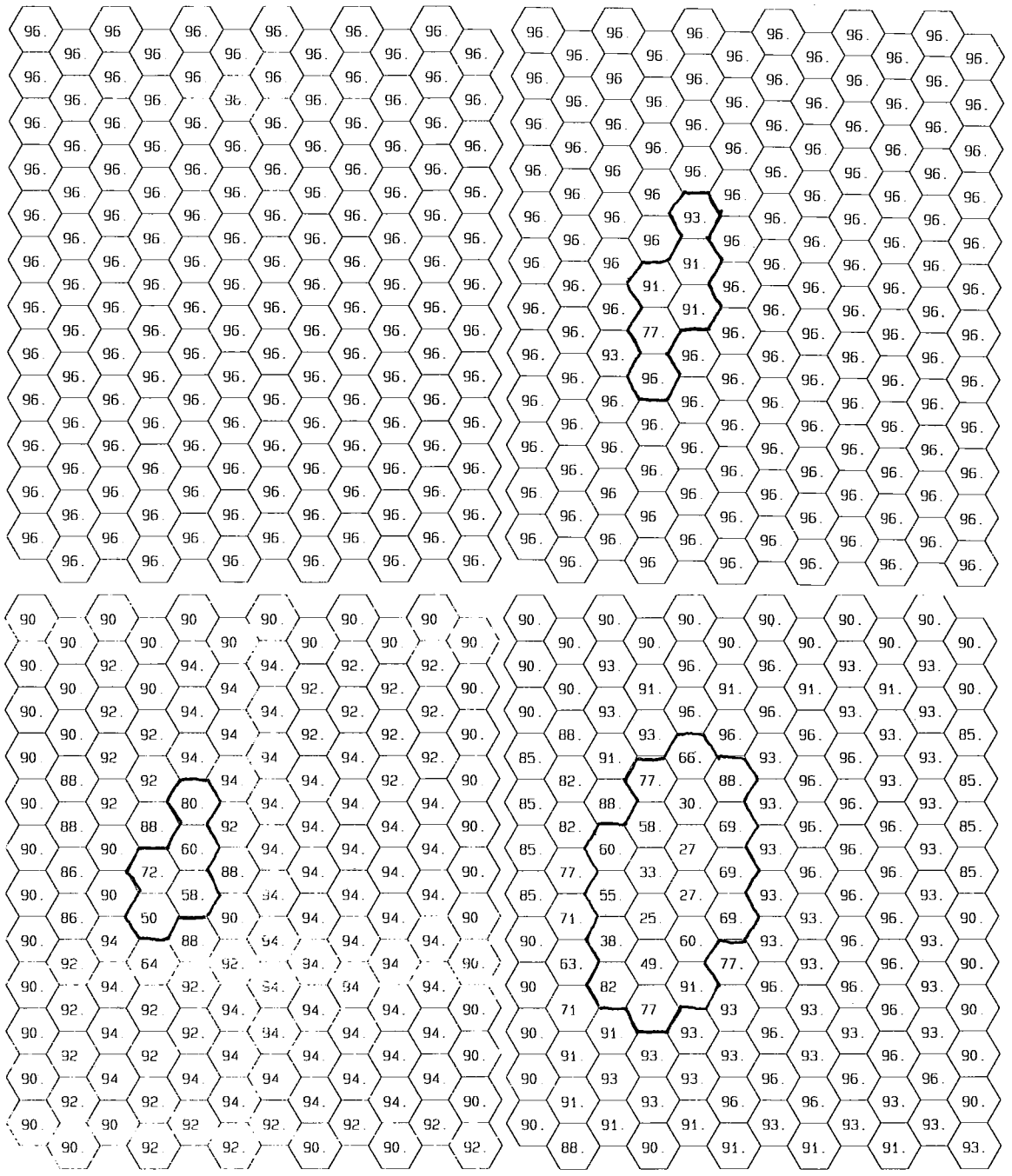

Time=0 ***Time=500***

Figure 7.3. Change in light regime over two years' growth. Plots show the x and y horizontal dimensions. The upper pair of plots represent $z = 2$ and the bottom pair $z = 1$, ground level. All units are W m^{-2}. Scale 1:11.3. North to the top.

The lack of an hourly directional treatment of light (i.e. calculation of hourly light from mean monthly conditions and proportional radiation incident at top of atmosphere) due to run time problems leads to an under-representation of the spatial heterogeneity of the light regime, even when the temporal variation is reintroduced as modelled. Given the present complexity of the light sub-model, this seems to be an imbalanced approach. It would seem desirable to simplify the light model in order to better represent hourly light. This would also simplify the interpretation of results, with the sun for each hour being represented as a fixed point source rather than a curve of varying intensity.

Figure 7.4. shows the modification of the wind profile by the individual plant. As this was part of the standard runs, the simplified wind model was used (i.e. no ray tracing), so no downwind sheltering effects are represented. At present, the ray tracing wind model is too slow to be practically applicable, and with the input direction as mean wind direction for each day, would be of little extra value. This is a significant shortcoming, particularly since there is no gradient of wind speed across the plant, although at these low wind speeds near ground level there will be little effects on growth. However, as the plant becomes larger, growing into faster air conditions, wind would be expected to have more effect, with this effect being concentrated at the most exposed points. This is an important controlling variable for plant form and as such is an important component of the modelling approach.

The modelling of wind direction presents a problem. As stated earlier, it would be possible to generate hourly values from a wind rose, but mean wind direction at 10 m is not necessarily representative of the wind direction at a particular point within the grid. With expansion of the grid to include more individuals, one would expect direction at canopy level to be heterogeneous due to the canopy structure. It is possible that wind direction would be more consistent and perhaps better approximated by a linear model at the higher wind speeds which are likely to have the greatest effect on the plant. This requires investigation.

Figure 7.4 shows results for two different sets of wind conditions, with wind speed shown in cm s^{-1} for ease of comparison. In the absence of a better approximation, the simpler wind sub-model produces variation about the mean wind speed for each layer much as expected, with the effect extending a little beyond the plant structure. This model may be appropriate for within-canopy air movement, where eddies make for variation in wind direction, but, again, this requires experimental investigation.

Due to the relatively low radiation experienced over the days sampled, and the good coupling of the isolated individual to the atmosphere, very little horizontal heterogeneity is

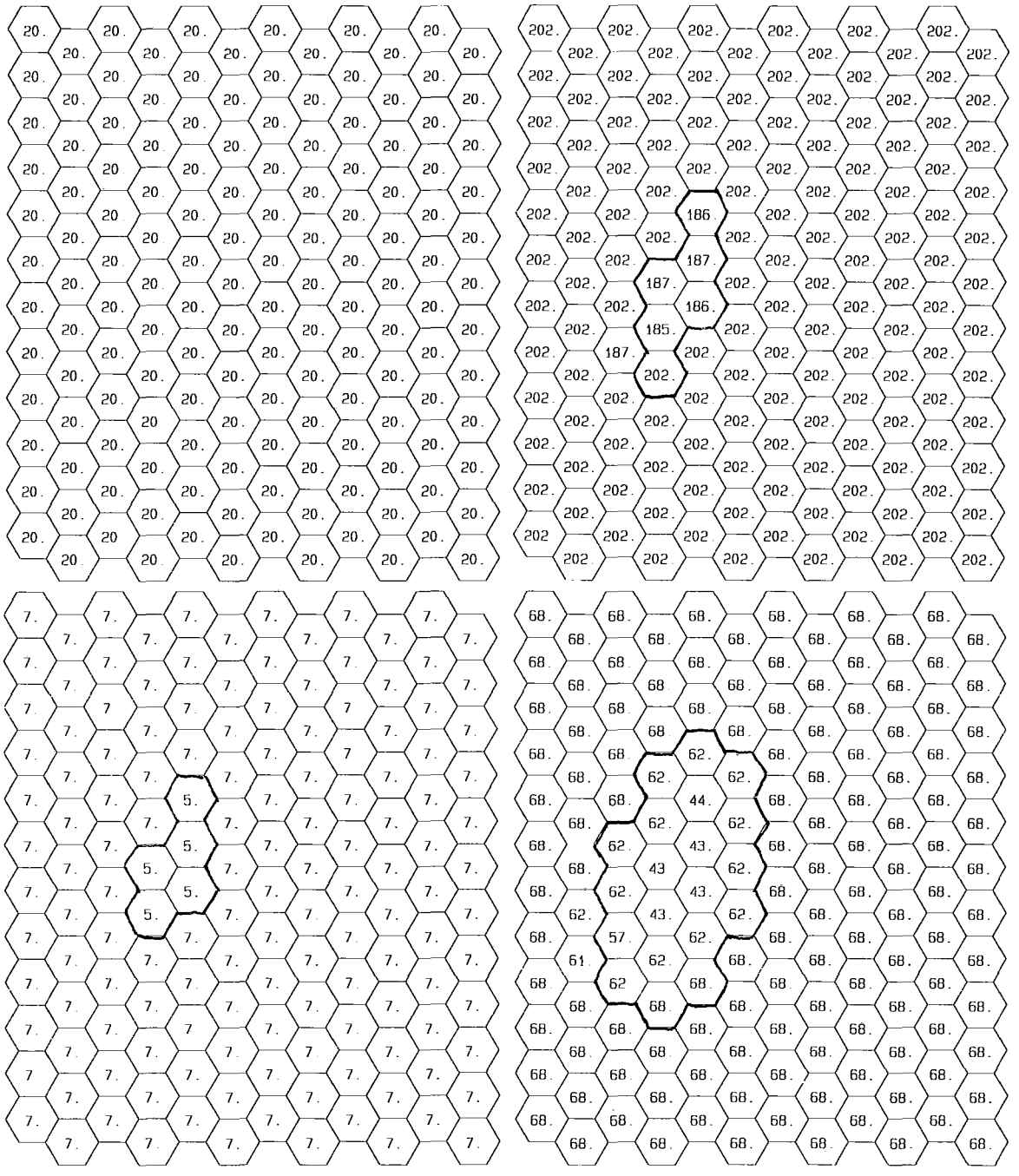

Figure 7.4. Change in wind regime over two years' growth. Plots show the x and y horizontal dimensions. The upper pair of plots represent z=2 and the bottom pair z=1, ground level. All units are cm s^{-1}. Scale 1:11.3. North to the top.

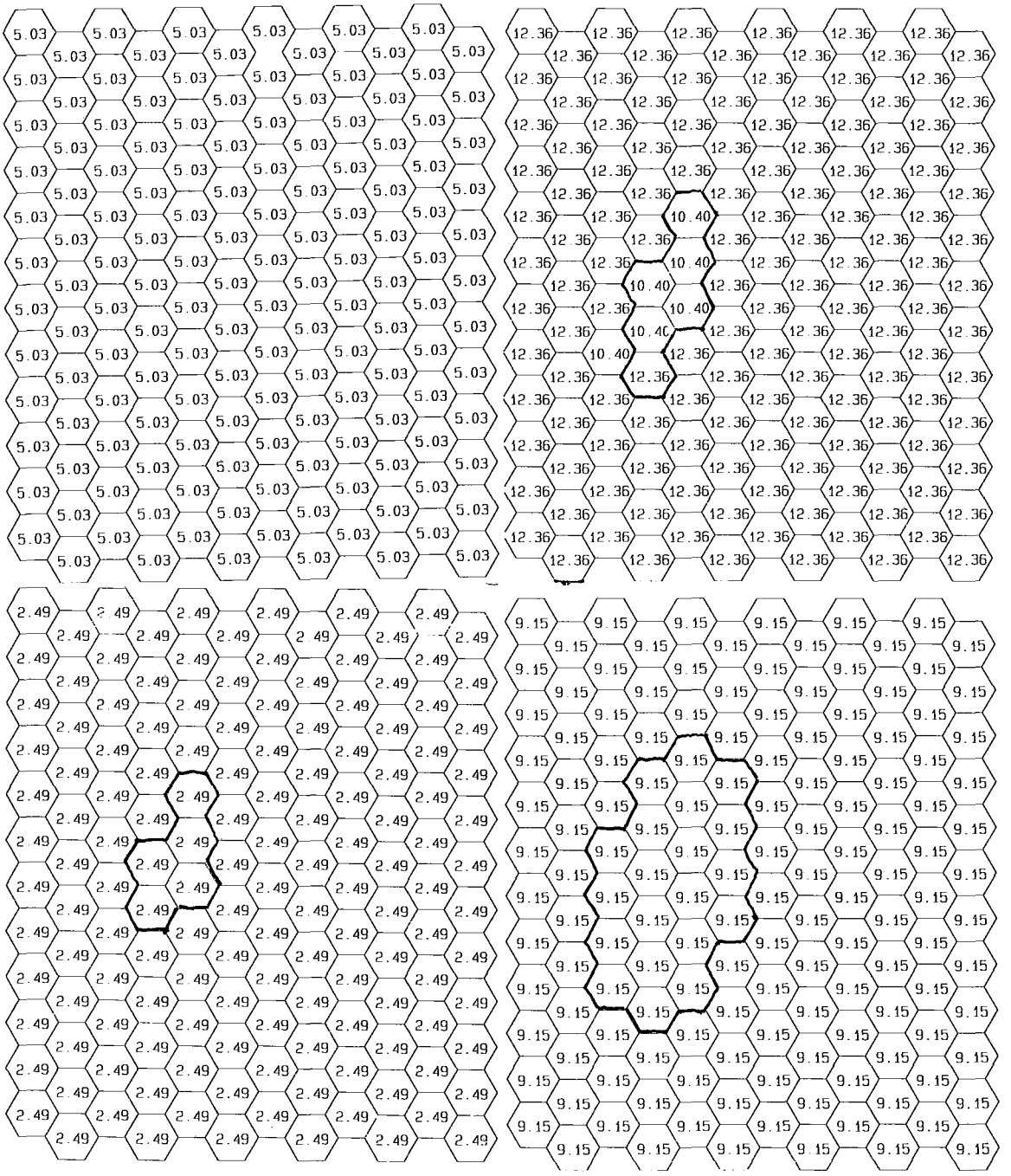

Figure 7.5. Change in temperature regime over two years' growth. Plots show the x and y horizontal dimensions. The upper pair of plots represent $z = 2$ and the bottom pair $z = 1$, ground level. All units are °C. Scale 1:11.3. North to the top.

demonstrated by the temperature sub-model (Figure 7.5). The differences between the initial regime and the regime after two years growth are largely attributable to different weather patterns from the stochastic weather generator. Model data from the ninth hour of daylight are shown. The only noticeable modification of microclimate by the plant is a cooling of the exposed top of the canopy due to increased wind-driven evaporation. This is much as would be expected for an isolated plant in low radiation. Heterogeneity is nevertheless evident in the vertical dimension, with both runs showing low temperatures in the layer closest to the ground. The degree of heterogeneity generated by the temperature sub-model would be expected to increase with increased plant structure (until closing of canopy) and radiation input, but at present appears to be functioning adequately.

Sensitivity of the model to stochastic elements

Random numbers are used in the model to generate weather patterns, to generate mortality and in the selection of new tiles. The short growing season lends particular significance to the timing of weather patterns relative to leaf density. Consequently there is considerable variation in the results obtained between runs starting from the same state, but using a different sequence of random numbers. In order to assess the sensitivity of the model to the seed number used in the random number generator (thus altering the sequence of events since the random number generator will produce the same series of numbers for each seed number), runs were performed for standard conditions at Moor House varying only the seed used in the random number generator. The approximately normal distribution shown in Figure 7.6 was generated, with a mean dry weight of 308 g and a standard deviation of 48.6 g. The model was run 45 times to achieve this distribution, and in two runs the model individuals died.

The extent of the variation is more than expected, with the highest generated value more than twice that of the lowest values. However, this variation appears at first sight to be of a similar order of magnitude to the variation in production between years at the same site, as described earlier, and is possibly a suitable amount. An attempt was made to correlate the variation in results with annual mean generated temperature, but there was no clear correlation due to the simultaneous action of other weather variables. As seen below, this variation is large compared to the variation between sites, and a simple test was carried out to separate some of the sources of variation. Figure 7.7 shows the distribution of results obtained from 30 runs (1 mortality) using mean monthly weather conditions. All variation thus generated comes from differences in the spatial allocation of resources in the spatial growth sub-model. Two distinct sources of variation, the weather sub-model and the spatial growth sub-model are

evident. Both sources of variation appear to be roughly the same order of magnitude. This indicates that both aspects of the model can have a significant effect on growth rates, as is evident in real plants. At present these share the same random number generator and are difficult to separate. It would therefore be desirable to modify the model to use two or more separate random number generators in the model, so that the same random sequence of events can be analysed for the separate sub-models.

Three possible reasons for the increased growth under the mean weather conditions with no snow are proposed:

a). Unfortunately it was necessary to disconnect the snow cover generator for this purpose due to its purely stochastic nature, thus increasing the number of days potentially available for growth.

b). An increased length of growing season resulting from a more stable temperature prehistory value (*hh=hcalc()*).

c). Mean monthly conditions are not necessarily representative conditions for that month.

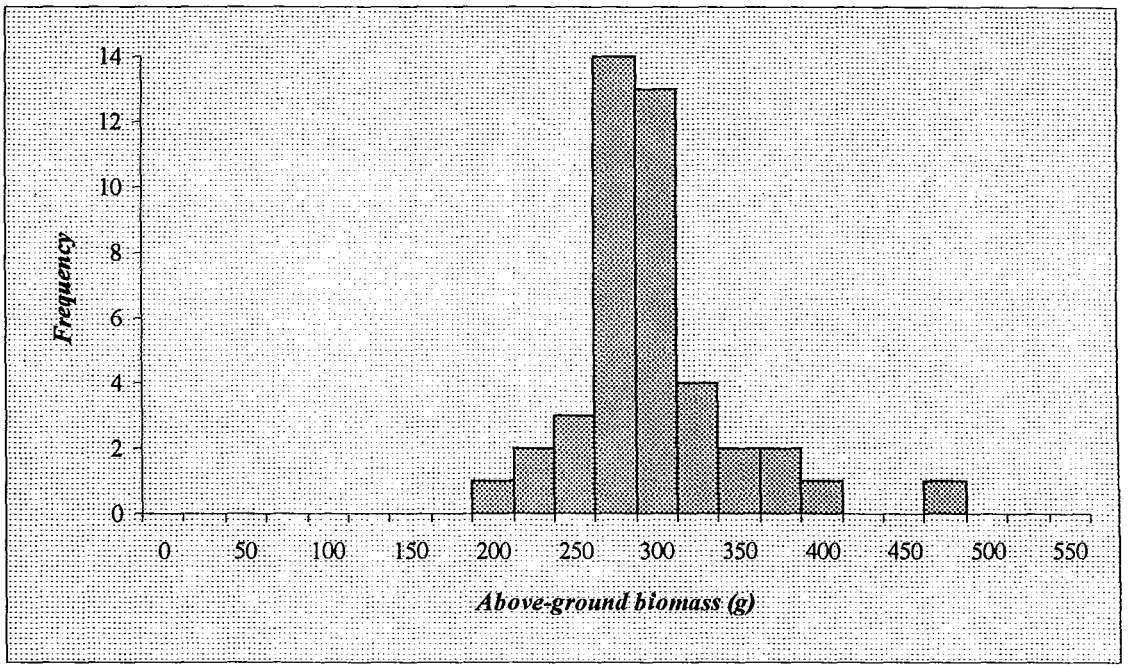

Figure 7.6. The distribution of results for standard conditions at Moor House for a single plant over five growing seasons, with an initial above-ground biomass of 100 g.

The simplified model results with variation from weather removed all fall in a narrower range than the full model as expected. Since these values are higher than the standard model and the results of increased growth are multiplicative one would expect an increase in variation simply from the increase in mean growth rate. This requires further

analysis, with a superior non-stochastic representation of the snow model. It is apparent that the spatial allocation of resources has an effect on the rate of plant growth. The significance of these separate sources of variation is discussed in Chapter 8. Due to the nature of the model, results are presented in the form of distributions, so the extent of variation within those distributions is critical to the understanding of model results.

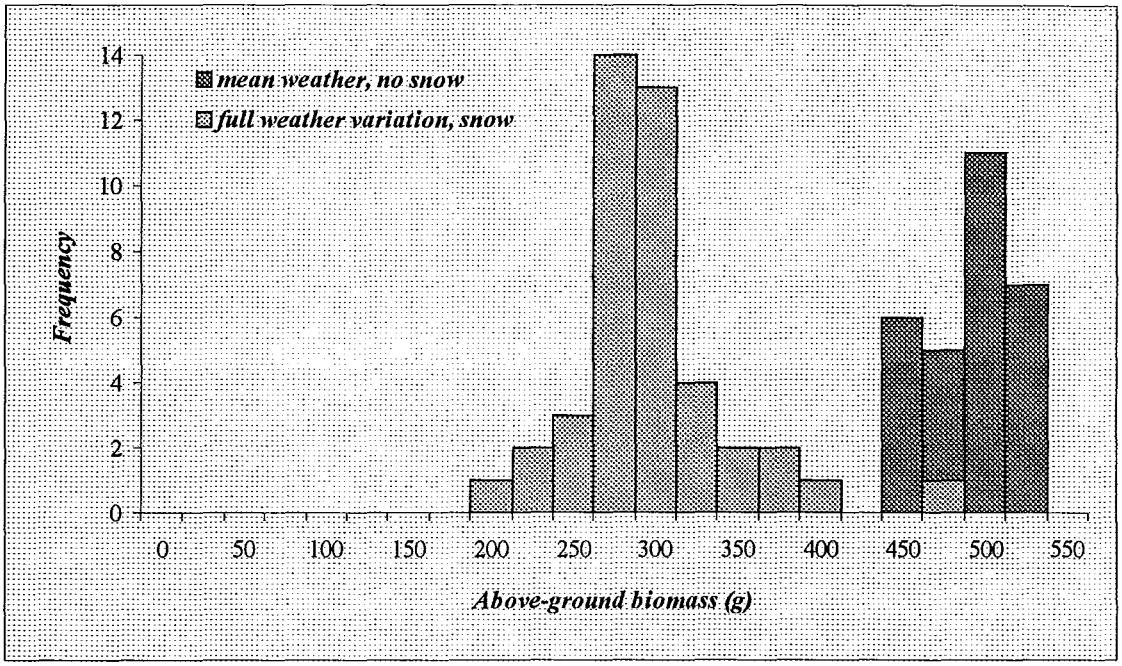

Figure 7.7 A comparison of the distribution of results from the standard model and the results from the model when set to constant weather.

Sensitivity to the rate of litter fall

It was noticed during the development of the model, that the rate and timing of litter fall can have a significant effect on the behaviour of the model. This rate influences the rate of turnover of leaves and has a direct influence on production. In the model, the variable *fallrate[sp][month]* can be adjusted to remove a daily proportion of leaves. This array was filled with a constant rate across the year increasing by a factor of five for four autumn months. The rate of conversion of living to dead material was determined by manual adjustment to approximate the expected distribution of biomass within the system. Due to the interdependence of the rates of leaf production and litter fall it is not possible to force the model to produce a specific amount of litter. Consequently, and undesirably, the method of manual adjustment must be used. Sensitivity was initially examined by halving the rate of litter creation across the year. Ideally other simulations would be carried out. The mean of the frequency distribution for thirty runs was found to be 355 g (S.D.= 53.4 g) compared with the standard 308 g (S.D.= 48.6 g). Although the two distributions overlap, the reduction in litter

fall (by 50%) is accompanied by a 15% increase in growth. Care should therefore be taken to ensure that the rates of leaf turnover are appropriate. It is likely that there will be certain critical levels of leaf loss which push the growth rate either to extinction or exponential growth. At present the model shows no sign of a reduction in growth rate over time. This may be appropriate for the initial stages of plant development, but it is hard to see where a reduction might come from. The rates of turnover of both leaves and roots will be critical to the realistic behaviour of the model.

Sensitivity to latitude

Three locations were chosen for model runs to investigate the effects of latitude, all at an elevation of 500 m above sea level. The sites were chosen at latitudes of 52°N, 54°65'N and 57°N, and solar radiation conditions calculated as described in section 4.4. The middle site at 54°65'N represents the Moor House study site, with the other two sites being situated approximately at the south and north coasts of Britain. This choice of sites enables an examination of the contention that (in the context of climate change), the combination of solar elevation and new climatic conditions will result in conditions with no geographical parallel (Department of the Environment, 1991). Each site was modelled at both current temperatures and under a regime of a three degree rise in each monthly average temperature. Importantly, the weather distributions, and all else apart from the sun angles and intensities have been kept constant, so variation between sites will be purely as a result of variation in solar conditions.

The effects of these conditions were examined for a single plant growing in the open, in a gap in a low canopy and in a continuous canopy. Open conditions were defined as for the standard runs with no above-ground structure. Conditions in the continuous canopy (Table 7.3) were taken at half the volumetric densities recorded by MacKerron (Gimingham, 1972). Gap conditions were defined as a low wall of vegetation around the outer two tile layers (i.e. where $2>x>9$ or $2>y>9$), with suitable vegetation densities (Table 7.3).

For both the gap and continuous canopy conditions, all individuals became energetically non-viable, dying either before the end of the first season, or more usually at the beginning of the second, when investment in leaf material is retarded by inadequate stores. As stated earlier, the stress-related mortality sub-model fails to represent the full range of an individual's responses, but examination of the long-term growth of these individuals (respiration consistently higher than photosynthesis) indicated that these results were appropriate. Plants growing under open conditions generally survived (some stochastic

Table 7.3. Vegetation densities used in the construction of gap and continuous canopy conditions.

height above ground (*ez*)	*absdens[x][y][z]* for gap conditions	*absdens[x][y][z]* for canopy
9	0	28
8	0	227
7	0	500
6	0	994
5	700	1221
4	2500	1079
3	2044	1022
2	1000	994
1	500	1020
0	1000	1136

mortality). This range of responses seems to be too large, indicating a fault in the mortality model. Real individual heather plants have a high resistance to stress, and may remain alive without any apparent increase in size for many years. The mechanisms underlying this are not clear. This topic is discussed further in Chapter 8.

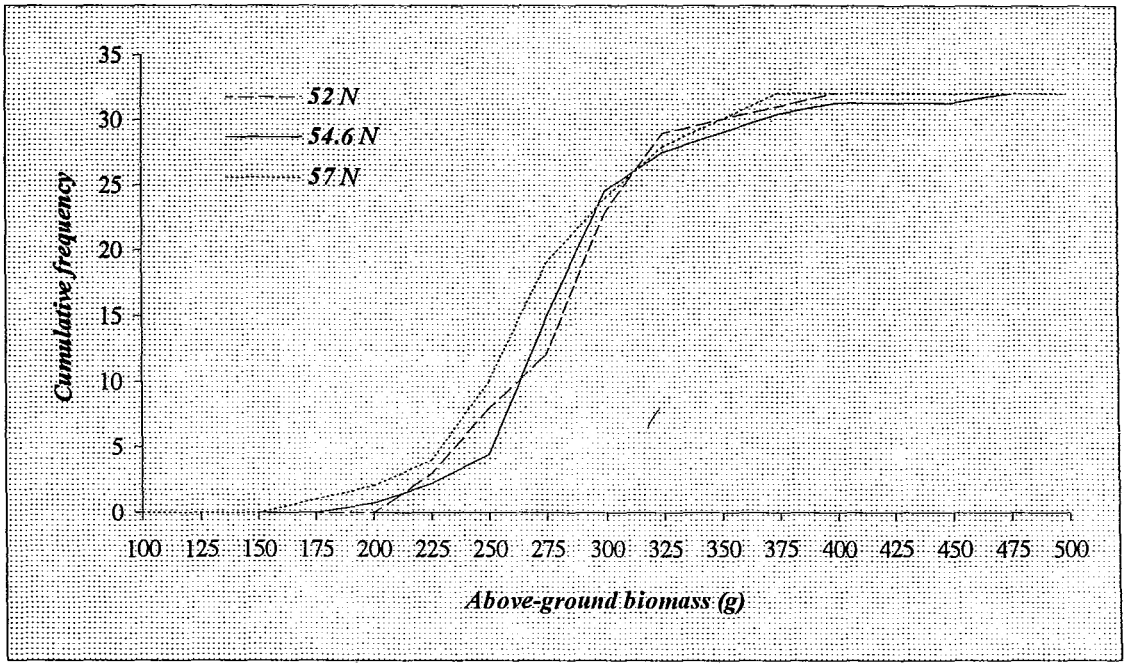

Figure 7.8. Cumulative frequencies of biomass after five seasons for three latitudes: 32 runs for each.

The variation within runs of the same solar conditions was greater than the variation between different treatments. Figure 7.8 shows the cumulative frequencies for above-ground biomass after 5 years for 32 runs in each treatment. As can be seen, there is little difference

between the treatments, and a larger sample size would be required before any further analysis could be carried out. It should be noted at this stage that the full effect of variation in latitude is not represented in the model since phenological responses are at present modelled only in response to time of year and temperature, and no solar response is modelled. The magnitude of the difference between treatments would be expected to increase with improved phenological response, but the sensitivity of the system to latitude is, at present, much less than its sensitivity to other inputs.

Sensitivity to climatic warming

As stated in the introduction, one of the design goals of the model was that it might be used to study the effect of climate change on vegetation without the violation of any model assumptions. The modelling approach allows for changing abiotic variables. Runs were performed for two scenarios of uniform warming, acting through the simple increase of each monthly mean temperature input (*tminmean[month]* and *tmaxmean[month]*) to the model by either 1°C or 3°C. Smaller sample sizes of 15 were used, so the results are not necessarily fully representative of the true distributions. The 1°C warming gave results broadly as expected, with the mean increasing a little to 323 g with a standard deviation of 41 g (compared to the standard 308 g; S.D., 48.6 g). However, the warming of 3°C produced results far outside the expected range, with a mean of 6741 g and a standard deviation of 325 g. This represents a phenomenal growth rate from 46 g in five seasons, leading to an above-ground biomass equivalent to 4350 g m^{-2}. This may be compared with the unusually high biomass measurement of 2930 g m^{-2} (Robertson & Davies, 1965) for a stand over 15 years old in Kincardineshire. Since the range of measured biomasses for heathlands goes down to 450 g m^{-2} (Allen, 1964) and the majority lie in the range 1800-2500 g m^{-2}, it is possible that the range could extend up to the generated value in exceptional circumstances. 4350 g m^{-2} is, however, approximately a quarter of the biomass of a forest ecosystem. The 12 × 12 × 15 grid is almost filled by these volumes of plant material and so the plant form becomes distorted and the ecological relevance minimised. At this point, as the grid becomes limiting, the performance of the model becomes suspect, with continued growth in a full grid invariably leading to disruption of the data structures leading to the model stopping due to error.

Such growth rates are only potentially possible in the absence of resource limitation from water and nutrients. The increased temperature would be expected to be accompanied by a corresponding increase in growth due to improved photosynthetic response, and due to an increased length of growing season. The 3 °C rise would be expected to have a significant

effect on the length of the growing season, increasing the potential season (i.e. temperature>5.6 °C, ignoring the higher temperature required for budburst) from 6 to 9 months at Moor House. Production per year would be expected to rise by 50% due to increased growing season alone. It is important to note here that the growth of successive years accumulate in the same way as compound interest, so a small deviation early in the plant's history will be magnified by successive seasons.

Although the biomass is possible, if unlikely, the rate of growth is high for a natural system. If averaged for the 5 years, the model produces 860 g m^{-2} yr^{-1}. Whittaker and Likens (1973) present productivity for a number of terrestrial vegetation types: grassland, 500 g m^{-2} yr^{-1} ; woodland and shrubland, 600 g m^{-2} yr^{-1}; temperate forest, 1200 g m^{-2} yr^{-1}. When taken as an average, the productivity is 43% higher than would be expected. Pakeman and Marrs (1996) predict an increase in bracken (*Pteridium aquilinum*) biomass of over 30% in some areas for a 1.4 °C rise in mean temperature without increased transpiration, and in the absence of competition, so the mean result remains within a plausible range. However, the productivity for the fifth season is approximately 2000 g m^{-2} yr^{-1}. This is not a reasonable value, and indicates that the model is behaving unrealistically. In a field study using open topped chambers to raise the temperature around 4 sub-Artic shrubs (*Empetrum hermaphroditum, Vaccinium vitis-idaea, V.uliginosum, V.myrtillus*) by about 4 °C, Parsons *et al.* (1994) found total above ground biomass unresponsive, although allocation of assimilate within the plants changed.

At present, no limitations on growth are imposed by nutrient limitation, water stress or by the physical structure of the plant. Where growth is not limited by light or temperature, this allows the plants to grow faster than real plants. It is hoped that the inclusion of responses to these limiting factors will reduce the possibility of unreasonable behaviour in the model. Indeed, it seems appropriate that the simple production model should behave unreasonably when placed in extreme conditions. Another drawback of the present model is that it has no facility for the inclusion of acclimation responses of plants in new conditions, which could limit the extent of response. This will be discussed further in Chapter 8.

7.4 Multiple individual simulation

Another design goal of the model was for it to be used to investigate interactions between plants. Because of the amount of computer time needed to undertake simulations, and the limited ecological value of simulations using partially validated sub-models, this analysis was

restricted to a single simulation involving four individuals. This was set up on a grid 15x × 20y × 15z. All four individuals were set to the same species, with the same characteristics for spatial spread. All individuals were initialised with a dry weight of 40 g spread between three tiles, with individuals A and D starting in a prostrate form and B and C starting as a single column (Table 7.4). Climate was set for a 3°C increase in order to accelerate the growth process due to run time considerations. As indicated above, this temperature regime may increase production to unrealistic levels. However, the purpose of this simulation is to demonstrate that the modelling approach can be used for a number of individuals simultaneously, and that these individuals will exhibit differences in growth rate attributable to differences in microclimate at the scale of the individual, thus generating competition. A simulation of three seasons was run, and the growth curves for the four individuals are recorded in Figure 7.9.

Table 7.4. Initial co-ordinates of four individuals for multiple simulation. Each individual occupies three tiles. Ground level is at $z = 1$.

dens[indiv][tile]	*indiv A*	*indiv B*	*indiv C*	*indiv D*
2100	4, 5, 1	7, 7, 3	12, 4, 3	16, 7, 1
2000	3, 5, 1	7, 7, 2	12, 4, 2	15, 8, 1
2000	3, 6, 1	7, ,7, 1	12, 4, 1	15, 7, 1

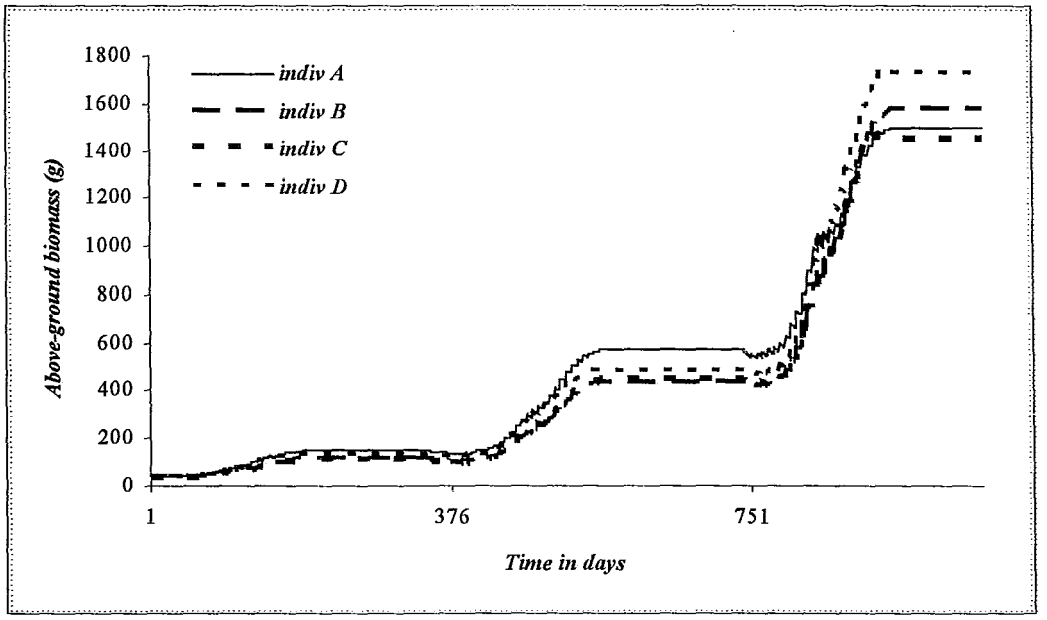

Figure 7.9. Growth curves for four competing model individuals.

It is interesting to note that the same individual does not remain dominant over the run period. Since the run is for such a short time period, and the individuals have not had time to reach any equilibrium, it is not appropriate attempt to determine the best competitor.

However, it is still useful to examine the changes occurring in the model over time. Figure 7.9. shows the structure (left) and light environment (right) after two seasons. The plants can be seen to be growing as two pairs, A & B and C & D. These results have been plotted on Microsoft Excel as contour graphs on a rectangular grid, and have afterwards been put back on to a hexagonal grid by hand. This results in a degree of distortion of form, but gives a good initial indication of general conditions within the plot. Some overlap between individuals is already evident. The starting positions are evident in the ground level *absdens[][][]* plan, with the vertical plants in the centre and the prostrate plants to the outside. Those plants near the edge are not conferred any great advantage, since the embedding profile begins to attenuate light even at this scale of vegetation, as evidenced by the outer ring of shade in the ground level light plan. The individuals can be seen to be competing as required by the model. All varaition in production is a result of the combination of form and microclimate, since all the individuals have an identical physiological response.

The shading effect of the four plants extends beyond the structures themselves, already significantly modifying the light environment in the plot such that it is apparent that other competitors would probably need to be shade tolerant. It is interesting to note that the dense canopy attenuates light to the extent that heterogeneity would eventually reduced after canopy closure. However, at present, the model generates a range of light values at ground level from full illumination down to near zero, providing a range of different potential germination sites.

7.5 Comment

It has not been possible to validate and fully demonstrate the full range of possible applications of this model. The model design is such that it could potentially be used to investigate any aspect of the dynamics of any terrestrial ecosystem. However, limitations of computing power and consequently run time, and the total available time for the project have severely restricted the possibilities for calibration, replication and investigation. It is hoped that the runs presented above illustrate both the working model mechanisms and the potential of the model.

Figure 7.10. (Overleaf) A four individual simulation after 500 days growth in dynamic microclimate. The page shows the structural state on the left, with no distinction between individuals, rising through *z* levels from the ground level (at bottom of page) to the top of the canopy (legend). Units of *absdens[x][y][z]* are used such that 3000 represents 30% volumetric occupancy. The right hand column shows the corresponding light environment (*lt[x][y][z]*) in Wm^{-2}. Scale 1:33. North lies to the left.

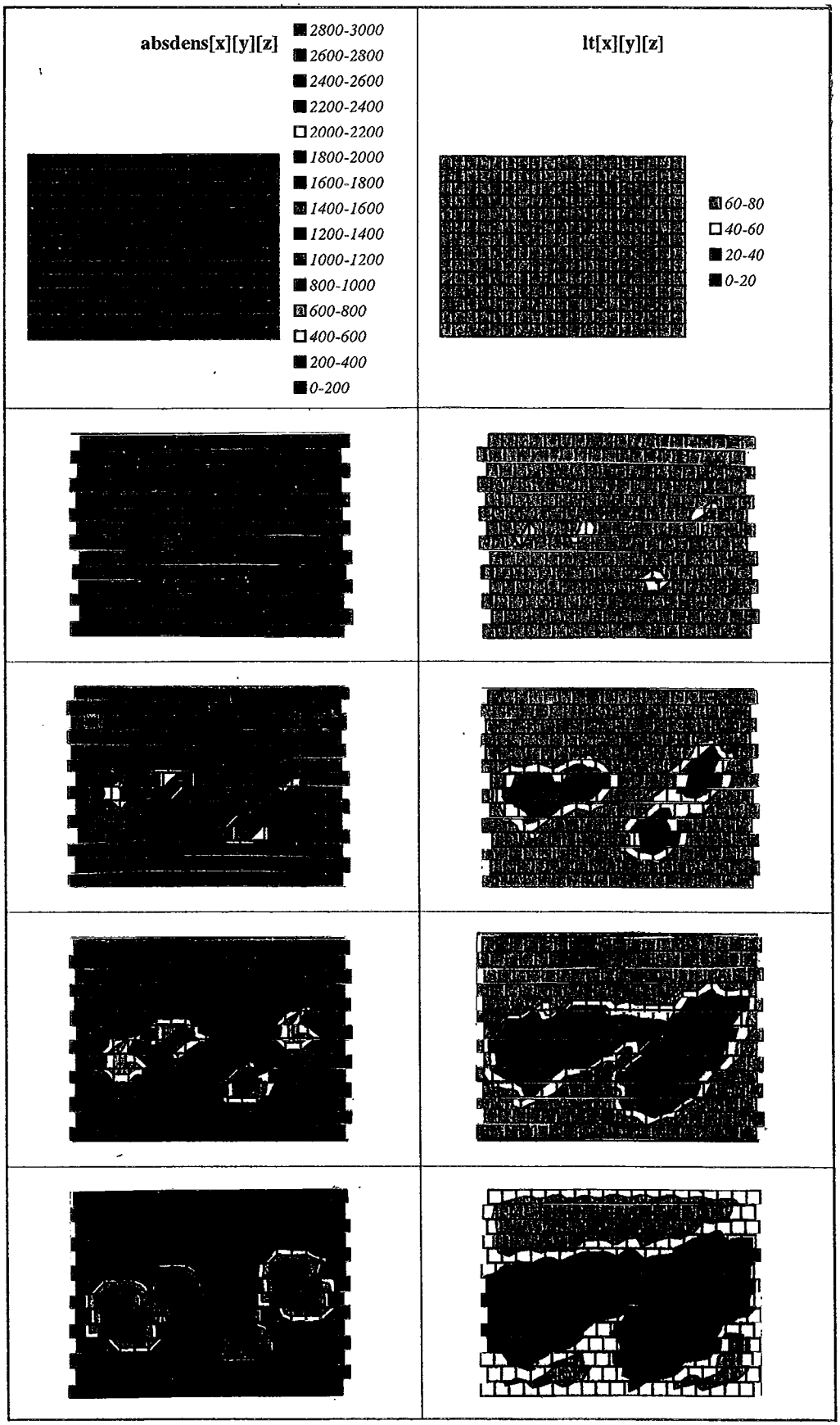

Figure 7.10. A four individual simulation after 500 days growth in dynamic microclimate.

8

Discussion

Contents

8.1 The modelling approach

The modelling approach used in the "Ecospace" model has been discussed in Chapter 2. As a prototype model it is of great importance that the "Ecospace" model can be shown to behave reasonably relative to the real system and to other individual-based models. The principle of a three-dimensional grid is sound and does not generate overly complex behaviour. Although expensive in computer time at present, advances in computing power, and more efficient use of both existing hardware and software, could lead to a more practical model in the near future. However, the model is, at present, far from complete and is some way from being a useful analytical tool.

The complex modelling approach

The modelling approach is a complex one, implemented for reasons described in Chapter 2, and carries with it disadvantages as well as advantages. Complex modelling approaches have been criticised for a number of reasons and are at present little respected by ecologists. Levin (1989) criticises

> "..the almost mindless inclination to include in many ecosystem models the full complexity of the biotic and abiotic environment, on the mistaken notion that highly detailed and reductionist approaches make the best tools for prediction and management."

Whilst there may be drawbacks in a complex approach, as there are in all other approaches, it is important to recognise that ecological modelling is at present in a primitive state and we are far from a position where we can determine the very best modelling approach for a given problem. It is not appropriate to consider modelling approaches as mutually exclusive, but rather as a series of alternatives each of which is suited to a different task. A modelling approach develops in tandem with field studies, and may be pursued for a number of years before becoming practical. Here we may consider the forest gap-dynamics models, where several generations of models have developed out of the original JABOWA model of Botkin *et al.* (1972). These models took a leap forward with variation in plot size leading to the gap dynamics model of Shugart and West (1977), five years after the initial model was published, and further advances have continued up until the present, using the same core approach. Similarly we may consider the development of the Lotka-Volterra equation, (Lotka, 1925; Volterra, 1931) with experimental work leading to the introduction of a non-linear functional response (Gause *et al*, 1936) and to further development of the modelling approach. It is necessary to subject any potentially useful modelling approach to rigorous experimental testing, possibly leading to further model development, before rejecting the approach.

This complex spatial approach has been shown to be a practical approach. The model demonstrates the potential capacity of computer-simulated models to describe a number of concurrent ecological and physical processes in three dimensions. Although complex, the model can produce output at a simple scale comparable to that of simpler, faster models, or produce more detailed information. It is a very adaptable approach, since any different sub-models could be substituted and linked through the spatially-distributed global variables, allowing them to be updated. It is felt that it is now appropriate to give this approach serious consideration when faced with a modelling problem.

A very similar approach has been developed independently by Williams (1996) for studying forest competition. The mechanistic model, "Arcadia", uses a 3-dimensional grid of hexagonal tiles (1 m between sides, 1.18 m tall) and grows trees as flexible cellular automata. Individual trees grow to occupy a number of tiles each, but occupation of a single tile is limited to a single individual. Competition is driven by the spatial distribution of light within the grid, calculated using a simplified ray tracing approach (arrays used to store the paths of selected rays, thus reducing calculation time). Photosynthesis is calculated three times a year using representative quasi-daily values for each tile occupied by an individual. Growth is applied using species-specific growth forms. The model produces reasonable output, although full validation is not possible due to the model complexity. "Arcadia" has no treatment of microclimate other than light, and generally models at a lower resolution than "Ecospace", but

the two models are very alike, having developed from a similar modelling philosophy. The lower resolution of "Arcadia" may be sufficient to capture much of the spatial heterogeneity of the real system.

An interesting result of the initial "Arcadia" model runs presented is that when the modelled solar regime is altered to simulate the treatment of light typical of forest gap-dynamics models (Shugart, 1984), very different dynamics are observed, with the resultant loss of heterogeneity leading to a reduction of species diversity. Although it is unlikely that the two models are directly comparable, this is the type of behaviour which one would expect to be the advantage of the complex spatial approach, allowing the continued existence of species which would become extinct in other, less complex models. When dealing with abiotic change, it is likely that the species which will be in optimum conditions after the change are currently in sub-optimum conditions. Although this does not necessarily imply that these species will be out competed in current conditions, it is essential that all these potential key species be allowed to survive if this is a realistic assumption.

A spatially rigorous approach to the modelling of mixed species forest has also been developed by Mou and Fahey (1993). They present a model of succession at the Hubbard Brook Experimental Forest, New Hampshire. The model, REGROW, uses a combination of ecological field theory (Wu *et al*, 1985) and a Markovian growth function to simulate vegetation dynamics on a 4 × 4 m torus. Competition is calculated at an individual level in both the horizontal and vertical dimensions from a few plant dimensions, combining abstractions of soil resource and light availability in relation to plant shape to give an index of "potential interference". This is largely a correlative rather than a mechanistic model, although modelling response to radiation and average temperature, and consequently requires a calibration variable with a significant influence on the growth rate to account for " a variety of unknown factors affecting photosynthesis and growth of each species". Currently running at a bi-monthly time step, this model operates at a high level of complexity, but avoiding explicit representation of individual plant form in favour of general species characteristics, thus requiring more complex extrapolations from the abstract forms to give the required response surfaces (Wu *et al*, 1985). In itself this is no reason for criticism, but it is possible that a more explicit treatment of plant form and microclimate would involve the introduction of little more complexity. Due to problems of estimation of resource capture (particularly below ground) and physiological response to resource supply, the model is not recommended in its present form for studies of vegetation response to abiotic change. This problem with information limits the "Ecospace" framework.

It has been suggested that one disadvantage of complex models is their complex behaviour (e.g. Kimmins & Scoullar, 1984). However, although the exact causes of the behaviour of a complex model may be difficult to determine, the increased number of feedbacks required by such an approach can also result in a more stable model if results are examined at the same ecological scale as simpler models. Thus although the model development may be hindered, the possibility of counter-intuitive behaviour can be reduced without the use of crude limits.

As a final comment on this question, the notions of complexity and simplicity are not absolute. The perspective from which a model is viewed is critical to the way in which it is viewed, in particular the scale (see section 8.2). Kimmins and Scoullar (1984) point out that what seems to be a high degree of complexity to a whole-plant modeller representing photosynthesis may well seem simple to the photosynthesis modeller. Similarly, the "Ecospace" model may be viewed as a fairly simple model at the scale of the single tile, although it is apparently complex when the individual units are combined, and a forest gap-dynamics model may be viewed as complex at the landscape scale. It is important to first determine the appropriate scale of study and then to determine the appropriate level of complexity at that scale and the hierarchical levels above and below.

Information requirements

Although it may be theoretically desirable to model plants at the individual level in three dimensions, the information required to develop, parameterise, calibrate and validate models of this type is incomplete. This is a problem common to all complex models, witness the validation problems of Williams (1996). Biological sciences have discovered many of the underlying mechanisms of the living world, and yet more still remain to be discovered. The reductionist approach to biology tends to focus on the minutia at the end of strands of knowledge and so we tend to believe that it is these minutia that we do not yet understand and often we ignore those principles which we do not understand higher up the tree of knowledge. When we examine plant growth, we find that we know what makes the plants grow, how that growth is applied at a cellular level and how that cellular growth responds to hormonal stimulation. It does not follow, however, that we know how plants grow into the shapes they do.

The study of the spatial structure of individual plants has been consistently neglected by biologists, with morphologists concentrating their studies at the cellular level and ecologists

concentrating on community structure. Descriptive measurements of growth forms (e.g. Hallé & Oldeman, 1975) have been limited largely due to the difficulty of effective measurement and statistical problems due to phenotypic variation and have tended to be qualitative. Spatial plant modelling has largely been carried out by computer graphicists (e.g. Prusinkiewicz & Lindenmayer, 1990; Aono & Kunii, 1984) until recently (Ford, Avery & Ford, 1990).

We can say that genetics control plant shape and that this is modified by the environment, and yet we do not know the mechanism for the action of the genetics upon the developing plant or the true nature and strategy of spatial resource allocation. We have only broad general principles to use as guidelines, and mechanistic modelling necessarily becomes increasingly speculative as one moves into these areas which are loosely defined scientifically. Great care must be taken to avoid applying inappropriate strategies, especially human-style cognitive mechanisms, to the growth of plants. One can work safely only with what has been proven: conjecture must be limited when producing a mechanistic model although some empirical relationships will usually be necessary.

If one is attempting to model plant growth in three-dimensions it is desirable that the three-dimensional structure of the model plant is authentic and that it responds spatially to environmental stimuli. The tile-based spatial plant growth system used in the "Ecospace" model is limited in that it has no explicit representation of the plant branching structure. This has advantages in that the plant can grow in any direction within growth rules, and in that the plant uses the same data structure as the microclimate sub-model. However, it is felt that a more morphologically-based spatial plant growth sub-model which can be related directly to the grid would represent dynamic plant structure more accurately.

Due to our poor understanding of vegetation structure, microclimatic measurements are not usually related to the three dimensional physical structure. Instead, measurements are related to properties of the whole canopy, or more frequently to coefficients representing aspects of vegetation structure (e.g. diffusivities, LAI). Microclimate has been studied almost exclusively as a one-dimensional process by physicists and is as yet far from fully understood (perhaps because it is a three dimensional process). It is consequently very difficult for biologists to correlate structural changes in plants with microclimatic variables, although the phenomena of phototropism and wind-pruning are well known. Similar problems arise in our treatment of directional root allocation, where the adequate description of both root structure and soil property distribution presents problems.

The information required for the completion of the "Ecospace" model is incomplete. It is not clear whether or when all the knowledge required will be available. This is a serious limitation of the approach. It may be some years before many of the crucial questions are answered. However, it is expected that the modelling framework would also require several years before nearing completion, especially if the recommended improvements and recoding are implemented. This would allow parallel development. As pointed out earlier, a modelling approach cannot be expected to yield instant results, and it is not therefore appropriate to compare the success of the approach at this stage with the gap-dynamics approach which has been developed for over twenty years and now consistently yields reasonable results for those field sites calibrated. However, it is appropriate to consider whether the approach is worth the future effort, and whether it could potentially function as well or better than other individual based approaches. Where there are information requirements which seem critical to the behaviour of the model, (e.g. nature of partitioning), it is worth asking how these elements are treated in other, simpler models. In order to not directly represent an element of ecosystem function it is necessary to use simplified variables representing a number of different processes. Such models require calibration, and are usually limited to the site for which they are calibrated. A more general approach requires some form of independent representation of all significant elements of the system in order to allow application across a range of systems.

The requirement for information is a major drawback of the complex approach, although it may be argued that in the lack of understanding remains whatever the modelling approach used, but only in a complex approach is it clearly lacking. Complex models are limited by the area of knowledge about which we know the least. It is common in models to use estimates where knowledge is limited. Thus, in the "Ecospace" model, a root-shoot ratio of 0.5 was used in common with most plant models. However, Røsberg *et al*, (1981), estimated allocation to roots in *Calluna* near Bergen in Norway to be as high as 90%, due to the rate of turnover of fine root hairs being as much as 3-4 time higher than the rate of leaf turnover. It is not clear to what extent this affects the model, since the correlative model of Grace (1970) may take account of this indirectly, although it is certain that if this estimate is true the growth patterns of the current model plants will be unreliable. Håkanson (1995) argues that uncertainty in the calculation or estimation of variables is additive and multiplicative such that no more than two to six compartments are reasonable in any model. However, such a simplification of a system itself introduces errors, and a balance must be sought as appropriate for the modelling task.

Run time

The "Ecospace" model has a long running time. The main time constraint lies in the ray tracing routines of the light and wind models. Here, for each tile, and for each ray, the shaft length in each tile passed through is calculated. If shaft lengths were stored directly as a data file, in order to minimise calculations, it could be quickly become unmanageably big for larger grid sizes. An alternative approach using a general formula based on the relative rather than the absolute positions of tiles might potentially be practical. Alternatively a simpler geometrical form than the hexagonal tile could be used.

The speed of simulation could be increased in two other ways, improvement of the computer hardware used and improvement of the software. The model was run on a Sun Microsystems SPARCcenter 1000E with six 60 MHz CPUs, with a main memory of 384 MB and a virtual memory of 1.5 GB. There are many faster computers which could potentially be used, often utilising parallel processing techniques for which this modelling framework is well suited. However, it would not be appropriate to use a larger computer without further improvements both to the model and the computer code. The code presented in the Appendix is written using a simple programming style, and it is felt that this could be considerably improved upon. The data structures used in the model are cumbersome and a more experienced programmer could use structures more appropriate for the hardware. The development of a complex model such as this requires a highly efficient programmer, to reduce both run time and development time.

It is critical that a model have a reasonable run time in order to be of practical application. The degree of variation between runs in the current version of the model requires that the model be run a number of times for each simulation. This increases the total run time required for a single set of conditions and represents a disadvantage of the modelling method. However, it is hoped that a proportion of the variation due to variation in plant form can be removed, thus improving the practicality of the model. A long run time is, however, an inevitable consequence of a complex modelling approach.

Generality

The "Ecospace" framework is suitable for application to a broad range of terrestrial vegetation. Modification of the tile size and grid dimensions could allow the grid to be scaled as appropriate for different systems if allowance is made for problems of scale. Most of the

modelling assumptions made are not specific to the heathland ecosystem permitting the representation of different vegetation types. The results from such a model should have a greater generality than those from an ecosystem-specific model (e.g. Coffin & Lauenroth, 1990) or a site-specific model (e.g. Phipps, 1979). This potentially allows comparisons between, or transitions between different systems.

The potential generality of a model should help balance the extra time required for development. A model which can be applied to all vegetation systems for a variety of studies without any major alterations would potentially save much modelling time.

Model performance

The "Ecospace" model has been developed as a prototype framework. As a complex mechanistic ecosystem model it is important that all aspects of ecosystem dynamics be addressed in some way. This may involve the use of assumptions where appropriate, to avoid representation, or the use of a reasonable approximation. In the model's present state, no dynamic water or nutrients are modelled. It is not appropriate to assume that these will have an insignificant effect on the system since they are well proven key features of the heath ecosystem (e.g.Heil & Diemont, 1983; Bannister, 1976), and because of the extent of their influence, a simple representation is likely to dominate the model performance. The model is therefore at present in an unfinished state; it is therefore not entirely surprising that some of its output is clearly unrealistic. It is not appropriate to judge the entire modelling approach from the model's present state, although a critical review of the performance of the current model is important.

A specific approach to the development of the modelling framework has been applied. The complex nature of the proposed model and the cross-influences between sub-models is such that it is inappropriate to attempt to model all aspects of the model to an equal level of detail simultaneously. The model has therefore been developed by using either simple constants or sub-models to describe inputs required for the sub-model under development. This allows a general framework with interconnecting variables between sub-models to be built up. The present temperature sub-model treats evapotranspiration indirectly, but it is necessary to have a spatial sub-model of temperature in order to develop a sub-model of water use in the system. The use of a mechanistic model of photosynthesis is severely limited at present by the lack of a water sub-model, but again this has an important influence on transpiration and is required as an input for a water sub-model. If viewed at a stage part way

through model development, such an approach will necessarily appear unbalanced. At the end of the chapter the areas of the model requiring attention are described.

"Ecospace" is currently a slow running model, although, as has been discussed, this could be improved in several ways. The amount of run time allocated to the calculation of the light, and potentially to the wind ray tracing sub-model seems to be rather high relative to the plant growth (particularly photosynthesis and partitioning). This reflects the level of detail used in each part of the model. It is important that the balance of detail within the model be appropriate. As the model is currently being developed, a simple correlative growth model has been used and it is suggested that a more detailed plant growth model be implemented.

The runs conducted with an elevated temperature of 3 °C give some cause for concern, as discussed in section 8.4. There is no evidence of self thinning or a self-imposed size limitation occurring, as would be expected due to self-shading. The plants therefore tend to outgrow the grid, resulting in unreasonable behaviour. This behaviour indicates that the model is at present unreliable. However, it may be expected that the phototrophic growth form could reduce problems of incorrect spatial allocation of photosynthate, bringing us closer to a self-regulating system.

8.2 Limitations of the hexagonal grid structure

The grid would ideally be designed such that each tile relates equally to all its neighbours (see section 3.2). The hexagon performs adequately in a single plane, but has an uneven relationship with its vertical and diagonal neighbours. The effects of this on the limitations of spatial spread can be reduced by making the tiles thinner in the vertical dimension as implemented in the model. Importantly, the plant structures resulting from this layer based approach are likely to be affected unevenly by this bias.

The complexity of the spatial form of the hexagonal tile introduces computational difficulties to the model which could be avoided in a simpler form. The use of a cubic grid, for example would simplify the calculation of the point of intersect of a line with the cube sides, and allow the use of simple general formulae to describe neighbour relations. It is felt that a a considerable proportion of the time taken to calculate the monthly light environment could be removed by the use of a simpler grid structure.

An alternative approach

In order to simplify the grid structure and the nature of calculations, a different unit of volume is proposed, that of a sphere approximating a dodecahedron. The sphere has the advantage that it is an entirely regular shape, with no orientation, having an equal relationship with all its neighbours. Its major disadvantage is that it does not tessellate, and there is consequently a considerable amount of free air between spheres. If one were to imagine a box filled with sponge rubber balls, these would fall into the pattern shown in Figure 8.1a below. By reducing the size of the box one could compress the balls until there was no air between them. At this point the point of contact between each ball would have been compressed into a flat pentagonal face and the balls would be twelve-sided solids, dodecahedrons.

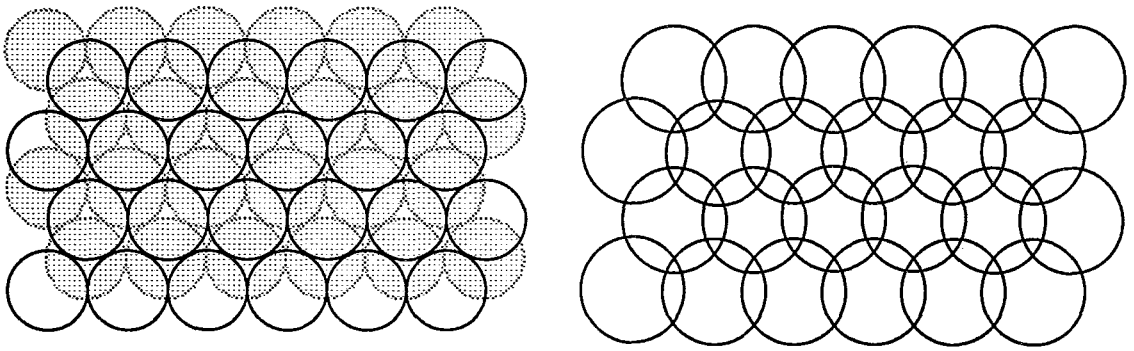

a) ***b)***

Figure 8.1. The use of spheres as an approximation of dodecahedrons. *a).* Two layers of a grid of normal spheres, with gaps between clearly visible. *b).* The top layer of the same grid with radius increased by a factor of 1.24 such that all volume is filled. In a dodecahedral structure there is a distortion of the hexagonal pattern.

This effect could also be produced by increasing the size of the spheres rather than decreasing the occupied volume. It is proposed that for a given volume to be modelled, this be first divided into normal spheres and then the radius of the spheres be increased until the total volume of the spheres is equal to the volume to be modelled. This radial increase is a constant 1.240701 times the radius of normal spheres. The resultant array of spheres overlap, as in Figure 8.1b, and can be used as an approximation of a tessellating grid of dodecahedrons for geometric calculations. Since the equation of the surface of each sphere is known, geometry can be simplified. The perfect symmetry of a sphere is such that the length of a straight line (chord) passing through a sphere can be determined directly from the nearest point between the line and the centre of the sphere. This could considerably simplify ray tracing calculations.

The surface geometry of the solids used in the grid is only used in calculations of ray tracing, disc overlap and potentially, moving vegetation. For all other calculations using the spatial structure it is the relative positions of neighbouring solids which are of importance.

Consequently, the unit of volume may equally well be visualised as a dodecahedron. As can be seen in Figure 8.1a, each sphere has six neighbours arranged in a hexagonal structure in a single plane. This pattern is repeated in three planes, two passing diagonally through the diagram, giving a total of twelve neighbours. When compressed until tessellation occurs, this structure is distorted, (each sphere will have two rings of five neighbours, one directly above and one directly below) so the positions of the centres of the spheres would also move, and this must be taken into account.

Scale

The use of a regular grid structure raises a complex problem of scale. It is necessary to choose the dimensions of the hexagonal tile. A side length of 0.05 m was chosen after the field studies as a suitable scale for heathlands. This scale allows a single heather plant to occupy over 100 tiles when fully grown, and appeared suitable for seedlings. However, if we consider the establishing seedlings and the moss carpet, it would perhaps be desirable to model them also at a sub-individual level, since that is the scale at which they compete. Equally the tile size is inappropriate for an emerging birch tree, which would require significant expansion of the grid. Importantly, one would expect the behaviour of a model individual to vary depending on the scale at which it is modelled. Legg (1995) points out that for heathlands, the level of study may determine the observed dynamics, and that the choice of scale is therefore critical to the results obtained from a field study. We would expect the same behaviour for a modelled system. This behaviour is demonstrated by the alteration of plot size until gap dynamics were produced in Shugart and West (1977). If the theory of vegetation dynamics presented in Chapter 1 is true at one scale, it is very likely true at other scales, particularly those scales close to that scale. The use of a fixed grid size forces us to consider scale below that of the individual. We can no longer use vague hierarchical terms such as the individual level, which surely implies an actual spatial scale varying across the plant's lifespan. This is illustrated by Legg (1995) for birch, showing how the scale at which an individual operates changes from centimetres at germination up to a hectare when full grown, with migration interactions occurring on a scale greater than 10 km^2.

An additional problem of scale is raised by O'Neill (1989) who points out that plant evolutionary strategies can operate across a broad range of scales. A species which may become locally extinct in 99% of cases at one scale may be forced, or have chosen to operate at a scale sufficiently larger than the local scale, thus competing at a separate hierarchical level from the dominant plants at the local scale. This gives added importance to the modelling

of survival of rarer plants, but presents problems regarding the interpretation of values from a local scale model. An advantage of the modelling approach producing output in the form of distributions is that this may allow the an estimation of the success of these species. However it must be recognised that a model operating at an inappropriate scale is unlikely to give a good indication of species dynamics.

The use of a rigid spatial scale presents problems for the modeller. The spatial forest regeneration model REGROW (Mou & Fahey, 1993) , is considered by the authors to be suitable only for the early stages of regeneration, and not for the resultant forest dynamics. The same applies to "Ecospace". The regular grid size results in each individual of a different size being modelled at a slightly different scale relative to the individual. This is likely to introduce bias in the model. It is possible that an irregular grid size could be introduced into the "Ecospace" model, to reduce the impact of the chosen scale. If the size of the tiles were increased at a suitable rate with distance above ground, it might be possible to simulate individuals of moss, shrub and tree with a similar number of tiles per individual, thus allowing an equal level of modelling detail for each species or age class. Such a sliding scale may seem ideal in the vertical dimension, but causes problems in the horizontal dimension. This technique is worthy of some investigation, since it would reduce the impact of modelling scale within a selected range. If applied to the pseudo-dodecahedrons proposed above, a simple radial increase as a function of height, could be applied in the vertical dimension, whilst maintaining the arrangement of the solids. This could result in an inverted trapezoid volume with greater horizontal area covered by the grid at the top than at the bottom. This is unlikely to be practical as a modelling solution, although the Cartesian sub-grid would prevent distortion of form.

8.3 Microclimate

The different components of the microclimate sub-model are discussed separately below. Importantly, the microclimate sub-model produces variation at a scale and magnitude similar to that observed in nature. Hopefully this should give a better representation of the range of microsites available within the stand of vegetation than would be given by a spatially simpler model. Consequently the model should give a more explicit representation of the process of competition in plant stands, allowing for the application of the model to a broader range of problems. However, it is not clear at this stage how representative each sub-model is of the real system. This requires more extensive validation.

The model runs presented demonstrate that the microclimate sub-model is responsive to changes in vegetation structure, and that the extent of the effect of vegetation structure varies between microclimatic variables.

Wind

The microclimate sub-model used in the model is unusual in that it models conditions in three-dimensions within the canopy. Air flow outside the canopy has been modelled in three dimensions, but within the canopy the complex effects of turbulence are poorly understood. Since the transfers of heat, moisture and CO_2 are all heavily dependent on the movement of air, it is essential that transfer of momentum is modelled effectively. In the "Ecospace" model, a very simple sub-model is used which can generate a three-dimensional wind pattern within the canopy, but this approach is based on little direct evidence. A number of one dimensional wind models have been developed, and it was the intention to work from these towards a three-dimensional distribution. A variation about the mean wind speed for each height above the ground is calculated according to the relative volumetric occupation of each horizontal tile and a simple straight ray-tracing approach. It is a reasonable assumption that volumes of dense vegetation will have a lower wind speeds than volumes of sparse vegetation, and that a mean composed of wind speeds from a number of volumes of different density will lie between the two extremes. It is likely, therefore, that this approach will be an improvement on the assumption that all points at a certain height above ground experience the same wind speed. Although the model produces the values we would expect if the above assumption is generally true, at present no suitable data exists for direct validation. It is apparent from the results that the variation between layers of air is greater than that within layers at the heights relevant to heath vegetation. Further analysis would be required to determine if this is appropriate, but the modelling philosophy has been influenced by the principle of Kimmins and Scoullar (1984), that a partial representation is superior to omission. The effects of eddying and vertical wind are not at present represented in any way in the sub-model, although it is suggested that the grid based approach might well be useful for a bottom-up modelling approach.

Most models of canopy microclimate (e.g. Sauer & Norman, 1995; Goudriaan, 1977) assume that wind speed is evenly distributed throughout each vertical layer, and it is felt that the current wind sub-model is an improvement, but does not introduce much further model complexity or run time. Another advantage of the current wind sub-model over other methods is that it is responsive to changes in 3 dimensional vegetation structure. Some models (e.g.

Cionco, 1978) allow an effect of the broad downwind area of the vegetation, but this is insufficient to capture the subtleties of a heterogeneous community.

In the model runs presented in the results section, run time limitations prevented the inclusion of the ray-tracing sub-model, resulting in a lack of downwind sheltering effects. This results in an under-representation of the extent of the effect of plant structure on surrounding microclimate. However, one must consider the complexity of wind direction within and immediately above the canopy. This cannot be expected to be closely correlated with the reference wind direction at 10 m, due to the effects of terrain and vegetation topography, particularly in heterogeneous canopies. This makes it difficult to select a suitable wind direction to use with the ray tracing model. The use of straight lines to represent wind is common with models of forest wind-throw, but this is for a regular monoculture. It is possible that the simplified wind model will give a better estimate of local wind speed, although the effects of strong directional winds will be biased. This requires further investigation.

Temperature

The temperature sub-model presented here has been developed as a prototypical three-dimensional model, to demonstrate the potential of the grid to generate heterogeneity. The sub-model demonstrates considerable behavioural validity (see Fig 4.11) but is not entirely rigorous. The vegetation-air interface is modelled as an open system with no conservation of energy. The model was developed using the leaf temperature equations of Friend (1995) as the main driving variable, assuming that the warming of the leaf and ground surface and the subsequent loss of energy to the surrounding air would be the main source of variation in local air temperature from background air temperature. In order to capture the effect of the loss of energy from the leaf to the surrounding air volume, an extra term was put into the equation to increase the effect of radiation and volumetric occupancy, assuming that the air acts as a temporary store for the accumulated lost energy, and that loss occurs in proportion to the difference between leaf and air temperature. The magnitude of this term was adjusted until the behaviour of the model was consistent with the behaviour of the natural system. Although the principles underlying this modelling decision are sound, there is a need for a critical examination of the modification of the equation and its implications. However, since the behaviour of the temperature sub-model is consistent with observed behaviour in the natural system, it was considered adequate in the absence of a closed-system approach, allowing the development of a water sub-model which would ideally be used as an input to an improved temperature model.

Mixing between air layers is modelled on a very simple basis, allowing for the build-up of heat and mixing with incoming air. Ideally a more mechanistic approach would be used, but this would require a method of deriving transfer coefficients from the grid structure, and to date no method has been developed to do this for any vegetation model.

The temperature and wind sub-models both represent processes and spatial distributions which have not as yet been fully empirically investigated. The lack of direct treatment of these processes in models results largely from insufficient knowledge. These sub-models do however illustrate an approach to the modelling of microclimate, showing how even simple representation of within-canopy variation can result in spatial distributions of microclimatic variables approximating those in the natural system. At the scale of the single tile, such an approach may well give a better indication of actual conditions than a stricter, more detailed one-dimensional representation. A grid-based approach could be extended to these more complex models.

Radiation

Radiation is an essential component of both the biotic and abiotic systems represented in the model. It is therefore essential that this be calculated accurately. The ray-tracing sub-model used in this model is based on reasonable assumptions and demonstrates good behavioural validity although a minor bug in the program is noticeable in the outer ring of tiles. Since light travels in straight lines, it follows that if the ray paths taken are representative of the sky conditions, and the transmission for each shaft is calculated correctly then the radiation conditions generated will be representative of the natural system.

The selection of representative rays is critical to the success of the model. In the "Ecospace" model rays are chosen at regular angular intervals for both azimuth and altitude, giving increased representation with higher elevation. Although compensation can be made for the relative areas of each slice of sky, the sample of rays is still biased. In low latitudes, where the vertical component of radiation is of greater significance, such an approach would be appropriate, but as one moves towards the poles the horizontal component is of increased significance. P. Sianturi (pers. comm.) has developed a model which distributes the selected rays evenly over the surface of the sky hemisphere, such that each ray is representative of a equal area of sky. Such an approach would appear to give a more generally applicable model.

In this radiation sub-model, care is taken to use the value of radiation taken normal to the ray direction rather than that projected on to a flat surface as is commonly used. As stated in section 4.4, this again reduces the emphasis on the vertical component. In a continuous canopy, where vertical attenuation is the predominant feature, little difference will be noted between the two approaches, but as one moves to sparser canopies the effects of horizontal rays become more significant. Increased latitude will also give an increased significance to the horizontal light component. The use of leaf angle distributions (adjusted by Cos(*elevation*) for flat surface models) in either approach can be used to calculate radiation interception accurately, so little improvement in rigour may actually be evident, although the approach outlined here avoids the multiplication by, directly followed by the division by Cos(*elevation*).

Figure 5.10. shows the light environment for a homogenous canopy. The rate of attenuation with height is broadly as expected, but within each horizontal layer there is unwanted variation. Since the canopy is homogenous, one would expect the model to produce a flat response surface (as in level 11, before attenuation) for each vertical level. However, a degree of variation of around 10 W m^{-2} is evident in each mid-canopy layer as a striping in line with the x columns. This would appear to be related to the hexagonal tile structure, and as such would appear to be the result of an error in calculation. Both level 8 and level 9 also show some edge effects, with a band of unusually high values to the left side of the grid, and a dip towards the nearest edges as viewed. It is unlikely that these edge effects will have a great effect on model behaviour if a sufficiently large grid size is used, but they are a cause for some concern. A significant amount of time has been spent trying to trace the source of these errors with no success.

Heterogeneity

One of the key features of the modelling framework is that it should be able to represent heterogeneity of the environment. The critical effect of heterogeneity on models is illustrated by Yatrebov (1996) where the introduction of heterogeneity significantly altered the dynamics of modelled monospecific stands. In the "Ecospace" model, heterogeneity of microclimate is evident in 3 dimensions surrounding and within the plant. The use of contour plots for the presentation of results allows one to see the general patterns of heterogeneity, but covers the fine scale variation between tiles.

Heterogeneity, particularly of the light environment, at ground level is critical to the dynamics of establishment. In the multi-individual simulation presented, the four plants can be

seen to have modified the light environment significantly, producing a range of light habitats from full light to near darkness. It is likely that the closure of the canopy would reduce the total light environment to the extent that the ground surface becomes near homogenous. This is much as expected for the real system (Delany, 1953). However, heterogeneity of the light environment is introduced as one moves towards the top of the canopy, allowing the development of plants on the woody *Calluna* stems. It is felt that the model has achieved its goal of producing heterogeneity at a suitable scale within the stand, although confidence in the sub-models is not complete.

8.4 Plant growth

It is demonstrated that this approach can produce growth rates broadly as expected. The individual plant growth sub-model performs adequately within standard conditions. Only a single growth form (*gform[sp]*=1) is demonstrated dynamically with the full model in Chapter 7, but the central stem-limited form (*gform[sp]*=0) is demonstrated in Chapter 6, growing in fixed conditions. The phototrophic form (*gform[sp]*=2) at present is performing poorly due to inadequate parameterisation, but since its form is determined by microclimatic conditions it could be a very suitable form for the model framework.

It is demonstrated in section 7.4 that several individuals can grow and compete within the model grid, modifying microclimate over time. However, since the model is at present largely unvalidated, such simulations have little more ecological implication than a three-dimensional cellular automaton. With adequate parameterisation and validation, the model could be used to represent interactions between specific species under different scenarios.

Variation in results

The model produces results in the form of distributions of potential growth, due to the use of stochastic sub-models. If we compare this form of results to models giving a single result, we must ask the question of where on the distribution does that single result lie? In addition we must be certain that the generated single result is representative of the distribution. Two sources of variation, the weather and spatial growth sub-models have been identified, and it is suggested that these are separated by the use of different random number generators. Both these sources of variation have a similar magnitude of effect in the model, which is consistent with the variation due to weather and phenotypic variation.

The sensitivity of the model to normal variation in the weather has significant implications for comparative ecological studies. If the model is representative of the real growth system then the extent of the year to year variation in single site performance must be considered. Most production studies are carried out for less than four years and it is doubtful whether this would be a reasonable sample if the model results are representative. The production results of Summers (1978) show a high degree of variation between 3 successive years at the same sites, with significant variation between years, as described in the results section. This supports the model results, although with such a small sample size it is hard to determine the appropriate scale of variation. It is possible that the inclusion of growth limitations will reduce the extent of the variation due to weather.

It is interesting that the extent of the year to year variation is such that there is no clear difference in growth rates between sites at either end of the country (with identical weather patterns), despite the significantly different radiation regimes. It was hoped that these radiation regimes could be related to plant structure (e.g. greater vertical component of light at lower latitude), but the shading induced by the fixed structures applied was too great at all latitudes. This is much as might be expected for the shade intolerant *Calluna*, although it is interesting that the gap size (approx. 0.866 m per side) did not allow in sufficient light for growth. Would a real plant die in these conditions? Since one can observe individual plants which are still living, but which have shown virtually no growth for years due to some limiting factor, this seems unlikely. Plant death will be discussed shortly. Real measurements of production across the length of the country suffer from variation due to weather and soil type and as such give little information as to the correct results, but remain within broadly the same range.

The sensitivity of the model to different spatial allocation strategies in the plant implies that the structure of an individual has an effect on plant growth even in the absence of neighbours. This supports the modelling approach, but underlines the need for an accurate spatial plant growth sub-model. In the real system plants have plastic responses to environmental factors, resulting in phenotypic variation about the genotype, and it is appropriate that we capture this dynamic plant strategy rather than treat individuals as idealised unresponsive forms. The spatial growth model used in the simulations presented in the results section (*gform[]*=1) is responsive to wind pruning, but not to light. It is hoped that the use of the phototropic form (*gform[]*=2), by minimising the use of random numbers for tile selection, and closer mimicking of the real plant allocation system will reduce the variation. In theory the model individuals are all genetically identical. We would expect, therefore, an identical response to the same conditions. Nevertheless, variation in

environmental conditions can produce variation in growth form with accompanying effects on growth rate. It is hard to quantify the extent of this variation, since it must be separated from genotypic variation, and thus hard to determine an acceptable level of variation due to variations in form. Here, a problem of complexity arises in the model, complicating the process of determining the variation due to variation in form independently of the varying abiotic variables, since ideally the abiotic variation will drive the variation in form. It is essential that this problem be addressed and an acceptable level of variation determined.

Abiotic change

Although the model broadly performs well, the investigation into the effects of climatic warming reveals a drawback in the model's present state. A key feature of this model is that it can theoretically be applied to the prediction of the effects of changes in climate on vegetation. In its present state the model appears to produce counter-intuitive results. Growth limitations due to water and nutrient limitation are not presently included, and, where climatic conditions permit, the plants will grow excessively. At present, the model growth is actually potential growth in the absence of these limitations. The crop surface photosynthesis model of de Wit (1959) assumed radiation to be the only limiting factor and predicted potential production rates greater than twice actual production for grass in the Netherlands; a difference which is largely attributed to water shortage in the summer months and low temperature in the winter months.

It is not clear whether the inclusion of these limitations would prevent the model from behaving unreasonably, but it seems unlikely. The complexity of plant response to abiotic change must be taken into account. Plants may not be expected to respond similarly in the short and long term, due to acclimation to the new conditions. Phenotypic plasticity of response can allow plants to survive in sub-optimal habitats (Bradshaw & Hardwick, 1989). Thus we would expect a change in the photosynthetic response over time with long-term change, although the mechanisms underlying this are not yet known. In addition, one would expect a change in allocation patterns within the plant. Parsons *et al*, (1994) studied the responses of four sub-Arctic dwarf shrubs, *Empetrum hermaphroditum, Vaccinium vitis-idaea, V.uliginosum* and *V.myrtillus* to elevated CO_2, temperature and nutrients. No change in total above-ground biomass was observed in response to elevated temperature, but a significant change in allocation towards more wood occurred in all species. Such a change would reduce the rate of expansion of the model plants under elevated temperature.

Most worrying is the lack of any sign of limitation of plant size or structure. It was hoped that these would be emergent properties, but in the model's present state the plants continue to grow until they fill the grid, causing unreasonable behaviour. It would be inappropriate to apply any exterior limitation until water and nutrient limitations and plasticity of growth rate and partitioning have been modelled and the model behaviour examined.

The problem of climate change has already been addressed at the individual level using forest gap models (Solomon 1986; Pastor & Post, 1988; Bonan *et al*, 1990). Although these models suffer from the theoretical limitations described in Chapters 2 and 6, and underestimate heterogeneity, they can still be used to generate potentially useful results. Although these results may not be absolutely accurate, they can give a good indication of some the species likely to be present in the new conditions. The same can be said for the simple use of Holdridge life zones (Holdridge, 1967) by Smith *et al* (1992) to give a broad indication of potential plant types, although no effect of latitude can be represented. The use of the complex "Ecospace" approach is, at present, a long way from producing useful results for the prediction of climate change, but could still work in the future, providing inputs or responding to the complex GCMs used to simulate potential weather patterns. The complex spatial model of Mou and Fahey (1993) is also considered by the authors to be inappropriate for studies of climate change due to inadequate validation. If climate change proceeds as predicted (IPCC, 1990), the need for accurate predictions will remain for at least several decades, allowing the development of a useful complex mechanistic approach.

Plant survival and allocation

Selection in and between communities is ultimately determined by survival at whichever scale is chosen, and this survival is directly related to the suitability of the plant strategy for the conditions experienced by that plant or group of plants. Mortality is frequently modelled as a random process or an age-related process, such that plants die independently of their physiological state at the time of dying. In order to represent the process of selection a more mechanistic approach is required. An alternative approach is to relate stochastic mortality to the growth rate, as in forest gap models, but although this is an improvement on purely stochastic models it does not deal directly with the process of plant death.

In the "Ecospace" model, mortality is represented as a constant stochastic rate representing herbivory and trampling plus an age dependent stochastic rate. In addition to these rates, which in all but a few cases will allow plants to live until they senesce, a mortality

rate linked to the sugar pool is used to kill plants which are no longer energetically feasible. It was hoped that this could be used to generate selective mortality. However, the mechanisms of plant survival near the point of death are not fully known. The model plants, especially the smaller and establishing individuals, often tread a fine line between a positive and a negative energy balance. Model individuals are allowed a period of negative energy balance defined by the variable *stress_tol[sp]*, and this can be adjusted empirically until plants die at the required rate. However, this is an approximation of a more complex process which we do not fully understand. It must be remembered also that plant death can occur for reasons other than energetic unfeasibility, particularly water and nutrient stress, and so in the present state of the model plant survival might be expected to be higher than otherwise.

Resource allocation within the plant is a key issue here. In a model such as this, with a delicate energy balance, it is essential that the partitioning of photosynthate, the storage and consequent utilisation, and the sacrifice of plant parts through dieback and leaf fall be adequately modelled. At present the function controlling partitioning between wood and leaf is dependent only on time after budburst, and the ratio of above-ground to below-ground allocation is set constant. This simplification and lack of dynamic response to stressful conditions ignores the complexity of species survival strategies, and is likely to affect the timing and rate of mortality. As such, the rates of mortality generated in the model will only be proportional to the real mortality at best. This is a very serious drawback with regards modelling competition between plants, although a simpler probability or growth rate related model could be substituted if a better treatment of resource allocation fails to reduce the energetic unfeasibility of plants.

Plant density and allocation

In the model runs presented and throughout the model development it has been evident that the rules for spatial growth are inadequate for all conditions. Plant growth is permitted in places where a real plant would not necessarily allocate material, particularly in the lower levels of the canopy. this may occur for one of two reasons. Firstly, the plant growth form may allocate growth in these positions. This may be limited by the use of a more mechanistically based growth form such as the phototropic form, which allocates to the volumes with the greatest illumination. Alternatively the plant may grow in unsuitable space because of material added in the recursive application of surplus growth which occurs in the growth sub-model when potential growth is blocked. This is a necessary safeguard for the growth model, ensuring that

in any time-step the appropriate amount of growth is allocated. However, this stage of growth application should ideally be avoided by the use of a more suitable growth allocation strategy.

No evidence of self-thinning is shown by the plants in the model. Indeed it is possible for plants to overfill the grid before stopping growth. Again this indicates that aspects of the spatial allocation of resources is inadequate, although it must be borne in mind that the majority of runs so far have been with isolated individuals. Some limitation on the maximum size of the plant with age , to represent the limitations of physical structure would be desirable. A variable of this type, *zmax[ageclass],* was used in the early development of the model, but this was removed because it seemed, like the dome form, to be limiting growth externally rather than internally. Problems of leaf fall distribution, leaf allocation, partitioning and stress strategies require to be addressed before a truly realistic plant shape is generated. At present the model fails to represent plant spatial growth accurately.

Domes and the model

The dome form was developed in response to field observations. The concept of a plant growth form which operates for a number of individuals is of interest, but the cause and effect of the processes must be considered. It is probable that the individuals comprising a dome adopt the form as a result of directional growth responses to unevenly distributed environmental variables rather than as a result of any predetermined strategy which can determine the plants position within a dome. The dome as applied in the model would therefore be an external structure imposed to simulate the effects of variables which are already explicitly represented. This runs contrary to the general modelling philosophy used herein, which is based on the principle of the model behaviour being determined from the behaviour of the components of the model. The approach invariably produced dome shaped plant canopies, but one cannot be sure whether these domes are in the right location or whether the conditions modelled would produce such well defined domes. A more desirable approach would be the one used in growth form two, where the plant grows towards the light, while at the same time plant material is lost from the more exposed extremities. One would expect these contrary factors to reach a point of equilibrium defining a surface which could easily be dome shaped. At present this growth form is not fully calibrated and tested, although it has demonstrated initial behavioural validity.

The potential for the model to deal with moving vegetation is of particular importance for *Calluna* based ecosystems, where the senescing stage provides the microclimate for the first pioneers of a new vegetation cycle. The use of the dome form to control this process, even

if not used for active limitation, might be of use, although again the process is very likely to be a predictable result of stem mechanical properties. This area appears at present to be a low priority, since it is more important to ensure that the more straightforward aspects of plant competition are functioning correctly.

8.5 Potential improvements

The "Ecospace" model is at present in an incomplete state, and requires a number of alterations and additions in order to be of practical use. The model is presently at a point where a water transport sub-model could reasonably be inserted. The conditions for evaporation and transport for each above-ground tile are known. It would be possible to link the precipitation generator to a soil water transport sub-model, allowing the direct treatment of root competition for uptake. Inputs and outputs for an individual plant could thus be represented and its water balance calculated dynamically.

In addition a number of other possible additions have been considered in order that the model should more explicitly represent the processes of plant competition. These are listed below.

- Decomposition, nutrient release. Some dynamic soil based representation of the decomposition of ground litter, and conversion into spatially distributed free nutrients.
- Spatial root growth sub-model. Growth of the roots according to a spatial sub-model, allowing interaction with local nutrient and water availability. It is not clear at present whether a branching system or a tile-based system would be most appropriate.
- Expansion of spatial plant description to include more detail on the spatial distribution of age, leading to an improved litter fall model. At present, all long shoots within the same tile are assumed to be of an equal age and all short shoots are assumed to be the same age. This simplification was necessary due the data structures required to implement the model.
- Completion of geometry for moving plant parts. A sub-model calculating the movement of plant parts attached to stems, allowing the simulation of the spreading and canopy thinning observed in older heather plants has been written, but not as yet linked to the modelling framework. Routines driving this movement would also be required. As stated earlier, this is a low priority.
- Improvement or validation of local leaf/air temperature model. The current temperature sub-model seems mechanistically unsatisfying, and may need to be replaced.

- Derivation of transfer coefficients/turbulence properties from grid structure. The adequate simulation of within-canopy transfer of heat, momentum and water depends on the calculation of transfer coefficients (K-values). At present no method exists to generate these from model plant structure, and use is limited to stands with field measurements.
- Improvement of photosynthesis sub-model to use more general equations. The correlative model used at present is suitable only for *Calluna*, and a more general and hopefully more flexible model of photosynthesis would be desirable.
- Separation of random number generators used for the weather and spatial growth sub-models, allowing more rigorous analysis of variation.

The model could also be improved by more radical changes, taking into account the lessons learned during this project. These are listed below.

- Improved code and data structures. At present the model is limited by the existing computer code. It is felt that this could be considerably improved by a specialist programmer.
- The use of a simpler grid structure. At the moment the grid calculation seem too rigorous for the model. Williams (1996) uses arrays to hold the radiation interception by single tiles rather than direct calculation. Perhaps this method could be used. Alternatively, the pseudo-dodecahedrons suggested in section 8.2 could be implemented, thus also increasing the rigour of the grid structure.
- The inclusion of changes in grid scale with height to compensate for problems of scale within the community. This is a complex problem and requires much thought.

8.6 Conclusions

The model has been designed as a prototype model in order to test the practicality of the spatial modelling approach. It has been demonstrated that is both possible and practical to model dynamic vegetation processes at the individual level with explicit spatial representation of plant structure and microclimate. At present, all the sub-models perform reasonably within narrow limits. However, difficulties with the light model (occasional untraced edge effects), and also problems with the growth model which led to high vegetation densities require attention before other aspects of the model are developed further.

This modelling study has nevertheless illuminated the potential of this spatial modelling approach to the study of vegetation dynamics. Consequently it is recommended that this approach be continued, and developed further. This might involve development of the current code or the development of new code based on a different grid system. In addition, such an approach will require extensive field studies to fill in the significant knowledge gaps we currently have, or at least allow reasonable estimates to cover these gaps. When faced with an ecological problem, the complex spatial approach should be considered alongside other modelling approaches.

The modelling approach used in "Ecospace" does not necessarily bring with it any increased accuracy of prediction. Gaps in knowledge leave obvious gaps in the model, leading to error. In addition, the errors from each sub-model could be additive. However, the rigorous approach avoids bias introduced by simpler models, with spatiotemporal heterogeneity giving a distribution of results which could potentially allow greater biodiversity and a more realistic simulation of vegetation than permitted in other models.

References

Aerts, R. and Heil, G.W. (1993). (eds.) Heathlands: Pattern and process in a changing environment. Kluwer Academic, Dordrecht-Boston-London.

Allen, S.E. (1964). Chemical aspects of heather burning. *J.Appl.Ecol.* **1**, 347-367.

De Angelis, D.L. and Rose, K.A. (1992). Which individual-based approach is most appropriate for a given problem? In De Angelis, D.L. and Gross, L.J., *Individual-Based Models and Approaches in Ecology.* Chapman and Hall. New York, London. 67-87.

Aono, M. and Kunii, T.L. (1984). Botanical tree image generation. *IEEE Comput. Graphics Applications*, **4**, 10-34.

Bannister, P. (1976). Introduction to Physiological Plant Ecology. Blackwell, Oxford.

Bardgett, R.D. and Marsden, J.H. (1992). *Heather condiation and management in the uplands of England and Wales.* English Nature, Peterborough.

Bardgett, R.D., Marsden, J.H., Howard, D.C. and Hossell, J.E. (1995). The extent and condition of heather in moorland, and the potential impact of climate change. In Thompson, D.B.A., Hester,A.J. and Usher, M.B. (eds.) *Heaths and moorland: Cultural landscapes.* HMSO.

Bartelink, H. H. (1993). FORFLUX. A spatial model of light interception by forest canopies. *Hinkeloord Reports*, **5**. Department of Forestry, Agricultural University, Wageningen.

Bassow, S.L., Ford, E.D. and Kliester, A.R. (1990). A critique of carbon-based tree growth models. In Dixon, R.K *et al.* (eds.) Process Modeling of Forest Growth Responses to Environmental Stress. Portland.

Bellamy, D.J. and Holland, P.J. (1966). Determination of the net annual aerial production of *Calluna vulgaris* (L.) Hull in northern England. *Oikos* **17**, 272-275.

Berendse, F. and Aerts, R. (1984). Competition between *Erica tetralix* L. and *Molinia caerulea* (L.) Moench as affected by the availability of nutrients. *Acta Oecologia* (Berlin), **62**,196-198.

Blad, B.L. and Lemeur, R. (1979). Miscellaneous techniques for alleviating heat and moisture stress. In Gerber, J.F. and Banall, B.J. (eds). Modification of the Aerial Environment of Plants. *Am. Soc. Agric. Engin. Mononogr.* **2**,409-425.

Boersma, M., van Schaik, C.P. and Hogeweg. P. (1991). Nutrient gradients and spatial structure in tropical forests: a model study. *Ecol. Model.* **55**, 219-240.

Bonan, G.B., Shugart, H.H. and Urban, D.L. (1990). The sensitivity of some high-latitude boreal forests to climatic parameters. *Clim. Change.* **16**, 9-29.

Botkin, D.B., Janak,, J.F. and Wallis, J.R. (1972). Some ecological consequences of a computer model of forest growth. *J. Ecol*, **60**, 849-872.

Bradshaw, A.D. and Hardwick, K. (1989). Evolution and stress: Genotypic and phenotypic components. *Biol. J. Linn.Soc.* **37**, 137-155.

Brock, T.D. (1981). Calculating solar radiation for ecological studies. *Ecol. Model.* **14**, 1-19.

Bunce, R.G.H., Howard, D.C., Clarke, R.T. and Deane, G.C. (1991). ITE Land Classification: Classification of all 1 km squares in Great Britain. Department of Environment, (unpublished).

Caldwell, M.M. and Pearcy, R.W. (1994) (eds.) *Exploitation of Environmental Heterogeneity by Plants: Ecophysiological Processes Above- and Belowground.* Academic Press. San Diego, New York, Boston, London, Sydney, Tokyo, Toronto.

Cannell, M.G.R., Grace, J. and Booth, A. (1989). Possible impacts of climatic warming on trees and forests in the United Kingdom: a review. *Forestry*, **62**, pp337-364.

Caswell, H. and John, A.M. (1992). From the individual to the population in demographic models. In De Angelis, D.L. and Gross, L.J., *Individual-Based Models and Approaches in Ecology.* Chapman and Hall. New York, London. 36-61.

Chapman, S.B. (1967). Nutrient budgets for a dry ecosystem in the south of England. *J.Ecol.* **55**,677-689.

Chapman,S.B., Rose, R.J. and Clarke, R.T. (1989) A model of the phosphorus dynamics of *Calluna* heathland. *J.Ecol.* **77**. 35-48.

Cionco, R.M. (1965) A mathematical model for air flow in a vegetative canopy. *J. Appl. Meteorol.* **4**, 517-525

Cionco, R.M. (1978) Canopy index values for various canopy densities. *Boundary-Layer Meteorol.* **15**, 81-93.

Clymo, R.S. (1978). A model of peat bog growth. In Heal, O.W. and Perkins, D.F.(eds.) *Production Ecology of British Moors and Montane Grasslands.* Springer-Verlag. Berlin, Heidelberg, New York.187-223.

Coffin, D.P. and Lauenroth, W.K. (1990). A gap dynamics simulation model of semi-arid grassland. *Ecol. Model.* **49**, 229-266.

Comins, H. N. (1982). Evolutionarily stable strategies for localized dispersal in two dimensions. *J. Theor. Biol.* **94**, 579-606.

Cooper, P. I. (1969). The absorption of solar radiation in solar stills. *Sol. Energy*, **12**: 3.

Davis, M.B. (1989). Insights from paleoecology on global climate change. *Bull. Ecol. Soc. Am.* **70**, 222-228.

Delany, M. (1953). Studies on the microclimate of *Calluna* heathland. *J. Anim. Ecol.* **22**, 227-239.

Department of the Environment, UK. Climate Change Impacts Review Group (1991). *The Potential Effects of Climate Change in the UK.* HMSO, London.

Diemont, W.H. and Heil, G.W. (1984). Some long term observations on cyclical and seral processes in Dutch heathlands. *Biological Conservation.* **30**, 113-120.

Diggle, P.J. (1976). A spatial stochastic model of inter-plant competetion. *J. Appl. Probab.* **13**, 662-671.

Drury, W.H. and Nisbet, I.C.J. (1973). Succession. *J. Arnold. Arboretum.* **54**, 331-368.

Duffie, J.A. and Beckman, W.A. (1980). *Solar Engineering of Thermal Processes.* Wiley-Interscience. New York.

Duncan, W.G. and Ohlrogge, A.J. (1958). Principles of nutrient uptake from fertiliser bands. II. *Agron.J.* **50**, 605-608.

Ebenhöh, W. (1994). Competition and coexistence: modelling approaches. *Ecol. Model.* **75/76**, 83-98.

van Eimern, J. Karshon, R., Razumova, L.A. and Robertson, G.W. (1964). *Windbreaks and Shelterbelts.* Technical Notes, World Meteorological Organisation, Geneva. No. 59

Ekschmitt, K. and Breckling, B. (1994). Competition and coexistence: the contribution of modelling to the formation of ecological concepts. *Ecol. Model.* **75/76**, 71-82.

Farquhar, G.D., von Cammerer, S. and Berry, J.A. (1980). A biochemical model of photosynthetic CO^2 assimilation in leaves of C3 species. *Planta*, **149**,78-90.

Farquhar, G.D. and von Cammerer, S. (1982). Modelling of photosynthetic response to environmental condition. In Lange, O.L., Nobel, P.S., Osmond, C.B. and Ziegler, H., *Encyclopedia of Plant Physiology*, vol 12B, *Physiological Plant Ecology.* Springer-Verlag. Heidelberg, Berlin, New York. 549-88

Feldman,W.M. (1935) *Biomathematics.* 480pp.Charles Griffin & Co.Ltd, London.

Finnigan, J.J. (1985). Turbulent transfer in flexible plant canopies. in Hutchinson,B.A. and Hicks, B.B. (eds.), *The Forest_Atmosphere Interaction.* D. Reidel Publishing Company, Dordrecht, Boston, Lancaster. 443-480

Fitter, A.H. (1994). Architecture and biomass allocation as components of the plastic response of root systems to soil heterogeneity. In Caldwell, M.M. and Pearcy, R.W., *Exploitation of Environmental Heterogeneity by Plants.* Academic Press, Inc., San Diego, California. 305-323.

Ford, E.D., Avery,A. and Ford, R. (1990). Simulation of branch growth in the Pinaceae: Interactions of morphology, phenology, foliage productivity, and the requirement for structural support, on the export of carbon. *J. Theor. Biol.*, **146**, 15-16.

Ford, E.D. and Diggle, P.J. (1981). Competition for light in a plant monoculture modelled as a spatial stochastic process. *Ann. Bot.* **48**,481-500.

Ford, E.D. and Sorrenson, K.A. (1992). Theory and models of inter-plant competetion as a spatial process. In De Angelis, D.L. and Gross, L.J., *Individual-Based Models and Approaches in Ecology.* Chapman and Hall. New York, London. 363-407.

Forrest, G.I. (1971). Structure and production of North Pennine blanket bog vegetation. *J. Ecol.* **59**, 453-479.

Forrest, G.I. and Smith, R.A.H. (1975). The productivity of a range of blanket bog types in the Pennines. *J. Ecol.* **63**, 173-202.

Friend, A.D. (1995). PGEN: an integrated model of leaf photosynthesis, transpiration, and conductance. *Ecol. Model.* **77**, 233-255.

Gardner, M. (1971). On cellular automata, self-reproduction, the Garden of Eden and the game of "life." *Sci. Am.* **224**, 112-117.

Gates, D.J. (1978) Bimodality in even-aged plant monocultures. *J. Theor. Biol.* **71**, 525-540.

Gause, G.F., Smaragdova, N.P. and Witt, A.A. (1936). Further studies of interaction between predators and prey. *J. Anim. Ecol.* **5**, 1-18.

Gimingham, C.H. (1972). *Ecology of Heathlands.* Chapman & Hall, London.

Gore, A.J.P. and Olson, J.S. (1967). Preliminary models for accumulation of organic matter in an *Eriophorum/Calluna* ecosystem. *Aquilo* (Ser. Botanica), **6**, 297-313.

Goudriaan,J. (1977). *Crop micrometeorology: a simulation study.* Pudoc,Wageningen. 249 pp.

Goudriaan,J. and van Laar,H.H. (1994). *Modelling Potential Crop Growth Processes.* Kluwer Academic, Dordrecht.

Grace, J. (1970). *The growth-physiology of moorland plants in relation to their aerial environment.* PhD. thesis, University of Sheffield.

Grace, J. (1971). The directional distribution of light in natural and controlled environment conditions. *J. Appl. Ecol.* **8**: 155-165.

Grace, J. and Woolhouse, H.W. (1973). A physiological and mathematical study of the growth and productivity of a *Calluna-Sphagnum* community III. Distribution of photosynthate in *Calluna. J. Appl. Ecol.* **10**, 77-91.

Grace, J. and Woolhouse, H.W. (1974). A physiological and mathematical study of the growth and productivity of a *Calluna-Sphagnum* community IV. A model of growing *Calluna. J. Appl. Ecol.* **11**, 281-295.

Grace, J. (1977). *Plant Response to Wind.* Academic Press. London, New York, San Fransisco.

Greig-Smith, P. (1964). *Quantitative Plant Ecology.* 2nd. edition. Butterworth, London,

Haefner, J.W. (1994). Parallel computers and individual-based models: An overview. In. De Angelis, D.L. and Gross, L.J., *Individual-Based Models and Approaches in Ecology.* Chapman and Hall. New York, London.126-164.

Haefner, J.W., Poole, G.C., Dunn, P.V., Deeler, R.T. (1991). Edge effects in computer models of spatial competition. *Ecol. Model.* **56**, 221-244.

Håkanson, L. (1995). Optimal size of predictive models. *Ecol. Model.* **78**:195-204.

Hallé, F. and Oldeman, R.A.A. (1975) *Essay on the Architecture and Dynamics of Growth of Tropical Trees.* Tr. B. C. Stone. Kuala Lumpur: Penerbit Universiti Malaya.

Hay, J.E. and Davies, J.A. (1980). Calculations of the solar radiation incident on an inclined surface. In Hay, J.E. and Won, T.K., *Proceedings of First-Canadian Solar Radiation Data Workshop* Canada: Ministry of Supply and Services; also New Jersey: Rowan and Allanshield, 59-72.

Heal, O.W., Jones, H.E. and Whittaker,J.B. (1975) Moor House UK. In Structure and Function of Tundra Ecosystems. *Ecol. Bull. (Stockholm)* **20**, 295-320.

Heal, O.W., Latter, P.M. and Howson, G. (1978). A study of the rate of decomposition of organic matter. In Heal, O.W. and Perkins, D.F.(eds.) *Production Ecology of British Moors and Montane Grasslands.* Springer-Verlag. Berlin, Heidelberg, New York. 136-159.

Heal, O.W. and Perkins, D.F.(eds.) (1978). *Production Ecology of British Moors and Montane Grasslands.* Springer-Verlag. Berlin, Heidelberg, New York.

Heil, G.W. and Bobbink, R. (1993). "Calluna" a simulation model for evaluation of impacts of atmospheric nitrogen deposition on dry heathlands. *Ecol. Model.* **68:** 161-182.

Heil, G.W. and Diemont,W.H. (1983). Raised nutrient levels change heathland into grassland. *Vegetatio* **53**, 113-120.

Hobbs, R.J. (1981). *Post-fire succession in heathland communities.* PhD. Thesis, University of Aberdeen.

Hobbs, R.J. (1983). Markov models in the study of post-fire succession in heathland communities. *Vegetatio.* **56**, 17-30.

Hobbs, R.J. and Legg, C.J. (1983). Markov models and initial floristic composition in heathland vegetation dynamics. *Vegetatio.* **56**, 31-43.

Hobbs, R.J. and Gimingham, C.H. (1987). Vegetation, fire and herbivore interactions in heathlands. *Adv. Ecol. Res.* **16**, 87-173.

Hobbs, R.J., Mallik, A.U. and Gimingham, C.H. (1984). Studies on fire in Scottish heathland communities. III Vital attributes of the species. *J. Ecol.*, **72**, 963-76.

Holdridge, L.R. (1967). *Life Zone Ecology.* Tropical Science Centre, San Jose.

Hossell, J. (1992). *Global warming and the British landscape: the sensitivity of land use and vegetation in Britain to climatic change.* PhD. thesis, University of Birmingham.

Hutchings, M.J. and De Kroon, H. (1994). Foraging in plants: the role of morphological plasticity in resource acquisition. In *Adv. Ecol. Res.* **25**, 159-238.

Hutchinson, G.E. (1958). Concluding remarks. *Cold Spring Harbour Symposia on Quantitative Biology*, **22**: 415-427.

Huston, M., DeAngelis, D. and Post, W. (1988). New computer models unify ecological theory. *BioScience.* **38**, 682-691.

Inoue, E. (1963) On the turbulent structure of airflow within crop canopies. *J. Meteorol, Soc. Japan Sec 11*, **41**, 317-332.

Intergovernmental Panel on Climate Change. (1990). *Climate Change: The IPCC Scientific Assessment*, Houghton, J.T., Jenkins, J. and Ephraums, J.J. (eds.). Cambridge University Press, Cambridge.

Jacobs, A.F.G., Vanboxel, J.H. and Elkinlani, R.M.M.(1995). Vertical and horizontal distribution of wind-speed and air temperature in a dense vegetation canopy. *J. Hydrol.* **166**, no.3-4, 313-326.

Jaeger. L. (1985) Estimations of surface roughness and displacement heights above a growing pine forest from wind profile measurements over a period of ten years.in Hutchinson, B.A. and Hicks, B.B. (eds.), *The Forest-Atmosphere Interaction.* D. Reidel Publishing Company, Dordrecht, Boston, Lancaster. 481-499

Jones, H.G. (1983). *Plants and Microclimate.* Cambridge University Press, Cambridge.

Jones, H.E. and Gore, A.J.P. (1978). A simulation of production and decay in blanket bog. In Heal, O.W. and Perkins, D.F.(eds.) *Production Ecology of British Moors and Montane Grasslands.* Springer-Verlag. Berlin, Heidelberg, New York. 160-186.

De Jong, T.J. and Klinkhamer, P.G.L. (1983) A simulation model for the effects of burning on the phosphorous and nitrogen cycle of a heathland ecosystem. *Ecol.Model.* **19**:263-284.

Jorgensen, S.E. (1992). Development of models able to account for changes in species composition. *Ecol.Model.***62**, 195-207.

Kauppi, P., Hari, P., and Kellomaki, S. (1978). A discrete time model for succession of ground cover communities after clear cutting. *Oikos* **30**, 100-105.

Kayll, A.J. (1966). Some characteristics of heath fires in north-east Scotland. *J. Appl. Ecol.* **3**, 29-40.

Kenkle, N.C. (1988). Pattern of self-thinning in jack pine: Testing the random mortality hypothesis. *Ecology* **69**, 1017-1024.

Kimball, H. H. (1921). Sky-brightness and daylight illumination measurements. *Mon. Weath. Rev.*, **49**, 481-8.

Kimmins, J.P. and Scoullar, K.A. (1984). The role of modelling in tree nutrition research and site nutrient management. In Bowen, G.D. and Nambiar, E.K.S. *Nutrition of Plantation Forests.* Academic Press, London.

Kurth, W. (1994). Morphological models of plant growth: possibilities and ecological relevance. *Ecol. Model.* **75/76**, 299-308.

Korzukhin, M.D. (1995). An individual tree-based model of competition for light. *Ecol. Model.* **79**, 221-229.

Kraalingen, D. W. G. van (1989). A three-dimensional light model for crop canopies. Internal Report 17, Dept. of Theoretical Production Ecology, Wageningen Agricultural University.

Lamb, H.H. (1950). Types and spells of weather around the year in the British Isles: Annual trends, seasonal structure of the year, singularities. *Quart. J. Roy. Met. Soc.* **76**, 393-348.

Lawton, J.H. and Strong. D.R. jr. (1981). Community patterns and competition in folivorous insects. *Amer.Nat.* **118**, 317-338.

Legg, C.J. (1995). Heathland dynamics: A matter of scale. In. Thompson, D.B.A., Hester,A.J. and Usher, M.B. (eds.) *Heaths and moorland: Cultural landscapes.* HMSO.

Leopold, A. C. (1961). Senescence in plant development. *Science* **134**, 1727-1732.

Leopold, A. C. (1980). Aging and senescence in plant development. In. *Senescence in plants,* Thimann,K.V.(ed.), 1-12. Boca Raton, FL:CRC Press.

Lettau, H.H. (1969) Note on aerodynamic roughness-parameter estimation on the basis of roughness element description. *J. Appl. Meteorol.* **8**, 828-834.

Levin, S.A. (1989). Challenges in the development of a theory of community and ecosystem structure and function. In Roughgarden, J. and Levin, S.A. (eds.). *Perspectives in Ecological Theory.* Princetown University Press, Oxford . pp 242-255.

Lewellen, W.S. (1985) Modelling turbulent exchange in forest canopies. In Hutchinson,B.A. and Hicks, B.B. (eds.), *The Forest_Atmosphere Interaction.* D. Reidel Publishing Company, Dordrecht, Boston, Lancaster. 481-499.

Linacre, E. (1992). *Climate and data resources: a reference and guide.* Routledge, London.

Li, Z., Lin, J.D. and Miller, D.R. (1989). Air flow over and through a forest edge: a steady- state numerical simulation. *Boundary-Layer Meteorol.* **46,** 333-354.

Lindenmayer, A. (1975). Developmental algorithms for multicellular organisms: A survey of L-systems. *J.Theor.Biol.* **54**, 3-22.

Lotka, A. (1925). *Elements of Physical Biology.* Williams and Wilkins, Baltimore.

Luan. J. (1994). *Simulation of forest ecosystem dynamics, with respect to the problem of hierarchy.* PhD. Thesis. University of Edinburgh.

McNaughton, K.G. and van den Hurk,B.J.J.M.(1995). A 'Lagrangian' revision of the resistors in the two-layer model for calculating the energy budget of a plant canopy. *Boundary-Layer Meteorol.* **74**, 261-268.

Mead, R. (1968). Measurement of competition between individual plants in a population. *J.Ecol.* **56**, 36-45.

Metcalfe, G. (1950). The ecology of the Cairngorms. Part II. The mountain Callunetum. *J.Ecol.*, **38**, 46-74.

Meteorogical Office (1972) . *Tables of temperature, relative humidity, precipitation and sunshine for the world.* Part III.HMSO, London.

Metz, J.A.J. and Diekmann. (1986). *The Dynamics of Physiologically Structured Populations.* Springer-Verlag. New York.

Meyers, T. and Paw U,K.T. (1986) Testing of a higher-order closure model for modelling airflow within and above plant canopies. *Boundary-Layer Meteorol.* **37**, 297-311.

Milankovitch. M. (1930). Mathematische Klimalehre und Astronomische Theorie der Klimaschwankungen. Handbuch der Klimatologie, Band 1 Tiel A. Gebruder Borntrager, Berlin, 298pp.

Miles, J. (1974). Effects of experimental interference with stand structure on establishment of seedlings in Callunetum. *J.Ecol.* **62**, 675-687.

Miles, J. (1981). Problems in heathland dynamics. *Vegetatio* **46**,61-74.

Monsi, M. and Saeki, T. (1953). Über der Lichtfaktor in den Pflanzengesell-schaften und seine Bedentung für die Stofffproducktion. *Japan.J.Bot.* **14**, 22-52.

Monteith, J. (1973). Solar radiation and productivity in tropical ecosystems. *J. Appl. Ecol.* **9**, 747-766.

Monteith, J.L. and Unsworth, M.H. (1990). *Principles of Environmental Physics.* 2nd. edition. Arnold. London, New York, Melbourne, Auckland.

Moon, P. (1940) Proposed standard solar radiation curves for engineering use. *J.Franklin Inst.*, **230**: 583-618.

Moon, P. and Spenser, D.E. (1942). Illumination from a non-uniform sky. *Trans. Illum. Engng. Soc.* N.Y., 37: 707-712.

Mou, P. and Fahey, T.J. (1993). REGROW: a computer model simulating the early successional process of a disturbed northern hardwood ecosystem. *J.Appl. Ecol.* **30**,676-688.

Munro, D.D. (1974). Forest growth models- a prognosis, In Fries, J. *Growth Models for Tree and Stand Simulation*, pp 385-393, Res. Notes 30, Department of Forest Yeild Research, Royal College of Forestry, Stockholm.

Nicholls, R. L. and Child, T. N. (1979). Solar radiation charts. *Sol. Energy*, **22**: 91-97.

Nielsen, N.S. (1992). Strategies for structural-dynamic modelling. *Ecol. Model.* **63**, 41-101.

Noble, I.R. and Slatyer, R.O. (1980). The use of vital attributes to predict successional changes in plant communities subject to recurrent disturbances. *Vegetatio*, **43**, 5-21.

O'Neill, R.V. (1989). Perspectives in hierarchy and scale. In Roughgarden, J. and Levin, S.A. (eds.). *Perspectives in Ecological Theory.* Princetown University Press, Oxford . pp 140-156.

Pakeman, R.J. and Marrs, R.H. (1996). Modelling the effects of climate change on the growth of bracken (*Pteridium aquilinum*) in Britain. *J. Appl. Ecol.* **33**, 561-575.

Parsons, A.N., Welker, J.M., Wookey, P.A., Press, M.C., Callaghan, T.V. and Lee, J.A. (1994). Growth responses of four sub-Artic dwarf shrubs to simulated environmental change. *J.Ecol.* **82**:307-318.

Parton, W.J. and Logan, J.A. (1981). A model for diurnal variation in soil and air temperature. *Agricultural Meteorology* **23**: 205-216.

Pastor, J. and Post. W.M. (1988). Response of northern forests to CO2-induced climatic change: Dependence on soil water and nitrogen availabilities. *Nature*. **334**, 55-58.

Peters, R.L. (1992). Conservation of biological diversity in the face of climate change. In Peters, R.L. and Lovejoy, T.E. *Global warming and biological diversity.* Yale University Press, New Haven , London. 15-30.

Philip, J.R. (1964) Sources and transfer processes in the air layers occupied by vegetation. *J.Appl. Meteorol.* **3**, 390-395.

Phipps,. R.L. (1979). Simulation of wetland forest dynamics. *Ecol. Model.* **7**, 257-288.

Pokrowski, J. (1929). Über einen scheinbaren Mie-Effekt und seine mogliche Roll in der Atmosphärenoptik, *Z,Phys.* **53**:67-71.

Prusinkiewicz, P. and Lindenmayer, A.(1990). The Algorithmic Beauty of Plants. Springer, New York.

Rabbinge, R. (1976) *Biological control of fruit-tree red spider mite.* Pudoc, Wageningen 234pp.

Raunkiaer, C. (1937). *Plant Life Forms.* Clarendon Press, Oxford.

Raupach,M.R. (1989). Stand overstorey processes. *Phil.Trans. R. Soc. Lond.* B, **324**, 175-190.

Raupach,M.R. and Shaw,R.H. (1982). Averaging procedures for flow within vegetation canopies. *Boundary-Layer Meteorol.* **22**,79-90.

Raupach, M.R. and Thom, A.S.(1981). Turbulence in and above plant canopies. *Ann. Rev. Fluid. Mech.* **13**, 97-129.

Robertson, R.A. and Davies, G.E. (1965). Quantities of plant nutrients in heather ecosystems. *J. Appl. Ecol.* **2**, 211-219.

Rodwell, J.S. (1991b). *British Plant Communities, Vol. 2 Mires and Heaths.* Cambridge University Press, Cambridge.

Røsberg, I. Øvstedal, D.O., Seljelid, R., Schreiner, Ø, and Goksøyr, J. (1981). Estimation of carbon flow in a *Calluna* heath system. *Oikos*, **37**, 295-305.

Sauer, T.J. and Norman, J.M. (1995). Simulated canopy microclimate using estimated below-canopy soil surface trnsfer coefficients. *Agric. For. Meteorol.* **75**, 135-160.

Shellard, H.C. (1976) Wind. In Chandler,T.J. and Gregory, S. (eds) *The Climate of the British Isles*, Longman Group, London. 39-73.

Shugart, H.H. (1984). *A Theory of Forest Dynamics.* Springer-Verlag, New York.

Shugart, H. H. and West, D. C. (1977). Development of an Appalachian deciduous forest succession model and its application to assessment of the impact of the chestnut blight. *J. Environ. Manage.* **5**, 161-179.

Shugart, H.H. and West, D.D. (1980). Forest succession models. *Bioscience*, **30**, 305-313.

Slatkin, M. & Anderson, D.J. (1984). A model of competition for space. *Ecology* **65**, 1840-1845.

Smith, T.M., Shugart, H.H., Bonan, G.B. and Smith, J.B. (1992). Modelling the potential response of vegetation to global climate change. *Adv. Ecol. Res.* **22**, 93-116.

Solomon, A.M. (1986) Transient response of forests to CO^2-induced climate change: simulation modeling experiments in eastern North America. *Oecologia.* **68**,567-579.

Steeves, T.A. and Sussex, I.M. (1989). *Patterns in Plant Development.* 2nd. edition. Cambridge University Press, Cambridge.

Stevenson, A.C. and Birks, H.J.B. (1995). Heaths and moorland: long-term ecological changes, and interactions with climate and people. In Thompson, D.B.A., Hester, A.J. and Usher, M.B. (eds.) *Heaths and moorland: Cultural landscapes.* HMSO.

Strandman, H., Väisänen,H., and Kellomäki, S. (1993). A procedure for generating synthetic weather records in conjunction of climatic scenario for modelling of ecological impacts of changing climate in boreal conditions. *Ecol. Modelling.* **70**, 195-220.

Summers, C.F. (1978). Production in montane dwarf shrub communities. In Heal, O.W. and Perkins, D.F.(eds.) *Production Ecology of British Moors and Montane Grasslands.* Springer-Verlag. Berlin, Heidelberg, New York.

Thomas, S.C. and Weiner, J. (1989). Including competitive asymmetry in measures of local nterference in plant populations. *Oecologia.* **80**: 349-355.

Thompson, D.B.A., Hester,A.J. and Usher, M.B. (1995). (eds.) *Heaths and moorland: Cultural landscapes.* HMSO. 400pp.

van Tongeren, O. and Prentice, I.C. (1986). A spatial simulation model for vegetation dynamics. *Vegetatio* 46, 163-173.

Troen,I. and Petersen, E.L. (1989). European Wind Atlas, Commission of the Economic Community, Risø National Laboratory, Roskilde, Denmark 656pp.

Waggoner, P.E. and Reifsnyder, W.E. (1968). Simulation of the temperature, humidity and evaporation profiles in a leaf canopy. *J.Appl.Meteorol.* **7**, 400-409.

Wang, Y.-P. and Jarvis, P.G. (1990). Description and validation of an array model- MAESTRO. *Agr. Forest. Meteorol.* **51**, 257-280.

Watson, A., Miller, G.R. and Green, F.H.W. (1966). Winter browning of heather (*Calluna vulgaris*) and other moorland plants. *Trans.Bot.Soc.Edinb.* **40**, 195-203

Watt, A.S. (1947). Pattern and process in the plant community. *J. Ecol.* **35**, 1-22.

Webb, N. (1986). *Heathlands.* Collins. London-Glasgow-Sydney-Auckland-Toronto-Johannesburg.

Weiner,J. and Conte, P.T. (1981). Dispersal and neighbourhood effects in an annual plant competition model. *Ecol.Model.* **13**, 131-147.

Weiss, A. and Norman, J.M. (1985). Partitioning solar radiation into direct and diffuse, visible and near-infra red components. *Agric.For. Meteorology* **34**, 205-213.

Whittaker, R.H. and Likens, G.E. (1973). Carbon in the biota. In Woodwell, G.M. and Pecan, E.V. (eds.) *Carbon and the biosphere.* D.C., Washington. pp281-302.

Williams, M. (1996). A three-dimensional model of forest development and competition. *Ecol. Model.* **89**, 73-98.

Wilson, B.F. (1995). Shrub stems: form and function. In Gartner. B.L. (ed.) *Plant stems: Physiology and Functional Morphology.* Academic Press. San Diego, New York, Boston, London, Sydney, Tokyo, Toronto. 91-102.

Wilson,N.R. and Shaw,R.H. (1977). A higher order closure model for canopy flow. *J. Appl. Meteorol.* **16**,1197-1205.

Wilson, C., Grace, J., Allen, S. and Slack, F. (1987). Temperature and stature: a study of temperatures in montane vegetation. *Funct. Ecol.* **1**, 405-413.

Wisiol, K. and Hesketh, J.D. (1987). *Plant Growth Modelling for Resource Management.* vol 1. C.R.C. Press Inc. Florida.

de Wit, C.T.(1959). Potential photosynthesis of crop surfaces. *Neth. J. Agric. Sci.* 7: 141-149.

Wu, H., Sharpe, P.J.H., Walker, J. and Penridge, L.K. (1985). Ecological field theory: a spatial analysis of resource interference among plants. *Ecol. Model.* **29**,215-243.

Volterra, V. (1931). *Leçons sur la théorie mathématique de la lutte pour la vie.* Marcel Brelot, Paris.

Yatrebov, A.B. (1996). Different tpyes of heterogeneity and plant competition in monospecific stands. *Oikos*, **75**,89-97.

Yoda, K., Kira, T, Ogawa, H. and Hozumi, K. (1963). Self-thinning in overcrowded pure stands under cultivated and natural consditions. *J. Inst. Polytech. Osaka City Univ. Ser. D.*, **14**, 107-129.

Appendix

"Ecospace" model listing

The model listing is given here in abridged form, with some of the functions not directly involved in the processes described in this thesis (data input functions and those for calculating the movement of trunks of vegetation through the grid) edited out for clarity. Functions are listed alphabetically. A full model listing is obtainable on request from the author. The program is written in the ANSI C language, largely using a few simple commands. A tree of model functions is presented below. First the *main()* program is shown, followed by four extensions to the tree in alphabetical order, *estab_master(), indiv_master, light_regime()* and *overhex()*. Dotted lines indicate a function which calls one or more other functions.

Function calling structure

```
main().....   set_up().....   anewlyprogrammedata()
                               read_dataA()
                               read_dataB()
                               read_dataC()
                               read_climdata()
                               dome_data()
                               randinput()
                               initialiseB()
                               light_regime().....see below
              snow_master()
              absdens_update()
              embdens_update()
              abiotic().....   season_master().....  sun_month()
                               light_regime().....see below
                               soiltemp()
                               weather_master().....  normal_distribution()
                                                      wind_direction().....  normal_distribution()
                               wind_master().....     wind_profile().....    wind_ht()
                                                                             wind_rough()
                                                      exposure().....        light_path()
                                                                             light_shaft().....
                               temp_record()
              phenology().....  dormant_calc()
              estab_master().....see below
              indiv_master().....see below
```

```
                dome_master()..... domegenerate()..... domerefresh()..... overhex().....
                                                                           dfill()
                                   domeallocate()
                                   domegrow()..... dome_align()..... domerefresh()
                                                   domerefresh()
                move_master().....currently disabled & not listed
                litter_master()..... litter_create()
                                   browning()..... hcalc()
                                   litter_level()
                                   litter_fall()
                outmaster().....controls output, not listed
end of main program
```

```
.....estab_master()..... germinate()..... germ_gap()
                                   seedbank()
                                   est_initialise()
                                   germ_rate()
                establishment()..... est_limits()..... response_ph()..... sindistribution()
                                                       response_sm()..... sindistribution()
                                   est_kill()
                                   indiv_remove()
                                   indiv_initialise()..... xyconvertB()..... stathexcord()
                                                                             slinegenerate().....
                                                                                          sgradcalc()
                                                                             shexpoint_test()
```

```
....indiv_master()..... temp_regime()..... tempvar()
                                   embtemp_update()
                                   radcalc()
                                   temp_leaf()
                est_grow()..... hcalc()
                                   phot_inputs()
                                   est_photo()
                                   est_resp()
                growth_gen()..... photosyntheather()...hcalc()
                                                       tempvar()..... sindistribution()
                                                       lvar()..... sindistribution()
                                                       phot_long()
                                                       phot_short()
                                                       prod_error()
                                   respiration()..... tempvar()..... sindistribution()
                                   {soil_limits().....} response_sm()..... sindistribution()
                                                       response_ph()..... sindistribution()
                                                       response_nit()..... sindistribution()
                                                       response_phos()..... sindistribution()
                mortality()
                grow()..... classify_age()
                                   ind_kill()
                                   store()
                                   senesc_test()
                                   partition()         rootgrow()..... rootdome().....
                greengrow()..... potentialindivgrow()..senesc_test()
```

	in greengrow()..		potformzero().....	overhex().....*see below*
				newtile()
			esmoothdisc()	
			potformone().....	nextscanB()
			potfromtwo().....	
			ddens_generate()	
			pressuredome()	
		appliedindivgrow()	nextscanA()	
			esmoothdd()	
		surplusindivgrow()	nextscanA()	
			newtile()	
			esmoothdd()	
		dens_update()	occtrigger()	newhextwo()
			part_again()	
			zenterzero()	xyconvertA()
	woodgrow().....	pot_wood()		
		appliedindivgrow().....*as above*		
		surplusindivgrow().....*as above*		
		dens_update().....*as above*		

....light_regime().....	light_direct().....	light_path()		
		light_shaft().....	stathexcord()	
			slinegenerate().....	sgradcalc()
			lintersects().....	dist_calc()
			light_horiz()	
			lvert_distribute()	
			ledgend()	
		light_attenuation()....	kcalc()	
			lembed()	
	light_diffuse()	light_path()		
		light_shaft()	stathexcord()	
			slinegenerate()	sgradcalc()
			lintersects()	dist_calc()
			light_horiz()	
			lvert_distribute()	
			ledgend()	
		soc()		
		light_attenuation()	kcalc()	
			lembed()	

....overhex()....	hexcord()		
	cpoint_test()		
	cside_test()		
	cintersects()		
	circhexarea().....	csmalldisc()	
		tcalc()	
		csegment()	
